

UNIVERSITY OF RIJEKA
FACULTY OF BIOTECHNOLOGY AND DRUG DEVELOPMENT

Franka Rigo

**ROLE OF REDOX RELATED GENES
IN THE REGULATION OF
METHAMPHETAMINE-INDUCED PHENOTYPES
IN *D. MELANOGASTER***

DOCTORAL THESIS

Rijeka, 2024

UNIVERSITY OF RIJEKA
FACULTY OF BIOTECHNOLOGY AND DRUG DEVELOPMENT

Franka Rigo

**ROLE OF REDOX RELATED GENES
IN THE REGULATION OF
METHAMPHETAMINE-INDUCED PHENOTYPES
IN *D. MELANOGASTER***

DOCTORAL THESIS

Thesis mentor: Assoc. Prof. Rozi Andretić Waldowski, Ph.D.

Rijeka, 2024

SVEUČILIŠTE U RIJECI
FAKULTET BIOTEHNOLOGIJE I RAZVOJA LIJEKOVA

Franka Rigo

**ULOGA GENA POVEZANIH S REDOKSOM
U REGULACIJI
FENOTIPOVA IZAZVANIH METAMFETAMINOM
U *D. MELANOGASTER***

DOKTORSKI RAD

Mentor: Izv. Prof. Rozi Andretić Waldowski, Ph.D.

Rijeka, 2024.

Doctoral thesis mentor: Associate Professor Rozi Andretić Waldowski, Ph.D.

Doctoral thesis was defended on _____ 2024, at the University of Rijeka, Faculty of Biotechnology and Drug Development, in front of the Evaluation Committee:

1. Associate Professor Jelena Ban, Ph.D.
2. Associate Professor Nicholas Bradshaw, Ph.D.
3. Associate Professor Dubravka Švob Štrac, Ph.D.

This doctoral thesis was completed at the Faculty of Biotechnology and Drug Development, University of Rijeka, under the guidance of Assoc. Prof. Rozi Andretić Waldowski, PhD. It is part of the postgraduate doctoral program in Medicinal Chemistry at the same faculty. The research was supported by the Croatian Science Foundation Research Grant #2794, "Influence of redox status on psychostimulant-induced neuronal plasticity".

Acknowledgement

First and foremost, I dedicate this thesis to my beloved daughter, Didi. Every effort and every late night have been for you. Your presence in my life has been my greatest motivation and inspiration.

My heartfelt gratitude goes to my incredible mentor, Rozi. From my first tentative steps as an undergraduate, you have guided me with patience and wisdom. Your unique ability to push me when necessary and grant me freedom when needed has profoundly shaped my journey. Thank you for being my steadfast support, for understanding when things didn't go as planned, and for always being there for me, both in and out of the lab.

Ana, you have been a pillar of support throughout my time in the lab. Everything I've learned, I owe to your patient teaching and guidance. Your insights, advice, and our cherished coffee breaks have been invaluable. Thank you for being there through every high and low.

I am deeply grateful to Milan for his assistance with data analysis. Your expertise has been essential in bringing this work to completion. Our shared laughs and crazy ideas helped, too.

To Bobi, Beti and Marta, thank you for filling the lab with laughter and joy. Your companionship has made this journey much more enjoyable. Also, to all my other fellow lab members and students, your company has created a wonderful environment that I will always treasure. Thanks to everyone at the faculty who offered a helping hand, wise advice, short talk or just shared a laugh.

My deepest gratitude goes to my family, especially my mother and father. Your unwavering support and willingness to help with everything during my long hours of work have been the backbone of my success. This achievement would not have been possible without you. I also want to extend my heartfelt thanks to my grandmother, my brother and his girlfriend, my aunts, and the rest of my family. Your love, encouragement, understanding and help with Didi have meant the world to me.

To my dancing family, thank you for being my sanctuary by providing me much-needed laughter, relaxation, and a break from the rigors of work. Special thanks to Elio, for supporting me in everything I do and always lifting my spirit.

Thanks to all my friends for being there, especially Ivana. Although being far from each other most of the time, I always feel your warm presence, care and support no matter what.

Thank you all, from the bottom of my heart.

Abstract

Addiction is a multifactorial neuropsychiatric disorder marked by compulsive drug-seeking behaviors despite adverse consequences. Neuroplasticity, the ability of the brain to adapt and reorganize, plays a crucial role in addiction, involving changes in gene expression, protein modifications, and synaptic plasticity. Alterations in redox homeostasis, particularly dysregulation of reactive oxygen species (ROS) signaling, are implicated in these neuroplastic changes. *Drosophila melanogaster*, with its well-characterized genome and genetic tools, serves as a valuable model for studying addiction-like behaviors such as drug self-administration (SA) and locomotor sensitization (LS). This research aims to identify genes and proteins involved in methamphetamine (METH) addiction using flies and approach integrating behavioral assays, genetic manipulations (selective breeding and genetic screen), and proteomic analyses.

We developed the FlyCafe assay to measure METH consumption and demonstrated flies' preferential SA of METH. Through 30 generations of selective breeding, we established fly strains with high (HP) and low (LP) preferences for METH, revealing distinct phenotypic profile of LP flies, including increased activity and body weight, decreased sleep and negative geotaxis and increased dopamine, tyramine and glutamate. Proteomic analysis of these strains identified differential proteins linked to metabolic processes, structural integrity, and protein turnover, including Bacchus, negative regulator of conversion of tyramine to octopamine, which was uniquely present in LP. Next, we showed that flies exhibiting LS displayed reduced preference for METH SA, and vice versa, suggesting shared molecular mechanisms through *period* gene. We conducted a genetic screen to identify redox-related genes that regulate LS to vMETH, uncovering several critical genes such as *Cat*, *Sod1*, *Sod2*, *Gapdh1*, and *Men*, which play functional roles in the regulation of LS. Remarkably, *Sod1*, *Gapdh1*, and *Men* are necessary in dopaminergic and serotonergic neurons for both LS and SA. Proteomic analysis of brain tissues from flies that did or did not develop LS after two administrations of volatilized METH identified a set of proteins unique

to the LS phenotype, highlighting significant changes in redox-related proteins. This included the upregulation of several antioxidative, glycolytic, and TCA enzymes (Cat, Prx3, Prx6c, Jafrac1, Gapdh1, Gapdh2, mAcon1, Mdh1, Mdh2) and the downregulation of enzymes related to oxidative phosphorylation (NADH dehydrogenases).

Combining these results, our study reveals that both LS and SA of METH are modulated by interconnected pathways involving peroxide regulation, glucose metabolism, NADPH production, and neurotransmitter systems. Together, these processes contribute to the development and maintenance of addiction-related neuroplasticity evident as LS and SA. Additionally, our findings highlight the importance of neurotransmitter tyramine in SA behavior, indicating that elevated tyramine levels, influenced by the Bacchus protein, may modulate the neural circuits involved substance preference and consumption. This research can serve as a foundation for exploring dietary and lifestyle interventions to maintain redox balance and metabolic health. For example, specific dietary supplements that enhance antioxidant defenses or support metabolic pathways, such as antioxidants, metabolic modulators, or NADPH boosters, could be investigated as adjunctive therapies for addiction.

Key words: addiction, methamphetamine, redox, neuroplasticity, *Drosophila*

Sažetak

Ovisnost je složen neuropsihijatrijski poremećaj karakteriziran kompulzivnim uzimanjem droge unatoč negativnim posljedicama. Neuroplastičnost, sposobnost mozga da se prilagodi i reorganizira kao odgovor na iskustva, ima temeljnu ulogu u razvoju ovisnosti. Taj proces uključuje kompleksne molekularne mehanizme, uključujući promjene u ekspresiji gena, modifikacije proteina i neuralnu plastičnost. Promjene u redoks homeostazi, posebice promjene u regulaciji signalizacije putem reaktivnih kisikovih vrsta (ROS), povezane su s neuroplastičnim promjenama i ovisnošću. *Drosophila melanogaster*, s obzirom na njen dobro karakteriziran genom te lako dostupne sofisticirane genetske alate, pokazala se je kao vrijedan modelni organizam za proučavanje ponašanja sličnih ovisnosti, poput samoadministracije droge (SA) i lokomotorne senzitivacije (LS), koja se lako mogu kvantificirati kod vinskih mušica. Glavni cilj ovog istraživanja je identificirati nove gene i proteine uključene u ovisnost o metamfetaminu (METH) koristeći *Drosophilu* kao model i pristup koji integrira bihevioralne testove, genetske manipulacije (selektivni uzgoj i genetski probir) te proteomske analize.

Razvili smo FlyCafe test za mjerenje konzumacije METH-a i pokazali da mušice preferencijalno samoadministriraju METH. Kroz 30 generacija selektivnog uzgoja, uspostavili smo sojeve mušica s visokom (HP) i niskom (LP) preferencijom za METH, otkrivajući različit fenotipski profil LP mušica, uključujući povećanu aktivnost i tjelesnu težinu, reducirano spavanje i negativnu geotaksiju te povećane razine dopamina, tiramina i glutamata. Proteomska analiza ovih sojeva identificirala je diferencijalne proteine povezane s metaboličkim procesima, strukturnim integritetom te sintezom i degradacijom proteina, uključujući Bacchus, negativni regulator pretvorbe tiramina u oktopamin, koji je jedinstveno prisutan kod LP mušica. Zatim smo pokazali da mušice koje pokazuju LS imaju smanjenu preferenciju za METH SA, i obratno, sugerirajući zajedničke molekularne mehanizme koji uključuju *period* gen. Proveli smo genetski probir kako bismo identificirali redoks-gene koji reguliraju LS na volatilizirani METH, otkrivajući nekoliko ključnih gena kao što su *Cat*, *Sod1*,

Sod2, *Gapdh1* i *Men*, koji imaju funkcionalne uloge u regulaciji LS-a. *Sod1*, *Gapdh1* i *Men* geni nužni su u dopaminskim i serotoninskim neuronima za oba fenotipa, LS i SA. Proteomska analiza moždanih tkiva mušica koje su razvile LS nakon dvije administracije volatiliranog METH-a identificirala je set proteina jedinstvenih za LS fenotip, naglašavajući značajne promjene u redoks-proteinima. To uključuje povećanu ekspresiju nekoliko antioksidativnih, glikolitičkih i TCA enzima (*Cat*, *Prx3*, *Prx6c*, *Jafrac1*, *Gapdh1*, *Gapdh2*, *mAcon1*, *Mdh1*, *Mdh2*) i smanjenje enzima povezanih s oksidativnom fosforilacijom (NADH dehidrogenaze).

Kombinirajući ove rezultate, naše istraživanje pokazalo je da su LS i SA METH-a modulirani međusobno povezanim putevima koji uključuju regulaciju peroksida, metabolizam glukoze, proizvodnju NADPH-a i neurotransmitterske sustave. Zajedno, ovi procesi doprinose razvoju i održavanju neuroplastičnosti povezane s ovisnošću, evidentne kao LS i SA. Dodatno, naši rezultati ističu važnost neurotransmitera tiramina u SA, ukazujući na to da povećane razine tiramina, pod utjecajem *Bacchus* proteina, mogu modulirati neuronske mreže uključene u preferenciju i konzumaciju droge. Ovo istraživanje može poslužiti kao osnova za istraživanje prehrambenih intervencija s ciljem održavanja redoks ravnoteže i metaboličkog zdravlja. Na primjer, specifični dodaci prehrani koji pojačavaju antioksidativnu obranu ili podržavaju metaboličke puteve, kao što su antioksidansi, metabolički modulatori ili NADPH pojačivači, mogli bi se koristiti kao dodatne terapije za ovisnost.

Ključne riječi: ovisnost, metamfetamin, redoks, neuroplastičnost, *Drosophila*

Contents

1. INTRODUCTION	1
1.1 Addiction as a brain disorder	1
1.1.1 Neurobiology of Addiction	2
1.1.2 Addiction-related behavioral phenotypes in humans and animal models	7
1.1.3 Addictive potential of methamphetamine	9
1.1.4 Addictive substances trigger neuroplastic changes in the brain	12
1.2 Redox biology in health and addiction	18
1.2.1 Redox regulation and effects of ROS on cellular signaling	19
1.2.2 Influence of ROS on neuroplasticity	23
1.2.3 Role and regulation of hydrogen peroxide in neuronal plasticity	26
1.2.4 Sources of ROS in the brain during substance abuse	27
1.2.4.1 Catabolism of dopamine as a source of ROS	28
1.2.4.2 Electron transport chain and the production of ROS	31
1.2.4.3 NOX as ROS producers	33
1.3 Role of Redox in Addiction.....	35
1.3.1 Effects of ROS on cellular function, signaling pathways, and metabolism in psychostimulant addiction	35
1.3.2 Behavioral effects of ROS in psychostimulant addiction	38
1.3.3 Effects of ROS modulation on psychostimulant-induced behavior	40
1.4 Addiction Research in <i>Drosophila melanogaster</i>	43
1.4.1 <i>Drosophila</i> as a model organism	43
1.4.2 Behavioral and genetic studies of psychostimulant addiction in <i>Drosophila</i>	45
1.4.3 Genetic screen and selective breeding in addiction research.....	48
2. AIMS	53
3. MATERIALS AND METHODS.....	54
3.1 Fly Strains	54
3.2 Assays and general protocols.....	55
3.2.1 Behavioral tests and protocols	55
3.2.1.1 FlyCafe assay	55
3.2.1.1.1 Experimental setup	55

3.2.1.1.2	Data collection and analysis.....	58
3.2.1.2	FlyBong assay.....	59
3.2.1.2.1	Experimental setup.....	59
3.2.1.2.2	Data collection and analysis.....	62
3.2.1.3	Activity and sleep tracking.....	62
3.2.1.4	Negative Geotaxis.....	63
3.2.1.5	Body weight measurement.....	64
3.2.2	Neurochemical Analysis.....	64
3.2.2.1	Sample preparation.....	64
3.2.2.2	Liquid Chromatography with Tandem Mass Spectrometry (LC-MS/MS).....	64
3.2.2.3	Data Analysis.....	65
3.2.3	Proteomic analysis.....	65
3.2.3.1	Brain dissection.....	65
3.2.3.2	Mechanical and chemical homogenization and protein isolation.....	66
3.2.3.3	Quantification of Total Proteins.....	67
3.2.3.4	Sample Preparation for Mailing.....	67
3.2.3.5	SDS-PAGE or 1D Electrophoresis.....	68
3.2.3.6	In-Gel Digestion of Samples and Preparation for Mass Spectrometry.....	68
3.2.3.7	Mass Spectrometry.....	70
3.2.3.8	Data analysis.....	70
3.2.4	Gene silencing using binary expression system UAS-GAL4.....	70
3.3	Approaches.....	72
3.3.1	Approach 1: Genetic screen and behavioral characterization.....	72
3.3.2	Approach 2: Selective breeding.....	74
3.3.3	Approach 3: Proteomic Analysis.....	75
3.3.3.1	Proteomics 1.....	76
3.3.3.1.1	Selective breeding.....	76
3.3.3.1.2	Proteomics and data analysis.....	77
3.3.3.2	Proteomics 2.....	78
3.3.3.2.1	FlyBong test.....	78
3.3.3.2.2	FlyBong data analysis.....	79
3.3.3.2.3	Criteria for separation into CTRL, LS and NLS groups.....	79
3.3.3.2.4	Proteomics and data analysis.....	81
3.4	Statistical Analysis.....	81
4.	RESULTS.....	82

4.1	Optimization of the CAFE method for measuring self-administration (SA)	82
4.1.1	Evaporation control	82
4.1.2	Amount of ingested food and side preference control	84
4.1.3	Flies preferentially self-administer METH food over regular food	87
4.2	Selective breeding for preferential consumption of METH	93
4.2.1	Selective breeding for 30 generations resulted in two divergent strains that differed in self-administration of METH food	93
4.2.2	Difference in self-administration of METH food was retained after the cessation of selective breeding	95
4.2.3	Behavioral and morphological characterization of HP and LP lines	96
4.2.3.1	Activity and sleep	97
4.2.3.2	Negative geotaxis	99
4.2.3.3	Adult males body weight	100
4.2.4	Selected lines differ in their neurochemical profile	101
4.2.5	Proteomic analysis	103
4.2.6	Role of tyramine and its regulation in METH preference	111
4.3	Self-administration and locomotor sensitization share a common molecular mechanism	112
4.3.1	Self-administration of METH food abolishes LS	112
4.3.2	Expression of LS abolishes preference for self-administration of METH food	115
4.3.3	<i>period</i> gene mutants do not develop LS nor preference of METH food	118
4.4	Identification of functional redox-related genes that regulate LS using genetic screen	121
4.4.1	Panneuronal silencing of redox related genes	124
4.4.2	Silencing of redox related genes in dopaminergic and serotonergic neurons (genetic screen using <i>ddc-gal4</i> driver)	130
4.4.3	Silencing of redox related genes in dopaminergic neurons (<i>ple-gal4</i> driver)	139
4.5	Identification of proteins involved in LS to vMETH using proteomic analysis	147
4.5.1	Upregulation and downregulation of proteins in the LS group	147
4.5.2	STRING analysis of overlapping proteins	149
4.5.3	<i>Proteins upregulated in LS</i>	149
4.5.3.1	Upregulation of redox-related proteins in LS: antioxidative and metabolic proteins	152
4.5.4	<i>Proteins downregulated in LS</i>	159
4.5.4.1	Downregulation of redox-related proteins in LS: ETC and Sod1	162

4.6	Overlapping multiple approaches	166
5.	DISCUSSION.....	173
5.1	Introduction to the Main Findings	173
5.1.1	Summary of the experimental design and approach.....	174
5.1.2	The significance of the FlyCafe assay	175
5.1.3	Methamphetamine preference and consumption.....	176
5.1.4	<i>Per</i> gene is a common genetic factor underlying LS and SA	177
5.1.5	Overview of selective breeding and genetic screen	179
5.2	Bacchus presence, alongside efficient metabolic regulation, protein turnover and structural integrity, underlies reduced METH preference	180
5.2.1	Stable divergence of high and low preference for METH SA after 30 generations of selection.....	180
5.2.2	A novel gene Bacchus defines low preference for METH	184
5.2.3	Efficient metabolic regulation, protein turnover, and structural integrity underlie reduced METH preference	186
5.2.4	Selective breeding summary and potential role of redox in preference for METH	190
5.3	Redox regulation of H₂O₂ levels, glucose metabolism and NADPH production underlies LS phenotype to vMETH	192
5.3.1	Expression of <i>Cat</i> , <i>Sod1</i> , <i>Sod2</i> , <i>Men</i> and <i>Gapdh1</i> in the dopaminergic and serotonergic neurons is necessary for LS phenotype	192
5.3.2	<i>Sod1</i> , <i>Gapdh1</i> and <i>Men</i> are common link in the overlapping regulation of LS and SA	199
5.3.3	Pleiotropic effect of redox-related genes.....	199
5.3.4	Large cluster of redox-related proteins is upregulated in flies that develop LS	201
5.3.5	Genes and pathways associated with LS identified by screen and proteomics	202
5.3.5.1	Combining behavioral genetics and proteomics in addiction studies.....	202
5.3.5.2	Antioxidative and metabolic adaptations are important for LS	204
5.4	Integration of findings and broader implications.....	205
5.4.1	Connecting the dots: genetic, behavioral, and molecular insights into LS and SA	205
5.4.2	Methodological considerations and experimental limitations	206
5.4.3	Future directions	208

6. CONCLUSION	209
7. REFERENCES	213
8. LIST OF ABBREVIATIONS.....	248
9. LIST OF FIGURES	252
10. LIST OF TABLES.....	255
11. SUPPLEMENT.....	256

1. INTRODUCTION

1.1 Addiction as a brain disorder

Addiction is a chronic, often relapsing brain disorder characterized by a compulsive urge to use drugs or engage in certain behaviors, despite harmful consequences (1). It is marked by alterations in the brain's structure and function, which manifest as changes in behavior, cognition, and emotional response. People with addiction, as severe substance use disorder, have an intense focus on using certain substances, such as alcohol or drugs, to the point that it takes over their life.

Addiction is a major public health problem with widespread consequences (2). It affects millions of people worldwide, leading to significant health, social, and economic burdens. Health consequences can range from overdose and death to the development of chronic health conditions, both physical and mental. The societal impact is also profound, including increased healthcare costs, lost productivity, increased crime, and substantial social welfare expenditures. Moreover, addiction strains relationships, diminishes quality of life, and can lead to stigma and social isolation.

Historically, addiction was often viewed through a moral or criminal lens, with sufferers seen as lacking in moral character or willpower (3). Over the centuries, the perception has shifted towards a more compassionate and scientifically grounded view. In the 19th century, advances in chemistry and medicine began to reveal the physiological properties of addictive substances, laying the groundwork for modern research, which views addiction as a complex interplay of genetic, environmental, and neurological factors (4). This shift has been influential in developing strategies for prevention, treatment, and rehabilitation, moving from punitive measures to evidence-based interventions.

Recent decades have seen emerging themes in addiction research that focus on the neurobiological basis of addiction (5,6). Studies have explored how addictive substances

alter brain pathways involved in reward, motivation, and memory (7). Researchers have also begun to examine the role of both genetics and environment in susceptibility to addiction, which has opened new avenues for personalized medicine (8–11). Additionally, the concept of neuroplasticity, or the brain's ability to adapt and change in response to experiences, including drug use, has become central to understanding addiction (12).

1.1.1 Neurobiology of Addiction

The capacity of human brain to adapt and learn from the environment is a fundamental evolutionary trait, shared with other animals (13). This adaptability is driven by a complex interplay of external stimuli and neurological responses that shape behavior, ensuring survival and prosperity through the mechanism of natural rewards (Figure 1). Central to these adaptive processes is neuroplasticity, the brain's ability to alter its neural pathways and synapses in response to experiences, underlying both learning and memory (14–16). However, this adaptive mechanism also reveals a more detrimental aspect when confronted with substances of abuse. Such substances activate specific brain circuits, “hijacking” the neuroplastic mechanisms intended for positive adaptation (Figure 1). Consequently, these substances induce profound and lasting neuronal changes, culminating in addictive behaviors that are both maladaptive and harmful.

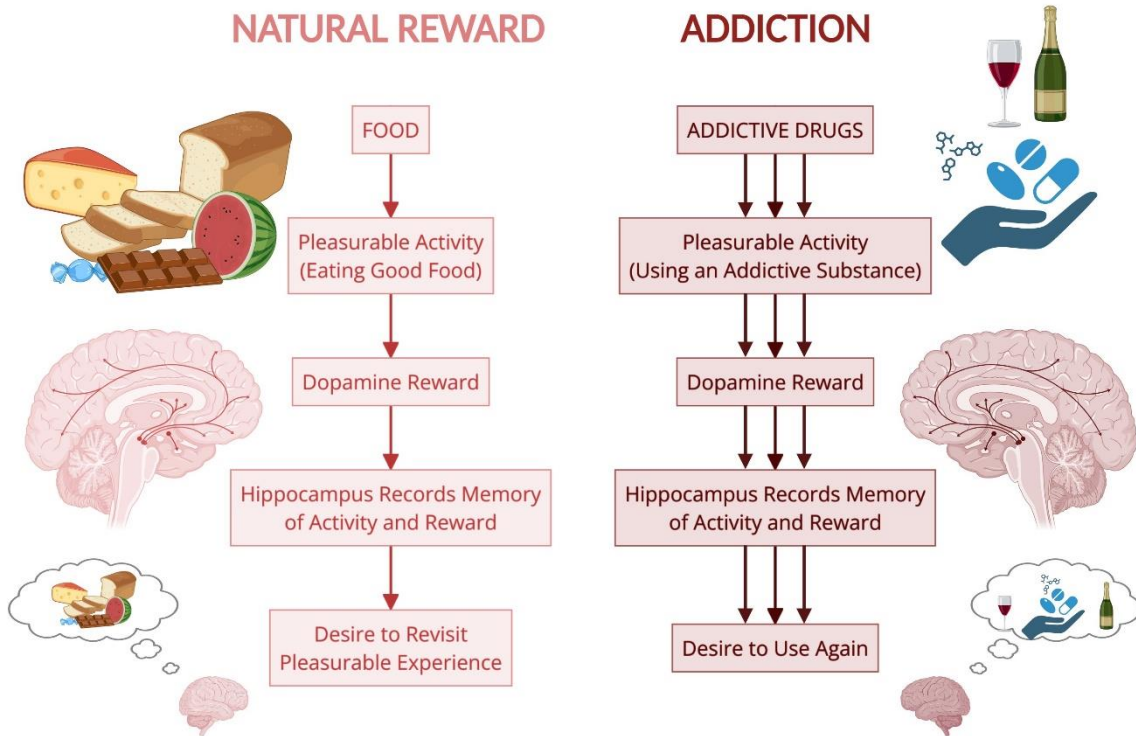


Figure 1. Addictive drugs “hijack” synaptic plasticity mechanisms in key brain circuits. Comparative visualization between the pathways of natural rewards and addiction. On the left, natural rewards, such as food, are pleasurable and trigger a dopamine-mediated reward signal in the brain. This is recorded in the hippocampus, creating a memory that contributes to the future desire to revisit the experience. On the right, the use of addictive drugs also leads to pleasurable activity, dopamine release, and memory formation in the hippocampus. However, the cycle of addiction is characterized by an amplified desire to use the substance again, often due to the stronger dopamine response compared to natural rewards. Created with BioRender.com.

Addiction affects the brain's complex circuitry, primarily altering the pathways involved in reward, motivation, and memory (17) (Figure 2). The mesolimbic and mesocortical dopamine pathways, central to these functions, include the ventral tegmental area (VTA),

nucleus accumbens (NAc), and prefrontal cortex (PFC) (18). Activation of the VTA releases dopamine into the NAc and PFC, which are critical for the perception of pleasure and reward. Neuroimaging studies have shown increased activity in these areas during drug use and cravings, highlighting their role in the addiction process (19).

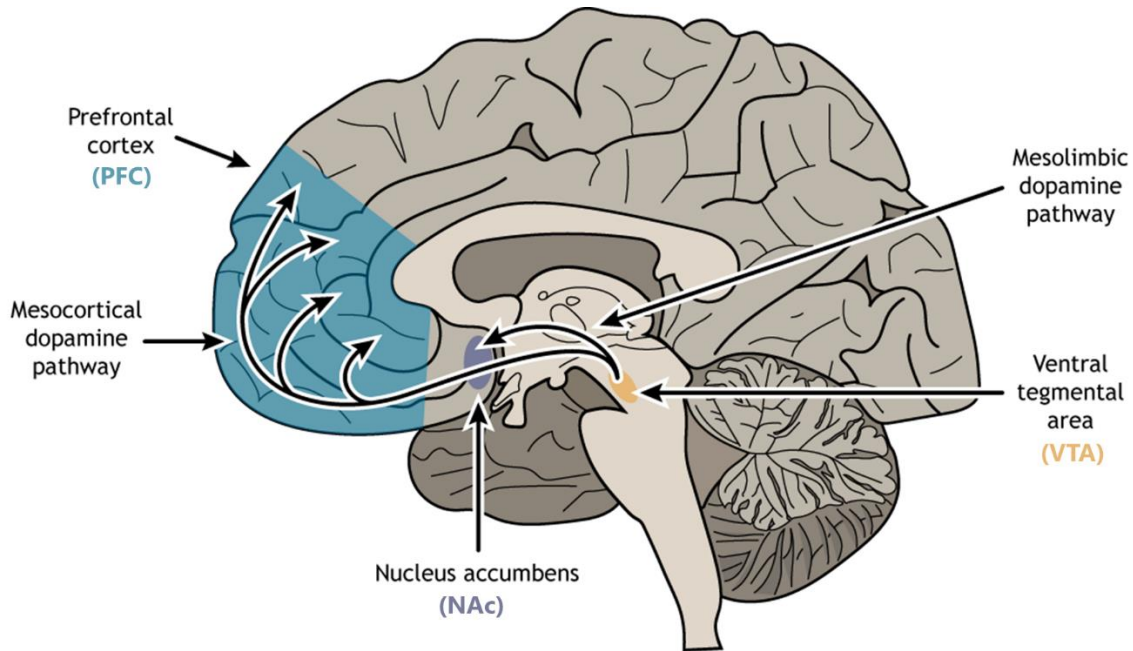


Figure 2. Mesolimbic and mesocortical dopamine pathways. *The ventral tegmental area (VTA), highlighted in orange, projects dopamine-rich signals to key brain regions via two primary pathways. Through the mesolimbic pathway, dopamine is transmitted to the nucleus accumbens (NAc), depicted in purple, playing a critical role in reward and motivation. Simultaneously, the VTA sends dopamine along the mesocortical pathway, to the prefrontal cortex (PFC), indicated in blue, which is essential for cognitive functions such as decision making and impulse control. Image source: 'Mesolimbic and Mesocortical Pathways' by Casey Henley is licensed under a [Creative Commons Attribution Non-Commercial Share-Alike \(CC BY-NC-SA\) 4.0 International License](https://creativecommons.org/licenses/by-nc-sa/4.0/).*

Dopamine (DA) is a neurotransmitter that plays a key role in the brain's reward system (20,21). It is associated with pleasure and reinforcement, motivating individuals to perform certain activities by providing a sense of enjoyment and satisfaction. In the context of addiction, DA role becomes complex and amplified (21). Addictive substances can cause the release of high levels of DA, far more than what natural rewards such as food or social interactions typically generate. This surge in DA contributes to the intense feeling of euphoria often described by individuals when they use addictive substances.

The brain's reward system adapts to these unnaturally high levels of DA by reducing the number of DA receptors or the amount of DA it produces (22). This leads to a diminished response to natural rewards, which can compel individuals to continue seeking out the addictive substance to achieve the same DA high, a process known as tolerance (23). Repeated exposure to these elevated DA levels conditions the brain to crave the substance, strengthening the neural pathways associated with drug use, and making it difficult to feel pleasure from previously enjoyable activities. This reinforces the behavior and creates a dependency or addiction, as the individual needs the substance to function normally or to feel pleasure.

Role of DA in addiction is well-documented, but its interaction with other neurotransmitters provides a broader understanding of addiction's complexity (21). Addictive substances can directly influence DA levels or alter the functions of other neurotransmitters which regulate DA activity within this system. For example, γ -Aminobutyric acid (GABA), opioid, serotonergic, cholinergic, and noradrenergic pathways are known to interact and modulate the activity of the mesolimbic DA pathway (24).

The serotonergic system, which involves the neurotransmitter serotonin (5-HT), interacts with DA. In the rodent brain it was shown those interactions have a role in regulating DA release through various 5-HT receptors, as revealed by microdialysis studies (25). They involve both facilitative and inhibitory effects on DA release by different serotonin receptor subtypes. This interaction significantly impacts various behavioral and psychological

functions such as reward processing, mood regulation, and decision-making. These critical aspects of cognitive function can be profoundly influenced by addictive substances, which often modify serotonin levels and disrupt its normal pathways, leading to alterations in mood and behavior that are characteristic of addiction disorders (26,27).

The noradrenergic system, which primarily relies on norepinephrine as its neurotransmitter, is essential for various brain functions, including arousal, attention, mood regulation, learning, memory, and responses to stress. In addiction studies using preclinical models, norepinephrine plays a crucial role in the stimulant effects of drugs, such as enhancing sensitization, aiding in drug discrimination, and triggering the relapse of drug-seeking behaviors. The interactions between norepinephrine and DA are integral to understanding the neurobiology of stimulant addiction (28). Despite the absence of DA transporters, experiments with knockout mice have demonstrated that DA release still occurs in response to stimulants, highlighting norepinephrine's significant independent role (29). The noradrenergic and dopaminergic systems are closely linked, with noradrenergic inputs into the mesolimbic pathway influencing dopaminergic activity in key areas like the ventral tegmental area (VTA) and prefrontal cortex through α 1-adrenergic receptors (30,31). Additionally, the overlap in substrate specificity between the norepinephrine and DA transporters, particularly in the prefrontal cortex, further exemplifies the complex functional coupling between these neurotransmitter systems (28).

GABA inhibits DA release, thus playing a critical role in modulating the brain's reward system and maintaining a balance in neural activity (32,33). This inhibitory action helps counteract the excessive stimulation that can occur with drug use, particularly with substances that can significantly increase DA levels. By controlling DA release, GABA helps to regulate mood, reduce the likelihood of compulsive behavior, and decrease the reinforcing effects of addictive substances. Therefore, disruptions in GABAergic signaling can contribute to the imbalance of neurotransmitter systems observed in addiction, leading to enhanced drug-seeking behaviors and increasing the risk of dependency and relapse(34).

Glutamate promotes DA release and, as the primary excitatory neurotransmitter, it is integral to the brain's ability to adapt and modify its connections in response to experiences, including drug use (35). By facilitating DA release, glutamate strengthens the neural pathways associated with drug-seeking behavior and intensifies the learning and memory processes that associate specific environmental cues with the rewarding effects of drugs (36). Consequently, the glutamatergic system has important role in the initiation and persistence of addictive behaviors. (37).

1.1.2 Addiction-related behavioral phenotypes in humans and animal models

The neurobiological mechanisms discussed in the previous section underlie behavioral phenotypes observed in both humans and animal models. These phenotypic manifestations provide observable evidence of the underlying changes within the brain's circuitry due to addictive substances. In humans, addiction is characterized by a spectrum of behavioral phenotypes, each deeply rooted in neurobiological changes. For example, compulsive drug seeking, and use is primarily driven by alterations in the brain's reward pathways, specifically the overactivation of dopaminergic systems which heightens the reward sensitivity to drugs (38). This change compels continued use despite detrimental consequences, driven by the brain's rewired response to drug-related stimuli. Tolerance develops as the brain adapts to the drug's presence, necessitating larger doses to achieve the same effects previously attained with smaller amounts (39). This neuroadaptation is complemented by withdrawal symptoms when drug use is decreased or stopped, where symptoms can range from mild anxiety to severe physiological distress, reflecting the central nervous system's dependency on the substance to function normally (40,41). Cravings are intense desires for the drug, often triggered by environmental cues like places, people, or emotions linked with drug use (42,43). These are a product of conditioned learning, where the brain's memory systems associate these cues with the pleasurable effects of drug use, reinforcing the addiction cycle. Impaired decision-making capabilities arise from dysfunction in the prefrontal cortex, a

region critical for judgement and impulse control (44). This impairment leads to poor choices and behaviors that prioritize immediate drug-related rewards over long-term well-being, perpetuating the cycle of addiction (45). Relapse, known as the resumption of drug seeking and taking after a period of abstinence, demonstrates the persistent changes addiction imprints on the brain (46,47). It highlights the challenge in maintaining long-term sobriety, influenced by enduring neurobiological changes and external triggers such as stress (48).

In animal models, these human behaviors are mirrored and studied under controlled conditions to gain deeper insights into the underlying mechanisms (8,49–51). Drug self-administration (SA) in animals, where they actively seek and consume drugs, closely mimics human patterns of addictive behavior, serving as a fundamental model for studying the reinforcing properties of substances (52–54). Conditioned place preference (CPP) reveals how environmental contexts associated with drug effects influence cravings, showing preference for places linked to drug experiences as a measure of the drug's rewarding impact (55,56). Locomotor sensitization (LS) in model animals illustrates the progressive nature of addiction where increased locomotor activity following repeated exposure to the same dose of the substance indicates neural sensitization to its effects (57,58). Similarly, observable signs of withdrawal in animals provide a parallel to human withdrawal, offering insights into the physiological dependencies developed on substances (50). Moreover, extinction and reinstatement studies in animals explore the dynamics of recovery and relapse (56,59). Extinction represents the reduction or cessation of drug-seeking behavior when the drug is no longer available, and reinstatement shows the ease with which behaviors can recur in the presence of drug cues or stress, mirroring human relapse scenarios (59).

From molecular changes to behavioral outcomes, interconnectivity of neurobiology and observable actions across species provides insights into the mechanisms of addiction, guiding the development of interventions that target both the biological basis and its behavioral manifestations. By bridging these aspects, researchers can better devise their

approach to treatment that address both the physiological basis and the behavioral consequences of addictive behaviors.

1.1.3 Addictive potential of methamphetamine

Methamphetamine (METH) is a central nervous system stimulant that is widely recognized for its high potential for addiction and significant health risks (60). METH is structurally similar to amphetamine and DA (Figure 3), a key factor in its action mechanism. It is a lipophilic compound allowing it to easily cross the blood-brain barrier and exert potent effects on the central nervous system. Its molecular formula is $C_{10}H_{15}N$, with a molecular weight of approximately 149.24 g/mol.

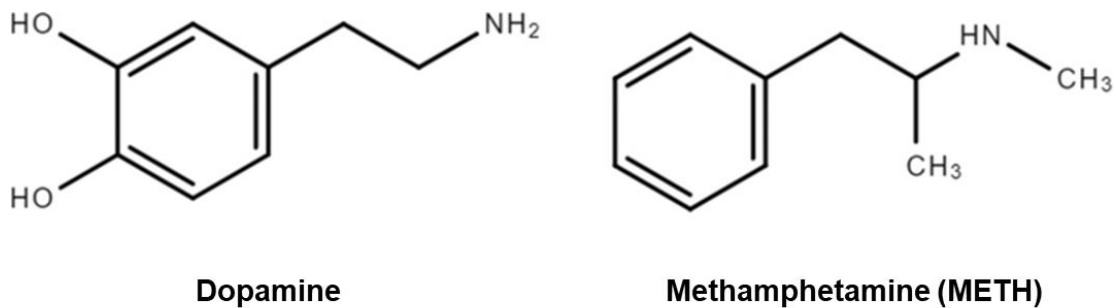


Figure 3. Chemical structures of dopamine and METH . Image source: (61)

METH primarily impacts the brain by altering the function of monoaminergic neurotransmitter systems, including DA, serotonin, and norepinephrine (62). Its effects start at the neuronal transporters. METH has a high affinity for the DA transporter (DAT), through which it enters the neurons. Once inside, METH induces reverse transport of DA, leading to increased extracellular DA levels (Figure 4). This action is not exclusive to DA as METH also

affects serotonin transporters (SERT) and norepinephrine transporters (NET), enhancing the extracellular concentrations of these neurotransmitters as well (62).

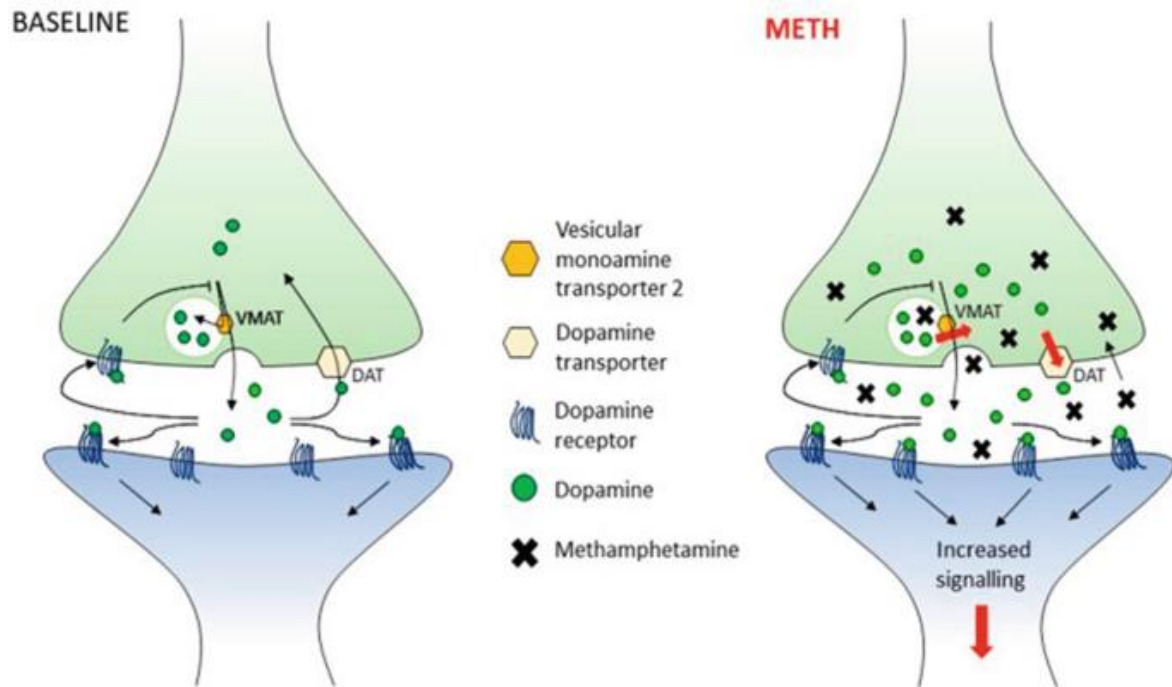


Figure 4. Dopamine Neurotransmission under Baseline and METH-Exposed Conditions.

Dark yellow shapes represent the Vesicular Monoamine Transporter 2 (VMAT2) responsible for packaging dopamine into vesicles; light yellow structures symbolize the Dopamine Transporter (DAT), which recycles dopamine back into the presynaptic neuron; blue structures depict dopamine receptors that bind dopamine to transmit signals across the synaptic gap; green circles indicate dopamine molecules; and black X marks represent METH molecules. Under baseline conditions, dopamine is synthesized and stored in vesicles within the presynaptic neuron, released into the synaptic cleft upon activation, binds to receptors on the postsynaptic neuron, and is then taken back up by DAT for reuse. In the METH-exposed scenario, METH disrupts this cycle by entering the presynaptic neuron through DAT, displacing dopamine from its vesicular storage via VMAT2 interference, and causing increased cytoplasmic dopamine levels. Additionally, METH reverses DAT function, leading

to increased dopamine release into the synaptic cleft and reduced reuptake. This results in prolonged and amplified activation of dopamine receptors on the postsynaptic neuron, enhancing signaling and contributing to METH's psychoactive and addictive effects, as indicated by the red arrow showing increased neurotransmission. Image source: (63)

METH also interferes with the vesicular monoamine transporter 2 (VMAT2), crucial for transporting monoamines into synaptic vesicles for storage. By disrupting VMAT2 function, METH causes an accumulation of neurotransmitters in the cytoplasm, making them more readily available for non-vesicular release into the synaptic cleft (64). Concurrently, METH inhibits monoamine oxidase (MAO), an enzyme responsible for the breakdown of monoamines, which further contributes to elevated neurotransmitter levels in the neuronal synapse (64).

The surge in neurotransmitter levels leads to sustained activation of their respective receptors. For DA, this means prolonged stimulation of both D1 and D2 receptors, contributing significantly to the drug's euphoric and addictive properties (65). Serotonin receptors across various neuronal subtypes also get overstimulated, affecting mood, perception, and other psychological functions (66). Overactivation of norepinephrine receptors results in increased alertness, elevated blood pressure, and heart rate, intensifying stimulant effects of METH (28).

These acute actions of METH on neurotransmitter systems lead to long-term changes in synaptic plasticity, notably affecting long-term potentiation and depression. Such changes are thought to underlie the persistent nature of addiction, as they can modify learning and memory processes (67). Moreover, METH activates downstream signaling cascades, including the cAMP response element-binding protein (CREB) and mitogen-activated protein kinases (MAPKs) (68,69). Activation of CREB can alter gene expression, promoting adaptations that sustain addictive behaviors, while chronic activation of MAPK pathways may lead to structural and functional neuronal changes.

Upon ingestion, METH quickly produces a surge of euphoria primarily due to its rapid increase of DA in the brain (60). This effect is accompanied by heightened alertness, increased concentration, and a feeling of increased energy. Physiologically, it can lead to increased heart rate, elevated blood pressure, and hyperthermia. Neurologically, it can cause changes in brain activity, as evidenced by increased metabolism in certain brain regions observed in imaging studies.

Chronic use of METH can lead to substantial neurotoxic effects, notably in the DA and serotonin systems (62,70). Neuroimaging studies have shown alterations in the activity of the limbic system, and reductions in the volume of the hippocampus and frontal cortex, which are associated with cognitive impairments, emotional dysregulation, and addictive behaviors (71). Long-term use also correlates with an increased risk of psychiatric disorders, including depression, anxiety, and psychosis (72).

A key factor in the neurotoxic effects of METH is the increase in reactive oxygen species (ROS) and subsequent oxidative stress. METH-induced oxidative stress has been shown to damage dopaminergic and serotonergic neurons, contributing to neurodegeneration (73). For instance, METH exposure led to elevated ROS levels, resulting in apoptosis of dopaminergic neurons (74). Similarly, De Vito and Wagner (1989) found that oxidative stress mediated by METH contributes to the long-term depletion of DA and serotonin in the brain (75). These studies highlight the role of ROS in disrupting cellular function and promoting neurodegenerative changes, further exacerbating the addictive and harmful effects of METH.

1.1.4 Addictive substances trigger neuroplastic changes in the brain

Development of addiction is a process which can be described as a complex interplay between environment and the genetic background (76). Genetics play a crucial role in determining an individual's susceptibility to addiction by affecting neurotransmitter systems

and brain circuitry. For instance, genetic variations can influence how DA is processed in the brain, which affects reward-seeking behavior (77). Environmental factors such as exposure to drugs, stress, and social surroundings interact with genetic predispositions to either intensify or mitigate the risk of developing addictive behaviors. Following repeated exposures to addictive substances, the drug naïve brain is modulated by specific early events, such as the short-lived modification or trafficking of existing proteins, leading to new gene expression and complex modulation of transcription, that leads to change in the neuronal morphology and function, a hallmark of neuronal plasticity (78).

Neuroplasticity plays a role in both learning and addiction, serving as the brain's ability to adapt structurally and functionally in response to various stimuli and experiences. This adaptability is manifested through mechanisms such as synaptic plasticity and structural plasticity (79–81), two basic types of neuroplasticity (Figure 5). Synaptic plasticity refers to the changes in the strength and efficacy of synaptic connections between neurons. These changes are critical for learning and memory, as they allow for the adjustment of neural circuits in response to new information (82). Structural plasticity involves more substantial changes, such as neurogenesis, formation of new synaptic connections, or the pruning of less-used pathways (81,83). Together, these mechanisms ensure that the brain remains dynamically adaptable across the lifespan.

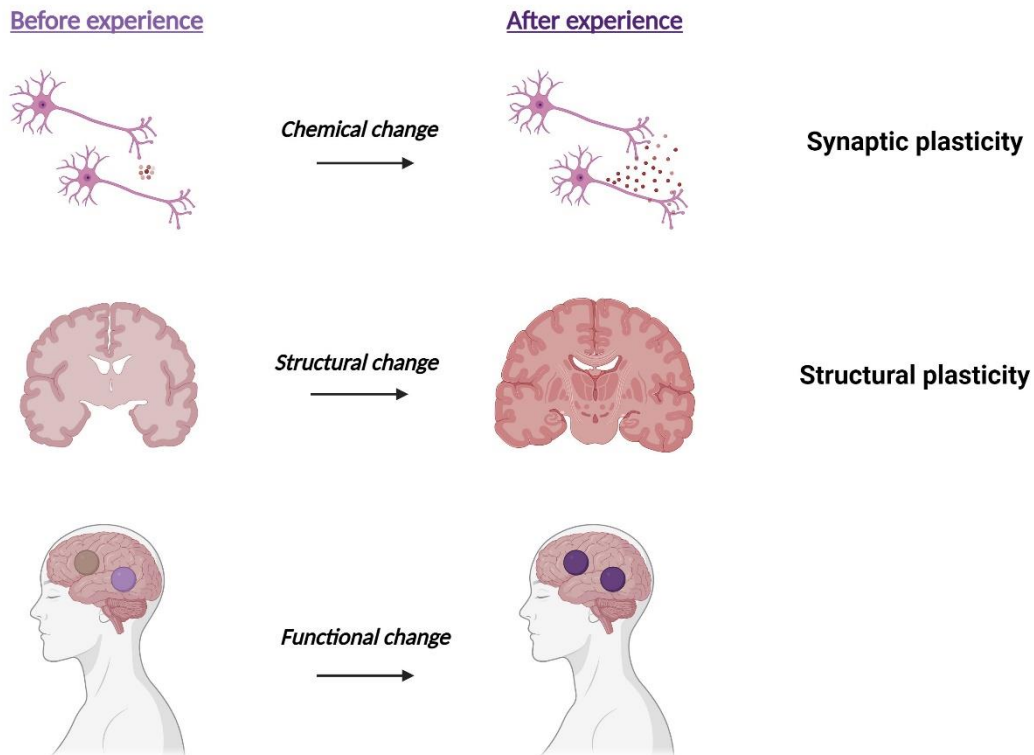


Figure 5. Basic neuroplasticity types. *Neuroplasticity, the brain's ability to reorganize itself by forming new neural connections, encompasses several fundamental types. Synaptic neuroplasticity involves changes in the release and reception of neurotransmitters between neurons, facilitating altered communication following new learning or experiences. Structural neuroplasticity refers to the physical changes in the brain's structure, such as the formation of new dendritic connections or the strengthening of synaptic connections, which occur in response to learning and experience. Lastly, functional neuroplasticity describes changes in the brain's activity in response to specific tasks or stimuli, often manifesting as altered brain activity patterns detectable via various neuroimaging techniques. Created with BioRender.com.*

In the context of addiction, neuroplasticity explains how initial voluntary substance use can eventually lead to compulsive and uncontrollable behavior (84). Over time exposure to

amphetamine, cocaine, nicotine, or morphine leads to long-term structural changes in the brain's neurons, particularly in regions responsible for reward and motivation, such as the NAc, and decision-making and self-control, such as the PFC. This results in a reorganization of synaptic connections, which alters brain function and contributes to the lasting effects and a pattern of addictive behaviors associated with these drugs (85).

Synaptic plasticity is the ability of synapses to strengthen or weaken over time. Short-term synaptic plasticity is a transient adjustment in synaptic strength, lasting from seconds to a few minutes, crucial for the dynamic processing of neural information (86). Long-term synaptic plasticity involves enduring changes in synaptic strength that significantly influence learning, memory, and behavior through the mechanisms of long-term potentiation (LTP) and long-term depression (LTD) (87). LTP is a long-lasting enhancement in signal transmission between two neurons that results from their synchronous stimulation. This mechanism is critical for several aspects of brain function, including learning and memory (88). Several studies found that either single or chronic cocaine exposure enhanced LTP in the PFC and VTA, leading to increased addictive behaviors (89–92). Expression of N-methyl-D-aspartate (NMDA) receptor 1 in the VTA has been found to be elevated after repeated use of psychostimulants, and these changes are linked to motor sensitization (93). At the molecular level, NMDA receptors are entered by calcium ions during LTP, activating kinases like CaMKII that enhance the function and number of α -amino-3-hydroxy-5-methyl-4-isoxazolepropionic acid (AMPA) receptors at the synapse (94). This strengthens the synaptic response to glutamate, reinforcing the connection between neurons.

Chronic METH exposure affects synaptic plasticity by inducing both LTP and LTD in different brain regions. For example, METH enhances LTP in the hippocampus, as shown in rat models (95), while it induces LTD in the striatum, contributing to synaptic weakening and addiction (96). These findings show the complex, region-specific effects of METH on neural circuitry, leading to both enhanced and weakened synaptic connections. LTD is the long-lasting decrease in synaptic strength that occurs due to the low-frequency activation of synaptic

connections (87). LTD involves a different set of molecular processes, primarily the internalization and dephosphorylation of AMPA receptors from the postsynaptic membrane. This process is mediated by phosphatases such as calcineurin, which respond to a lower rise in intracellular calcium, typically facilitated by milder or prolonged activation of NMDA receptors. By removing AMPA receptors from the synapse, the efficiency of synaptic transmission is reduced, which is crucial for deleting old or less useful synaptic connections, thereby optimizing neural circuitry (87). LTD in the NAc, facilitated by the endocytosis of AMPA receptors, is essential for the development of amphetamine-induced behavioral sensitization (97). Blocking AMPA receptor endocytosis effectively prevents this form of neural plasticity, suggesting a potential therapeutic approach for addressing addiction.

Structural plasticity involves changes in the physical structure of the brain, including the growth and formation of new neurons and synapses, alongside the removal or pruning of neurons and synapses that are no longer necessary (88,98,99). This type of plasticity is evidence of the brain's dynamic nature, reshaping its architecture to meet the demands of various physiological activities and experiences. A study by Thompson et al. (2004) highlighted how METH abuse causes long-term changes in brain structure and function. Using magnetic resonance imaging (MRI) and new computational brain-mapping techniques, the study identified the pattern of structural brain alterations associated with chronic METH abuse in human subjects (100). METH abusers had 7.8% smaller hippocampal volumes than control subjects, significant white-matter hypertrophy, and impaired memory performance. Studies in mice have also shown that chronic psychostimulant use leads to significant dendritic spines alterations. For instance, research by Kasahara et al. (2019) demonstrated that METH exposure resulted in changes to the dendritic spine density in the NAc, a region associated with reward and addiction behaviors (101). Cocaine also induced dendritic remodeling by increasing spine density induced by repeated cocaine treatment (102). This synaptic restructuring is a key component of how addiction alters neural circuitry.

Several proteomic studies on different brain regions have detected neuroplasticity-related proteins altered by one or multiple METH administrations, revealing significant changes that contribute to its impact on neuronal structure and function. These studies have identified key proteins involved in synaptic function, cytoskeletal organization, and signal transduction. For example, Iwazaki et al. found changes in synapsin II, hippocalcin, and SNAP-25 in the striatum of rats with METH-induced behavioral sensitization, all crucial for synaptic vesicle trafficking and neurotransmitter release (103). They also observed alterations in N-tropomodulin, GDI alpha, and beta actin, which regulate the cytoskeleton in the rat striatum after acute METH treatment, which indicates that neuroplastic processes could be triggered after only one METH administration (104). Yang et al. investigated protein alterations in the prefrontal cortex, cingulate cortex, hippocampus, striatum and nucleus accumbens in rats following the induction of METH-induced CPP and highlighted changes in profilin-2, syntaxin, and neurofilament, essential for synaptic plasticity and structural support (105). Another study by Iwazaki et al. on the amygdala revealed changes in synapsin-2b and tropomyosin, further indicating METH's widespread impact on proteins regulating cytoskeletal dynamics and synaptic function (106). These proteomic changes underline the profound impact of METH on neuroplasticity, providing insights into its long-term effects on brain function.

An integral part of both the initial events and later long-lasting structural and functional changes of affected neurons are the changes in metabolic processes. The understanding of the interplay between metabolism and neuronal plasticity is still very limited. Lately the research shows that redox-related processes and genes that regulate redox homeostasis have important role in the neuroplastic changes related to drug use (107). Although drugs of abuse produce divergent effects in the brain, a unifying characteristic of drug addiction is altered redox status (108). Except their well-known neurotoxic effects, recent studies show that ROS can act as signaling molecule by briefly and reversibly modifying protein function and consequently regulating several cellular processes (109,110). ROS molecules play a key role as messengers in the normal cell signal transduction and cell cycling, and modulate the

physiological processes of neuronal development, neuronal polarization, connectivity, and plasticity (111,112). This shows the importance of tight connection between metabolism and regulation of redox homeostasis to ensure proper functioning of the brain.

1.2 Redox biology in health and addiction

Redox biology refers to the delicate balance between the production of reactive oxygen species (ROS) and their neutralization within brain cells (113). This equilibrium is crucial for various cellular processes, including signal transduction, gene expression, and modulation of ion channels and receptors. ROS, though often perceived as harmful, play essential roles in normal cellular functions at moderate levels (114) (Figure 6.). However, when this balance tips, leading to oxidative stress, it can contribute to numerous disorders, including addiction (115).

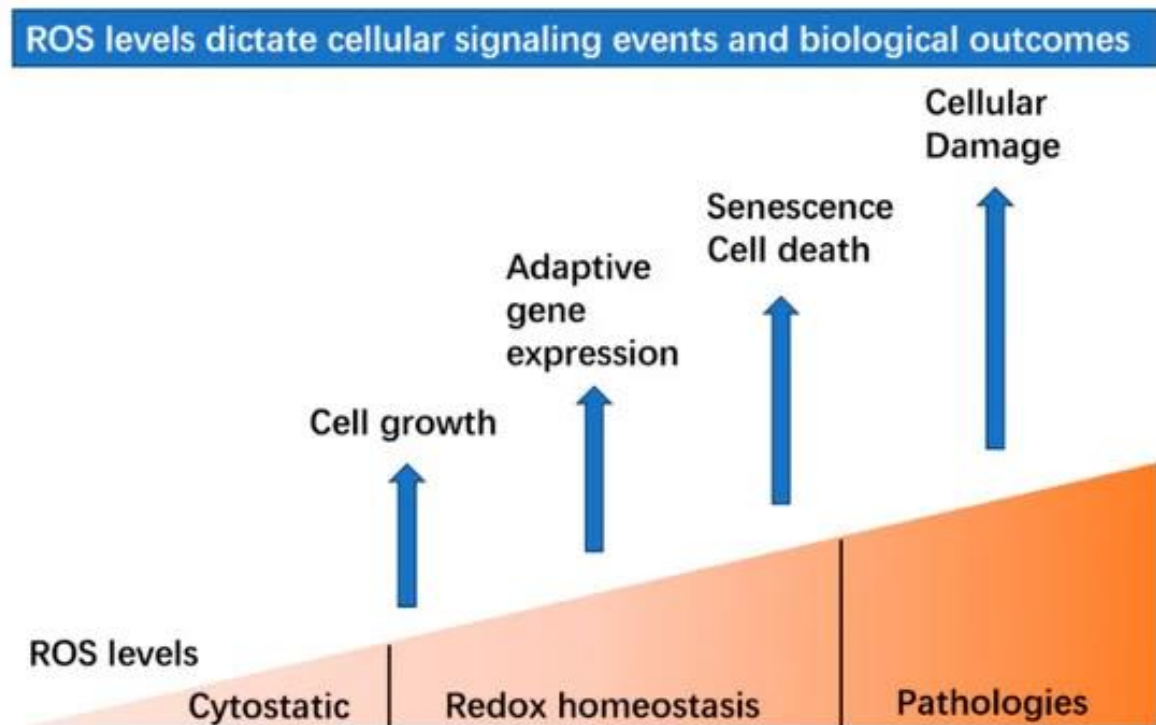


Figure 6. The Impact of ROS Levels on Cellular Signaling and Outcomes. *Within the normal physiological range, ROS are crucial for various cellular functions, maintaining redox balance. At low concentrations, ROS stimulate cell proliferation and differentiation. As ROS levels increase, they trigger adaptive responses, including the upregulation of antioxidative genes. However, exposure to higher ROS concentrations can initiate cellular senescence or lead to cell death. Image source: (116)*

Oxidative stress occurs when there is an imbalance between the generation of ROS and the brain's capacity to detoxify these reactive molecules or repair the resultant damage (117,118). In the context of addiction, substances like METH and cocaine exacerbate this imbalance by either increasing ROS production or diminishing antioxidant defenses (119). Enhanced ROS production, often through mechanisms such as increased metabolic activity, mitochondrial dysfunction, and activation of specific enzymes like NADPH oxidase, leads to significant cellular damage (120,121).

Importantly, there is a state that exists between normal physiological conditions and developed pathology. This intermediate state involves the signaling pathways and neuroplasticity changes that precede pathological conditions. In addition these changes involve synaptic plasticity modifications that lead to long-term alterations in the brain's response to stimuli, thereby contributing to addictive behaviors (93). These early signaling disruptions are critical as they set the stage for more severe neurotoxic changes if the imbalance persists.

1.2.1 Redox regulation and effects of ROS on cellular signaling

Under a physiological state, the level of cellular ROS is in a dynamic equilibrium, and this balance is modulated by cellular processes that produce and eliminate ROS (122). This carefully orchestrated redox system works to keep the homeostasis in place. Upon external perturbations, by sensing the metabolic state of the cells through specific molecules that

act as redox sensors, redox system adapts by modulating signaling to maintain homeostasis. Important redox sensors are active redox couples (such as NAD^+/NADH , $\text{NADP}^+/\text{NADPH}$, GSSG/GSH) which are present in the cell at the same time in the oxidized and reduced states (123). They take part in sensing and adjusting numerous cellular reactions. Ratios of the oxidized and reduced forms of these compounds are important redox parameters and their crosstalk with the components of the redox system, for example antioxidative proteins glutathione peroxidases (GPx), glutathione reductase (GRx), peroxiredoxins (Prx), superoxide dismutase (SOD), catalase (CAT) or ROS producers such as NOX or electron transport chain components, further dictate the direction of redox adjustments. (124–126). These processes either stimulate or restrict production of molecules that could act as redox second messengers. Main metabolically produced forms of ROS are superoxide (O_2^-) and the hydroxyl radical ($\cdot\text{OH}$). Normally, due to its high reactivity, superoxide is quickly converted to the less reactive hydrogen peroxide (H_2O_2) (114).

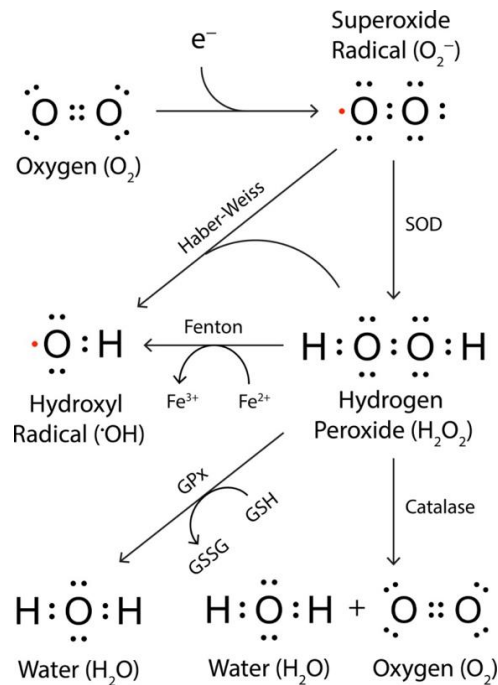


Figure 7. Reactive Oxygen Species (ROS) and Antioxidant Defense Mechanisms. *Starting with molecular oxygen (O_2), an electron transfer leads to the formation of the superoxide radical (O_2^-). Superoxide dismutases (SOD) then convert superoxide radicals into hydrogen peroxide (H_2O_2), which can further participate in the Fenton reaction to produce hydroxyl radicals ($\cdot OH$). This sequence also includes the Haber-Weiss reaction linking superoxide radicals and hydroxyl radicals. The diagram shows that hydrogen peroxide is detoxified into water and oxygen through the action of catalase and glutathione peroxidase (GPx), which utilizes glutathione (GSH) and converts it to its oxidized form (GSSG), further emphasizing the crucial role of antioxidant defenses in maintaining cellular redox balance. Image source: (127)*

It seems that nature evolutionary selected for ROS as a signal transduction mechanism to allow for adaptation to environmental changes, for example nutrients availability or defense against pathogens. The term redox signaling implies reversible modifications, such as oxidation or formation covalent adducts which then results in conformational or activity changes of target proteins, thus resulting in the change in signal transduction (128). Specific cysteine residues within proteins show the highest susceptibility to oxidation, and this susceptibility and specificity depend both on kinetics and proximity to ROS molecules. These modifications include formation of disulphide bridges and generation of sulphenic, sulphinic, and sulphonic acids. (129). Moreover, important oxidative post-translational modifications are S-glutathionylation, S-nitrosylation and the incorporation of fatty acids and advanced glycation products to amino acid side chains. They affect the activity of enzymes related to the ROS and cellular metabolism, regulate the activity of proteins that have the active cysteine residue, regulate the oxidoreductive pathway of signal transduction, and participate in the regeneration of antioxidant enzymes (130). Irreversible modifications, such as carbonylation of proteins, can also occur as a mark for proteolysis to counteract large aggregates formation and inactive proteins accumulation. Products of proteolysis of carbonylated proteins can function as secondary ROS messengers that target the cell nucleus (131).

It was shown that ROS have impact on several signaling pathways and proteins involved in cell-signaling such as ion channels, kinases, phosphatases, transcription factors and Ubiquitination/Proteasome System (132). For example, a link between dephosphorylation and protein cysteine reduction/oxidation occurs through the redox sensitivity of critical cysteine residues in protein phosphatases. ROS can regulate diverse kinase signaling pathways via different mechanisms. One such mechanism involves oxidizing kinase interacting modulators, such as thioredoxin or glutathione-S-transferases, which then alters their activity (133,134). Another mechanism involves the inhibition of counteracting phosphatases, such as PTEN, by oxidizing cysteine residue in the active site (135–137). Important ROS-influenced signaling pathways include the Activator Protein-1 (AP-1), Nuclear Factor-kappa B (NF-κB), p53, Keap1-Nrf2-ARE, and Mitogen-Activated Protein Kinase (MAPK) pathways (116). These pathways are involved in regulating gene expression, cell growth, apoptosis, and stress responses. Hence, this consequential interplay between ROS, other messenger molecules and metabolism safeguards tight regulation of redox signaling, thus controlling cellular functions such as proliferation, differentiation, apoptosis, response to stimuli and others.

ROS are normally generated and removed as part of metabolic reactions, but external factors, such as addictive drugs, can lead to significant increase in ROS. Neurotoxic consequences of increased ROS levels after administrations of psychostimulants have been extensively studied (138,139). However, a single administration of a psychoactive drug is sufficient to disturb the redox balance, a cellular event that has been mostly neglected, considering that it can lead to modulation of intracellular signaling pathways that are susceptible to ROS molecules, such as H₂O₂ (104). Function of enzymes and other proteins that contain cysteine residue can be altered as H₂O₂ or other ROS molecules oxidize or modify susceptible cysteines (140). In this way a change in the redox metabolism modulates function of proteins and signaling pathways during normal functioning. However, when the endogenous antioxidative system is insufficient to maintain balanced redox regulation

accumulation of ROS molecules can lead protein modification that have a long-term effect on protein function including the change in transcriptional activity (140).

1.2.2 Influence of ROS on neuroplasticity

ROS, highly reactive molecules which can play both harmful and beneficial roles in the brain, can also influence various aspects of neuronal plasticity, including synaptic plasticity, neurogenesis, dendritic arborization, myelination and neuronal survival (141).

Studies done in rodents that investigated effects of psychostimulants on brain functioning has implicated ROS as a modulator of neuronal plasticity (103,104,106). For example, proteomic studies showed changes in the expression of proteins related to both neuroplasticity and redox homeostasis (103,106). These studies focused on changes in protein expression in mice that show behavioral sensitization, which is considered a form of neuroplasticity because it involves long-term changes in the brain's response to stimuli, often associated with alterations in synaptic strength and connectivity (57,58). The role of ROS in this process highlights their importance in modulating the underlying mechanisms of synaptic plasticity that contribute to behavioral changes. Additionally, the alteration in redox-sensitive proteins underscores the role of oxidative stress in modulating synaptic function and potentially in the pathology of neuropsychiatric disorders.

The precise role of ROS in addiction-related processes such as behavioral sensitization is still under investigation, but it is well known that ROS act as important signaling molecules that modulates LTP and LTD in general (79,82,142). ROS can activate various signaling pathways, including protein kinase C (PKC), MAPK), and cyclic AMP (cAMP) signaling pathways, which can in turn modulate the activity of transcription factors and gene expression related to neuronal growth and plasticity (114,128,143,144).

Studies have revealed that ROS also play a crucial role as regulators and modulators of signaling pathways and gene expression, many of which are essential for brain plasticity.

Early *in vivo* research provided direct evidence that ROS regulate synaptic terminal growth under pathological conditions. For instance, in a *Drosophila* model of the lysosomal storage disease, oxidative stress activated the JNK cascade and the immediate early genes c-Jun and c-Fos (AP-1), leading to changes in the growth of neuromuscular junction terminals (145). This, along with prior research by Sanyal and colleagues (146), identified AP-1 as a key adaptive response to ROS in neurons. The JNK/AP-1 signaling pathway is well-known for its role in various neuronal functions, mediating both synaptic and oxidative stress responses (147).

ROS can also act as second messengers to modulate the activity of various ion channels and receptors, including NMDA receptors and AMPA receptors, which are critical for synaptic plasticity. For example, ROS can increase NMDA receptor activity by promoting the phosphorylation of the NR1 subunit, which can lead to an increase in LTP (148). One study found that ROS scavengers increased NMDA receptor whole-cell currents by 100% (149). Another study found that the NMDA-induced increase in ROS was mediated by NADPH oxidase through NO, cGMP and PKG (150). ROS can affect neurogenesis by modulating the activity of signaling pathways involved in cell proliferation and differentiation (151). At low concentrations, ROS can promote neurogenesis by activating certain signaling pathways, such as Nrf2/ARE pathway (152,153). However, at high concentrations, ROS can cause oxidative damage to DNA, impairing cell proliferation and differentiation.

Neurons employ various adaptive plasticity mechanisms, including utilizing the plasticity of dendritic arbors, and ROS can affect dendritic arborization (154). In *Drosophila* embryo and larva, motor neurons use dendritic arbors as homeostatic devices, with their growth and connectivity adapting to changes in synaptic input. This is particularly evident as dendritic arbors are exclusively postsynaptic. It was discovered that ROS serve as new plasticity signals that play a key role in this form of dendritic adjustment (154). In *Drosophila* larvae, overactivation of motoneurons led to increased mitochondrial ROS levels at presynaptic neuromuscular junctions, resulting in altered synaptic terminal growth and the formation of

smaller synaptic varicosities (155). Additionally, postsynaptic dendrites undergo structural adjustments in response to activity-generated ROS, which results in smaller dendritic arbors and reduced synaptic input sites (156). Neuronal ROS exert their effects through DJ-1 β , a redox-sensitive protein. When DJ-1 β is oxidized it enhances its inhibitory interactions with the phosphatase PTEN, subsequently activating PI3K signaling, which regulates synaptic terminal growth (157,158). ROS are essential for activity-regulated structural plasticity of synaptic terminals. Inhibiting neuronal ROS signaling disrupts the homeostatic adjustments of the locomotor network, leading to abnormal motor function (155).

The process of myelination facilitates the rapid and efficient transmission of electrical impulses between adjacent nerve cells, while also preserving the strength of the impulse signal as it traverses the axon (159). ROS can affect myelination by modulating the activity of signaling pathways involved in oligodendrocyte differentiation and myelin formation (160). At low concentrations, ROS can promote myelination (161). However, at high concentrations, ROS can cause oxidative damage to lipids, impairing these processes (162).

The effects of ROS on neuronal plasticity are complex and depend on the concentration and duration of exposure to ROS (155). Moderate levels of ROS are important for normal neuronal function and plasticity, whereas excessive levels can impair neuroplasticity and contribute to neurodegeneration. Maintaining a balance between oxidant and antioxidant signaling pathways is important for promoting healthy neuronal plasticity. The specific signaling pathways activated by ROS depend on the type and location of neurons being studied, as well as the specific stage of neuronal development or plasticity (155).

The connection between ROS and addiction, particularly through the lens of behavioral sensitization, shows up the necessity to delve deeper into the underlying mechanisms. Future research could focus on identifying which specific ROS are most important in signaling pathways related to addiction. Understanding the interactions between ROS and neuroplasticity could reveal how ROS modulates synaptic strength and connectivity in response to addictive substances. Investigations could also explore which genes and

molecular mechanisms are influenced by ROS during neuroplastic changes associated with addiction. Additionally, it would be valuable to study the role of second messengers, such as H_2O_2 in ROS-mediated signaling pathways, their sources and interactions with antioxidative system and redox sensitive proteins, and how these interactions influence the expression of genes related to neuronal growth and plasticity.

1.2.3 Role and regulation of hydrogen peroxide in neuronal plasticity

Hydrogen peroxide (H_2O_2), a type of ROS, acts as a secondary messenger and participates in signal transduction pathways, influencing synaptic function and plasticity (163). H_2O_2 is most often produced by enzymes such as NOX and can also be generated through mitochondrial respiration. Sophisticated fine-tuning of H_2O_2 levels in the cell is carried out by a range of antioxidant enzymes, such as peroxiredoxins, glutathione peroxidases, and catalase, and their associated backup systems (164,165).

Peroxiredoxins are a family of antioxidant enzymes that can rapidly reduce H_2O_2 to water using a cysteine residue in their active site, and in the process, they become oxidized (166,167). The oxidized peroxiredoxin is then reduced by another enzyme called thioredoxin, which is in turn reduced by a reductase enzyme. Glutathione peroxidases use glutathione as a cofactor to reduce H_2O_2 to water, and in the process, they oxidize glutathione (165). The oxidized glutathione is then reduced by glutathione reductase, which uses NADPH as a cofactor. Catalase is an antioxidant enzyme that is found in peroxisomes and is responsible for converting H_2O_2 to H_2O and O_2 . It can rapidly degrade high concentrations of H_2O_2 , and this is especially important in tissues with high metabolic activity. Overall, the regulation of H_2O_2 in the cell is a complex process that involves the activity of multiple antioxidant enzymes and backup systems. This fine control of H_2O_2 is important for maintaining cellular homeostasis and preventing oxidative damage to cells and tissues.

In neurons, H_2O_2 can modulate synaptic strength and LTP via various mechanisms. H_2O_2 can directly affect the activity of ion channels such as NMDA and AMPA receptors, influence the

phosphorylation state of proteins involved in LTP, such as ERK and CaMKII and regulate gene expression and alter the synthesis of proteins that contribute to synaptic plasticity (168,169).

However, the effects of H₂O₂ on neuronal plasticity are complex and context dependent. The neurotoxic or beneficial effects of H₂O₂ depend on the concentration and duration of exposure, as well as the neuronal type and brain region. In general, low concentrations of H₂O₂ can act as a signaling molecule and promote neuronal plasticity, whereas high concentrations can lead to oxidative stress and neurotoxicity (170). Studies have reported that concentrations of H₂O₂ in the range of 10-100 μM can promote synaptic plasticity and enhance memory formation in the hippocampus and prefrontal cortex (170). However, higher concentrations of H₂O₂ (above 100 μM) have been shown to cause neuronal damage and apoptosis in various regions of the brain, including the hippocampus, cortex, and striatum (170). The precise concentration and duration of H₂O₂ exposure necessary for its beneficial or neurotoxic effects may differ depending on the specific experimental conditions and brain region being studied. Understanding the role of H₂O₂ in neuronal plasticity may have implications for the development of treatments for neurological disorders that involve alterations in synaptic plasticity.

1.2.4 Sources of ROS in the brain during substance abuse

Energetically demanding consequences of psychostimulants administration affect redox signaling and result in increased production of ROS. Increased monoaminergic signaling is a consequence of the direct action of psychostimulants on cellular and vesicular transporters on the presynaptic neuron (171). These primary effects result in the increased extracellular concentration, cause significant dysfunction in synthesis, catabolism and recycling of monoamines and increase the neuronal excitability of postsynaptic neurons, and together contribute to the increase of ROS (172). Additional sources of ROS are mitochondrial

electron transport chain (ETC) leakage due to high metabolic demand and NADPH oxidases (Figure 8).

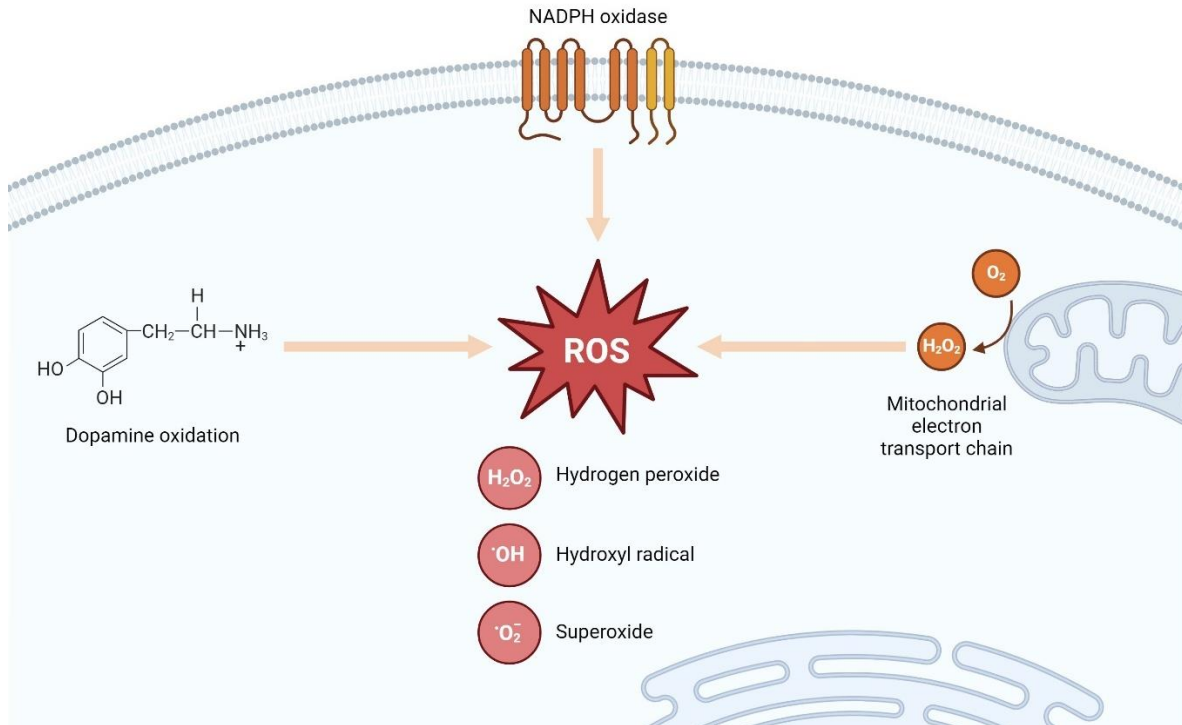


Figure 8. Main sources of ROS in the neurons upon psychostimulant abuse. Dopamine oxidation directly leads to the production of ROS, which includes hydrogen peroxide (H₂O₂), hydroxyl radicals (·OH), and superoxide (O₂^{·-}). The figure also details the role of NADPH oxidase on the cell membrane and the mitochondrial electron transport chain as significant contributors to the cellular ROS pool. Created with BioRender.com

1.2.4.1 Catabolism of dopamine as a source of ROS

Addictive potential of different abused substances and behaviors is mediated by rewarding potential that DA signaling has within the brain reward circuit by potentiating neural connections that result in the acquisition of harmful behaviors that characterize addiction (20,22). After the administration of psychostimulants released DA contributes to the

increase in ROS in two ways: by causing an increase in neuronal excitability and through the degradation of the excess DA (21,173,174). ROS produced from these two sources modulates signaling pathways that regulate gene transcription, chromatin structure, DNA and histone modifications that change the long-term activity and responsiveness of a neuron (126,144). For example, ROS can influence the activity of histone-modifying enzymes such as histone acetyltransferases (HATs) and histone deacetylases (HDACs) (175). Oxidative stress can inhibit HDACs, leading to increased histone acetylation and a more open chromatin structure, facilitating gene transcription.

To regulate the energetically demanding neuronal excitability and to remove the excess DA, the nervous system has developed mechanisms by which to control the excessive amounts of DA that accumulates in the extracellular and intracellular space. However, this comes with the cost of increased ROS production. DA degradation occurs through enzymatic and non-enzymatic process that leads to oxidative stress (Figure 9). Monoamine oxidase A (MAO_A) present on the outer side of the mitochondrial membrane deaminates DA to H₂O₂ and reactive 3,4-dihydroxyphenylacetaldehyde (DOPAL). The predominant pathway is further oxidation of DOPAL to the carboxylic acid 3,4-dihydroxyphenylacetic acid (DOPAC) by alcohol dehydrogenase (ADH) or aldehyde dehydrogenase (ALDH). 3-O-methylation of DOPAC by catechol-O-methyltransferase COMT leads to homovanilic acid (HVA), one of the main degradation products of DA (174).

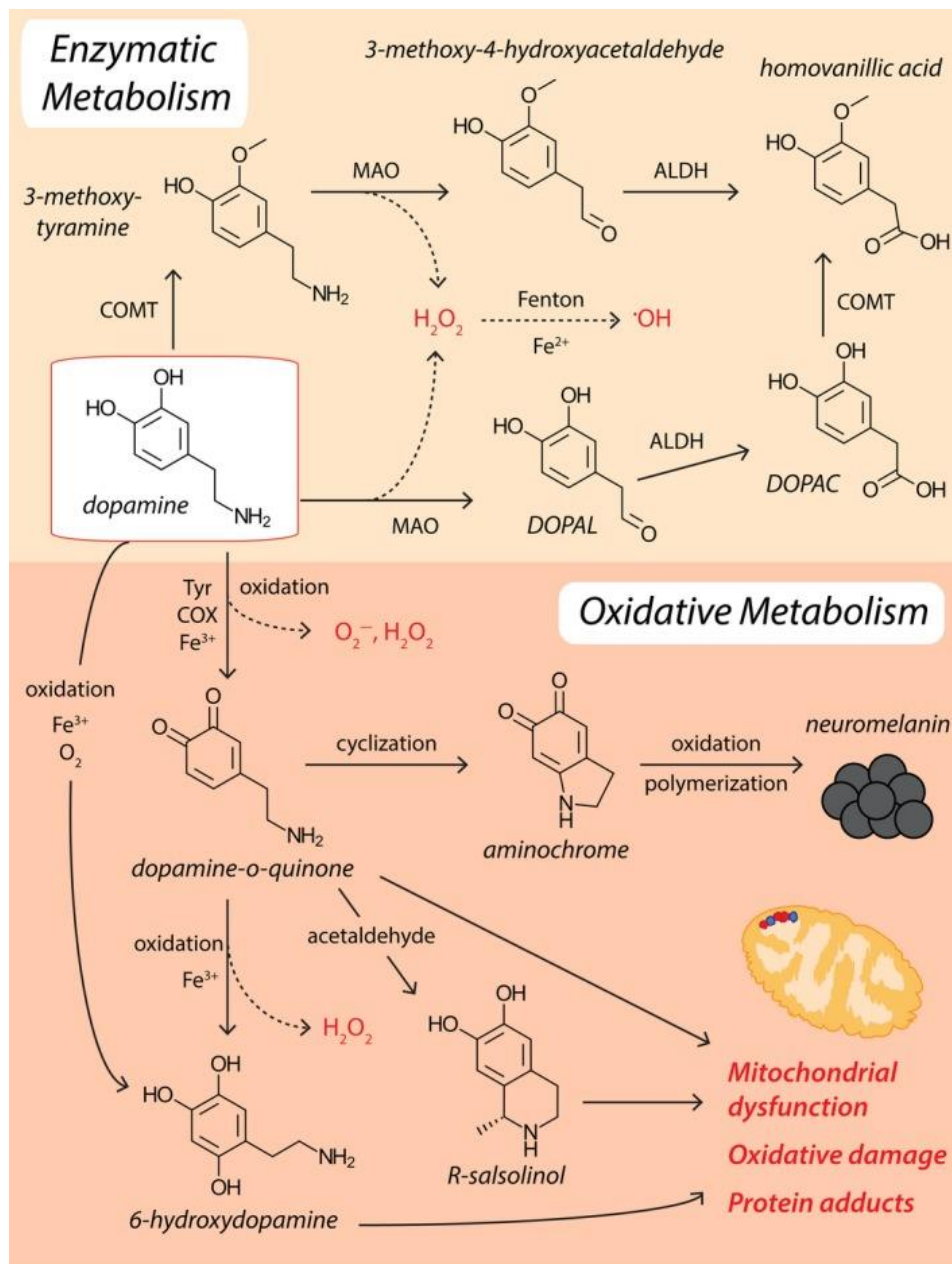


Figure 9. Neuronal DA metabolism and ROS production. Monoamine oxidase (MAO), catechol-*o*-methyl transferase (COMT), and aldehyde dehydrogenase (ALDH) facilitate the conversion of dopamine to homovanillic acid. Conversely, dopamine can be oxidized to dopamine-*o*-quinone by tyrosinase (Tyr), cyclooxygenase (COX), or labile ferric iron (Fe^{3+}). These dopamine-*o*-quinones act as reactive intermediates, leading to the formation of more harmful compounds like 6-hydroxydopamine and R-Salsolinol. The endogenous

detoxification process involves the cyclization of dopamine-o-quinones to produce aminochrome, followed by oxidation and polymerization to form neuromelanin. Hydrogen peroxide (H₂O₂), originating from MAO activity, dopamine oxidation, and dopamine-o-quinone formation, participates in Fenton chemistry, reacting with labile ferrous iron (Fe²⁺) to generate detrimental hydroxyl radicals (·OH). Image source: (127)

Another significant source of oxygen radical is the DA auto-oxidation that can also occur extracellularly (176,177). DA and DOPA are prone to spontaneous auto-oxidation at their electron-rich catechol moiety yielding the highly reactive electron-poor ortho-quinones, DOPA-quinone and DA-quinone and H₂O₂ (178). Quinone can via Haber-Weiss/Fenton reaction create a highly toxic ·OH. Quinones can undergo an intramolecular cyclization and formation of insoluble neuromelanin or can participate in a cascade of oxidative reactions as redox intermediates or react nonspecifically with many cellular components and can lead to mitochondrial damage (179,180). LaVoie and Hastings' study provides evidence linking the formation of DA quinones to METH-induced striatal neurotoxicity, suggesting a role for these quinones in protein modification and oxidative stress within the striatum, thus expanding our understanding beyond the conventional role of extracellular DA in METH-induced toxicity (181).

1.2.4.2 Electron transport chain and the production of ROS

Mitochondria are a significant source of physiological ROS, which form as obligate byproducts of respiratory ATP synthesis by 'leakage' of the electron transport chain (ETC), where premature electron transfer at complexes I and III leads to the natural generation of superoxide radicals (O₂⁻) (182–184) (Figure 10). These radicals can trigger the formation of highly reactive hydroxyl radicals (·OH), which are known to cause primary neuronal oxidative damage (185). In response, mitochondria are equipped with superoxide dismutases (SOD1

and SOD2) that convert O_2^- into the less damaging H_2O_2 , a reaction that is crucial for mitigating oxidative stress within the mitochondrial matrix and intermembrane spaces (186,187).

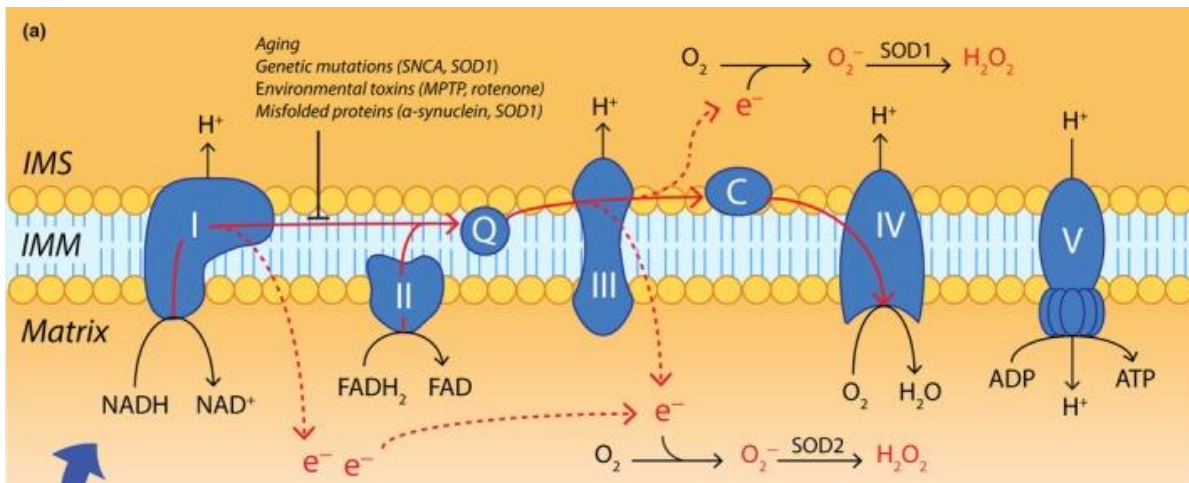


Figure 10. Reactive oxygen species are an inherent by-product of oxidative phosphorylation in the mitochondrial ETC. *Electrons generated by the tricarboxylic acid cycle in the mitochondrial matrix are shuttled to ETC complexes I and II by NADPH and FADH₂, respectively. They are then transferred to complex IV of the ETC with the help of inner mitochondrial membrane (IMM) electron shuttles (Q, coenzyme Q; C, cytochrome c) where they reduce molecular oxygen to water, a process which simultaneously drives ATP production by ATP synthase (ETC complex V). A small amount of premature electron leakage occurs naturally during oxidative phosphorylation, whereby electrons bound within ETC complexes I and III diffuse into both the mitochondrial matrix and intermembrane space (IMS). Here, they may cause incomplete reduction of molecular oxygen (O₂), generating superoxide radicals (O₂⁻) that may subsequently be converted to hydrogen peroxide (H₂O₂) through the action of superoxide dismutase 1 or 2 (SOD1/2). Image source: (127)*

In the context of addiction, this mitochondrial function becomes critically relevant. The enhanced ROS production seen with psychostimulant use can disrupt the redox balance and

lead to oxidative stress, neuronal damage and changes in signalization that may exacerbate addictive behaviors and neurodegeneration (188). Also, an increase in ROS due to DA oxidation affects the functionality of electron transport chain in mitochondria, causes proton leakage and leads to further ROS production (189). Due to the increase in dopaminergic signaling and neuronal stimulation activity of MAO is higher (190) resulting in greater metabolic demands, higher metabolic rates, and elevated ROS production. Oxidative deamination of DA by MAO produces H₂O₂ and hydroxyl radical that can disrupt mitochondrial respiration (191).

1.2.4.3 NOX as ROS producers

Studies show that psychostimulants can activate NADPH oxidases (NOX) and generate ROS in various regions of the brain, which can contribute to neurotoxicity, affect neuroplasticity, and contribute to the development of addiction (120,192–195). Membrane-bound NOX transfers electrons from NADPH to molecular oxygen through the conversion of NADPH to NADP⁺, leading to the production of superoxide anion radical (O₂⁻). Evidence suggests that NOX enzymes are involved in generating ROS in response to psychostimulant exposure (196). This response is initiated by DA release, which activates NOX, resulting in the production of superoxide (O₂⁻). DA influences NOX activity through its receptors, notably the D5 receptor, which has been found to specifically modulate NOX activity and alter ROS production in murine models (197). Several studies have also suggested that NOX-derived ROS play a key role in reward, motivation, and synaptic plasticity. METH, at levels relevant to human abuse, can activate a NOX complex, leading to the activation of ERK1/2 signaling and phosphorylation of Cav-1 at Tyr14 (198). There is also an important contribution of brain oxidative stress derived from NOX2 in cocaine-induced brain dysfunctions and neurotoxicity (196). Blocking NOX activity reduces the generation of ROS and attenuates the behavioral effects of amphetamine (199). O₂⁻ produced by NOX can be converted to H₂O₂ by

extracellular SOD3 and transported to the cytoplasm through aquaporins, where it contributes to intracellular redox signaling (200).

Understanding both the sources of ROS and their specific actions within the brain is crucial for developing effective strategies to modulate ROS levels and mitigate their harmful effects. The detailed examination of ROS origins, such as DA catabolism, mitochondrial electron transport chain leakage, and NADPH oxidase activity, provides insights into how psychostimulants elevate ROS production. Concurrently, elucidating the mechanisms by which ROS influence neuroplasticity, including their impact on signaling pathways, ion channels, and gene expression, highlights the potential for targeted interventions.

1.3 Role of Redox in Addiction

In the brain, particularly within the domain of addiction, ROS molecules can induce significant changes at both the cellular and behavioral levels. This section explores how ROS generated after psychostimulant use modifies neuronal pathways, potentially contributing to addictive behaviors. The focus on cellular and molecular impacts provides a foundation for better understanding of the effect that addictive substances have on the brain function and highlights potential targets for therapeutic intervention.

1.3.1 Effects of ROS on cellular function, signaling pathways, and metabolism in psychostimulant addiction

ROS play a crucial role in modulating cellular function, signaling pathways, and metabolism. Although there are limited studies that directly link ROS to neuroplasticity in psychostimulant addiction are very limited, the observed effects of ROS can be inferred from electrophysiological and genetic studies of neuronal plasticity, a basis of addiction-related behavior. This chapter provides a comprehensive review of how ROS impact these processes, drawing on studies conducted in humans, rodents, and flies.

The administration of psychostimulants results in the production of ROS, which subsequently affects synaptic plasticity and neuronal function through multiple mechanisms. Firstly, ROS can directly alter proteins involved in synaptic plasticity, such as NMDA and AMPA receptors. These modifications can affect receptor function and trafficking, leading to changes in synaptic strength and plasticity (201–203). Specifically, METH and amphetamine have been shown to increase NMDA receptor levels, and NMDAR activation further elevates ROS production (150,204) Secondly, ROS influence various signaling pathways that regulate gene expression and protein synthesis, resulting in long-term alterations in neuronal function and synaptic plasticity (114). Thirdly, ROS can inflict

oxidative damage on cellular components including DNA, lipids, and proteins, contributing to neurodegeneration and cognitive impairment (203). In addition to directly damaging cellular components, ROS production can activate inflammatory signaling pathways and promote the release of pro-inflammatory cytokines, such as interleukin-1 β (IL-1 β) and tumor necrosis factor-alpha (TNF α). These cytokines exacerbate neuroinflammation and neuronal damage (205). Furthermore, ROS produced by psychostimulants can lead to the formation of protein adducts, such as carbonyl and nitrotyrosine residues, which can alter protein structure and function (117,206,207). This can disrupt key signaling pathways involved in synaptic plasticity and neuronal function, such as the extracellular signal-regulated kinase (ERK) and cyclic AMP response element-binding protein (CREB) pathways, which can affect learning and memory (68,208).

Overall, ROS produced by psychostimulant administration negatively impacts synaptic plasticity and neuronal function by disrupting neurotransmission balance, altering receptor expression and function, causing oxidative damage and inflammation, and interfering with critical signaling pathways. These effects contribute to the development of addiction as well as the cognitive and behavioral impairments associated with chronic psychostimulant use. ROS interference with signaling pathways in the earlier stages of addiction may also affect neuroplasticity in a way of reinforcing addictive behaviors before the neurotoxic detrimental effects overtake.

ROS are known to activate receptor tyrosine kinases (RTKs) through the oxidation of cysteine residues, leading to downstream signaling cascades involving Ras, Raf, MEK, and ERK, which ultimately regulate gene expression for cell proliferation and differentiation (114). METH and amphetamine activate the MAPK/ERK signaling pathway, which can lead to increased CREB phosphorylation and activation of transcription factors involved in synaptic plasticity and reward learning (69,209). METH inhibits the AKT/mTOR signaling pathway, which is involved in protein synthesis and cellular growth, leading to decreased synaptic plasticity and neuronal survival (210) and activates the JNK signaling pathway, which can lead to

increased c-Jun phosphorylation and activation of transcription factors involved in cell death and inflammation (211). One study suggests that METH induces neuroinflammation via activation of TLR4 in microglia, leading to an increase in proinflammatory cytokines and elevation of DA in the NAc, and inhibition of TLR4 signaling attenuated the rewarding effects of METH. (212). In the NF- κ B pathway, ROS activate the I κ B kinase complex, leading to the phosphorylation and degradation of I κ B, thereby freeing NF- κ B to translocate to the nucleus and promote the transcription of genes involved in inflammation and cell survival. The study by Lepsch et al. showed that cocaine induced cell death and activated NF- κ B in PC12 cells, partially due to the activation of D1 receptors (213). In the PI3K/Akt pathway, ROS activate RTKs and PI3K, resulting in the production of phosphatidylinositol (3,4,5)-trisphosphate (PIP3) and the recruitment and activation of Akt, which phosphorylates various substrates to support cell survival, growth, and metabolism. Akt and its downstream kinase, GSK3, play a crucial role in dopaminergic neurotransmission and are known to be involved in regulating behaviors induced by psychostimulants. Miller et al. demonstrated the activation of GSK3 signaling pathway by cocaine in mice (214).

Psychostimulant-induced ROS can activate or inhibit various signaling pathways involved in addiction-related neuroplasticity, such as the DA, MAPK/ERK, AKT/mTOR, NF- κ B, and PI3K/Akt pathways. The specific effects of ROS on these pathways can vary depending on the type and duration of the psychostimulant exposure, as well as the cellular context in which they are induced (144).

ROS significantly affect metabolic processes, especially in the context of psychostimulant addiction. Both METH and cocaine alter cellular metabolism through oxidative stress, leading to energy deficits and metabolic dysregulation (215,216). In human studies, METH impairs glucose metabolism in the brain, exacerbating oxidative stress and neuronal injury(217). Cocaine disrupts mitochondrial function, decreasing ATP production and increasing oxidative damage (218) Rodent models reveal that METH-induced oxidative stress disrupts mitochondrial dynamics, impairing oxidative phosphorylation and ATP

synthesis (219). Cocaine similarly affects metabolic enzymes, leading to an imbalance in energy homeostasis and increased ROS production (220) In *Drosophila*, METH exposure results in metabolic reprogramming characterized by increased glycolysis and impaired oxidative phosphorylation, contributing to ROS generation and neuronal damage (118).

The role of ROS in psychostimulant addiction is complex, influencing cellular function, signaling pathways, and metabolism. Studies across various models, including humans, rodents, and flies, consistently demonstrate that METH and cocaine induce significant oxidative stress, leading to neuronal damage and dysfunction. These findings emphasize the detrimental consequences of ROS on neurodegeneration and psychosis associated with addiction. Recent studies that focused on behavioral effects of ROS modulation in addiction suggest that targeting ROS production may have beneficial effects, potentially preventing the neural plasticity mechanisms underlying addictive behaviors. Understanding these mechanisms provides valuable insights into the pathophysiology of addiction and highlights potential therapeutic targets for mitigating oxidative stress-related damage in individuals with psychostimulant use disorders.

1.3.2 Behavioral effects of ROS in psychostimulant addiction

The interplay between ROS and behaviors induced by addictive substances can be studied combining the results of different approaches. One is to correlate the changes in ROS production after drug administration with behavioral consequences, while the other is to interfere with ROS production using antioxidant treatment and follow the behavioral effects.

There is evidence that ROS generated by psychostimulants can lead to behavioral changes, including increased drug-seeking behavior, impaired cognitive function, motor deficits, changes in social behavior (221,222). In addition, ROS relates to the hallmark addiction phenotypes, such as locomotor sensitization and self-administration, which can be studied in model animals (49).

One of the major effects of ROS is the increase in expression of the transcription factor, FosB, which plays a critical role in addiction development, related to drug-seeking behavior (223). The AP1 transcription factor Δ FosB, a splice variant of FosB, accumulates in the brain due to chronic insults like drug abuse and Alzheimer's disease, mediating long-term neuroadaptations by forming heterodimers with other AP-1 factors such as JUND, regulated by a cysteine-based redox switch. This study reveals the structural basis of the redox switch by determining the crystal structure of the Δ FosB /JUND bZIP domains and identifies thiol-reactive compounds that target this switch, validated biochemically and in cell assays. It demonstrates that Δ FOSB and related AP1 transcription factors can be selectively targeted by ROS to modulate their function, despite being previously considered undruggable (224).

In addition, generation of ROS by psychostimulants can be correlated with cognitive impairments, including deficits in attention, working memory, and executive function (54,225,226). One study investigated the cognitive and biochemical effects of repeated crack cocaine inhalation on male adult Wistar rats (227). The results showed that rats exposed to crack cocaine exhibited impaired spatial working memory and increased errors in a delayed task performance compared to a sham group. Biochemically, crack cocaine inhalation led to decreased lipid peroxidation in the hippocampus and increased levels of advanced oxidation protein products (AOPP) and SOD activity in the striatum, indicating oxidative stress (227). Studies also suggest that psychostimulants can induce motor deficits such as impairments in coordination and balance and alter social behavior in animals, leading to decreased sociability and increased aggression (51). Although the role of psychostimulant-induced ROS is not yet clear, similar mechanisms that are activated after drug administrations, such as dysregulation of the dopaminergic system and intensified ROS production, have been connected to aggressive behavior in rodents (228).

Psychostimulant-induced ROS production can lead to behavioral changes such as LS and SA. LS is a phenomenon where repeated exposures to psychostimulants lead to an enhanced locomotor response to subsequent drug exposure. Studies have shown that ROS plays a

crucial role in the development of LS to psychostimulants (229,230). *Drosophila melanogaster* was used to explore the role of ROS in cocaine-induced behavioral changes, specifically focusing on LS (229). Results demonstrated that cocaine exposure significantly increases ROS levels and activates antioxidant defenses, particularly catalase and H₂O₂, in dopaminergic and serotonergic neurons. Notably, feeding flies the antioxidant quercetin abolished LS, highlighting the critical roles of DA and H₂O₂ in cocaine-induced neuronal plasticity. These findings suggest that dietary interventions targeting redox balance could be a promising strategy for managing addiction. SA is a measure of the reinforcing properties of a drug, and psychostimulants have been shown to increase ROS levels in the brain regions involved in reward, which may contribute to the development of drug-seeking behavior (231). Furthermore, it has been shown that NADPH oxidase, one of the primary sources of ROS in the brain, plays a role in psychostimulant-induced behavioral changes. Inhibition of NADPH oxidase by apocynin has been shown to reduce motor-activating effects of METH in animal models (199).

1.3.3 Effects of ROS modulation on psychostimulant-induced behavior

Given the role of ROS in psychostimulant-induced behavioral changes, studies have been conducted to examine the effects of ROS modulation on psychostimulant-induced behavior. Studies have mainly been performed on rodents, aiming to better understand the link between oxidative status in the brain and psychostimulant-induced behavior. These studies have shown that compounds with antioxidative properties, for instance 4-hydroxy-2,2,6,6-tetramethylpiperidine-1-oxyl (Tempol), N-tert-butyl- α -phenylnitron (PBN), N-acetylcysteine (NAC), melatonin, resveratrol and quercetin can modulate response to psychostimulants and change the drug-related behavioral phenotypes such as self-administration, conditioned place preference and locomotor sensitization.

Initial studies analyzed the ability of Tempol, the superoxide-selective antioxidant, to attenuate cocaine-induced oxidative damage and behavioral response. Acute cocaine

treatment significantly increased oxidative stress in prefrontal cortex and nucleus accumbens in rats and decreased total antioxidant capacity. Tempol prevented the elevation of oxidative stress markers in these areas and attenuated both the development and expression of locomotor sensitization normally induced by cocaine (232). Additionally, Tempol prevented the elevation of oxidative stress markers in rats which showed sensitization to cocaine (232).

Beiser et al. also reported that pretreatment with Tempol reduced the development and expression of cocaine-induced psychomotor sensitization in rats and reduced cocaine-induced oxidative stress, (233). Two studies from Jang et al. as well showed the effectiveness of Tempol in both cocaine and methamphetamine related phenotypes. (234,235) They have shown that enhancement of ROS production in the neurons of NAc contributes to the reinforcing effect of cocaine by monitoring metabolic neural activity by temperature and oxidative stress. (234) Pre- or post-treatment with Tempol or PBN (another ROS scavenger which is less specific) at the systemic level significantly decreased both cocaine (234) and methamphetamine (235) self-administration, without affecting food intake and attenuated METH-induced locomotor activity without affecting generalized behavior in METH-naïve rats. Cocaine self-administration was also inhibited by infusion of Tempol into the NAc. Increased oxidative stress was found mainly in neurons, but not in other cell types in NAc of rats self-administering cocaine or METH. Tempol also significantly attenuated DA release induced by cocaine. Similar results were obtained in a study with amphetamine (236). Tempol pretreatment attenuates the induction of locomotion and oxidative stress generated in Nac by acute amphetamine administration. Tempol also attenuates the increase of DA induced by amphetamine in Nac (236).

The impact of polyphenol resveratrol on stimulant neuropsychopharmacology was also studied in rodents (237). Although an acute resveratrol treatment was not effective, repeated seven-day treatment decreased METH-induced hyperactivity in mice, but did not

affect cocaine-induced hyperactivity. These data suggest that resveratrol tends to minimize the effects of METH to increase locomotor activity and evoke DA release.

N-acetyl cysteine (NAC) is one of the most extensively used antioxidants in clinical, animal and cell culture studies. It is believed that antioxidative activity of NAC stems from the ability to act as cysteine source for increased biosynthesis of glutathione (GSH). (238) There have been several studies in animals and humans reporting beneficial role of NAC in context of psychostimulant addiction. A study in mice reports that NAC attenuates sensitization-induced locomotor enhancement (239). NAC also prevents increased amphetamine sensitivity in social isolation-reared mice (240). Studies in cocaine-dependent patients show that NAC can normalize elevated glutamate levels. (241) These studies could be valuable as abnormal glutamate levels are related to relapse, and treatment with NAC prevented relapse in animal studies (242,243). NAC has also been found to reduce craving for methamphetamine in human trials (244).

Melatonin is a hormone involved in broad spectra of cellular processes, amongst it can act as a free radical scavenger and has antioxidative properties (245). It is also involved in the regulation of circadian rhythms, which are disrupted in drug users. Furthermore, it has been demonstrated that melatonin can modulate the reinforcing effects of several addictive drugs and may therefore play a role in substance use disorder. (246) For example, melatonin reduces motivation for cocaine self-administration and prevents relapse-like behavior in rats (246). It is also reported that melatonin administration decreased cocaine-induced locomotor activity in naïve and pinealectomized rats at different times of day (247). Melatonin is efficient in reducing oxidative stress, either via direct detoxification of ROS or indirectly by stimulating antioxidant enzymes while suppressing pro-oxidant enzymes (248).

It is known for some time that flavonoid quercetin demonstrates antioxidative properties, but recently it was found that it can mitigate aberrant mitochondrial morphology and mitochondrial dysfunction (249). Chen et al. showed the ability of quercetin to alleviate METH-induced anxiety-like behavior and improve neuron number and mitochondria

dysregulation by decreasing the levels of ROS and increasing the oxygen consumption rate and ATP production.

All these results imply that change of the redox balance in the brain reward system by psychostimulants is accompanied with behavioral changes and that enhancement of ROS in the brain contributes to the reinforcing effect of psychostimulants. It can be concluded that redox balance can be modulated by treatment with compounds which interfere with ROS production. Results of all these behavioral studies indicate that studying the relationship between ROS regulation and behaviors induced by addictive drugs is necessary for better understanding of the mechanistic background of psychostimulant addiction and for the development of better treatment strategies.

1.4 Addiction Research in *Drosophila melanogaster*

1.4.1 *Drosophila* as a model organism

Drosophila melanogaster is an excellent model for studying addiction for several reasons (250). Firstly, flies share many genetic and molecular pathways with mammals, including those involved in neurotransmitter systems like DA and serotonin. The conservation of these pathways means that findings in flies can often be translated to understand mechanisms in more complex organisms, including humans. For example, genes involved in DA synthesis, release, and reception are conserved, allowing researchers to study the fundamental aspects of addiction biology in a simpler system. Secondly, flies are cost-effective and efficient. They are inexpensive to maintain and have a short generation time, allowing for rapid experimentation. A complete life cycle from egg to adult takes about two weeks, facilitating quick genetic studies and the ability to observe the effects of genetic modifications over multiple generations within a short period. This efficiency makes large-scale genetic screens feasible and cost-effective compared to rodent models. Thirdly, there are ethical advantages to using flies. Employing *Drosophila* in research adheres to the 3Rs

principle (Replacement, Reduction, Refinement) by reducing the need for higher animals (251). As invertebrates, flies are not subject to the same ethical concerns and regulatory restrictions as mammals, allowing for more extensive and flexible experimentation. Lastly, *Drosophila* benefits from advanced genetic tools, such as RNA interference (RNAi) and the GAL4/UAS system, which facilitate the manipulation and study of specific genes (252). RNAi allows for the targeted knockdown of gene expression, while the GAL4/UAS system enables spatial and temporal control of gene expression. These tools are powerful for studying the roles of individual genes and neural circuits in addiction-related behaviors.

Drosophila and mammals share significant similarities in their genetic makeup, particularly concerning the neurotransmitter systems involving DA, serotonin, and glutamate (253). Both flies and mammals have conserved neurotransmitter systems. In *Drosophila*, the DA pathway is particularly critical in addiction-like behaviors, much like in mammals. DA in flies regulates reward, aversion, and motivation, mirroring its effects in mammalian brains. Serotonin influences diverse brain functions, including walking, circadian entrainment, sleep, aggression, and olfactory learning and memory. Similar to its role in mammalian systems, it is also influencing behavioral responses to addictive substances (254,255). These systems play crucial roles in reward, motivation, and learning processes associated with addiction. Behavioral responses to psychostimulants, such as increased locomotion and arousal, are observed in both flies and mammals, providing measurable endpoints for studying the effects of drugs (58). Additionally, both exhibit neuroplastic changes in response to drug exposure, a hallmark of addiction. These shared pathways suggest that findings in *Drosophila* can provide foundational insights into the neurochemical bases of addiction, which are applicable to more complex organisms, including humans. However, flies lack the complexity of mammalian brains, including highly specialized regions like the PFC and NAc. These regions are critical in humans for executive function and reward processing, making the human brain's response to addiction more complex. Moreover, flies use octopamine instead of norepinephrine, which serves a similar role in modulating arousal

and reward but operates through different receptors and pathways. This difference necessitates careful interpretation when translating findings from flies to mammals.

1.4.2 Behavioral and genetic studies of psychostimulant addiction in *Drosophila*

The use of flies in psychostimulant addiction research began in the late 1990s, pioneered by studies such as McClung and Hirsh (1998), which explored molecular and neural mechanisms of acute volatilized cocaine responses (256). Since then, *Drosophila* has been more extensively utilized to study addictions to substances like cocaine and METH (250). Researchers have employed various assays, including volatilized drug exposure, oral administration, and self-administration assays, to investigate behaviors such as locomotor activity, arousal, learning, memory, drug craving, and SA (250). Some of the main studies showed that, like other animal models, *Drosophila* exhibits sensitivity (SENS) to acute psychostimulant doses by increasing locomotor activity. SENS has been explored in flies in response to cocaine and METH (256,257). Volatilized cocaine induces varying behaviors in flies based on dose, from increased locomotor activity at lower doses to stereotypical behaviors at moderate doses and akinesia or death at higher doses (256). Oral administration of METH enhances activity and reduces sleep, mirroring effects observed in mammals (258). These studies have highlighted similarities between fly and human responses, particularly in dopaminergic signaling and neuronal plasticity, providing valuable insights into the neurobiological mechanisms of addiction.

In laboratory settings, addiction studies often use simple, drug-induced behavioral phenotypes in animal models. These studies typically involve easily quantifiable drug-induced behaviors, with the experimenter controlling drug administration (non-contingent) (259). This method is relatively straightforward and employs a rigorously controlled drug administration protocol. In contrast, studies where animals self-administer drugs of abuse (contingent) rely on operant learning. These procedures necessitate animal training and often involve complex setups and analyses. Contingent studies are considered to have

higher face validity because they more closely mimic human drug-taking behaviors, whereas the face validity and relevance to human addiction in non-contingent studies have been questioned.

Behavioral sensitization is a well-studied non-contingent behavior (260–262). Although most drug classes can be studied for their impact on this behavior, research predominantly focuses on psychostimulants such as cocaine and METH. These studies have demonstrated that molecular events triggered by behavioral sensitization lead to long-term changes in brain homeostasis, involving transcriptional changes and long-lasting epigenetic remodeling (263). Behavioral sensitization has even been observed in flies, which develop LS to cocaine by either increasing the amount of locomotor activity or by enhancing the intensity of stereotypical drug-induced behavior (264,265). Flies also develop sensitization to ethanol, evident as disinhibited courtship behaviors (266). Since sensitization to addictive drugs is not easily demonstrable in humans, it raises debates about the neuromodulatory contributions of behavioral sensitization to the development of drug abuse. Proponents of the incentive-sensitization theory of addiction suggest that sensitization can explain compulsive drug-seeking and drug-taking behaviors, supported by evidence of changes in the mesolimbic dopaminergic system (58).

Because behavioral sensitization represents one form of long-lasting neuronal change, studies in this area can significantly advance our understanding of neuroplasticity in brain circuits involved in drug-seeking and taking behaviors. A suitable method for quantification of LS to psychostimulants is Flybong test, which was previously developed in our lab (267). It was shown that exposure to volatilized cocaine (268) or METH (269) in Flybong leads to increase in locomotor activity indicating sensitivity to an acute dose. Further increase in locomotion following second dose represents LS. Because of its high-throughput nature, FlyBong can be used in genetic screens or in selection experiments aimed at the unbiased identification of functional genes involved in acute or chronic effects of volatilized psychoactive substances.

Besides locomotor response, several methods were developed to study more complex behaviors such as self-administration and rewarding effects of the drugs. Self-administration assays in *Drosophila* reflect drug-seeking behavior and rewarding properties of substances and are designed to study voluntary drug intake and preference. In pivotal ethanol self-administration studies using Capillary Feeder (CAFE) assay, flies were provided a choice between ethanol-laced food and regular food (270). This method was originally developed to quantify food consumption, but later underwent modifications to allow quantification of preferential consumption of one food source over the other (271–273). A preference for ethanol-laced food over time indicates SA, suggesting the rewarding effects of ethanol. Further genetic manipulation is employed to elucidate the role of specific genes, for example related to Notch pathway, in ethanol preference and tolerance (274).

SA studies for cocaine and METH preference were also done using CAFE assay which measures voluntary self-administration of a group of flies by quantifying the consumption of METH-laced food (275). This method is essential for studying SA, where flies choose to consume substances containing addictive drugs, reflecting the rewarding properties of these substances. In the CAFE assay, flies are provided with a choice between capillaries containing regular food and food mixed with a psychostimulant. The volume of food consumed from each capillary is measured to determine preference and intake. This assay is straightforward and does not require extensive training like in rodent models, making it particularly useful for examining the voluntary intake of addictive substances and for conducting preference tests. The CAFE assay has several advantages, including a simple setup that requires minimal specialized equipment and is easy to implement. It also allows precise measurement of drug preference and consumption. However, there are significant limitations to the CAFE assay that need to be addressed to make it suitable for genetic screening and selection studies. One major issue is the reproducibility of data across different laboratories, which can vary due to differences in experimental conditions. Additionally, the assay typically measures group behavior rather than individual, which can obscure individual variations in drug intake and preference. To improve its suitability for genetic screening, the CAFE assay would need

to incorporate mechanisms for high-throughput analysis and better standardization across labs. Innovations such as tracking individual fly consumption and enhanced data collection techniques could help address these limitations.

1.4.3 Genetic screen and selective breeding in addiction research

Genetic screens and selective breeding are crucial in addiction research as they help identify specific genes and genetic variations that influence addictive behaviors, providing insights into the underlying mechanisms of addiction and potential therapeutic targets. These techniques enable the development of animal models that mimic human addiction, facilitating the study of genetic and environmental interactions in substance abuse.

The utility of *Drosophila melanogaster* as a model organism is largely due to the effectiveness of forward genetic screens in pinpointing genes crucial to various biological processes (276). These methods are particularly valuable because of the fly's genetic tractability and the ability to rapidly uncover and manipulate genes involved in addiction, offering a powerful model for the understanding of genetic basis of addictive behaviors. Traditional mutant screens can sometimes fall short in identifying all genes related to a particular phenotype, especially when some genes have redundant functions. In these instances, the GAL4-UAS system is employed to screen for phenotypes resulting from misexpression or overexpression of genes in anatomically localized brain areas (276). One such approach was applied to study the cocaine sensitivity. It involved genetic screen designed to identify *Drosophila* mutants with altered acute responses to cocaine and revealed effects of a mutation in the dLmo gene. Mutant was identified due to heightened sensitivity to cocaine-induced impairment of negative geotaxis measured in the "crackometer" (277). Flies with loss-of-function mutations in dLmo show increased cocaine sensitivity, whereas those with gain-of-function mutations, resulting in dLmo overexpression, exhibit a decreased response to the drug. This opposite correlation

between dLmo activity and cocaine sensitivity suggests that dLmo regulates the expression of genes that directly influence the response to cocaine (277).

Another screen in flies was performed for altered ethanol responses and isolated the gene encoding Ras suppressor 1 (Rsu1) as a regulator of ethanol responses in flies and confirmed this finding in humans (278). A study by Devineni and Heberlein (2009) identified several genes that affect ethanol-induced behaviors, including those involved in the Notch signaling pathway. Such findings in flies can be further explored in rodent models or directly compared to human genetic data, facilitating a translational approach to addiction research.

The GAL4/UAS system has been a transformative tool in *Drosophila* genetics, enabling researchers to manipulate the expression of a specific gene in specific neurons. This system allows for spatial and temporal control over gene expression, providing insights into the contributions of various neural circuits to drug responses. Such genetic screens can uncover novel genetic components of addiction, providing new targets for further investigation and potential therapeutic intervention. Although many behavioral studies indicated the relation of ROS and addictive behaviors, a screen that would focus on the functional role for redox related genes in psychostimulant induced behaviors has not been done. Furthermore, genetic screens have so far not been performed for endpoints such as locomotor sensitization due to the laborious method of monitoring group behavior. The high-throughput nature and objective monitoring of individual flies in the FlyBong now enables genetic screens for identification of genes that regulate locomotor sensitization to volatilized cocaine or METH.

Selective breeding, while more commonly utilized in rodent models, has also shown promise in *Drosophila* research for traits like aggression, sleep and longevity (279,280). Selective breeding for drug-related behaviors, although not extensively explored in flies, presents a valuable opportunity. By selectively breeding flies for preference or sensitivity to drugs like METH, researchers can create distinct lines that exhibit divergent responses to drug exposure. This approach can provide a model to study the genetic basis of addiction-related

behaviors, much like how selective breeding in rodents has been used to study traits such as alcohol or METH preference and resistance to addiction. Rodent models are frequently used due to their high face validity, which stems from the complexity of their brains that closely mimic human neurobiology. In these models, selective breeding for traits like METH preference, sensitivity to various drugs, and complex behaviors like self-administration is common. For instance, selectively bred lines of mice that differ in their sensitivity to METH have provided insights into the genetics of stimulant addiction (281). Research on rats selectively bred for high saccharin intake has demonstrated elevated drug-seeking behaviors, suggesting a genetic overlap between preferences for sweet substances and addictive drugs (282–285). Similarly, mice selectively bred for high alcohol consumption exhibit increased sensitivity to nicotine and cannabinoid rewards, highlighting potential genetic pathways shared across different forms of substance dependence (286). These findings are further supported by studies showing that selective breeding for high and low responses to METH and morphine can aggregate addiction traits, making these models invaluable for large-scale genetic experiments (287).

Genetic factors significantly influence individual susceptibility to METH addiction, as demonstrated by selectively breeding mouse lines to consume high (MAHDR) or low (MALDR) amounts of METH. Researchers used a lickometer system to analyze the microstructure of METH and water intake in these lines during limited access sessions, finding that MAHDR mice consumed more METH, had more frequent and longer drinking bouts, and exhibited higher blood METH levels, indicating a genetic predisposition to higher METH consumption (288). Additionally, a model to investigate binge-level METH use was developed using MAHDR and MALDR lines, where progressively increasing METH concentration and manipulating the METH to water bottle ratio resulted in MAHDR mice showing significantly higher METH intake similar to human binge users, while MALDR mice showed minimal escalation (289). The sustained high intake of MAHDR mice, even after extended withdrawal periods, underscores their genetic predisposition to binge-level METH consumption. Furthermore, gene expression analysis in MAHDR and MALDR mice revealed

differential regulation of genes associated with apoptosis and immune pathways in the NAc, suggesting that genetic predisposition influences METH consumption and provides a valuable model for studying the neurobiological and pharmacological aspects of METH addiction (281).

Collectively, these studies underscore the significance of selective breeding in identifying genetic vulnerabilities and developing targeted interventions for addiction, providing a robust foundation for future research in the field of behavioral genetics and addiction biology. Selective breeding in *Drosophila* for addiction research offers advantages over rodents, such as a shorter lifespan and rapid generation time making large-scale genetic studies feasible. While METH selection has not yet been done in *Drosophila*, the availability of high-throughput methods and advanced genetic tools could make the basic research more efficient.

The central focus of this study is to identify genes and proteins that regulate behavioral responses to METH in *Drosophila*, with a particular focus on genes involved in redox regulation. For the first time, we will conduct a genetic screen to identify genes that regulate LS to METH, targeting genes involved in redox processes. This approach is designed to uncover genes that regulate neural plasticity induced by METH, identifying those with a direct functional role in LS. This will be complemented by a proteomic analysis of brain tissues from flies that developed LS, examining the overlap between the genetic screen and proteomic data. Additionally, we will optimize the CAFÉ assay to enable the tracking of individual flies. This modification will facilitate the selection process for preferential METH consumption, allowing us to crossbreed flies with the highest and lowest preferences for METH. If distinct populations are isolated, subsequent proteomic analysis of their brain tissues will reveal the impact of selection on protein expression and identify overlaps with the LS phenotype. Furthermore, we will analyze the potential bidirectional influence of SA and LS, exploring whether SA affects LS and vice versa. This integrated approach aims to

provide a comprehensive understanding of the genetic and proteomic foundations of METH-induced neural plasticity and behavioral responses.

2. AIMS

The primary aim of this study is to identify genes and proteins that regulate behavioral responses to methamphetamine in *Drosophila melanogaster*, with a focus on genes involved in redox regulation. To achieve this, we have outlined several sub aims:

1. **Development of a modified CAFÉ assay:** Development of a modified version of the CAFÉ assay which will enable precise and high-throughput measurement of METH SA in individual flies. Data analysis will provide the quantification of individual preference for METH, locomotor activity and the location in the environment during SA.
2. **Selection of fly strains based on methamphetamine preference:** Using the new CAFÉ method select two distinct strains of flies with high and low preference for SA of METH. This will enable identification of genes and proteins that regulate voluntary consumption.
3. **Proteomic analysis of brain tissues from selected strains:** Proteomic analysis of the brain tissue derived from flies with high and low preference for METH SA. This will define the proteomic changes that accompany changes in preferential SA and show potential overlap with the LS phenotype.
4. **Genetic screen for redox-related genes:** Genetic screen for the unbiased identification of redox related genes that regulate LS to vMETH. This approach will identify genes that have a functional role in the regulation of LS.
5. **Proteomic analysis of brain tissues:** Proteomic analysis of brain tissues derived from flies that did or did not develop LS after two administrations of vMETH. This approach will identify all the proteins that are unique to flies that develop LS but without the distinction of their functional role in the process.

3. MATERIALS AND METHODS

3.1 Fly Strains

We used *wild-type (wt) Drosophila* male flies, *Canton S* strain, and *period* mutant flies (*per*⁰¹) from the laboratory of C. Helfrich Forster, University of Würzburg, Germany. Driver lines (*elav-gal4*, *ddc-gal4* and *ple-gal4*) used in genetic screen were obtained from Bloomington Drosophila Stock Center (BDSC) and RNAi lines from Vienna Drosophila Resource Center (VDRC) and Bloomington Drosophila Stock Center (BDSC) as shown in the Table 1. Upon arrival of each strain, flies were placed in the quarantine for at least two weeks. Flies were maintained on standard cornmeal/agar medium at 25°C and 70% humidity on a 12-hour light/dark cycle. Three to five-day old male flies were anesthetized using CO₂ and collected one day prior to experiments.

Table 1. List of RNAi lines obtained from Vienna Drosophila Resource Center (VDRC) and Bloomington Drosophila Stock Center (BDSC)

Vienna Drosophila Resource Center (VDRC)					
<i>Gene</i>	<i>Full name</i>	<i>Annotation Symbol</i>	<i>FlyBase Gene Number (FBGn)</i>	<i>VDRC ID</i>	<i>VDRC Library</i>
<i>Cat</i>	<i>Catalase</i>	CG6871	FBgn0000261	103591	KK
<i>Gclc</i>	<i>Glutamate-cysteine ligase catalytic subunit</i>	CG2259	FBgn0040319	108022	KK
<i>Gclm</i>	<i>Glutamate-cysteine ligase modifier subunit</i>	CG4919	FBgn0046114	108737	KK
<i>Grx1</i>	<i>Glutaredoxin 1</i>	CG6852	FBgn0036820	101410	KK
<i>GstE1</i>	<i>Glutathione S transferase E1</i>	CG5164	FBgn0034335	110529	KK
<i>MBD-like</i>	<i>Methyl-CpG binding domain protein-like</i>	CG8208	FBgn0027950	111000	KK
<i>Sod1</i>	<i>Superoxide dismutase 1</i>	CG11793	FBgn0003462	108307	KK
<i>Sod2</i>	<i>Superoxide dismutase 2 (Mn)</i>	CG8905	FBgn0010213	110547	KK
<i>Sod3</i>	<i>Superoxide dismutase 3</i>	CG9027	FBgn0033631	37793	GD

Bloomington Drosophila Stock Center (BDSC)				
<i>Gene</i>	<i>Full name</i>	<i>Annotation Symbol</i>	<i>FlyBase Gene Number (FBGn)</i>	<i>Bloomington Stock Number</i>
<i>Ckl1beta</i>	<i>Casein kinase II β subunit</i>	CG15224	FBgn0000259	RRID:BDSC_31254
<i>E(spl)m3-hlh</i>	<i>Enhancer of split m3, helix-loop-helix</i>	CG8346	FBgn0002609	RRID:BDSC_25977
<i>Gapdh1</i>	<i>Glyceraldehyde 3 phosphate dehydrogenase 1</i>	CG12055	FBgn0001091	RRID:BDSC_36842
<i>Gapdh2</i>	<i>Glyceraldehyde 3 phosphate dehydrogenase 2</i>	CG8893	FBgn0001092	RRID:BDSC_26302
<i>Jafrac1</i>	<i>Peroxiredoxin 2</i>	CG1633	FBgn0040309	RRID:BDSC_38926
<i>Men</i>	<i>Malic enzyme</i>	CG10120	FBgn0002719	RRID:BDSC_41652
<i>ND-51</i>	<i>NADH dehydrogenase (ubiquinone) 51 kDa subunit</i>	CG9140	FBgn0031771	RRID:BDSC_29534
<i>PHGPx</i>	<i>Glutathione peroxidase homolog with thioredoxin peroxidase activity</i>	CG12013	FBgn0035438	RRID:BDSC_33939
<i>Prx3</i>	<i>Peroxiredoxin 3</i>	CG5826	FBgn0038519	RRID:BDSC_60475
<i>Prx5</i>	<i>Peroxiredoxin 5</i>	CG7217	FBgn0038570	RRID:BDSC_64998
<i>Sni</i>	<i>sniffer</i>	CG10964	FBgn0030026	RRID:BDSC_31978
<i>Tbh</i>	<i>Tyramine β hydroxylase</i>	CG1543	FBgn0010329	RRID:BDSC_27667
<i>Trx-2</i>	<i>Thioredoxin 2</i>	CG31884	FBgn0040070	RRID:BDSC_33721

3.2 Assays and general protocols

3.2.1 Behavioral tests and protocols

3.2.1.1 FlyCafe assay

3.2.1.1.1 Experimental setup

We developed the FlyCafe assay by combining two systems: the standard two-choice Capillary Feeder (CAFE) assay (ref.) and the Drosophila Activity Monitoring System (DAMS) (TriKinetics, Waltham, MASS). Individual flies were placed in standard DAM system glass tubes (65 mm long with a 5 mm diameter). To modify the tubes, a 1.5 cm long rubber tube was attached to cap each end. The exterior end of the rubber cap was covered with nylon mesh and secured with parafilm to allow the entry of water vapor and prevent dehydration. At the upper middle position of each rubber cap a hole was drilled to fit a 200 μ l pipette tip vertically, which was adapted to securely hold a 5 μ l glass capillary (Hirschmann) (see Fig. 1a).

Capillaries were filled, via capillary action, with mineral oil to minimize evaporation and then with liquid food. Sugar food was 100 mM sucrose+5% yeast solution, while

methamphetamine (METH) food was a mix of Sugar food with different concentrations of METH diluted in distilled water. Methamphetamine-hydrochloride ($\geq 97.5\%$) and mineral oil were purchased from Sigma–Aldrich. Sucrose and yeast were purchased from a local store. The height of liquid food in the capillary was measured using a ruler and capillaries were then inserted into the pipette tip in a way that was easily accessible to the flies to feed. The amount of consumed liquid in the capillaries was measured every day at 09:00 and were then replaced with freshly prepared capillaries.

To obtain data for locomotor activity, dwell position and rest periods for each of the 32 individually housed flies in the glass tubes, we used DAM5M monitor (Trikinetics), sized 33.0 x 8.3 x 2.6 cm, which emitted four infrared beams per glass tube. For each FlyCafe experiment 10 control and 22 experimental flies were placed in the DAM5M monitor. Control flies had a choice of Sugar liquid food from both capillaries, while experimental flies were divided in two groups of 11 with METH and Sugar food offered at alternate sides of the tubes to abolish potential side bias (Fig.1c). For each experiment, aside from the daily amount of consumed Sugar and METH food, we collected additional data: counts (locomotor activity), and dwells (percent of time spent at each end of the tube), every minute for the duration of the experiment (three or seven days).

DAM5M monitor was placed into a plastic tub on a pedestal to prevent contact with one liter of tap water, and then covered with cling film to minimize humidity fluctuations and evaporation. Monitor was connected to a computer using a PSU9 Power Supply Interface Unit (TriKinetics). The tub was placed inside an incubator set at 24°C in constant darkness to prevent the possibility of side preference due to environmental cues (Fig.1b). To correct for spontaneous evaporation, we had additional tubes with liquid food in both capillaries but without flies. The tubes were placed in the same conditions as DAM5M. Each day the amount of consumed food was corrected for average evaporation using the evaporation control tubes.

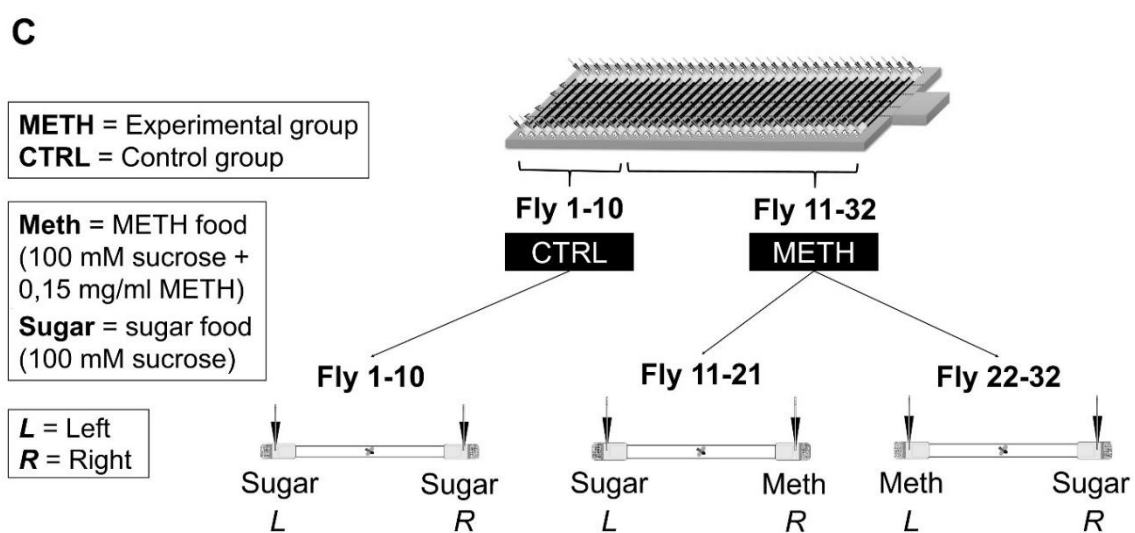
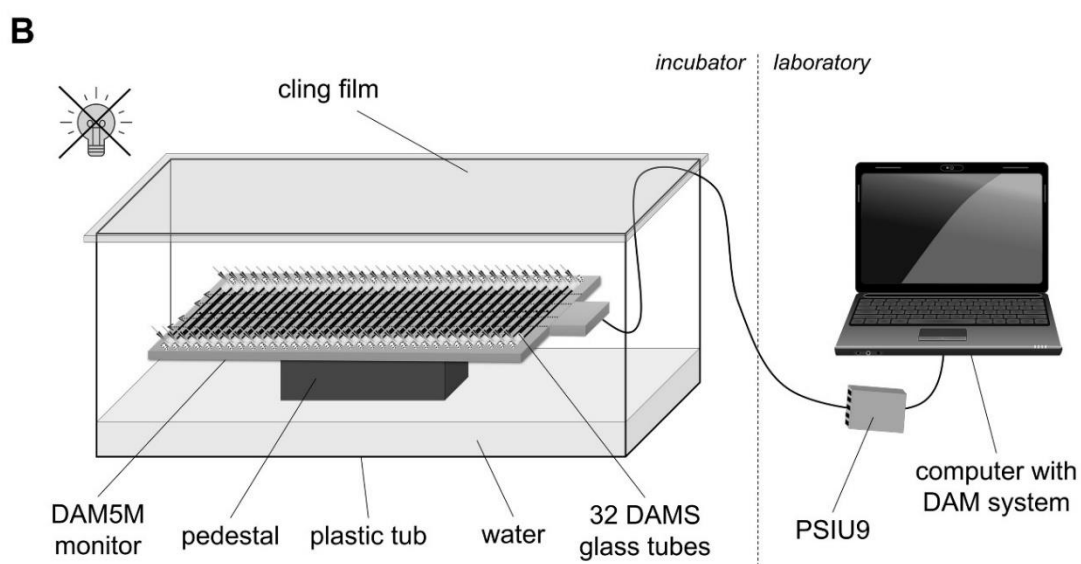
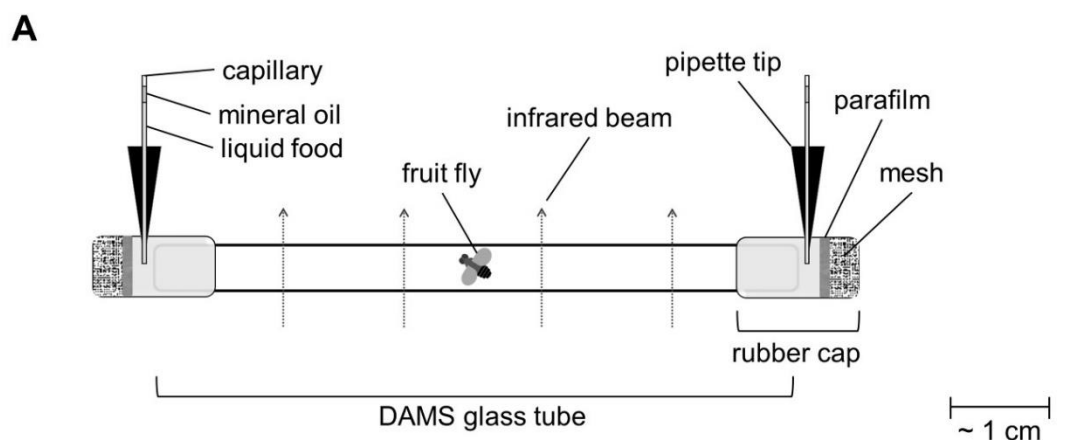


Figure 11. FlyCafe: a novel method for measuring preferential consumption of food in individual flies. **A.** *Drosophila Activity Monitoring System (DAMS) glass tube with modified ends for insertion of glass capillaries with liquid food.* **B.** *FlyCafe experimental setup consisting of DAM5M monitor that holds 32 glass tubes with individual flies, placed in a sealed container with water and connected to a computer that collects locomotor activity data every minute during a 24-hour period.* **C.** *Standard procedure for positioning glass tubes in a DAM5M monitor.*

3.2.1.1.2 Data collection and analysis

The daily change of the meniscus position of liquid food and mineral oil in the glass capillaries (in centimeters) was measured using a ruler. To determine the amount of ingested liquid food, the evaporation correction was subtracted, and the result was multiplied by the cross-sectional area of the capillary to obtain the volume in microliters. Preferential consumption was defined as the consumption difference between METH food and Sugar food. MS Excel was used to analyze individual fly food consumption in the FlyCafe assay.

The assessment of the locomotor activity (counts) and the percentage of time spent at the ends of the glass tube by the food source (dwell) in the DAM5M monitor was done on data acquired using the Data Acquisition Software, DAMSystem310. Data, recorded at one-minute resolution over 24 hours for the experiment's duration, were saved as .txt files. The DAM5M monitor generated a matrix of 28,800 lines and 42 rows per day, where each line corresponded to counts, moves, dwell, position, and rest detected by one of four beams (5 parameters x 4 beams x 1440 minutes per day). Rows represented individual fly values (32 flies per monitor). The focus in the analysis was on counts and dwell.

For the analysis of DAM5M output data, a newly developed open-source software in the Python programming language was used. This software enabled the selection of specific time intervals or individuals and facilitated calculations of mean, sum, standard deviation,

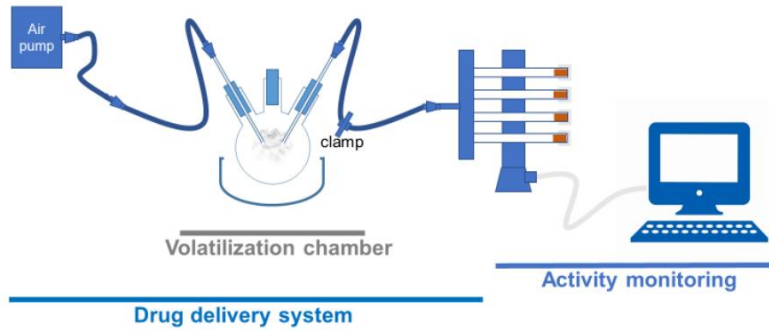
and standard error on the chosen data. The resulting values could be visually represented as a line graph in the user interface or exported in another file format for additional statistical analysis. In our experiments, files were exported to MS Excel for further analysis. The software for the analysis of raw data is available as open source using the following link: <https://github.com/DAMS-software/DAM4-gui> and was written in collaboration with Milan Petrović, Faculty of informatics and digital technologies.

3.2.1.2 FlyBong assay

3.2.1.2.1 Experimental setup

FlyBong assay was previously developed in our laboratory as a high-throughput method for quantifying the levels of locomotor activity induced by exposure to volatilized cocaine (264). Briefly, 75 µg of METH or COC dissolved in 96% ethanol was placed in a triple neck flask through the middle, widest neck. The flask was connected through a glass and rubber tubing system to an air pump using one of the narrower necks, and MAN2 Gas Distribution Manifold on the other narrow neck. Prior to drug administration a glass stopper was placed in the middle neck of the flask to enable a closed system. 32 flies were individually loaded in plastic tubes with two small holes that allow for the air flow and food on one end and placed in a vertical DAM2 Drosophila Activity Monitor with a single infrared beam crossing the midline of the tube. The monitor was connected to a Gas Distribution Manifold on one end and a computer on the other using PSIU9 data acquisition hardware.

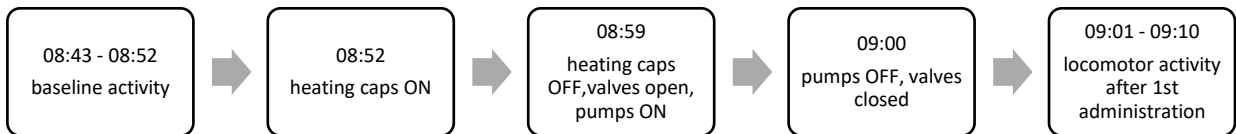
A



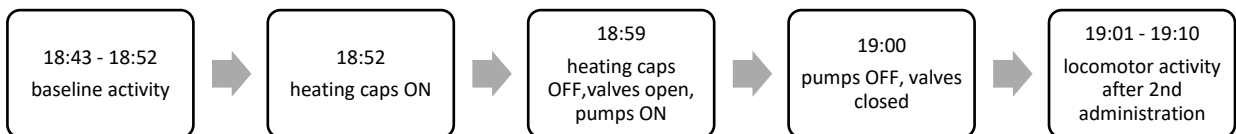
B

vMETH:

1. dose:



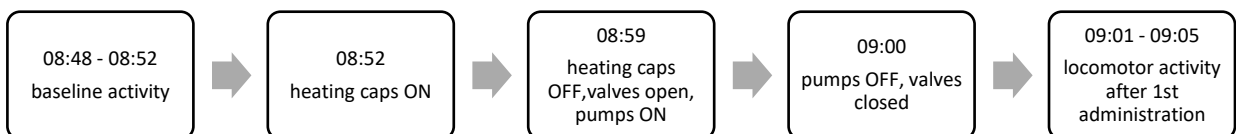
2. dose:



C

vCOC:

1. dose:



2. dose:

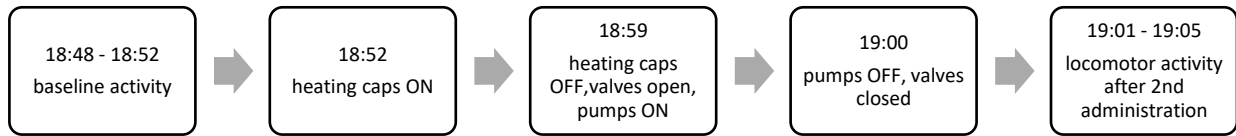


Figure 12. FlyBong platform for measuring changes in locomotor activity of *Drosophila* after delivery of psychostimulants. A. METH or cocaine dissolved in ethanol is pipetted into a three-neck flask, which is then heated to the temperature of psychostimulant volatilization. Individual flies are placed in tubes in the vertical *Drosophila* monitor (TriKinetics). Flies are subjected to volatile psychostimulant for one minute by activating the air pump and opening the valve/clamp. The flies' locomotor activity is continuously observed by measuring the number of midline crossings in the tube per minute, before and after the psychostimulant exposure. B. FlyBong protocol for two administrations of vMETH C. FlyBong protocol for two administrations of Vcoc. Image source: (264)

The first step in the FlyBong procedure is to increase the temperature inside the flask using a heating cap for seven minutes to achieve the volatilization temperature for methamphetamine-hydrochloride or cocaine-hydrochloride (172-174°C). vMETH or vCOC is then administered for one minute to all 32 flies, evenly and simultaneously, using an air pump (3.5 L/min air flow) which pumps the aerosol through automatic valves powered by an electric motor. The experimental group of flies received two doses of volatilized METH (vMETH) at 09:00 and 19:00 PM (Figure 2B) or volatilized cocaine (vCOC) at 09:00 and 15:00 (Figure 2C), while the control group always received heated airflow without the psychostimulant.

3.2.1.2.2 Data collection and analysis

The DAM2 data were gathered using the DAMSystem310 Data Collection Software and then extracted into .txt files using DAMFileScan111. Each .txt file consisted of 32 columns, each representing individual flies, and 1440 rows, accounting for each minute in a day. The extracted .txt files were analyzed using custom-made software, created by Milan Petrović from the Faculty of Informatics and Digital Technologies, accessible at <https://github.com/DAMS-software/DAM1-GUI>. The average population locomotor activity in counts per minute was quantified for the 10 minutes before and after the administration of vMETH (experimental) and heated air (control) or 5 minutes before and after the administration of vCOC (experimental) and heated air (control). Periods of heating (seven minutes) and drug administration (one minute) were excluded from the data analysis.

The average baseline locomotor activity is then subtracted from the average locomotor activity after the administration to calculate the response as a difference of those two parameters (locomotion – baseline) after each administration for both controls (CTRL first and CTRL second) and experimental group (vMETH first or vCOC first , and vMETH second or vCOC second). If the activity after the vMETH first or vCOC first was significantly higher than CTRL first, it indicated that flies were sensitive (SENS) to the motor-activating effects of psychostimulant. If the second response was significantly higher than the CTRL second, it indicated that the effect was drug- specific. Finally, if the activity after the second administration was higher than first, and the first was higher than the baseline, for an individual fly, it indicated that the fly developed locomotor sensitization (LS).

3.2.1.3 Activity and sleep tracking

The activity and sleep patterns of flies were quantified using the DAMS system (Drosophila Activity Monitoring System). Each fly line or control was assigned one DAMS monitor, which accommodated a total of 32 flies. Individual flies were carefully aspirated into glass tubes containing food sealed with parafilm at one end, and a sponge at the other end to prevent their escape. These glass tubes were then placed in monitors, which were connected to a

computer, and the entire setup was maintained in a controlled environment with a 12-hour light and 12-hour darkness cycle (LD conditions) at a constant temperature of 24°C. In some experiments, the same procedure was repeated but the monitors were kept in constant darkness (DD conditions).

To monitor the flies' activity, an infrared (IR) light was passed through the center of the glass tubes. Whenever a fly crossed the center of the tube, the interruption of the IR light was detected and recorded as a count on the computer. Beam interruptions were collected every minute during 24 hours for the duration of the experiment. The sleep was defined as no beam interruption for 5 minutes or more.

The activity and sleep patterns were monitored continuously for five consecutive days. From the recorded data, the total average activity (number of glass tube crossings in a 24-hour period) and sleep duration (in minutes during a 1-hour period) were calculated for each experiment.

3.2.1.4 Negative Geotaxis

Flies possess an inherent negative geotaxis response, demonstrating their natural reflex to climb against the force of gravity. One day prior to experiment, approximately 50 male flies per group were anesthetized, separated by sex (10 flies per vial) and placed on a 3 ml of fresh food.

After one day of recovery from the anesthesia, all flies from the food vials were transferred to empty vials marked at the midpoint (three cm from the tube bottom). Flies were left for 20 minutes to adapt to new environment. After 20 minutes five vials with flies from one experimental group were placed in a wooden frame, secured with screws and a camera was positioned 30 cm in front of the frame with the vials. The wooden frame was tapped against the surface three times to ensure that all flies fall to the bottom of the vials, and a stopwatch was started. After 5 seconds, the vials were photographed to capture the number of flies

that crossed the midline mark. After one minute, the frame was tapped three times again, and the flies were photographed after five seconds. This procedure was repeated five times for each experimental group.

3.2.1.5 *Body weight measurement*

To measure the body weight of *Drosophila*, three to five days old flies were collected and briefly immobilized by freezing, groups of five flies were weighted in triplicates using analytical balance, ensuring the consistency and accuracy of the measurements.

3.2.2 Neurochemical Analysis

3.2.2.1 *Sample preparation*

Three to five days old male flies were selected, placed on ice, and dissection scissors and tweezers were used to separate heads from the body. Fifteen heads per sample were then immersed in 300 μ L of 0.1 M perchloric acid (95%, Sigma Aldrich, Buchs, Switzerland) and mechanically homogenized on ice for 15–20 seconds. The samples were centrifuged for 45 minutes at 12 °C and 45000 rpm right after the homogenization. The resulting supernatant was transferred to 1 mL glass vial using cellulose filters with 0.20 μ m pores (Macherey-Nagel, Chromafil Xtra RC-20/13, 0.20 μ m, 13 mm) and a syringe to facilitate rapid flow-through filtration. The vial was sealed using a stopper equipped with a septum.

3.2.2.2 *Liquid Chromatography with Tandem Mass Spectrometry (LC-MS/MS)*

An Agilent 1260 series HPLC chromatograph, equipped with a degasser, binary pump, autosampler, and column oven, was linked to an Agilent 6460 triple quadrupole mass spectrometer (QQQ) featuring an AJS ESI source. The quantitative analyses were performed for monoamines (dopamine, octopamine, and tyramine) and semi-quantitative analyses of glutamate, acetylcholine, and gamma-aminobutyric acid (GABA). Chromatographic

separation utilized a Purospher STAR RP-18 Hibar HR column (50 mm × 2.1 mm, 1.7 μm, Merck, Darmstadt, Germany). The mobile phase consisted of (A) 1% formic acid in milliQ water and (B) acetonitrile. The gradient elution proceeded as follows: 0–0.9 min with a linear gradient from 1% to 10% B, 0.9–3 min from 10% to 20% B, 3–4.5 min from 20% to 25% B, 4.5–6 min from 25% to 30% B, 6–6.1 min from 30% B to 99% B, 6.1–6.2 min from 99% B to 1% B, and 6.2 to 10 min at 1% B. The post time was set to two min, and the flow rate was 0.33 mL/min. The column oven was maintained at 25 °C, and the sample injection volume was 2.5 μL, injected in triplicate. For AJS-ESI-QQQ, the parameters were configured as follows: capillary voltage was 3.5 kV in both positive and negative modes, nozzle voltage was 0.5 kV, ion source temperature was 300 °C, gas flow was 5 L/min, nebulizer pressure was 45 psi, drying gas temperature was 250 °C, and sheath gas flow was 11 L/min. Nitrogen served as the collision gas. Data processing was carried out using MassHunter Qualitative Analysis version B.07.00 (Agilent Technologies, Santa Clara, CA, USA). In cases of compounds semi-quantified without standards, calculations were based on extracted ion chromatograms (EIC) of deprotonated ions.

3.2.2.3 Data Analysis

All data generated through MassHunter Qualitative Analysis software version B.07.00 (Agilent Technologies, Inc., Santa Clara, CA, USA; 2014) was processed in MS Excel and was visualized in GraphPad Prism.

3.2.3 Proteomic analysis

3.2.3.1 Brain dissection

Three-five days old males were separated from females using CO₂ anesthesia and a microscope. Male flies were collected in a clean vial, sealed with a cotton plug, and then placed in an ice bath to remain alive but immobilized until brain dissection. Prior to

dissection, the flies underwent rinsing in 70% ethanol followed by cold PBS × 1. Using a dissecting microscope and two forceps, the brain was extracted from the head and transferred to an empty and pre-weighed Eppendorf tube. Dissection was performed in a cold PBS × 1 solution. As many individuals as possible were dissected within a 10-minute period to prevent sample degradation due to reaching room temperature. After dissection, the samples were stored at -80 °C for further processing.

3.2.3.2 Mechanical and chemical homogenization and protein isolation

Protein isolation from fly brain tissue utilized RIPA extraction buffer with the addition of a protease inhibitor, which was prepared as outlined in Table 2. The pH was adjusted to 8 using 1 M HCl. Subsequently, 10 mL from the prepared 50 mL RIPA solution was pipetted, and a protease inhibitor tablet was added.

Table 2. Composition for 50 mL RIPA (RadioImmunoPrecipitation Assay)

CHEMICAL	AMOUNT
50 MM TRIS-HCL	0.3028 g
150 MM NAACL	0.4233 g
0.1% NP-40	500 µL of a 10% solution
0.5% SODIUM DEOXYCHOLATE	2.5 mL of a 10% solution
0.1% SDS	500 µL of a 10% solution

Collected samples underwent mechanical homogenization on ice for 5-15 seconds. Then a cold solution of RIPA extraction buffer was added to the sample, and using a homogenizer, all cellular components were disrupted for 20-30 seconds. The added buffer volume follows a ratio of 30, averaging 5 mg of tissue to 300 µL of RIPA buffer. Following homogenization,

samples were centrifuged at 14,000 rpm, +4 °C, for 30 minutes. After centrifugation, the supernatant was transferred to a clean and labeled Eppendorf tube for further analysis.

3.2.3.3 Quantification of Total Proteins

The concentration of total proteins in brain extracts was quantified using the BioDrop device. For quantification, 3 μ L of dH₂O is pipetted to establish a referent value, followed by gently wiping the sampling area. Subsequently, 3 μ L of the sample is pipetted for measuring the γ (μ g/mL) of the protein extract.

3.2.3.4 Sample Preparation for Mailing

After quantifying the total protein concentration in the sample, precipitation was achieved by adding cold acetone overnight at -20 °C. This step is crucial for samples to dissolve in Laemmli buffer, resulting in a final protein concentration of 50 μ g/mL in all samples. Precipitation is performed at a ratio of 1 μ L lysate to 4 μ L cold acetone. After precipitation, samples were centrifuged to remove the supernatant, and 30 μ L of Laemmli buffer was added (Table 3.). The samples were then resuspended using an ultrasonic probe, transferred to transport tubes. The samples were sent to the Proteome Center Tuebingen (PCT), a proteomics core facility affiliated with the University of Tuebingen, Germany, to undergo subsequent analysis steps, conducted in collaboration with Dr. Ana Velić, including 1D SDS-PAGE, In-Gel digestion of samples, sample preparation for mass spectrometry, as well as mass spectrometry itself and the initial phase of data analysis.

Table 3. Composition of Laemmli Buffer

CHEMICAL	AMOUNT
GLYCEROL	1 mL
0.5 M TRIS HCL PH 6.8	1.25 mL

10% SDS	2 mL
2M DDT	0.5 mL
WATER	

3.2.3.5 SDS-PAGE or 1D Electrophoresis

Upon receipt, 1D SDS-PAGE was conducted on the samples without additional fractionation, as it involves non-specific analysis without additional labeling. Materials used for sample preparation included NuPAGE 12% Bis-Tris gel, Invitrogen (NP0341BOX), NuPAGE LDS sample buffer (4x), Invitrogen (NP0007), NuPAGE MOPS SDS Running buffer (20x), Invitrogen (NP0002), and NOVEX colloidal blue staining kit, Invitrogen (LC6025).

Samples were mixed with LDS sample buffer (4x) and β -mercaptoethanol as a reducing agent following the NuPAGE protocol in triplicate. They were then applied to a 12% precast gel with a maximum sample volume of 45 μ l per well. An empty well was left between each sample to prevent contamination. Gel electrophoresis was run at 200 V for 10 minutes, with a working distance between gels of 0.5 - 1.0 cm. After electrophoresis, the gel was stained using the NOVEX colloidal blue staining kit. Each sample was entirely excised from the gel, including a 1-2 mm buffer in front of the dye, diced into pieces, and extracted following the In-Gel Digest protocol.

3.2.3.6 In-Gel Digestion of Samples and Preparation for Mass Spectrometry

On day 1, stained gel was placed on a glass plate and cut into sample strips using a scalpel. Gel pieces were thoroughly rinsed for approximately 10 minutes with 100 μ l of distilled water of HPLC purity. After rinsing, excess water was discarded. Gel pieces were then bleached for 10 minutes using 100 μ l of a 40% solution of acetonitrile (ACN) at 60 °C,

followed by the removal of the supernatant. The gel was washed again for 10 minutes with 100 μ l of ACN solution (40%) at room temperature, and then rinsed for an additional two minutes with 100 μ l of ACN solution (100%). If the gel pieces still appeared blue, three additional washing steps with 40% and 100% ACN were repeated. The destained gel pieces were completely dried under a laminar flow for 10 minutes, and then 100 μ l of 5 mM dithiothreitol (DTT) solution was added and incubated at 60 °C for 15 minutes. The sample was allowed to cool to room temperature, as iodoacetamide is not thermally stable. Next, 100 μ l of 25 mM iodoacetamide solution was added and incubated in complete darkness at room temperature for 45 minutes, followed by discarding the excess liquid. Subsequently, two washes for 10 minutes each with 100 μ l of ACN solution (40%) and 2 minutes with 100 μ l of ACN solution (100%) were performed. The gel pieces were dried again in the laminar flow.

Before digestion, a trypsin solution was prepared by dissolving 25 μ g of trypsin in 50 μ l of 50 mM acetic acid to a final concentration of 0.5 μ g/ μ L. An aliquot of 5 μ g was prepared and stored at -20 °C until use. The final trypsin solution for digestion was prepared by dissolving one aliquot (10 μ l) in 1980 μ l of freshly prepared 50 mM ammonium bicarbonate solution. Twenty to forty microliters of this prepared trypsin solution were added to the gel and incubated overnight at 37 °C. The tube was wrapped with parafilm to reduce evaporation.

On the second day, trypsin and peptide mixture were acidified by adding 10 μ l of a 2.5% solution of trifluoroacetic acid (TFA) in distilled water of HPLC purity and incubated at room temperature for 15 minutes. Then, 80 μ l of 0.5% TFA/50% ACN were added and incubated for 15 minutes at room temperature, followed by the addition of 80 μ l of 0.5% TFA/100% ACN and another 15-minute incubation at room temperature. The samples were then dried in a SpeedVac at 35 °C and stored at -20 °C or directly analyzed by mass spectrometry.

3.2.3.7 Mass Spectrometry

The prepared samples were analyzed using the Q Exactive HF instrument (ThermoFisher). This instrument is an LC-MS/MS setup that enables separation based on polarity with liquid chromatography (LC) and a hybrid MS/MS detector that is quadrupole-Orbitrap.

3.2.3.8 Data analysis

The analysis of raw data was performed at the University of Tübingen by our collaborator dr. Ana Velić using the MaxQuant software (in this case, version 1.6.7.0), generating .txt files that were further statistically analyzed using Perseus¹.

We obtained MS Excel files containing the complete list of identified proteins, along with lists specifically highlighting proteins showing significant differential expression following sample comparisons. The acquired data underwent subsequent analysis and visualization through STRING² (Search Tool for the Retrieval of Interacting Genes/Proteins) to evaluate protein-protein interaction networks and conduct functional enrichment analysis. Additionally, ShinyGO³, an online tool, was utilized for gene ontology enrichment analysis, functional categorization, and elucidating biological significance.

3.2.4 Gene silencing using binary expression system UAS-GAL4

Mutations in genes associated with the regulation of redox status are often lethal. To have consistent results of inactivation of different genes we used transgenic flies with silenced genes of interest only in specific tissues/cells.

¹ <https://maxquant.net/perseus/>

² <https://string-db.org/>

³ <http://bioinformatics.sdstate.edu/go74/>

To silence genes at the post-transcriptional level, Gal4/UAS-RNAi (252) expression system was employed. The Gal4/UAS-RNAi system is a versatile tool utilized in *Drosophila* research for targeted gene knockdown with spatial and temporal control (Figure 3). This system operates through the interaction of two main components: the Gal4 transcription factor (driver) and the Upstream Activating Sequence (UAS) promoter sequence. Firstly, a tissue-specific promoter, such as those derived from the enhancer of genes expressed in specific cell types or developmental stages, drives the expression of Gal4. Upon Gal4 binding to the UAS sequence, transcriptional activation occurs. This results in the production of double-stranded RNA (dsRNA) or short hairpin RNA (shRNA) molecules, which are processed into small interfering RNAs (siRNAs) by the cellular RNAi machinery. These siRNAs then guide the RNA-induced silencing complex (RISC) to the complementary mRNA transcripts of the target gene, leading to their degradation or translational repression. Consequently, the expression of the target gene is selectively and efficiently suppressed in the tissues or developmental stages where Gal4 is active, enabling precise investigation of gene function in a spatially and temporally controlled manner.

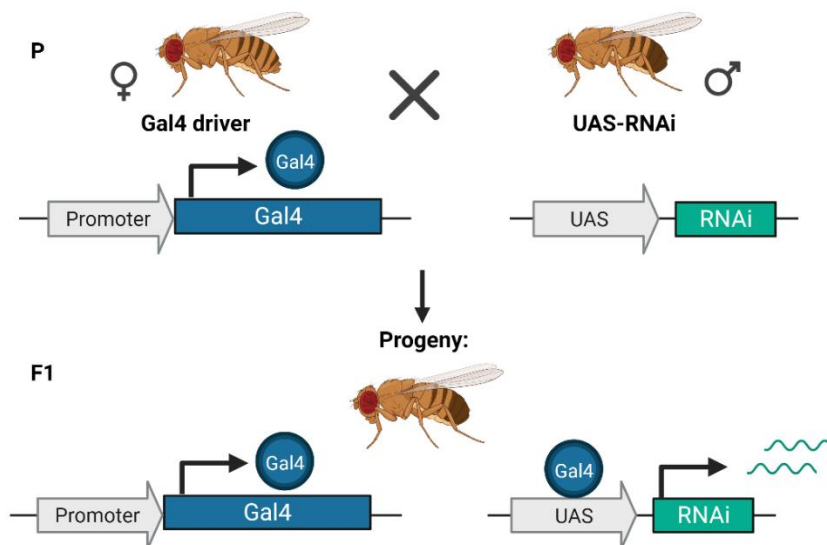


Figure 13. Transgenic flies used in the genetic screen were generated using the Gal4/UAS expression system. *Transgenic virgin females carrying GAL4 construct are crossed with males carrying UAS-RNAi construct. In their progeny the Gal4 transcriptional activator is expressed under the promoter specific cells/tissue and binds to the UAS (upstream activation sequence) regulatory region. This initiates specific expression of interfering RNA that binds to the mRNA of the gene of interest, preventing translation and thereby leading to gene silencing in a cell specific manner.*

We chose different Gal4 driver lines, depending on the tissue or cells of interest, such as *elav-gal4* driver line for silencing in all neurons, *ddc-gal4* line for gene silencing in dopaminergic and serotonergic neurons and *ple-gal4* for only dopaminergic neurons.

Crosses were established by pairing 10-15 virgin females from the driver line with 5 males harboring the RNAi gene silencing construct. F1 progenies were collected at 3-5 days old and tests were performed, depending on the approach. In case of genetic screen, behavioural tests, including FlyBong (vMETH and vCOC administration), FlyCafe (measuring preference for METH), negative geotaxis assay, activity and sleep tracking were done on F1 progeny. Gene silencing is also used to silence *Tbh* gene before the SA test in FlyCafe.

3.3 Approaches

3.3.1 Approach 1: Genetic screen and behavioral characterization

Genes that regulate redox processes were selected using Flybase. RNAi lines for selected genes and the tissue specific driver lines were ordered from VDRC and BDSC. 10-15 virgins of Gal4 line were put in the same vial with 5 males of UAS-RNAi lines for breeding. Three to five days old males of F1 progeny were collected and tested in Flybong, using standard procedure for the delivery of two doses of vMETH.

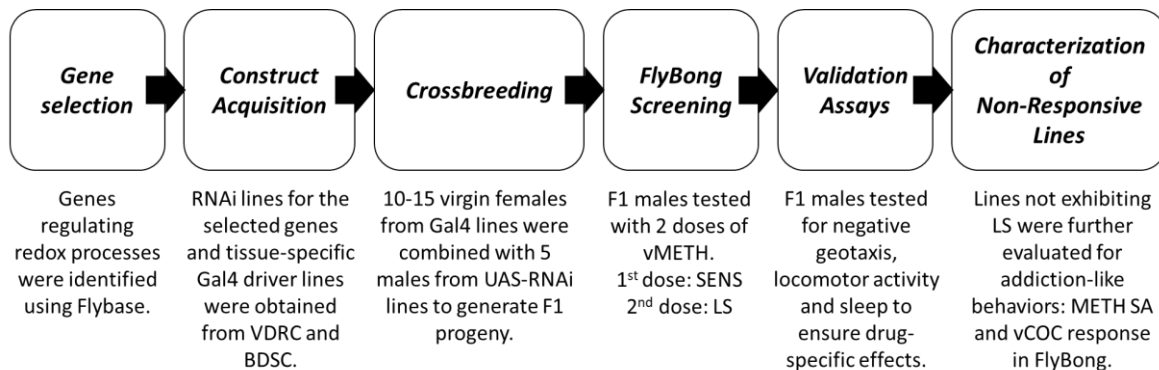


Figure 14. Flow chart of the genetic screen for the identification of redox-related genes involved in LS in *Drosophila melanogaster*.

To ensure that LS is drug-specific and to exclude any motor neuron deficits caused by gene silencing, which can affect the ability of flies to develop LS, negative geotaxis (vertical climbing ability), locomotor activity and sleep were quantified in all transgenic flies, in a way described in section “assays and general protocols”. Negative geotaxis was measured as a percentage of flies that climb over the center of a vial five seconds after flies have been dropped to the bottom of the vial. For Locomotor activity and sleep assay, flies were put in glass tubes with food which were placed in DAMS monitors with infrared beam used to track the activity. Flies are considered sleeping when they do not cross the IR beam for at least five minutes. Average 24-hours, day and night activity and sleep was calculated based on a five-day recording.

Following the identification of lines lacking LS, we conducted further characterization using additional tests to evaluate addiction-like behaviors, including METH SA and response to COC in FlyBong. These additional assessments allow for a better understanding of the behavioral phenotype of identified lines, shedding light on potential differences in addictive susceptibility and responses to various psychostimulants.

3.3.2 Approach 2: Selective breeding

Selective breeding was employed to establish two distinct lines: the High Preference (HP) line, characterized by a high preferential consumption of METH, and the Low Preference (LP) line, displaying a low preference for METH. The selection process involved the utilization of FlyCafe, as previously described in general protocols, which enables the quantification of drug preference (269).

Individual male flies from parental generation (P0) were housed in glass DAMS tubes and offered liquid food in capillaries placed on opposite sides of the tube. One capillary contained Sugar food (sugar and yeast solution), while the other capillary in addition contained 0.15 mg/ml METH. Over a three-day period, the amount of ingested food was measured daily, and fresh capillaries with food were provided. Preference was calculated for each of the 22 experimental flies by determining the difference between the amount of Sugar food and METH-laced food ingested. To control for assay variations, 10 flies were used as side preference controls.

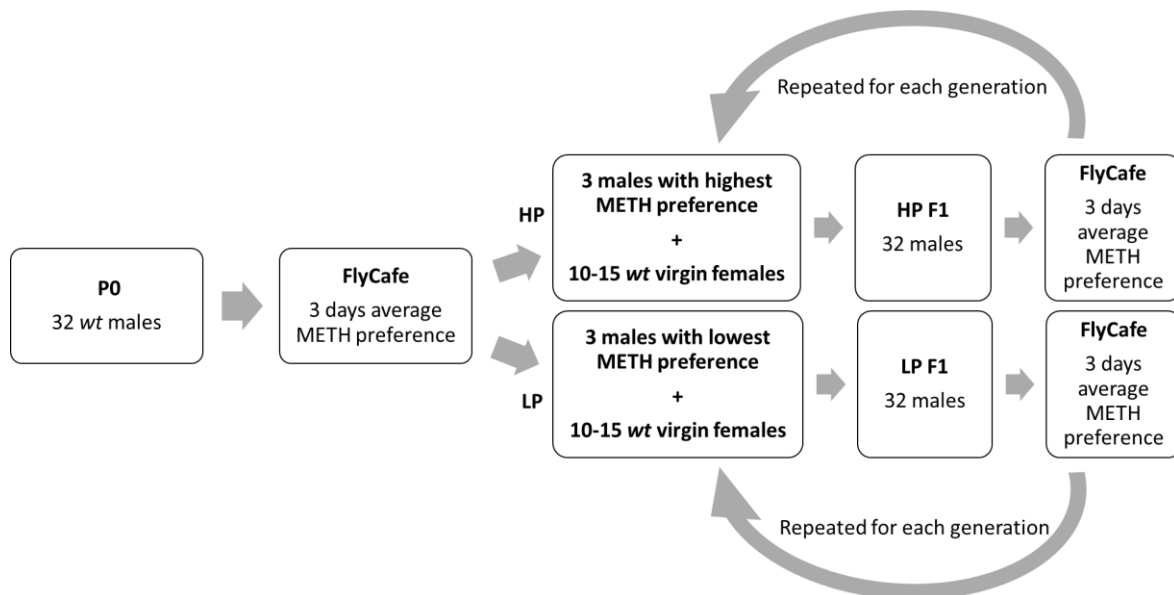


Figure 15. Flow chart of the selective breeding for the high and low METH preference. *Male flies from the parental generation were offered sugar-only or sugar-METH options over three days in FlyCafe. Based on the METH preference score, the top three HP and bottom three LP males were selected in each generation for breeding with virgin females from the parental line, their progeny was collected and tested in FlyCafe again. The breeding continued for 30 generations.*

In the parental (P0) line, three males with the highest average three-day preference were selected and bred with *wt* virgins to establish the first generation of the HP line. Similarly, three flies with the lowest average three-day preference were chosen and bred with *wt* virgins to start the first generation of the LP line. Once the F1 progeny emerged, we collected 32 HP males (22 experimental + 10 controls) and 32 LP males (22 experimental + 10 controls). These flies underwent FlyCafe testing, and the three individuals with the highest preference were chosen for the HP line, while the three with the lowest preference were selected for the LP line. This breeding and selection process was repeated for a total of 30 generations.

FlyCafe experiments during the selection process were exclusively conducted on male flies and were crossed with virgin females from P-line. Flies that perished during any of the three days of FlyCafe were excluded from further analysis to ensure the accuracy and reliability of the preference measurements.

3.3.3 Approach 3: Proteomic Analysis

Two distinct proteomic analyses were conducted (Figure x). The first targeted proteins associated with low and high preferential METH SA phenotypes achieved through selective breeding (Proteomics 1). The second focused on differences in brain proteomes among flies

that either developed or did not develop LS to METH after they received two doses of vMETH in FlyBong (Proteomics 2).

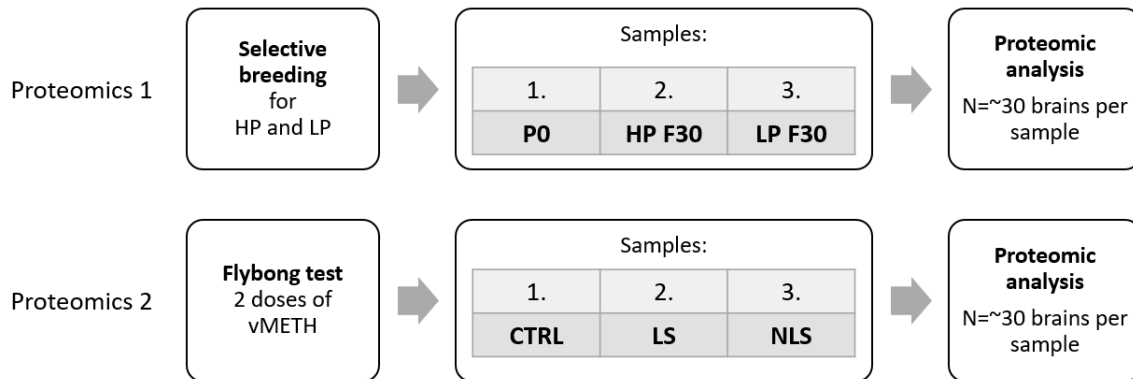


Figure 16. Proteomic analyses of fly brains after selective breeding for high and low METH preference (Proteomics 1) or exposing *wt* flies to two doses of vMETH (Proteomics 2). *PO* – parental generation in selective breeding, *HP F30* – 30th generation of HP line, *LP F30* – 30th generation of LP line; *CTRL* – *wt* flies exposed to heated air in FlyBong, *LS* – *wt* flies exposed to two doses of vMETH in FlyBong

The primary aim of Proteomics 1 was to identify proteins that changed because of selective breeding for METH preference, thereby defining the HP or LP phenotype. Proteomics 2 aimed to identify proteins in *wt* flies that were induced after the two doses of vMETH, depending on whether they developed LS compared to flies that did not develop LS and control flies.

3.3.3.1 Proteomics 1

3.3.3.1.1 Selective breeding

Selective breeding yielded highly divergent strains with varying preferences for METH, HP and LP, determined by quantifying their consumption of Sugar food with and without METH. Subsequently, adult males from strains with high and low METH preference were selected

to form two experimental groups of 30 flies each. The control group comprised males from the P0 generation, which had no prior exposure to METH.

3.3.3.1.2 *Proteomics and data analysis*

For proteomic analysis, brain tissue samples were collected from male flies representing the control P0 generation and the F30 progeny of both HP and LP lines, which were developed through 30 generations of selective breeding using the FlyCafe assay. The brain tissue samples from the HP, LP, and CTRL lines underwent proteomic analysis following the protocol outlined in the "General Assays and Protocols" section.

In summary, brain dissection was followed by protein isolation using RIPA extraction buffer, with subsequent quantification of the extracted proteins. Samples were then prepared using Laemmli buffer and sent to the University of Tübingen for further analysis. There, 1D SDS-PAGE, InGel digestion, and LC-MS/MS were performed in collaboration with Dr. Ana Velić. For fragmentation, the twelve most highly charged ions were selected for higher-energy collision dissociation (HCD). Raw data files were processed using the MaxQuant software suite version 1.6.7.0, with spectral analysis conducted using the Andromeda search engine within MaxQuant. The analysis targeted the Uniprot *D. melanogaster* complete proteome database, along with a database containing frequently observed contaminants. Raw data analysis was performed with a false discovery rate (FDR) setting of 1%. The processed data were exported as .txt files for further statistical examination using the Perseus tool.

We received the results in .xls format, providing a comprehensive list of all detected proteins in the samples, along with comparisons highlighting proteins with differential abundance across the samples. For annotation and enrichment analysis, detecting significant molecular pathways and data visualization, we employed STRING⁴ online tool.

⁴ <https://string-db.org/>

3.3.3.2 Proteomics 2

3.3.3.2.1 FlyBong test

Three to five-day-old *wt* male flies were collected one day before testing (a total of 128 flies) using CO₂ anesthesia, loaded into plastic DAMS tubes with food, and placed in 4 vertical DAMS monitors (32 flies per monitor). The monitors were then connected to the FlyBong system. In 3 out of 4 volatilization chambers, 75 µl of methamphetamine (METH-HCl) dissolved in 96% ethanol at a concentration of 10 mg/ml was added. In one volatilization chamber, which served as a control, no METH was added.

On the day of the test, flies were exposed to two doses of vMETH with a 10-hour interval (at 09:00 and 19:00 PM), and the change in their locomotor activity was quantified. The control group underwent the same protocol but without vMETH exposure, being exposed only to heated air.

1. dose:



2. dose:



Figure 17. FlyBong test procedure for exposing *wt* flies to two doses of vMETH before Proteomics 2.

The test procedure began with the measurement of initial locomotor activity (baseline) 10 minutes before each administration of vMETH or heated air (Figure x.). Subsequently, a 7-minute heating period was employed to attain the optimal temperature for METH volatilization. Following this, vMETH or heated air was administered for 1 minute using pumps. Finally, locomotor activity was measured 10 minutes after vMETH or heated air administration.

3.3.3.2.2 FlyBong data analysis

DAMS monitors collect data on the locomotor activity of flies by recording a signal (count) each time a fly crosses the infrared beam passing through the center of the plastic tubes where individual flies are housed.

Locomotor activity data were analyzed immediately after completing the test at the level of individual flies. For each fly, the change in average locomotor activity 10 minutes after the first and second administrations was calculated relative to the baseline locomotor activity. Subtracting the baseline activity from the locomotor activity after administration resulted in the response to the 1st dose (vMETH 1st) which is a measure of sensitivity to vMETH and response to the 2nd dose (vMETH 2nd) which indicates whether flies developed LS or not.

3.3.3.2.3 Criteria for separation into CTRL, LS and NLS groups

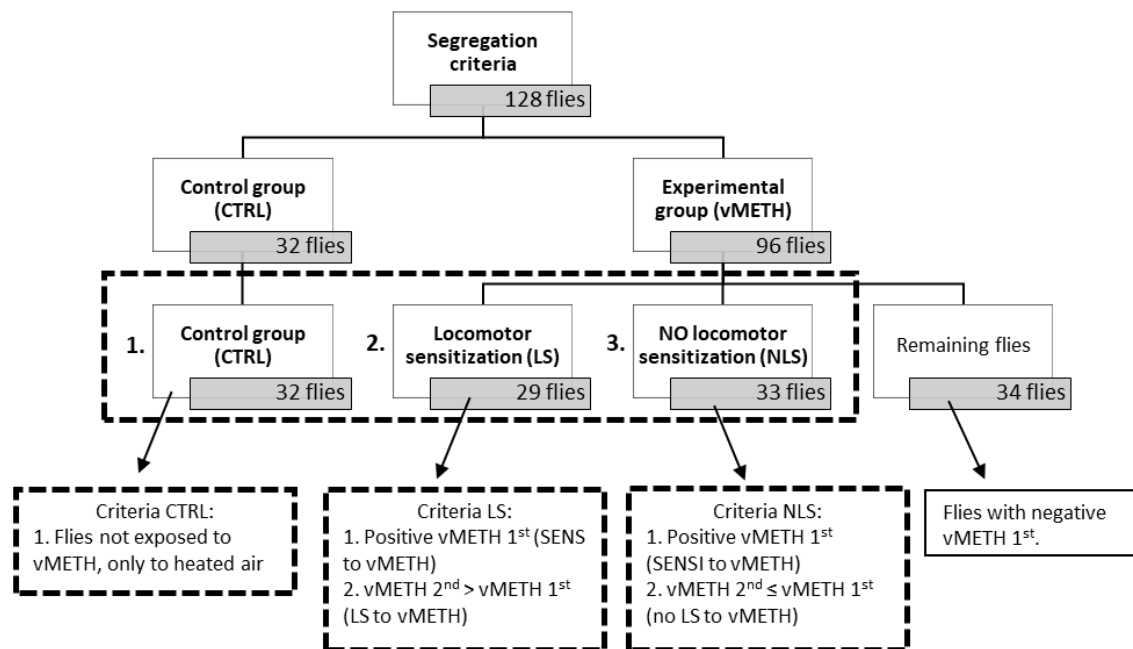


Figure 18. Criteria for segregation into CTRL, LS and NLS groups for proteomic analysis.

Flies were categorized into three groups (Figure 18.), including control group exposed only to heated air (CTRL), flies that developed locomotor sensitization to vMETH (LS) and flies that did not show locomotor sensitization to vMETH (NLS). The fourth group was excluded from the further analysis because their first response was negative, meaning they did not show SENS to the first dose of vMETH.

The criteria for the CTRL group specified that flies were exclusively exposed to heated air, with no exposure to vMETH. For the locomotor LS group, the criteria involved a positive response to vMETH during the first administration (indicating sensitivity, SENS) and a subsequent increase in locomotor activity following the second vMETH administration compared to the first (indicating LS). Conversely, the criteria for the NLS group entailed a positive response to vMETH during the first administration (indicating SENS), but no increase in locomotor activity following the second vMETH administration compared to the first (indicating that LS was not developed).

3.3.3.2.4 *Proteomics and data analysis*

After data analysis files were collected from the monitors, grouped as CTRL, LS and NLS and the proteomic analysis was performed as described in "Proteomic analysis" section of "General Assays and Protocols".

We received the list of all identified proteins as MS Excel files, as well as the lists of proteins that were significantly differentially expressed after the comparison of all the samples (CTRL vs. LS, CTRL vs. NLS, LS vs. NLS), compared by t-tests.

Obtained data was then further analyzed and visualized using STRING⁵ to assess protein-protein interaction networks and functional enrichment analysis. ShinyGO⁶ online tool was used for gene ontology enrichment analysis, functional categorization, and biological significance.

3.4 Statistical Analysis

The statistical analysis was conducted using GraphPad Prism software for Windows, version 10.0.0. To compare two groups, an unpaired two-tailed Student's t-test was employed. For comparisons involving two or more groups, one-way analysis of variance (ANOVA) was utilized. In cases where there were two different categorical independent variables and one continuous dependent variable, a two-way ANOVA was performed. Subsequently, a Tukey or Bonferroni post hoc tests were applied to evaluate multiple comparisons.

⁵ <https://string-db.org/>

⁶ <http://bioinformatics.sdstate.edu/go74/>

4. RESULTS

4.1 Optimization of the CAFE method for measuring self-administration (SA)

The CAFE assay is used to quantify the average volume of consumed food from a group of flies placed in a vial, however this method is not conducive for easy monitoring of behavior of individual flies (290). We used the basic foundations of the CAFE technique to construct a method that enabled quantification of liquid food consumption in individual flies, from which it is possible to calculate the preference for regular food containing METH (METH food) against regular food in a two choices assay. Combining Drosophila Activity Monitoring System with CAFE into new assay named FlyCafe, we were able to measure locomotor activity and dwell time spent at each end of the tube for each individual fly with one-minute resolution. Control flies were offered a choice of both capillaries with regular food (control for side preference), while experimental flies were offered one capillary with regular food and the other with METH food. The amount of consumed food was monitored daily from each capillary. To control for the side preference and humidity we performed optimization procedures described in Methods, with the results shown in the following figures.

4.1.1 Evaporation control

To ensure the accuracy of liquid food measurements, we recognized the need for evaporation optimization based on previous experiences with the regular CAFE assay. It was evident that optimizing evaporation was crucial to reduce result inconsistencies and enhance reproducibility. This optimization was essential for calculating the precise amount of food ingested by the flies, especially considering the substantial fluctuations observed during initial preliminary tests.

The optimization of the FlyCafe assay involved adjusting environmental conditions, specifically focusing on humidity and temperature, which directly influence the evaporation

of liquid food. Food evaporation was measured under three distinct conditions: at room conditions (22 °C, 60% humidity), inside the incubator (24 °C, 75% humidity), and within the evaporation control system (ES). The ES system comprised a plastic tub containing 1 liter of water, sealed with cling film, and placed in the incubator. This comprehensive optimization aimed to establish controlled conditions for liquid food measurements, ensuring reliable and reproducible results in subsequent experiments.

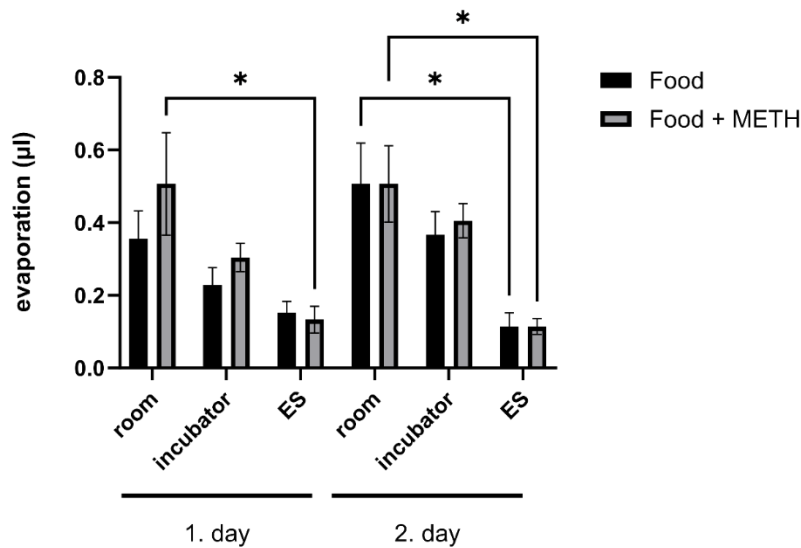


Figure 19. Evaporation of liquid food is significantly lower when the capillaries are placed in evaporation control system (ES).

The amount of liquid food which evaporated from capillaries was measured 2 days in a row. N=4-6 capillaries per group.

We showed that use of ES significantly reduced the amount of liquid food that evaporated from the capillaries (Figure 19.). Based on these results, we ensured an adequate evaporation control system for each subsequent FlyCafe experiment.

4.1.2 Amount of ingested food and side preference control

After ensuring optimal humidity/temperature conditions, we were able to continue the optimization. We checked if the flies always ingest similar total amount of food, whether this amount varies across the time and whether the control flies have stable absence of side preference.

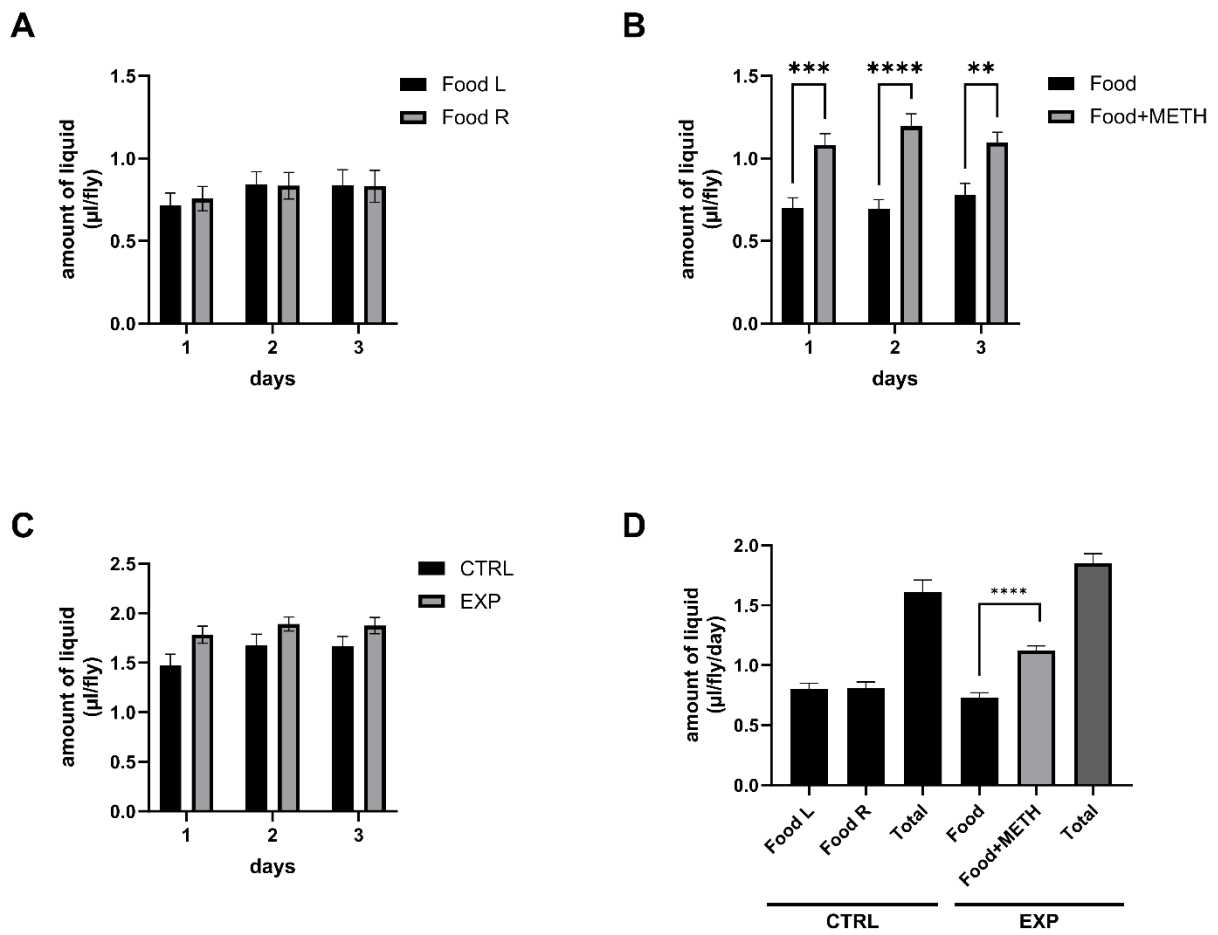


Figure 20. Experimental group (EXP) consumes more METH food than regular food, but the total amount does not differ from the control group during 3-day experiment.

A. Mean amount of consumed food \pm SEM per day for control group (CTRL, n=35 flies). **B.** Mean amount of consumed food \pm SEM per day for experimental group (METH, n=74 flies) **C.** Mean total amount of consumed food \pm SEM for experimental group (METH, n=74 flies) and control (CTRL, n=35 flies). **D.** Average amount of liquid regular food, METH food and total food consumed for 3 days \pm SEM is shown. Control flies for side preference had regular food choice in both capillaries (CTRL, n=35), experimental flies had a choice between regular food and 0.15 mg/ml METH food (EXP, n=74 flies). **** $p < 0.001$, t-test for independent samples.

In FlyCafe experiment, the control group exhibited no side preference, consuming equivalent amounts of regular food from both capillaries over a three-day period (Figure 20A). On the contrary, the experimental group consistently consumed a significantly higher quantity of METH food across all three days, with no observable variation in consumption levels between days (Figure 20B). Importantly, there was no evident difference in the total food intake between the control and experimental groups across the three-day duration of the experiment (Figure 20C).

Figure 20D shows the average daily consumption over the course of the three-day experiment for both capillaries in controls (Food L and Food R) and experimental (Food and Food+METH) group, as well as total amount of consumed food. Despite the differential intake of METH food by the experimental group, both groups exhibited similar average consumption levels of liquid food. This finding underscores the selective preference for METH food in the experimental group while highlighting the maintenance of comparable overall consumption patterns between the groups.

As we have shown that flies consume the same total amount of food, to simplify the graphical representations of FlyCafe measurements, we will use preference as a measure of preferential SA of psychostimulants.

Table 4. Example of amount of ingested food and preference calculations for FlyCafe assay.

One row represents one fly. After performing the same calculations for each fly in the experiments, mean values \pm SEM for amount of liquid and/or preference were calculated for each group and shown on graphs.

	BASELINE/cm (DAY 0)		MEASUREMENT/cm (DAY 1)		DIFFERENCE 1/cm (MEASUREMENT-BASLINE)		DIFFERENCE 2/cm (DIFFERENCE 1 - EVAPORATION)			AMOUNT/ μ (DIFFERENCE 2 * 1.52)			PREFERENCE/ μ (FoodMETH-Food) or (Food RIGHT - Food LEFT for CTRL)
	Food LEFT 1 (Food LEFT, Food RIGHT)	Food RIGHT 1	Food LEFT 2	Food RIGHT 2	Food LEFT	Food RIGHT	Food LEFT- EVAPORATION Food	Food RIGHT- EVAPORATION Food	TOTAL	Food LEFT in μ	Food RIGHT in μ	TOTAL	
CTRL (Food LEFT, Food RIGHT)	2.30	2.30	1.60	1.60	0.70	0.70	0.70	0.70	1.40	1.06	1.06	2.13	0.00
EXP1 (Food LEFT, FoodMETH RIGHT)	2.30	2.30	1.90	1.30	0.40	1.00	Food- EVAPORATION Food	FoodMETH- EVAPORATION FoodMETH	TOTAL	Food in μ	FoodMETH in μ	TOTAL	0.91
EXP2 (FoodMETH LEFT, Food RIGHT)	2.30	2.30	1.30	1.90	1.00	0.40	FoodMETH- EVAPORATION FoodMETH	Food- EVAPORATION Food	TOTAL	FoodMETH in μ	FOOD in μ	TOTAL	0.91

EVAPORATION	Food	FoodMETH
	0.37	0.35

Table 4 represents a detailed step-by-step process for calculating preference in the FlyCafe assay. The baseline measurement is taken on the initial day, representing the initial height of the liquid food meniscus inside the capillary in centimeters before the experiment begins. After 24 hours, the height of the meniscus is remeasured (Measurement) for each capillary. The difference between the measurement and baseline (Difference 1) is calculated in centimeters for each of the two capillaries per glass tube housing one fly. Next, the average evaporation, measured and calculated for each type of food, is subtracted from Difference 1 (Difference 2). To determine the volume of consumed food in microliters (Amount), Difference 2 is multiplied by the cross-sectional area of the capillary (1.52 cm²). Finally,

preference is calculated by subtracting the amount in the left capillary from that in the right for the control group, or by subtracting the amount of regular food from the amount of METH food for the experimental group. Cases where preference is equal to zero indicate an equal consumption of METH and regular food, values greater than zero represent a preference for METH, and values below zero indicate METH avoidance.

4.1.3 Flies preferentially self-administer METH food over regular food

To measure whether voluntary SA of METH in *Drosophila* males is dose dependent we exposed flies to 0.10, 0.15, 0.20 and 0.25 mg/ml of METH food and compared results to a control group with the choice of regular food in both capillaries. Each male was held in glass tubes for three days and the amount of METH and regular food that each fly consumed was quantified for each 24-hour period and preference was calculated.

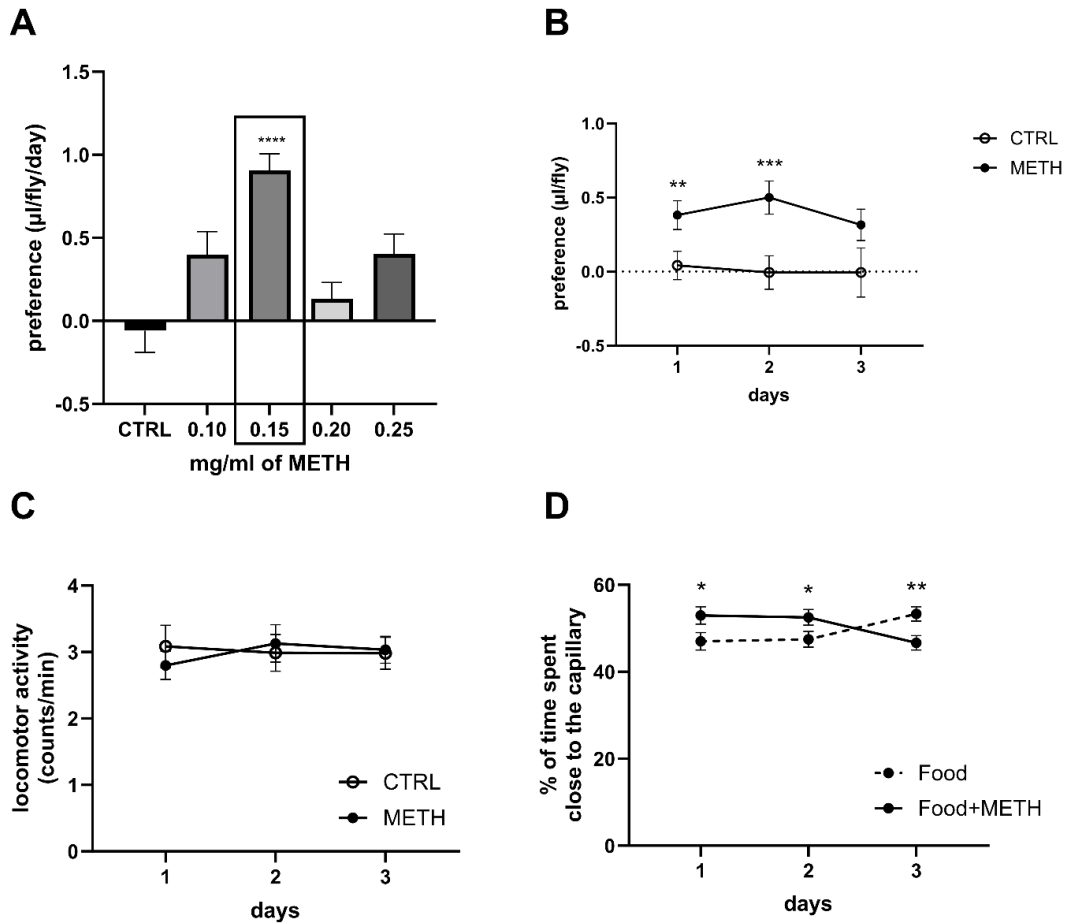


Figure 21. *Drosophila* males preferentially consume METH food over regular food. A. Dose dependent preference for METH food. Average preference during a 3-day experiment \pm SEM is calculated for METH concentrations of 0.10 mg/ml ($n=12$ flies), 0.15 mg/ml ($n=14$ flies), 0.20 mg/ml ($n=12$ flies) and 0.25 mg/ml ($n=13$ flies). Flies had one capillary with regular food and another with METH food, at varying concentrations. **** $p<0.001$, One-way ANOVA with Bonferroni correction. CTRL group ($n=11$ flies) for side preference had regular food in both capillaries. **B.** Daily preference for 0.15 mg/ml METH food. Mean preference \pm SEM per day for experimental group (METH, $n=74$ flies) and control (CTRL, $n=35$ flies). ** $p=0.0430$, *** $p=0.0060$, Two-way repeated measures ANOVA with Bonferroni correction **C.** Average

*daily locomotor activity ± SEM per day for experimental group (METH, n=74 flies) and control (CTRL, n=35 flies) D. Average daily % of time spent close to the capillaries containing METH food (Food+METH, n=74) and regular food (Food, n=74) for experimental group (EXP) . *p=0.0751, *p=0.0751, **p=0.0160, t-tests for dependent samples.*

The highest average preferential consumption during the three days was for 0.15 mg/ml METH food ($p < 0.001$, One-way ANOVA with Bonferroni correction) (Figure 21A), so we chose that concentration for further experiments. When SA of 0.15 mg/ml METH versus regular food is analyzed for each day during a 3-day experiment we observed a significant preference for METH food on the first day and second day ($p = 0.0430$ and $p = 0.0060$, Two-way RM ANOVA with Bonferroni correction) (Figure 21B).

To test if this preference can last longer than 3 days, we exposed flies to 0.15 mg/ml METH food for 7 days. The average preferential consumption for METH food for all 7 days was significant compared to the control group ($p = 0.0023$, t-test for independent samples), similar as the average 3 days consumption ($p = 0.0179$, t-test for independent samples) (Figure 22). Average preferential consumption for METH food was not significantly different between seven days, although we noticed a trend for increased consumption for second compared to the first day, after which preference for METH food remained stable and positive over subsequent days (Figure 22B).

To confirm that preferential consumption of METH does not change the overall amount of consumed food we compared the total consumption of food between control and experimental group in 3-day (Figure 21D) and 7-day experiment (Figure 22E). In both cases there was no significant difference in the total quantity of food that control, or experimental groups consumed. However, when analyzed by group, control group consumed the same quantity of regular food from both capillaries, while experimental group consumed significantly more METH than regular food ($p < 0.001$, t-test for independent samples).

The preferential consumption of METH food in either 3-day (Figure 21C and Figure 22) or 7-day experiment (Figure 22C) caused no significant increase in the locomotor activity. In the 3-day experiment, experimental group spent more time by the capillary containing METH food on the first ($p=0.0751$), and second day ($p=0.0751$), and less on the third day ($p=0.0160$, t-tests for dependent samples) (Figure 21D). However, average dwell time for 3 days is not significantly different between control and METH groups, and the same result was observed for the average 7-day dwell time (Figure 22D).

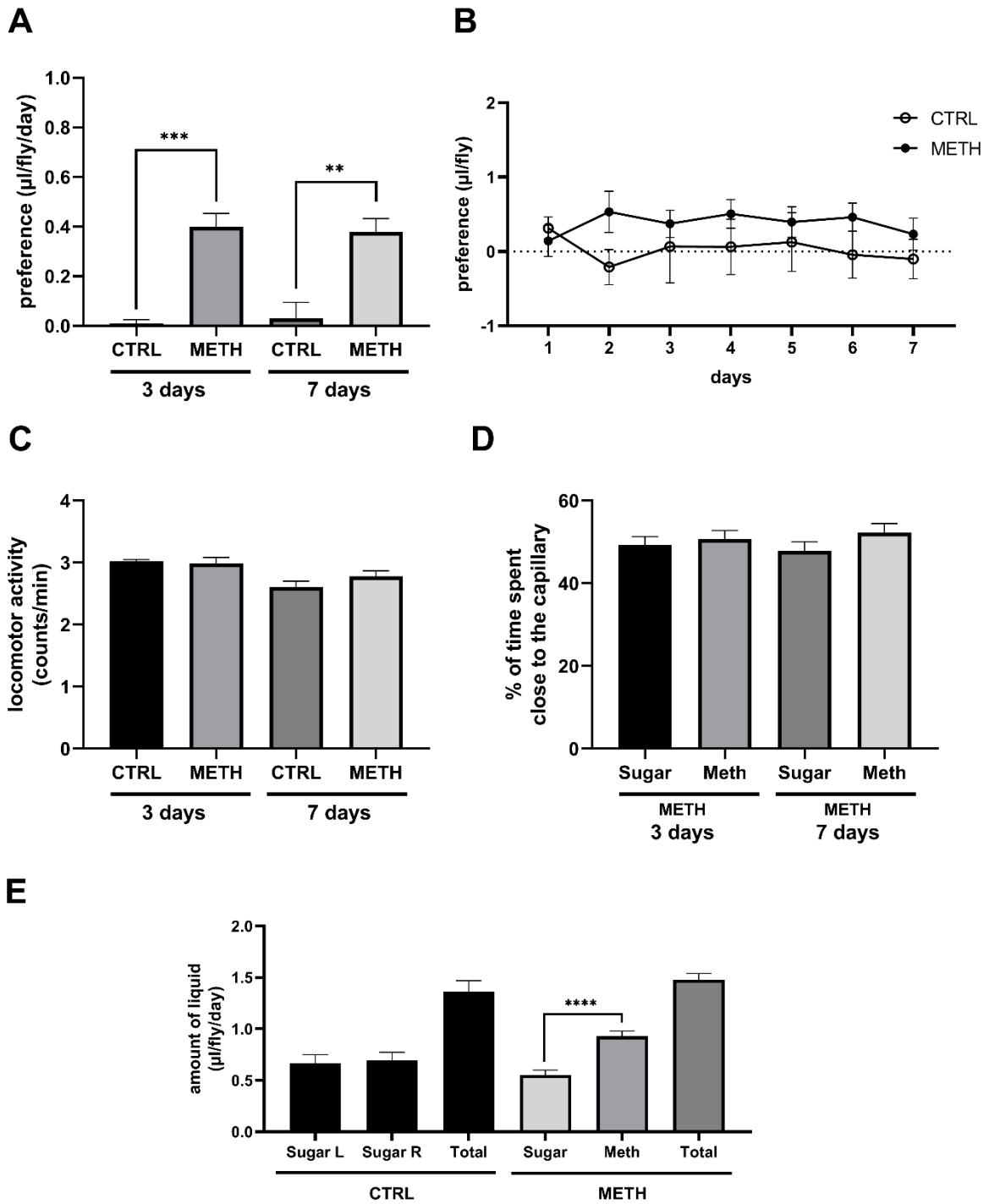


Figure 22. Preferential self-administration of METH food is long lasting.

A. The average preference for 0.15 mg/ml METH food for 7 days \pm SEM for the experimental group (METH, n=19 flies). Control flies had a regular food choice in both capillaries (CTRL, n=7) in comparison to the 3-day experiment (CTRL, n=35 flies, METH, n=74 flies)*** $p=0.0023$, ** $p=0.0179$, t-test for independent samples **B.** Average daily preference \pm SEM for 0.15 mg/ml METH food over a 7-day period for experimental group (METH, n=19 flies) and control (CTRL, n=7 flies) **C.** The average locomotor activity over a 7-day period \pm SEM for the experimental group (METH, n=19 flies) and the control (CTRL, n=7 flies), in comparison to the 3-day experiment (CTRL, n=35 flies, METH, n=74 flies) **D.** Mean percent of time spent close to the capillaries containing METH food (Meth, n=19) and regular food (Sugar, n=19) over a 7-day period \pm SEM for experimental group (METH), compared to the 3-day experiment (Sugar, n=74 flies, Meth, n=74 flies) **E.** The average amount of liquid regular food (Sugar), METH food and total food consumed during 7-days experiment \pm SEM. The control group had a Sugar food choice in both capillaries for side preference (CTRL, n=7), and the experimental group had a choice between regular food and 0.15 mg/ml METH food (METH, n=19 flies). **** $p<0.001$, t-test for independent samples.

Based on these findings, we can determine that a 3-day experiment duration is adequate for assessing whether flies exhibit preferential consumption of psychostimulants. Consequently, we employed this approach in all subsequent experiments which we conducted in FlyCafe.

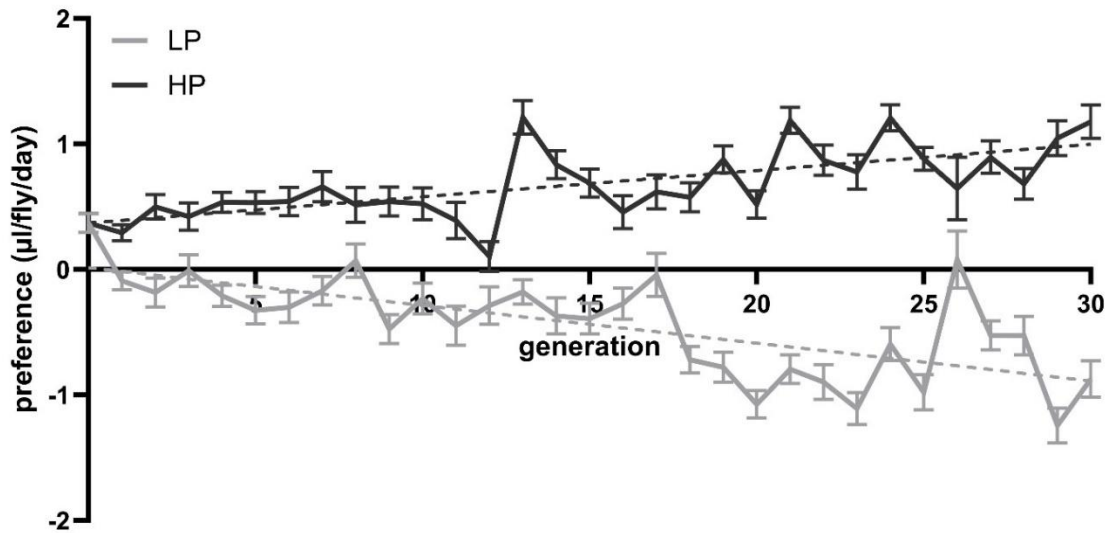
4.2 Selective breeding for preferential consumption of METH

We aimed to identify and select flies with a high or low preference for METH through a targeted breeding strategy. Utilizing the newly developed FlyCafe, we bred males exhibiting the highest or lowest preference for METH in each generation. This selective breeding process continued for 30 generations, until the response stabilized, marked by the absence of a consistent increase or decrease over several generations. The average preference was determined by calculating the mean of individual 3-day preference scores. Subsequently, three males with the highest or lowest average preferences were chosen and crossed with 10-15 female virgins to establish the next generation.

Our underlying hypothesis posits that this selective breeding approach can enable us to pinpoint genes that regulate the motivation for preferential consumption of METH. Upon the completion of the selection process, we characterized the generated lines and employed brains from the selected lines for proteomic analysis.

4.2.1 Selective breeding for 30 generations resulted in two divergent strains that differed in self-administration of METH food

A



B

Line \ Generation	1	2	3	4	5	6	7	8	9	10	11	12	13	14	15	16	17	18	19	20	21	22	23	24	25	26	27	28	29	30	
HP													*								*			*			*		*	*	
LP		*		*	*	*	*		*	*	*	*	*	*	*	*		*	*	*	*	*	*	*	*	*		*	*	*	*

C

Generation	1	2	3	4	5	6	7	8	9	10	11	12	13	14	15	16	17	18	19	20	21	22	23	24	25	26	27	28	29	30	
HP vs LP		*		*	*	*	*		*	*	*		*	*	*	*	*	*	*	*	*	*	*	*	*	*		*	*	*	*

Figure 23. Two highly divergent lines of flies with Low Preference (LP) and High Preference (HP) for METH were generated through 30 generations of selective breeding. A. The x-axis represents the generations (0 to 30th), while the y-axis represents the preference score, calculated as the difference in ingestion between regular food and 0,15 mg/ml METH-laced food measured using FlyCafe assay during three days. wt (CS) flies were used as the parental population (P line). To establish subsequent generations, three male flies with the highest preference for METH in the HP line and for the lowest preference in the LP line were selected and mated with female virgin flies to produce the next generation. The process was repeated for 30 generations, maintaining the same selection criteria. N=16-22 male flies per group in

each generation. B. Representation of statistical significance for each generation of HP and LP flies relative to the 0. generation. Statistical analysis: two-way ANOVA with Tukey post-hoc test. C. Representation of statistical significance between HP and LP flies for each generation. Statistical analysis: two-way ANOVA with Sidak post-hoc test.

Selective breeding was performed for 30 generations to establish two distinct lines of flies: High Preferring (HP) and Low Preferring (LP) flies (Figure 23A). A comparison with the initial wild-type (CS) line revealed significant differences in preference behavior (Figure 23B). For LP flies, all generations, except for generations 1, 3, 8, 17, and 26, exhibited significantly lower preference compared to the parental line. In HP flies, generations 13, 21, 24, 27, 29, and 30 showed significantly higher preference compared to the parental line. When comparing HP and LP in each generation, there was always significant difference in mean 3-day preference except in generations 1, 3, 8, 12 and 26 (Figure 23C). These results highlight the successful generation of divergent preference phenotypes through selective breeding, demonstrating the impact of genetic selection on preference behavior in the studied flies.

4.2.2 Difference in self-administration of METH food was retained after the cessation of selective breeding

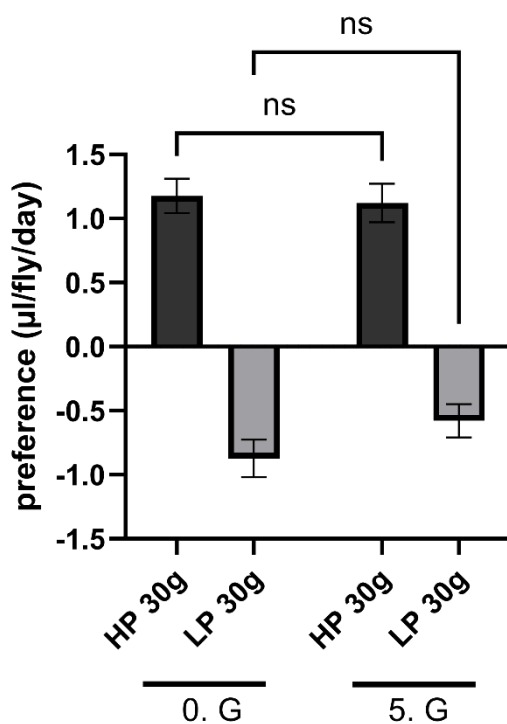


Figure 24. Phenotypes of high and low preferential consumption of METH are stable after the end of selective breeding. *The average preference for 0.15 mg/ml METH food for 3 days \pm SEM for the 30th generation of HP and LP lines (0.G, n=22 flies) and for their progeny collected after 5 generations (5.G, n=21 flies). Two-way ANOVA with Sidak post-hoc test*

To assess the stability of the established lines after the end of the selection process, we conducted a test on the progeny of the 30th generation after five generations without selection using FlyCafe. The results indicated that the preference and aversion scores remained unchanged, demonstrating the stable phenotype of the HP and LP lines even after five generations without selection (Figure 24).

4.2.3 Behavioral and morphological characterization of HP and LP lines

After the successful selection, further experiments were conducted to investigate if HP and LP flies exhibit differences in some phenotypes other than preference for METH. Such

differences would suggest that we either inadvertently selected for additional phenotypes or that differences in selected HP and LP lines have a neural basis that also regulates other behaviors. Phenotypes that were measured include locomotor activity and amount of sleep in regular light-dark conditions and in constant darkness, vertical climbing ability (negative geotaxis) and body weight. All the tests were performed on the progeny of 30th generation of selected flies.

4.2.3.1 Activity and sleep

The investigation of activity differences between the selected HP and LP lines in both LD (light:dark) and DD (dark:dark) conditions, alongside comparison to the initial P line, is crucial to understanding the impact of selective breeding for METH preference on behavioral traits.

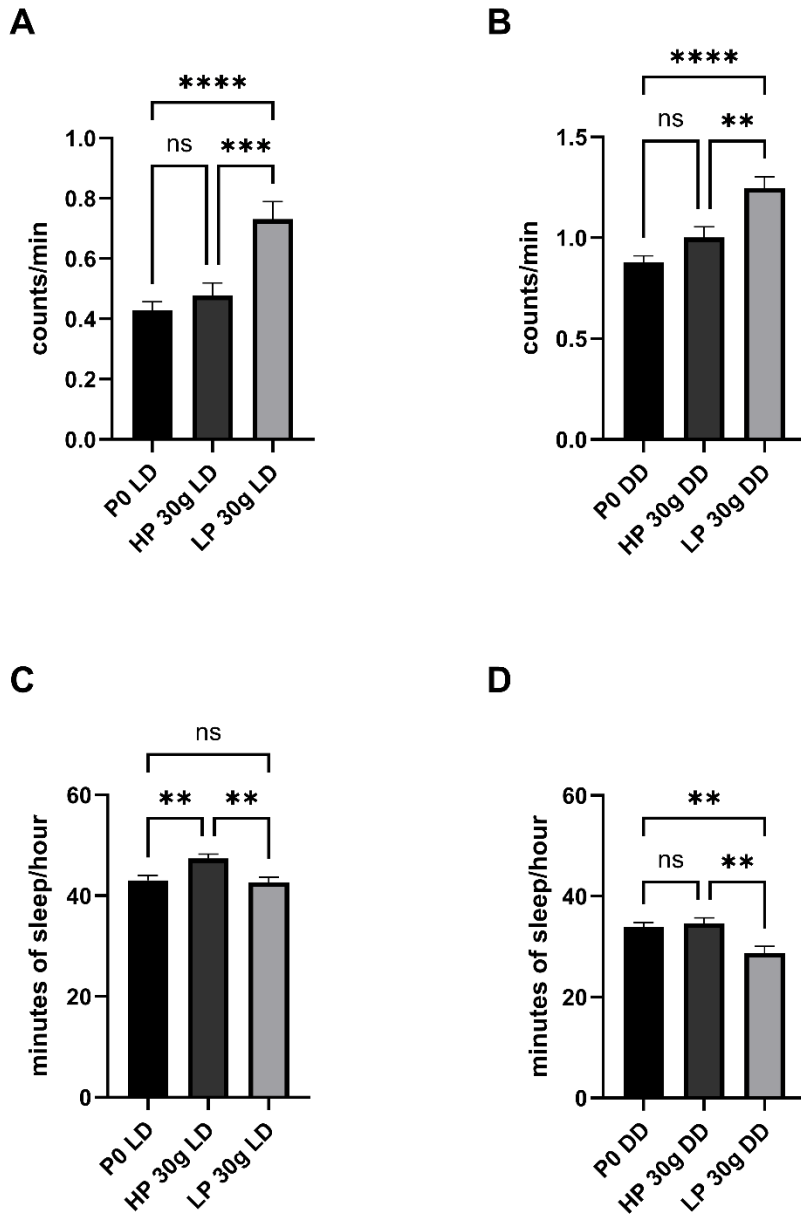


Figure 25. Increased locomotor activity in LD and reduced sleep in DD conditions in LP. Locomotor activity is measured in counts per minute for P0, HP, and LP flies in LD (A) and DD (B) conditions. Sleep is measured as the minutes of sleep in one hour for P0, HP, and LP flies in LD (C) and DD (D) conditions N=28-32 flies per group, Statistical analysis: One-way ANOVA with Tukey post-hoc test. P0: flies with wt background, P line

The LP line showed higher locomotor activity in LD that was further increased in DD conditions, while HP lines showed similar activity as the parental line. (Figure 25A and 25B). Interestingly, average sleep per hour in HP and LP lines did not mirror change in the activity. HP lines had increased sleep in LD, but not in DD conditions (Figure 25C and 25D). LP lines showed no difference in sleep amount in LD conditions despite significant increase in activity (Figure 25A and 25C). LP lines did however show a decreased amount of sleep in DD conditions (Figure 25D).

4.2.3.2 *Negative geotaxis*

To determine if the selection affected flies' vertical climbing ability and motor neurons, the selected HP and LP lines were evaluated for their negative geotaxis scores and compared to the initial *wild-type* P line (P0).

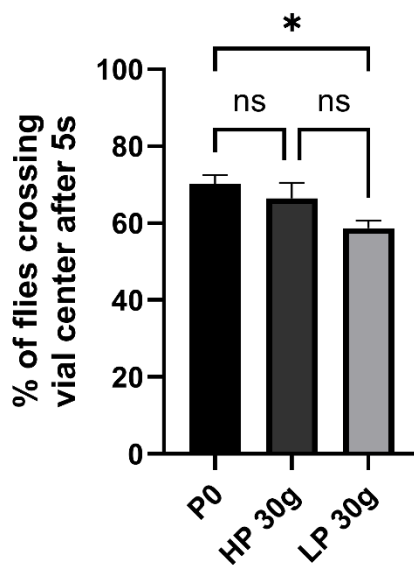


Figure 26. LP male flies have reduced vertical climbing ability compared to P0. *Negative geotaxis was measured in 3-5 days old HP and LP flies. N=5 repetitions per experiment. The average percentage of flies that crossed 3 cm after 5 seconds is shown.*

Figure 26 demonstrates that LP male flies exhibited a significant reduction in vertical climbing ability when compared to CS flies, while there was no significant difference between HP and the other two lines. This observation indicates that the low preference for METH in the LP line is associated with impaired climbing performance.

4.2.3.3 *Adult males body weight*

We conducted measurements on body weight, a widely used indicator of overall health and metabolic status, in HP and LP lines and compared it with P line. By comparing the body weight of these lines, we aimed to determine if preference selection is correlated with alterations in body weight, which could signify underlying physiological differences between HP and LP flies.

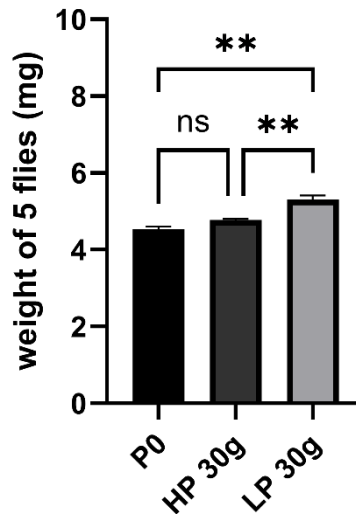


Figure 27. LP male flies have increased body weight compared to *wt* and HP. *Average body weight for P0, HP, and LP flies. N = 3 measurements, 5 flies per measurement.*

The results revealed significant differences in body weight among the tested lines (Figure 27). Specifically, LP flies exhibited significantly higher body weight compared to both HP and *wt* lines. However, no significant difference in body weight was observed between *wt* and HP flies. These findings suggest that the selection for low preference may be associated with an increase in body weight, highlighting a potential link between preference behavior and metabolic regulation in *Drosophila*.

4.2.4 Selected lines differ in their neurochemical profile

To investigate potential differences in the neurotransmitter profiles among HP, LP and their P control we quantified the concentration of dopamine (DA), octopamine (OA), tyramine (TA), glutamate (GLU), acetylcholine (ACh), and gamma-aminobutyric acid (GABA).

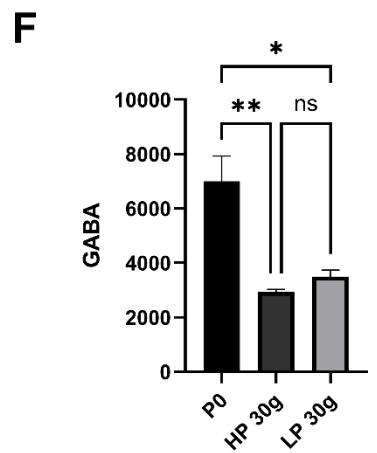
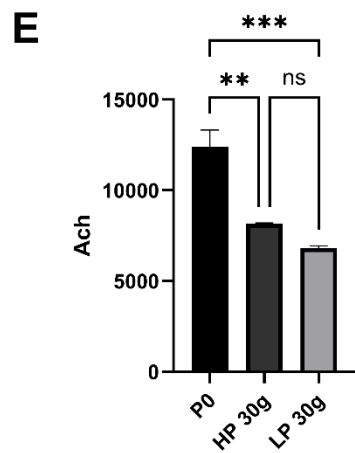
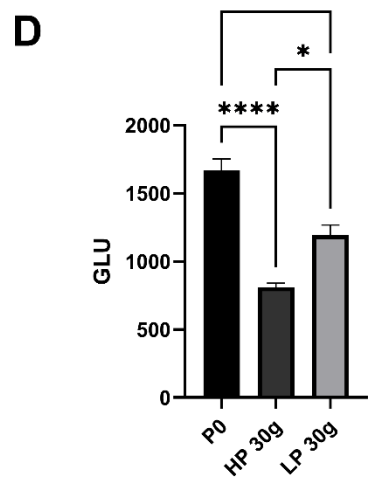
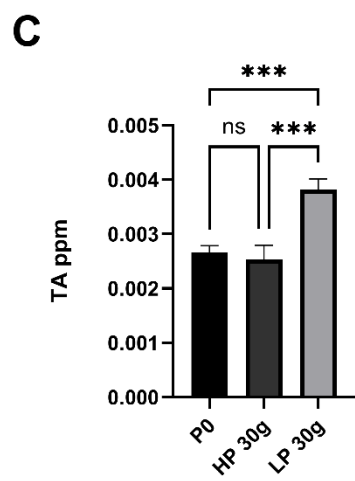
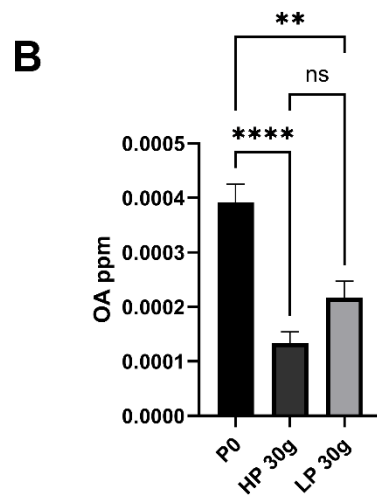
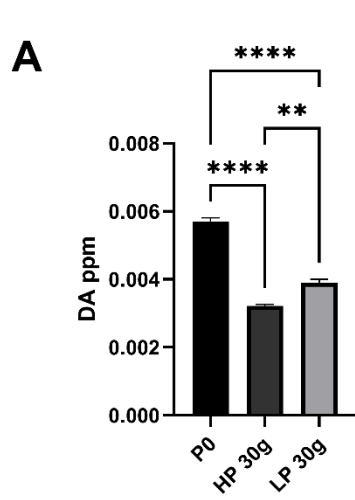


Figure 28. LP flies have increased tyramine compared to P0, while other neurotransmitter concentration are lower in HP and LP lines compared to P0.

Dopamine (A), octopamine (B), tyramine (C), glutamate (D), acetylcholine (E), and GABA (F) were measured in male wild-type flies (P0), high-preferring (HP) flies, and low-preferring (LP) flies. Measurements were obtained from duplicate measurements of sample homogenates of 15 male fly heads.

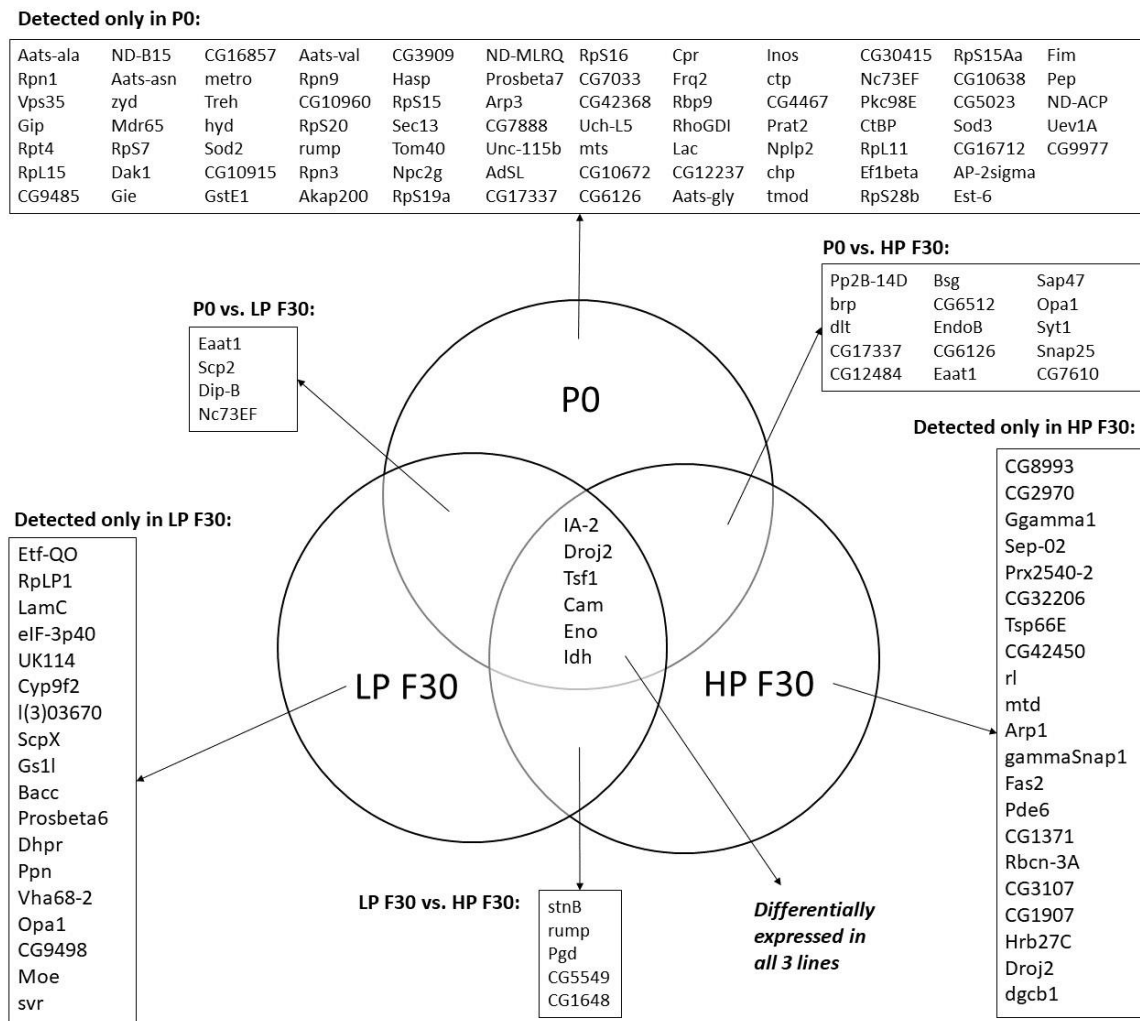
Surprisingly, most neurotransmitters did not show significant difference between HP and LP lines, however in all cases there was a significant difference between selected lines and P line (Figure 28). For example, OA, Ach and GABA (Figure 28B, 28E and 28F) concentrations were significantly lower in HP and LP lines relative to the P line but did not differ between HP and LP. There were two exceptions, DA and GLU (Figure 28A and 28D), which were significantly higher in LP line compared to HP, while both HP and LP had significantly lower levels of DA and GLU relative to P line. The most intriguing finding pertained to TA concentration (Figure 28C). The LP line showed significantly elevated levels of this neurotransmitter relative to both the P and HP lines, while there were no differences between the HP and P lines.

4.2.5 Proteomic analysis

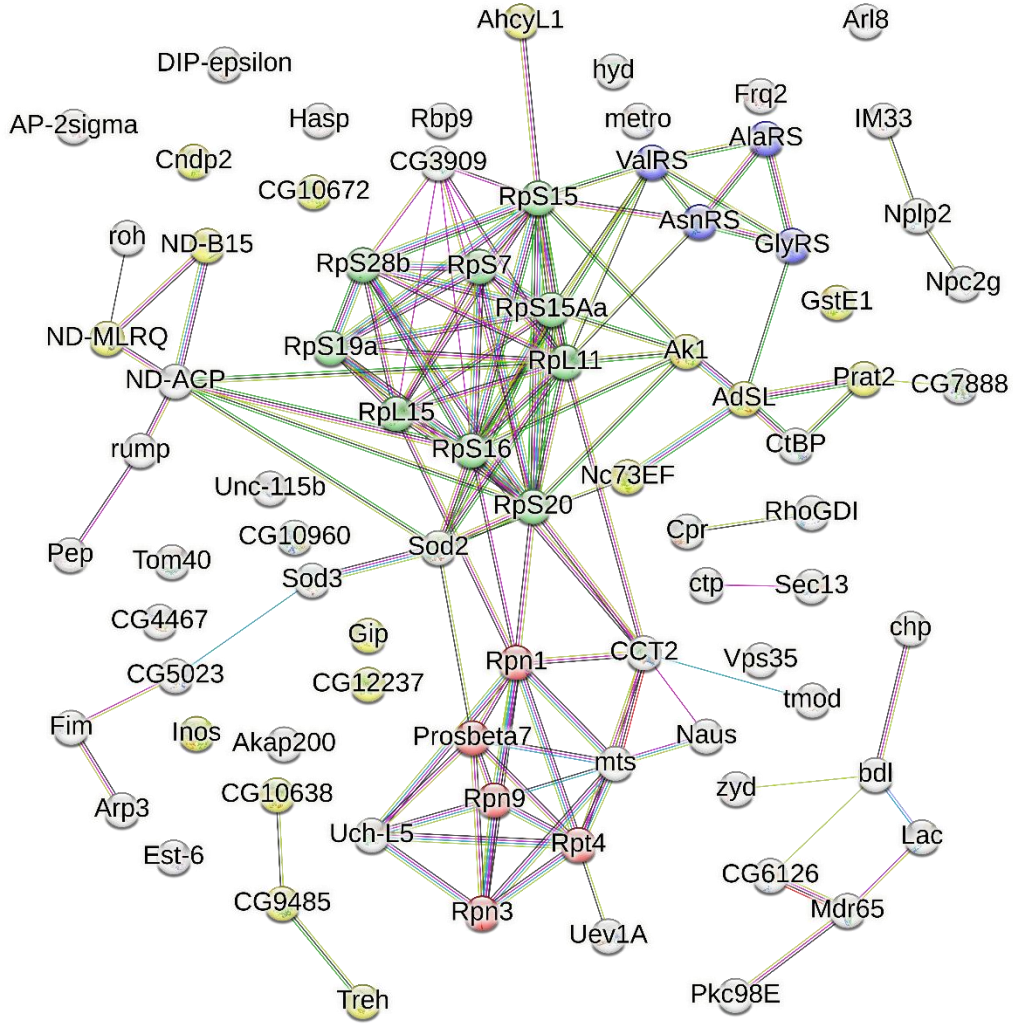
The decision to perform proteomic analysis on selected lines stems from their consistent and distinct behavioral and neurochemical phenotypes between selected and paternal lines and the uniqueness of the LP line. This suggests that LP flies may possess unique genetic and molecular characteristics that contribute to their specific traits.

Proteomics was performed on samples isolated from 30 brains per group extracted from drug-naïve progeny of 30th generation of selected HP and LP flies, and P line was used as a control. After conducting brain dissection, protein isolation, and quantification, we sent the samples to the University of Tübingen for SDS-PAGE, InGel digestion, and LC-MS/MS analysis. Processing the data with MaxQuant software yielded a list of differentially expressed proteins among the groups which we received in MS Excel format. Subsequently, we conducted enrichment analysis to reveal the biological pathways and functions associated with these proteins.

A



B



KEGG Pathways			
<i>description</i>	<i>count in network</i>	<i>strength</i>	<i>false discovery rate</i>
Proteasome	5 of 51	1.23	0.0012
Aminoacyl-tRNA biosynthesis	4 of 42	1.21	0.0063
Ribosome	9 of 132	1.07	1.54e-05
Metabolic pathways	16 of 1111	0.39	0.0209

Figure 29. Proteomic analysis of P0, HP and LP lines yielded a list of differentially expressed proteins among those 3 groups. A. The proteins which are detected only in one group and proteins detected in multiple groups which were significantly differentially expressed B. Proteins specific for P0 line visualized in STRING with enriched KEGG pathways and its belonging proteins.

Of 1380 detected proteins, only a limited number of proteins were deemed significant in our analysis (Figure 29A). 82 proteins were detected only in P0 line, 21 protein only in HP and 18 proteins only in LP. Six proteins which were detected in all three lines were significantly differentially expressed. Proteins which were detected and significant in two out of three lines were: five proteins in LP vs. HP comparison, four proteins in P0 vs. LP comparison and 15 proteins in P0 vs. HP comparison. Despite utilizing various annotation and enrichment programs such as STRING and ShinyGO, no significant pathways were detected, except for a list of proteins exclusively present in the P0 group and absent in HP and LP. Notably, four main KEGG pathways exhibited significant enrichment (Figure 11B): proteasome (5 proteins), aminoacyl-tRNA biosynthesis (4 proteins), ribosomes (9 proteins), and metabolic pathways (16 proteins).

Given the consistent divergence in phenotype observed in previous experiments between the LP line and both P and HP lines, we conducted a more in-depth examination of the 18 proteins exclusively detected in the LP sample.

Table 5. Proteins unique in LP line *Metabolism efficiency, protein turnover, and structural and signaling proteins are related to METH low preference phenotype*

<i>Group</i>	<i>PROTEIN</i>	<i>DESCRIPTION</i>
<i>Metabolism</i>	Etf-QO	Electron transfer flavoprotein-ubiquinone oxidoreductase, isoform a; Electron transfer flavoprotein-ubiquinone oxidoreductase (ETF-QO) is a mitochondrial membrane-bound

		protein. ETF-QO acts as a hub with wal and fuels electrons from fatty acid oxidation by matrix dehydrogenases into the respiratory chain (604 aa)
	Cyp9f2	Probable cytochrome P450 9f2; May be involved in the metabolism of insect hormones and in the breakdown of synthetic insecticides (516 aa)
	ScpX	Sterol carrier protein X-related thiolase; Phospholipid transporter activity; transferase activity, transferring acyl groups other than amino-acyl groups. It is involved in the biological process described with: phospholipid transport; metabolic process; Belongs to the thiolase family (544 aa)
	Gs1l	Probable pseudouridine-5'-phosphatase; Dephosphorylates pseudouridine 5'-phosphate, a potential intermediate in rRNA degradation (231 aa)
	Dhpr	Dihydropteridine reductase, isoform a; 6,7-dihydropteridine reductase activity. It is involved in the biological process described with: metabolic process (235 aa)
Protein Synthesis / Folding / Degradation	RpLP1	Large subunit ribosomal protein lp1; 60S acidic ribosomal protein P1; Plays an important role in the elongation step of protein synthesis (112 aa)
	eIF-3p40	Eukaryotic translation initiation factor 3 subunit h, isoform a; Eukaryotic translation initiation factor 3 subunit H; Component of the eukaryotic translation initiation factor 3 (eIF-3) complex, which is involved in protein synthesis of a specialized repertoire of mRNAs and, together with other initiation factors, stimulates binding of mRNA and methionyl-tRNAi to the 40S ribosome. The eIF-3 complex specifically targets and initiates translation of a subset of mRNAs involved in cell proliferation (338 aa)
	UK114	2-iminobutanoate/2-iminopropanoate deaminase; RutC family protein UK114; Molecular chaperone. Seems to fulfill an ATP- independent, HSP70-like function in protein folding. May protect essential factors of cell proliferation during heat shock. No role in calpain activation (138 aa)
	Prosbeta6	Proteasome subunit beta type-1; The proteasome is a multicatalytic proteinase complex which is characterized by its ability to cleave peptides with Arg, Phe, Tyr, Leu, and Glu adjacent to the leaving group at neutral or slightly basic pH. The proteasome has an ATP-dependent proteolytic activity; Belongs to the peptidase T1B family (235 aa)
	svr	Carboxypeptidase D; Required for the proper melanization and sclerotization of the cuticle; Belongs to the peptidase M14 family (1439 aa)

Structural Proteins	LamC	Lamin c, isoform a; Lamin-C; Lamins are components of the nuclear lamina, a fibrous layer on the nucleoplasmic side of the inner nuclear membrane, which is thought to provide a framework for the nuclear envelope and may also interact with chromatin (By similarity). In spermatocytes, regulates cytokinesis during meiosis (640 aa)
	Chchd3	Coiled-coil-helix-coiled-coil-helix domain-containing protein 3, mitochondrial; Lethal (3) 03670 (223 aa)
	Moe	Moesin/ezrin/radixin homolog 1; Involved in connections of major cytoskeletal structures to the plasma membrane. Together with wgn, involved in control of axon targeting of R8 and R2-R5 photoreceptors, independent of egr. In the nucleus, recruited to sites of active transcription by RNA polymerase II where it has a role in nuclear mRNA export together with the mRNA export factor PCID2 and other messenger ribonucleoprotein (mRNP) particles (649 aa)
	Ppn	Papilin; Essential extracellular matrix (ECM) protein that influences cell rearrangements. May act by modulating metalloproteinases action during organogenesis. Able to non-competitively inhibit procollagen N-proteinase, an ADAMTS metalloproteinase; Belongs to the papilin family (2898 aa)
Signaling and Regulation	Bacc	Bacchus, isoform c; Bacchus; Negatively regulates tyramine beta-hydroxylase tbh and thus the conversion of tyramine (TA) to octopamine (OA). In tyrosine decarboxylase 2 (Tdc2) neurons, acts in an amine-mediated signaling pathway to negatively regulate acute ethanol sensitivity probably via tbh-mediated depletion of TA (152 aa)
	Vha68-2	V-type proton atpase catalytic subunit a isoform 2; Vacuolar H[+] ATPase 68 kDa subunit 2 is a component of the V1 subunit of the vacuolar ATPase, which acidifies endosomal compartments including the lysosome and influences the activity of several signaling pathways (614 aa)
	Opa1	Optic atrophy 1 ortholog, isoform a; Optic atrophy 1 (Opa1) is a dynamin-related GTPase that mediates fusion of the inner membrane of mitochondria. Opa1 usually works with Marf to coordinately fuse both mitochondrial membranes. Opa1 activity is regulated by proteolytic processing; Belongs to the TRAFAC class dynamin-like GTPase superfamily. Dynamin/Fzo/YdjA family (972 aa)
	CG9498	Uncharacterized protein; FI04444p; Transferase activity, transferring phosphorus-containing groups (424 aa)

There was no specific pathway of interest detected among 18 proteins unique for LP line (Figure 30), but we observed the function of listed proteins (Table 5). These proteins encompass diverse functional categories and include those involved in energy metabolism, such as Electron Transfer Flavoprotein-Ubiquinone Oxidoreductase (Etf-QO); ribosomal proteins like Large Subunit Ribosomal Protein lp1 (RpLP1); and nuclear structural components, exemplified by Lamin C (LamC). Additionally, proteins implicated in translation initiation, such as Eukaryotic Translation Initiation Factor 3 Subunit H (eIF-3p40), and molecular chaperones, like 2-iminobutanoate/2-iminopropanoate Deaminase (UK114), were also detected. Another group of proteins identified includes those potentially involved in detoxification mechanisms, exemplified by Probable Cytochrome P450 9f2 (Cyp9f2); mitochondrial functions, such as Coiled-Coil-Helix-Coiled-Coil-Helix Domain-Containing Protein 3 (Chchd3); and phospholipid transport, represented by Sterol Carrier Protein X-Related Thiolase (ScpX). Furthermore, proteins associated with RNA degradation, such as Probable Pseudouridine-5'-Phosphatase (Gs1l), and neurotransmitter regulation, like Bacchus (Bacc), were also observed. Other proteins identified include those involved in proteasome-mediated protein degradation (Proteasome Subunit Beta Type-1, Prosbeta6), metabolic processes (Dihydropteridine Reductase, Dhpr), extracellular matrix organization (Papilin, Ppn), and intracellular pH regulation (V-Type Proton ATPase Catalytic Subunit A Isoform 2, Vha68-2). Lastly, proteins implicated in mitochondrial fusion (Optic Atrophy 1 Ortholog, Opa1), cytoskeletal organization (Moesin/Ezrin/Radixin Homolog 1, Moe), and cuticle structure development (Carboxypeptidase D, svr) were also detected. Importantly, these proteins were specific to the low-preference phenotype, suggesting their involvement in mediating responses to METH exposure and addiction-related behaviors in *Drosophila*.

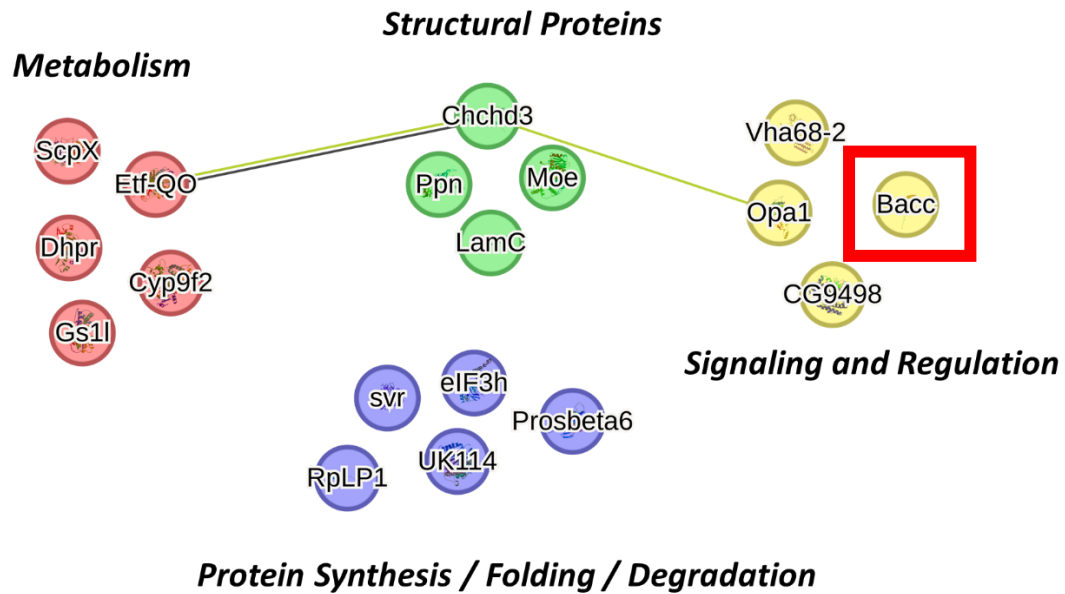


Figure 30. Bacchus, a negative regulator of tyramine beta-hydroxylase, is detected among proteins present only in the brains of LP flies and is not present in HP nor CS lines. 18 proteins specific for LP line visualized in STRING.

We selected Bacchus for further analysis due to its potential relevance to addiction-related behaviors, particularly considering its involvement in neural processes associated with ethanol addiction (291). Notably, Bacchus was detected exclusively in the LP line, where elevated TA levels were observed in our neurochemical analysis. This observation suggests a potential connection between Bacchus and TA metabolism in addiction-related phenotypes. Bacchus is known to negatively regulate tyramine beta-hydroxylase (Tbh), an enzyme involved in the conversion of TA to OA. This regulatory function of Bacchus on Tbh-mediated metabolism of TA could have implications for addiction-related responses to METH exposure in *Drosophila*. Therefore, our findings point to a potential interplay between Bacchus, Tbh, and TA metabolism in modulating addiction-related behaviors, highlighting the need for further investigation into the underlying neurobiological mechanisms.

4.2.6 Role of tyramine and its regulation in METH preference

Building upon the findings from neurochemical analysis (where LP were shown to have elevated TA) and proteomic analysis (where we detected Bacchus, a negative regulator of *Tbh*, among proteins specific for LP line), we investigated the impact of silencing *Tbh* on the preference for METH. *Tbh* plays a crucial role in the conversion of TA to OA, neurotransmitters implicated in various behavioral processes, including reward and addiction. By targeting *Tbh*, we aimed to disrupt the synthesis of OA and subsequently increasing the TA levels, similar to elevated TA observed in LP line, thereby potentially altering the neural circuitry associated with METH preference. We used UAS-RNAi/Gal4 expression system to silence *Tbh* in all neurons by crossing *UAS-Tbh RNAi* line with panneuronal *elav-gal4* driver. This approach not only provides mechanistic insights into the neurochemical basis of preference behavior but also offers a means to manipulate preference phenotypes.

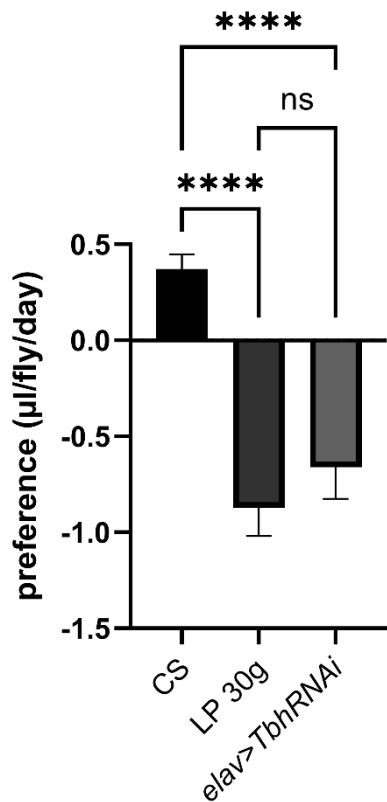


Figure 31. Panneuronal silencing of *Tbh* mimics LP phenotype.

*Average preference ± SEM for 0.15 mg/ml METH-laced food for 3 days shown for 30th generation of LP flies (n=22) and flies with *Tbh* gene silenced in all neurons (*elav>TbhRNAi*, n=22 flies).*

Average preference for METH in flies with silenced *Tbh* in all neurons was the same as preference of the 30th generation of LP flies and was significantly lower than the preference in *wt* flies (CS) (Figure 31.). These results show significant alteration in drug preference behavior and suggest an important role for *Tbh* and TA in modulating METH preference.

4.3 Self-administration and locomotor sensitization share a common molecular mechanism

We aimed to investigate the potential relationship between LS and METH SA as a way to investigate if these two phenotypes share a common neuronal or genetic basis. We designed two complementary experiments. In the first flies were tested for their SA phenotype using the FlyCafe, followed by a transfer to the FlyBong apparatus to evaluate LS. Conversely, in a different group of flies we first measured the LS in the FlyBong, followed by three days of METH SA in the FlyCafe. Our experimental setup allowed us to observe potential bidirectional effects between LS and SA and to examine whether the induction of LS affects preference for METH or if initial preference for METH impacts the development of LS.

4.3.1 Self-administration of METH food abolishes LS

To assess the impact of METH food self-administration on LS to vMETH, we housed flies in FlyCafe for three days with the option of regular food or 0.15 mg/ml METH food. On the

fourth day, they received two doses of 75 μ g vMETH, spaced 10 hours apart, in the FlyBong (Figure 32A).

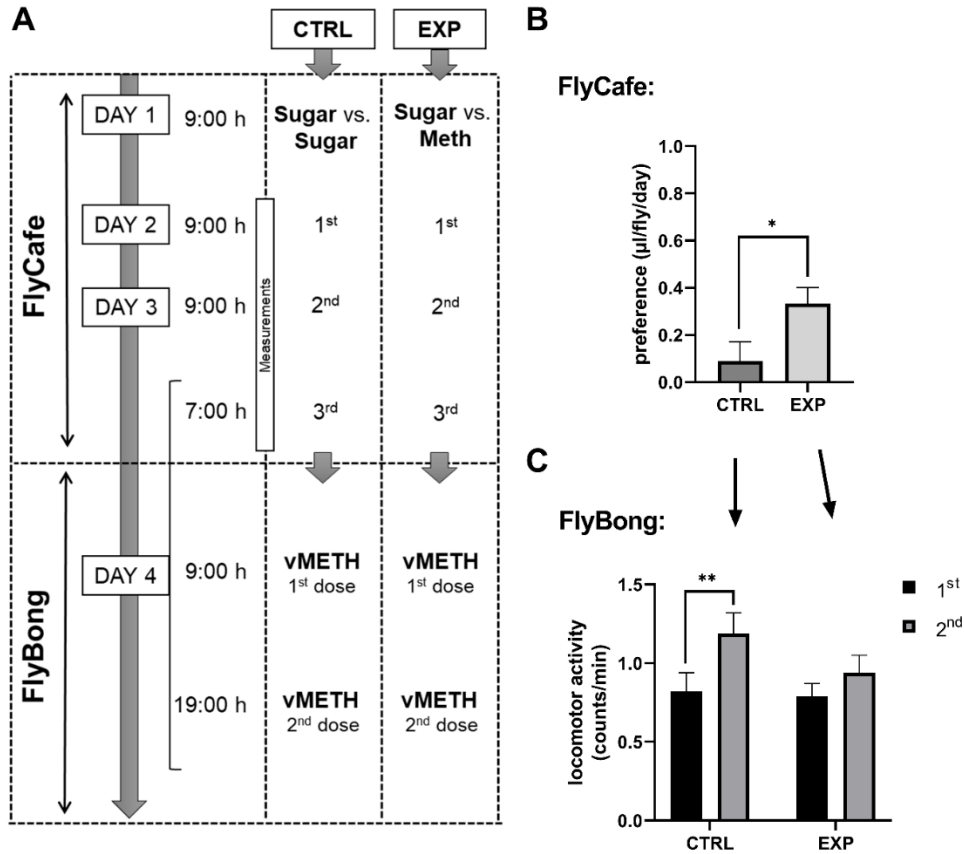


Figure 32. Preferential self-administration of METH precludes LS to vMETH. **A.** Timeline of experimental manipulations. **B.** Average preference \pm SEM for 0.15 mg/ml METH food during 3 days for control (CTRL, $n=19$ flies) and experimental (EXP, $n=39$ flies) group. $*p=0.0825$, t -test for independent samples **C.** The average locomotor activity after the 1st and 2nd exposure to 75 μ g vMETH given at 10 h interval for flies that previously self-administered food in FlyBong (CTRL, $n=19$ flies and EXP, $n=39$ flies). The difference between 1st and 2nd exposure was calculated by subtracting the baseline activity, 10 minutes before exposure, from the response, 10 minutes after the exposure to vMETH. $**p=0.0436$, t -tests for dependent samples.

We confirmed the preference for METH food in the experimental group during the pre-treatment in FlyCafe ($p=0.0825$, t-test for independent samples) (Figure 32B). Following exposure to two administrations of $75 \mu\text{g}$ of vMETH, distinct behavioral phenotypes emerged in the experimental and control groups. The control group, provided only sugar food in FlyCafe, exhibited an increased response to the second dose of vMETH, an expression of LS to vMETH ($p=0.0436$, t-tests for dependent samples), similar to the behavior of naïve flies (Figure 32C). In contrast, the experimental group, which showed preference for METH food in FlyCafe, did not develop LS, as the levels of locomotor activity after the first and second exposure to vMETH were not significantly different (Figure 32C).

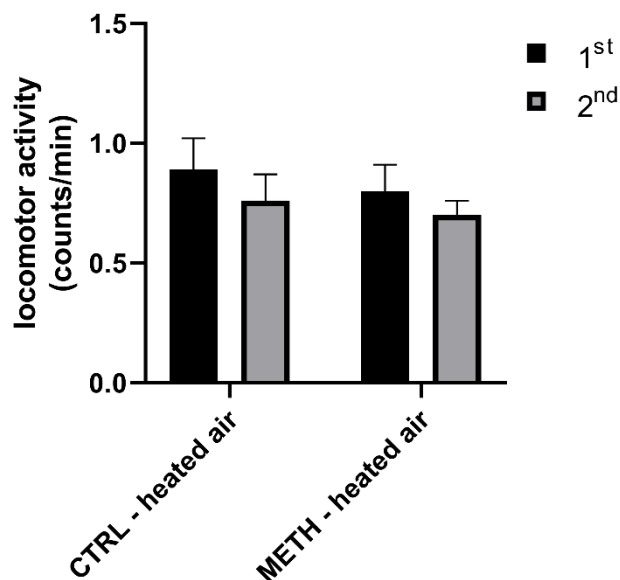


Figure 33. Flies exposed to heated air after the SA experiment show no LS. *Change in the average locomotor activity after the 1st and 2nd exposure to heated air given at 10 h intervals for flies that previously underwent the self-administration experiment. Control group offered only regular food choice in FlyCafe followed by mock treatment in FlyBong (CTRL-heated air,*

n=16 flies) and group that preferentially consumed METH over regular food in FlyCafe exposed to mock treatment (METH-heated air, n=22 flies). The change is a difference between the baseline activity, 10 minutes before, to the response 10 minutes after the exposure to heated air.

To account for potential influence of the FlyBong experimental protocol on our findings, we conducted control experiments where exposure to heated air alone did not induce LS. This had a comparable effect on flies that predominantly consumed METH food and those that exclusively consumed regular food (Figure 33). Our findings indicate that the preferential self-administration of METH food impacts the ability to develop LS to vMETH.

4.3.2 Expression of LS abolishes preference for self-administration of METH food

To investigate the influence of LS on the preferential consumption of METH food, we exposed naïve flies to two doses of vMETH in the FlyBong, then transferred them to FlyCafe to monitor their consumption of METH versus regular food for 3 days. We administered 75 µg of vMETH to two identical groups of flies, spaced 10 hours apart. Subsequently, one group (control) received only sugar choice, while the other (experimental) had the option of sugar food versus 0.15 mg/ml METH food (Figure 34A).

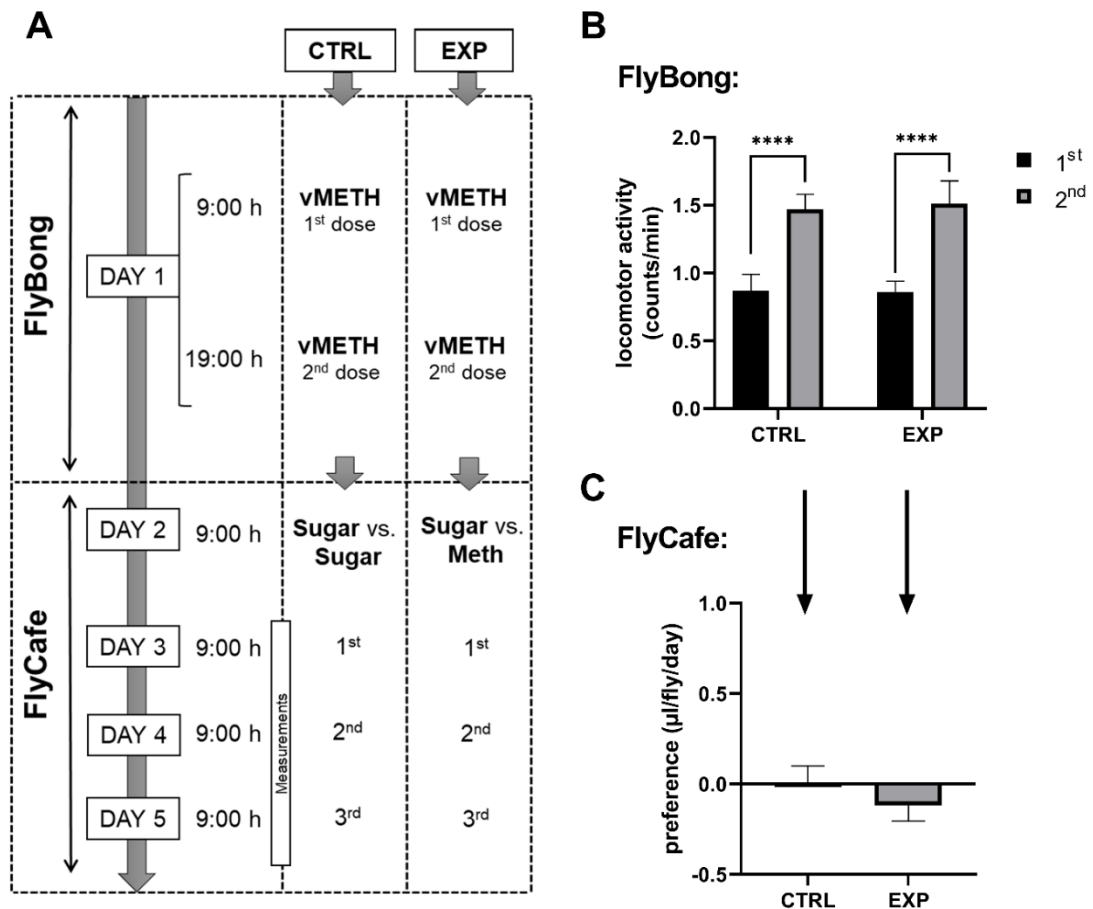


Figure 34. LS to vMETH precludes preferential self-administration of METH food. A. Timeline of experimental manipulations. **B.** The average locomotor activity after the 1st and 2nd exposure to 75 μg vMETH given at a 10 h interval for control group that subsequently received regular food (CTRL, n=25 flies) and experimental group that subsequently received the choice of METH or regular food (EXP, n=65 flies). The change was calculated by subtracting the baseline activity 10 minutes before the exposure from the vMETH response 10 minutes after the exposure to vMETH. **** p=0.0006, ****p=0.0007, t-tests for dependent samples. **C.** Average preference ± SEM for 0.15 mg/ml METH food during 3 days for control (CTRL, n=25 flies) and experimental (EXP, n=65 flies) group previously exposed to two doses of 75 μg vMETH.

Both groups of naïve flies exposed to two doses of vMETH developed LS ($p=0.0006$, $p=0.0007$, t-tests for dependent samples) (Figure 34B). However, exposure to vMETH in the FlyBong significantly decreased the preference for METH food in the experimental group compared to flies not subjected to the FlyBong procedure. The FlyBong pre-treatment did not affect the side preference of the control group, and the preference for METH remained evident in the METH-naïve control group.

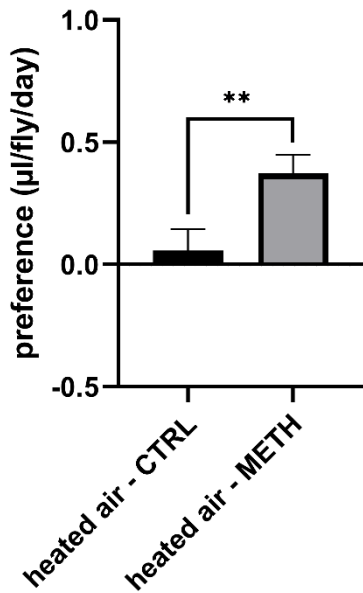


Figure 35. Mock treatment with heated air in the FlyBong does not affect preferential consumption of METH in the FlyCafe. *The average preference \pm SEM for 0.15 mg/ml METH food during 3 days for flies first exposed to heated air and then to only regular food (heated air-CTRL, $n=21$ flies), or those exposed to heated air and then given a choice between METH and regular food (heated air-METH, $n=36$ flies). ** $p=0.0123$, t-test for independent samples.*

As an additional control to rule out the possibility of the observed result being an artifact of the experimental manipulations, we subjected flies to heated air in the FlyBong before

transferring them to the FlyCafe. Flies exposed to heated air in the FlyBong still developed a preference for METH food ($p=0.0123$, t-test for independent samples), with no impact on side preference in the control group (Figure 35), indicating that the loss of preference for METH food was a result of previous exposure to vMETH and was not influenced by the experimental manipulation. These findings demonstrate that brief exposure to vMETH has a lasting effect on SA and preference for METH food.

4.3.3 *period* gene mutants do not develop LS nor preference of METH food

Having validated our hypothesis regarding the reciprocal interactions between LS and SA, we hypothesized the existence of a genetic counterpart influencing both behaviors. Our candidate gene, *period* (*per*), was selected due to its significant involvement in various drug-induced behaviors observed in both *Drosophila* and rodents. To examine this hypothesis, we evaluated the behavioral phenotypes of *per*⁰¹ mutant flies in comparison to their *wt* counterparts, employing the FlyBong and FlyCafe paradigms.

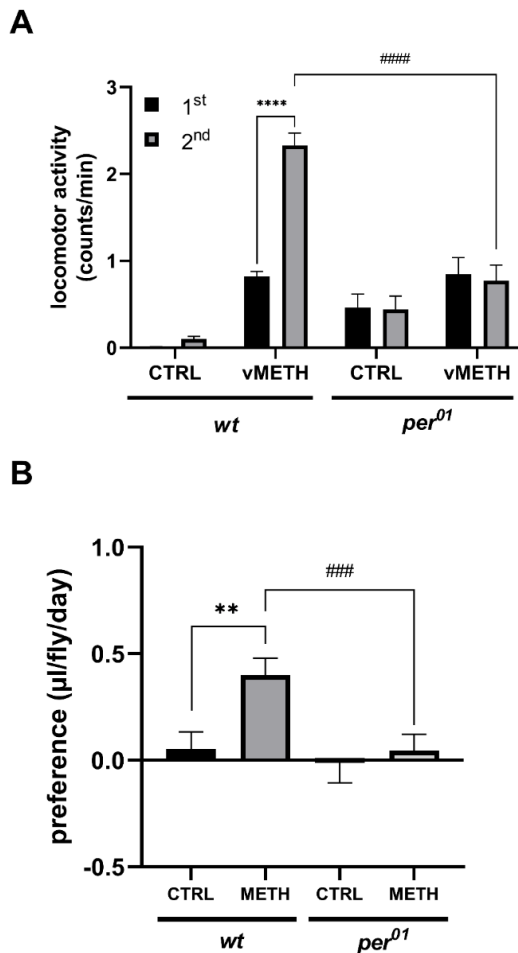


Figure 36. *per⁰¹* mutant flies do not develop LS to vMETH and do not preferentially self-administer METH food. **A.** The average locomotor activity after the 1st and 2nd exposure to 75 µg vMETH ($n = 32$) or heated air (CTRL, $n = 32$) given at a 10 h interval for *per⁰¹* mutant flies compared to *wt* flies. The change was calculated by subtracting the baseline activity, 10 minutes before the exposure, from the response 10 minutes after the exposure to vMETH. :**** $p < 0.001$, ##### $p < 0.001$, Two-way ANOVA with Bonferroni correction **B.** Average preference for 0.15 mg/ml METH food during 3 days \pm SEM for *per⁰¹* mutants compared to *wt* flies. Control flies had regular food choice in both capillaries (CTRL, $n=26$ *wt* flies, $n=27$ *per⁰¹* flies), experimental flies had a choice between regular food and 0.15 mg/ml METH food

(METH, $n=54$ wt flies, $n=50$ per^{01} flies). ** $p=0.0388$, ### $p=0.0046$, One-way ANOVA with Bonferroni correction.

In contrast to wt flies, per^{01} flies failed to exhibit LS following exposure to two doses of $75 \mu\text{g}$ vMETH (Figure 36A). Similarly, per^{01} flies over the course of three days did not show preference for METH food, unlike wt flies (Figure 36B).

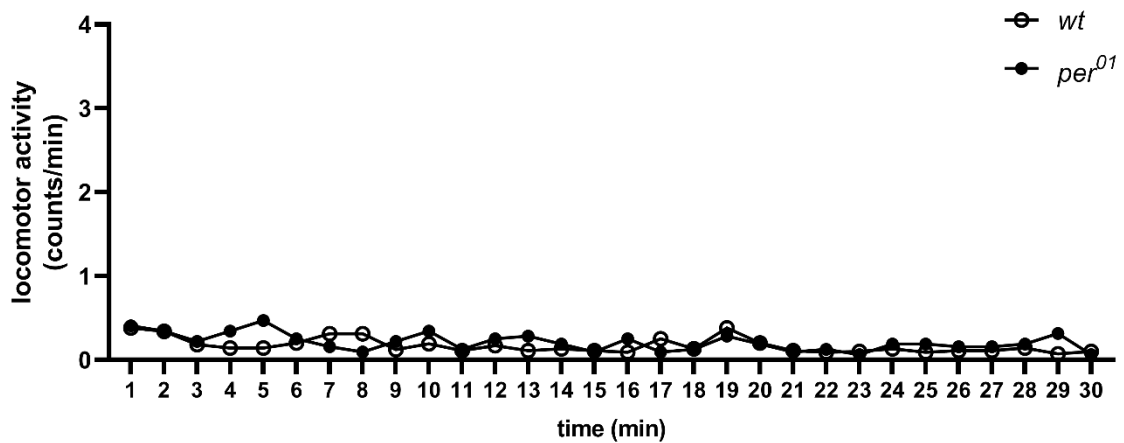


Figure 37. There is no difference in baseline locomotor activity between wt and per^{01} flies.

A. Kinetic graph of mean locomotor activity is shown for wt ($n = 32$) and per^{01} ($n = 32$) flies 30 min before administration (baseline) of $75 \mu\text{g}$ vMETH.

The difference between wt and per^{01} flies in the FlyBong and FlyCafe phenotype does not depend on the baseline level of locomotion since there are no differences in their baseline activity (Figure 37). These findings indicate that the per gene might be a common genetic link influencing LS to vMETH and preferential SA of METH food.

4.4 Identification of functional redox-related genes that regulate LS using genetic screen

Selection of the potential genes that regulate redox processes that could be involved in the development of LS was performed using a comprehensive database of *Drosophila* genes called Flybase. Genes were chosen because of their functional and structural properties, with the priority for genes known to be involved in redox processes, such as those encoding antioxidant enzymes, oxidoreductases, or proteins involved in redox signaling pathways, as well as genes which code for proteins with specific domains, such redox-sensitive thiol groups, which can easily be subjected to redox regulation.

RNAi lines (UAS constructs) for selected genes and the tissue specific driver lines (GAL4 constructs) were ordered from Vienna and Bloomington stock centers. We employed Gal4 lines targeting all neurons, only dopaminergic and serotonergic neurons together, or dopaminergic neurons alone. By comparing the effects of gene silencing in all neurons versus dopaminergic / serotonergic neurons specifically, we can discern whether potential phenotypic differences stem from the global neural perturbations or are specific to dopaminergic circuitry.

The experimental protocol consisted of gene silencing achieved by crossing different RNAi lines with specific GAL4 lines, testing the progeny for their ability to develop LS, data analysis and phenotypization. For every cross, 10-15 virgins of *Gal4* line were put in the same vial with five males of *UAS-RNAi* lines. Three to five days old males of F1 progeny were collected and tested in Flybong with two exposures to vMETH given ten hours apart, at 09:00 AM (1st) and 07:00 PM (2nd). Baseline activity was measured 10 minutes before exposure and the locomotion was measured 10 minutes after the exposure, and the response was calculated as a difference of those two parameters (baseline subtracted from locomotion) after each administration for both controls (CTRL 1st and CTRL 2nd) and experimental group (vMETH 1st and vMETH 2nd). If locomotor activity after vMETH 1st was significantly higher than CTRL 1st, flies were considered to be sensitive to vMETH. If flies were sensitive and the vMETH 2nd

response was significantly higher than vMETH 1st, indicating that the second response is higher than first, flies were considered to develop LS to vMETH.

The results of greatest interest to us were those in which flies exhibit sensitivity to vMETH without displaying LS. This meant that the response to the second vMETH exposure was not significantly higher than the response to the first exposure (Figure 38).

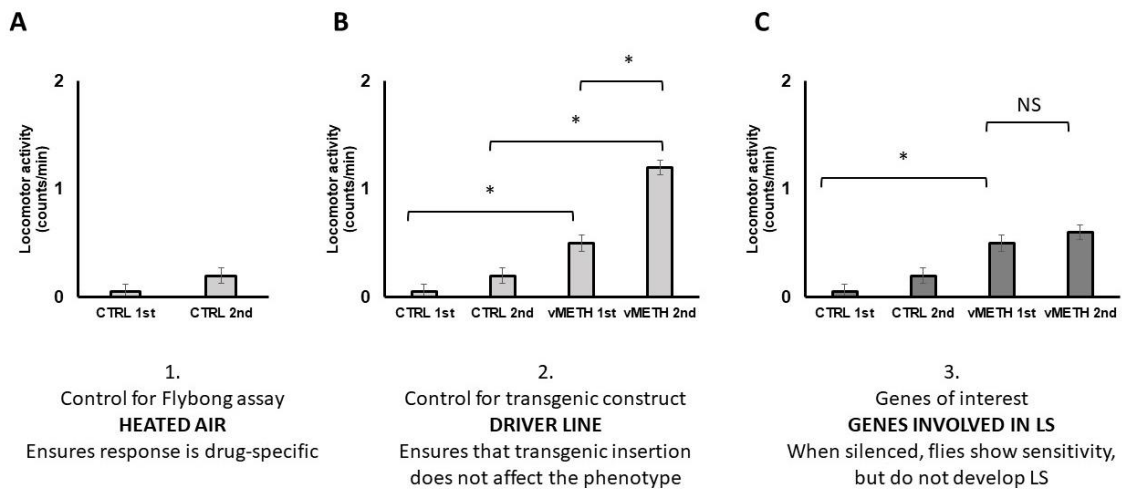


Figure 38. Hypothetical results and their controls. **A.** Control for FlyBong assay shows no difference to the first or second hot air exposure **B.** Control for transgenic construct shows normal development of LS **C.** Silencing of a specific gene results in sensitivity to vMETH but lack of LS.

To ensure that LS is drug-specific and to exclude any motor neuron deficits caused by gene silencing, which can affect the ability of flies to develop LS, we quantified negative geotaxis (vertical climbing ability), locomotor activity and sleep in all transgenic flies. Dysregulation of DA and serotonin systems, for example, which are implicated in addiction, may influence motor behavior, and negatively impact geotaxis performance. It was shown that genes and molecular pathways associated with addiction-related behaviors also regulate motor function in *Drosophila*. Therefore, genetic manipulations targeting addiction-related genes

or pathways may concurrently affect negative geotaxis behavior, which can then interfere with our assessment of FlyBong data.

We reasoned that quantifying negative geotaxis will be useful for several reasons. As mentioned, it provides a sensitive measure of motor function and coordination, ensuring that observed changes in addiction-related behaviors are not merely due to underlying motor deficits. Additionally, negative geotaxis serves as a baseline measure of locomotor activity and vitality, allowing for comparisons between control and experimental groups. Moreover, potential correlations between negative geotaxis and addiction phenotypes can offer insights into the interplay between motor function and addictive behaviors. Lastly, assessing negative geotaxis in flies subjected to genetic manipulations targeting redox-related genes enables the exploration of genetic interactions between redox pathways and motor function, contributing to our understanding of addiction-related traits at the genetic level.

Negative geotaxis was measured as a percentage of flies that climb over the center of a vial 5 seconds after flies have been dropped to the bottom of the vial. For locomotor activity and sleep assay, individual flies were placed in glass tubes with food into a DAMS monitors where an infrared beam is used to track the activity. Flies are considered sleeping when they do not cross the infrared beam for at least 5 minutes. Activity was presented as average counts for one-minute periods during 24h and sleep as the sum of 5 minutes sleep periods.

Flies that did not develop LS we further characterized using other tests to measure addiction-like behaviors, such as METH SA and response to cocaine (COC) in FlyBong. Results of this approach informed us about the specific effects that redox related genes have on development of LS to vMETH versus other METH and COC-dependent behaviors.

4.4.1 Panneuronal silencing of redox related genes

Panneuronal silencing of redox related genes allows for comprehensive coverage of neural circuits, enabling assessment of the overall impact of gene silencing on LS and addiction-related behaviors across the nervous system.

Table 6. Summary of tested phenotypes for pan-neuronal silencing of redox related genes.

(+) - altered phenotype, (-) - normal phenotype, (blank) - no data, + - flies show sensitivity to vMETH but do not sensitize

	vMETH	Negative geotaxis	Activity	Sleep
<i>elav-gal4</i>	ctrl	ctrl	ctrl	ctrl
<i>Cat</i>	+	-	+	+
<i>Gclc</i>	+	-	+	+
<i>Gclm</i>	+	-	+	+
<i>Grx1</i>	+	-	+	+
<i>GstE1</i>	+	-	+	+
<i>MBD-like</i>	+	-	+	+
<i>Sod1</i>	+	-	+	+
<i>Sod2</i>	+	-	-	+
<i>Sod3</i>	+	-	-	+
<i>E(spl)m3-hlh</i>	+	-	-	-
<i>Gapdh1</i>	+			

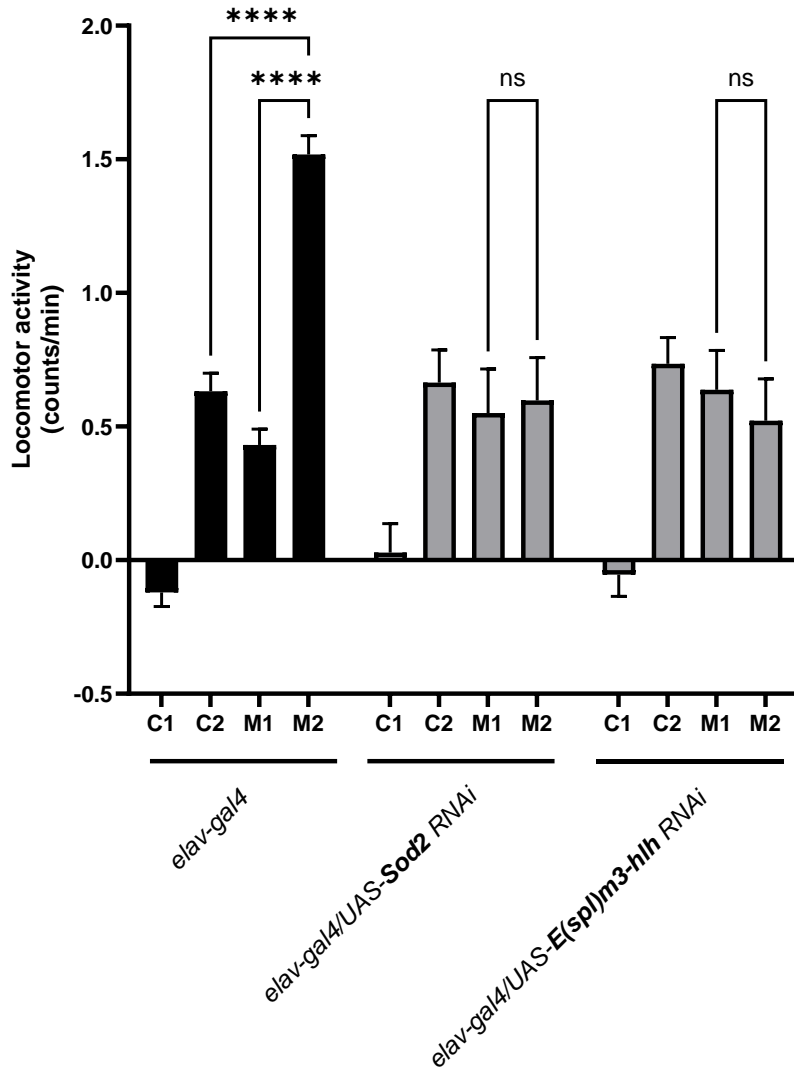


Figure 39. Panneuronal silencing of *Sod2* or *E(spl)m3-hlh* prevents the development of LS . Change in average locomotor activity is shown after the 1st and 2nd dose of 75 μ g vMETH (experimental group – vMETH) or hot air (control group - CTRL) administered 10 hours apart. The change is calculated by subtracting the baseline activity (10 minutes before exposure) from the response to the dose (10 minutes after exposure). Two-way ANOVA with Tukey correction.

We examined the impact of panneuronally silencing redox-related genes on sensitivity to vMETH and the development of LS in response to METH exposure. The change in average locomotor activity following the administration of the first and second doses of 75 μ g vMETH or heated air (control group - CTRL), given 10 hours apart, is depicted (Figure 39.). This change in activity is calculated by subtracting the baseline activity recorded 10 minutes before exposure from the locomotor response measured 10 minutes after exposure.

Our results reveal that panneuronal silencing of *Sod2* or *E(spl)m3-hlh* prevents the development of LS over repeated exposures to vMETH, as evidenced by the absence of a significant increase in locomotor activity following the second dose of vMETH relative to the first. These findings suggest that *Sod2* and *E(spl)m3-hlh* may play a role in cellular changes induced by vMETH that lead to the development of LS. Silencing other redox-related genes had more systemic effects and affected multiple phenotypes, including sensitivity to heated air and first dose of vMETH, so we were not able to precisely determine their effect on LS (supplemental figure).

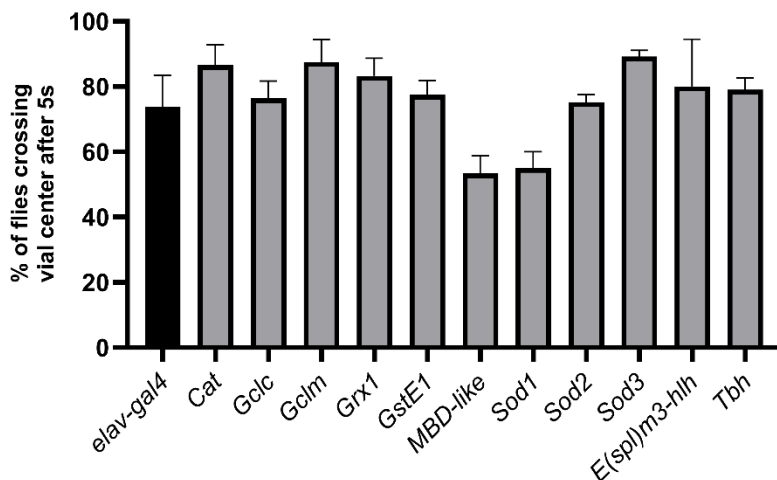


Figure 40. Redox-related genes do not affect negative geotaxis. *Negative geotaxis was measured in 3-5 days old male progeny of elav-GAL4 x UAS-RNAi crosses. N=5 repetitions per experiment. The average percentage of flies that crossed 3 cm after 5 seconds is shown.*

We investigated the impact of silencing selected redox-related genes in all neurons on negative geotaxis behavior. Negative geotaxis, a measure of climbing behavior, was assessed in 3-5 days old male progeny resulting from GAL4 x UAS-RNAi crosses. The average percentage of flies that crossed 3 cm after 5 seconds was used as the metric for evaluating negative geotaxis. There was no significant difference in negative geotaxis among the tested groups (Figure 40.). Flies with redox-related genes silenced in all neurons displayed comparable climbing behavior to the control group.

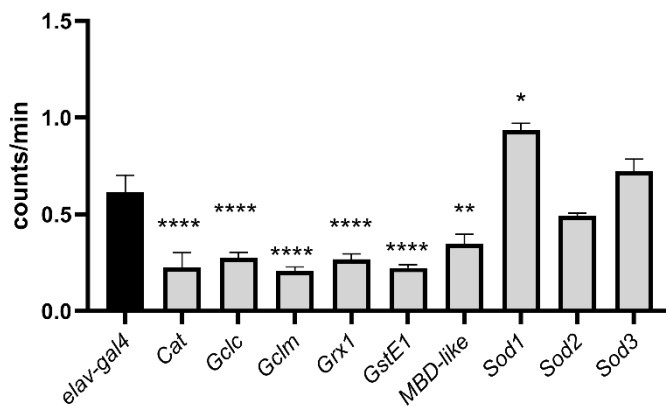


Figure 41. Flies with panneuronally silenced *Cat*, *Gclc*, *Gclm*, *Grx1*, *GstE1*, and *MBD-like* exhibit significantly reduced, while *Sod1* shows increased locomotor activity. *The average locomotor activity per minute was measured over a 5-day period in 3-5 days old progeny of the respective GAL4xUAS-RNAi crosses. n=16 flies per group. One-way ANOVA with Bonferroni correction.*

To quantify locomotor activity, we measured the average activity per minute over a 5-day period in the progeny resulting from respective GAL4xUAS-RNAi crosses established to silence redox-related genes of choice in all neurons. Flies used in the study were males aged between 3 to 5 days.

The locomotor activity of flies with silenced *Cat*, *Gclc*, *Gclm*, *Grx1*, *GstE1*, and *MBD-like* genes was significantly reduced compared to controls (Figure 41.), while flies with silenced *Sod1* exhibited increased locomotor activity compared to controls.

These results suggest that, in most cases, silencing redox-related genes in all neurons reduces the average activity of flies. However, the observed increase in locomotor activity upon silencing of *Sod1* highlights a unique role for this gene in modulating locomotion in *Drosophila*.

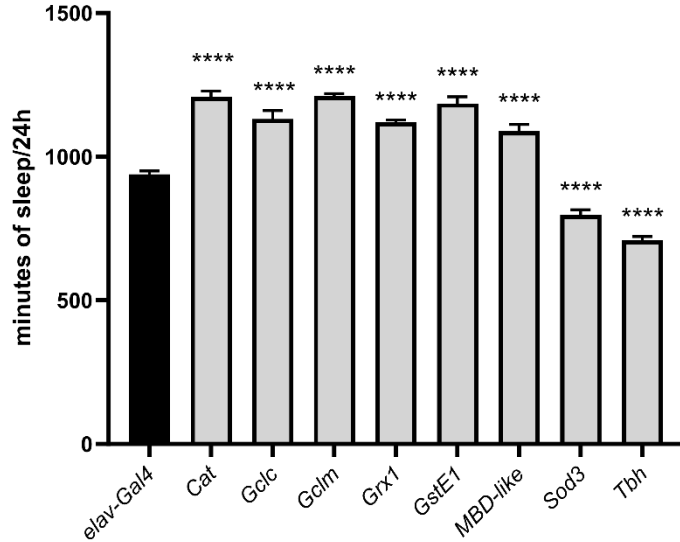


Figure 42. Silencing redox-related genes in all neurons affects the amount of sleep. *The average amount of sleep in minutes is measured for 5 days and is depicted as the average for 24-hour period in 3-5 days old progeny of the respective GAL4xUAS-RNAi crosses. n=16 flies per group. One-way ANOVA with Bonferroni correction.*

Silencing redox-related genes in all neurons significantly affected the amount of sleep (Figure 42.). Flies with silenced *Cat*, *Gclc*, *Gclm*, *Grx1*, *GstE1* and *MBD-like* genes slept longer than controls, while flies with silenced *Sod3* and *Tbh* exhibited lower amount of sleep per 24h. These findings indicate that the sleep phenotype is very sensitive to the general perturbation of redox regulation in the brain.

4.4.2 Silencing of redox related genes in dopaminergic and serotonergic neurons (genetic screen using *ddc-gal4* driver)

Focusing on dopaminergic and serotonergic systems provides insight into the involvement of redox-related genes in modulating pathways that are known to regulate addiction-related behaviors, such as reward processing and motor-activating effects.

Table 7. Summary of tested phenotypes when redox-related genes were silenced in dopaminergic and serotonergic neurons.

(+) - altered phenotype, (-) - normal phenotype, (blank) - no data, + - flies show sensitivity to vMETH but do not sensitize

	vMETH	Self-administration	Negative geotaxis	Activity	Sleep
<i>ddc-gal4</i>	ctrl	ctrl	ctrl	ctrl	ctrl
<i>Cat</i>	+	-	-	-	+
<i>Gclc</i>	+		-	-	+
<i>Gclm</i>	+		-	-	+
<i>Grx1</i>	-		-	-	+
<i>Gste1</i>	-		-	-	+
<i>MBD-like</i>	+		-	-	-
<i>Sod1</i>	+	+	-	-	+
<i>Sod2</i>	+	+	-	-	+
<i>Sod3</i>	+		-	+	+
<i>E(spl)m3-hlh</i>	+		-	-	+
<i>Gapdh2</i>	+		-		
<i>Tbh</i>	+		-		

ND-51	+		-	-	+
CklIbeta	+		-	-	+
Sni	+		-	-	-
Trx-2	+				
PHGPx	+		-	+	+
Gapdh1	+	+	-	-	+
Jafrac1	+		-	-	+
Men	+	+	-	-	+
Prx3	+		-	-	+
Prx5	+		-		

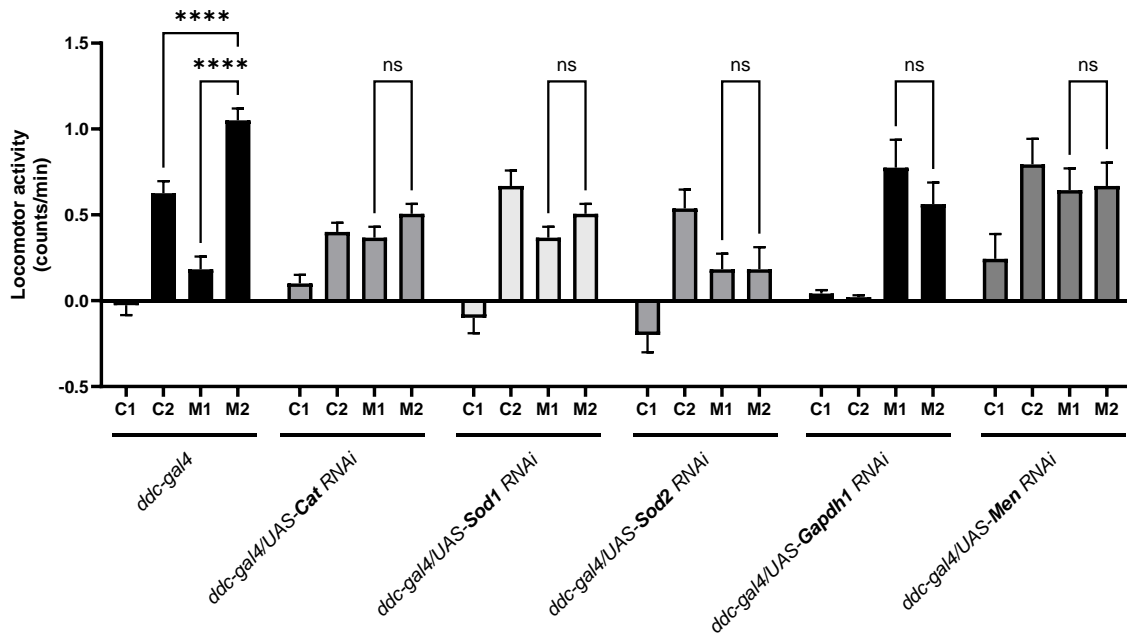


Figure 43. Silencing of *Cat*, *Sod1*, *Sod2*, *Gapdh1* or *Men* in dopaminergic and serotonergic neurons prevents LS to vMETH. Change in average locomotor activity is shown after the 1st and 2nd dose of 75 μ g vMETH (experimental group – vMETH) or heated air (control group - CTRL) administered 10 hours apart. The change is calculated by subtracting the baseline activity (10 minutes before exposure) from the response (10 minutes after exposure).

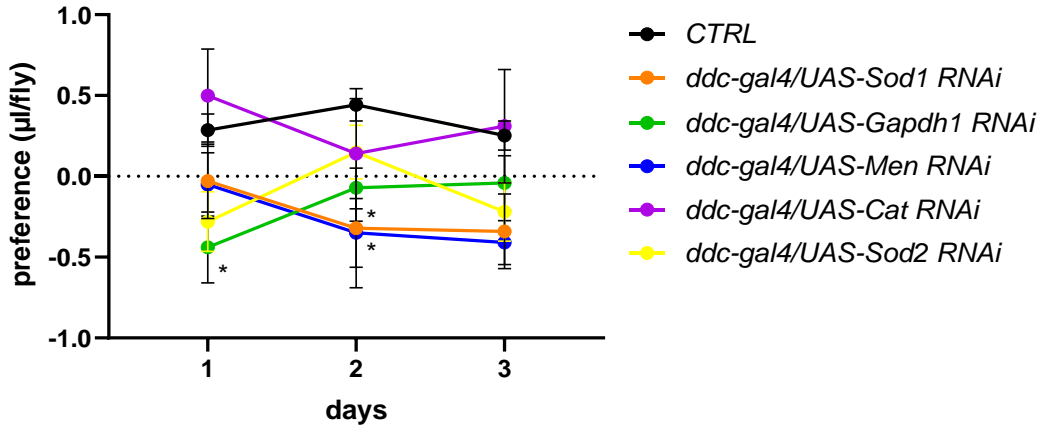
We investigated the effects of silencing redox-related genes specifically in dopaminergic and serotonergic neurons on sensitivity to vMETH and the development of LS in response to METH exposure. The figure presents the change in average locomotor activity following the administration of the first and second doses of 75 µg vMETH or heated air (control group - CTRL), given 10 hours apart. This change in the activity is calculated by subtracting the baseline activity recorded 10 minutes before exposure from the locomotor response measured 10 minutes after exposure.

Our findings demonstrate that silencing of *Cat*, *Sod1*, *Sod2*, *Gapdh1* and *Men* in dopaminergic and serotonergic neurons results in increased sensitivity to vMETH, as indicated by higher locomotor activity compared to controls (Figure 43.). Furthermore, this manipulation prevents the development of LS over repeated exposures to vMETH, as evidenced by the absence of a significant increase in locomotor activity following the second dose of vMETH relative to the first. This suggests that inactivation of specific genes that regulate redox processes in a limited number of neurons have a significant effect on the development of LS.

Other tested lines either developed the LS (*Grx1*) or showed decreased sensitivity (*MBD-like*, *Sod3*, *ND-51*, *ckIIbeta*, *Trx-2*, *Jafrac1*). Several strains developed LS, however, this response cannot be considered METH-specific, as the same, or even stronger, response was observed to the heated air (controls) (supplemental figure).

We then tested the impact of silencing *Cat*, *Sod1*, *Sod2*, *Gapdh1*, and *Men* genes in dopaminergic and serotonergic neurons on the preference for METH. The experimental group of flies was provided with a choice between food containing 0.15 mg/ml METH and regular food (yeast + sugar) over a 3-day period, with the amount of consumed food measured at 24-hour intervals.

A



B

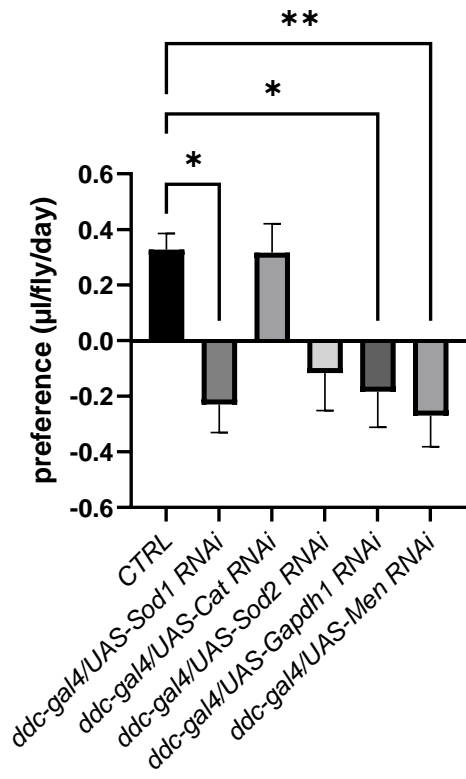


Figure 44. Silencing *Sod1*, *Gapdh1*, and *Men* genes in dopaminergic and serotonergic neurons results in the loss of preference for METH. *The experimental group of flies was given a choice between food with added 0.15 mg/ml METH and regular food (yeast + sugar) over a 3-day period. The amount of consumed food was measured at 24-hour intervals. Graph A depicts preference over days, while graph B illustrates the average preference for 3 days for each line. Statistical significance: A. Two-way ANOVA, $p < 0.05$, $n=10-22$ males in each group; B. One-way ANOVA, $p < 0.05$, $n=10-22$ males in each group.*

In graph A (Figure 44.), the experimental group, with *Sod1*, *Gapdh1*, and *Men* genes silenced, displayed a loss of preference for METH compared to controls. This loss of preference persisted over the 3-day period. Graph B further confirms these findings, showing that the average preference for METH over the 3-day period was significantly lower in the flies with *Sod1*, *Gapdh1* and *Men* silenced compared to controls. Silencing *Cat* did not affect the METH preference, while flies with silenced *Sod2* exhibited lower preference trend, which was not statistically significant.

These results highlight the crucial role of *Sod1*, *Gapdh1*, and *Men* genes in modulating the preference for METH in dopaminergic and serotonergic neurons.

Most of the identified genes which are required for the development of the LS regulate the preferential voluntary SA of METH food (Figure 44). Silencing of *Sod1*, *Gapdh1*, and *Men* genes in the dopaminergic and serotonergic neurons led to negative preference for METH food during all 3 days of the test (Figure 44) resulting in a significantly decreased average preference (Fig.25b). This finding suggests that perturbation of the specific redox pathways in dopaminergic and serotonergic neurons affects multiple behaviors induced by METH exposure.

To exclude the effect of gene silencing on climbing ability, was quantified the negative geotaxis in male progeny aged 3-5 days resulting from crosses of *ddc-GAL4* driver with UAS-

RNAi lines targeting the selected genes. Utilizing the average percentage of flies that crossed three centimeters after five seconds as the measure for evaluating negative geotaxis, our analysis revealed no significant difference among the tested groups (Figure 45). These findings indicate that inability to develop LS to repeated doses of vMETH and lack of preferential SA of METH is not caused by flies' inability to climb.

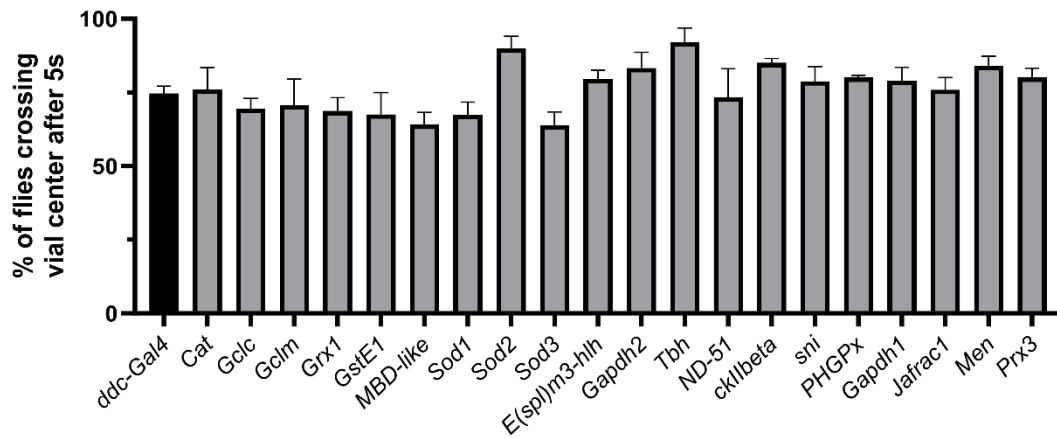


Figure 45. Silencing redox related genes in dopaminergic and serotonergic neurons does not affect climbing ability. *Negative geotaxis was measured in 3-5 days old male flies of the first generation of transgenic flies. N=5 repetitions per experiment. The graph depicts the average percentage of flies that crossed 3 cm after 5 seconds.*

To assess locomotor activity, we monitored the average activity per minute over a 5-day period in the offspring resulting from respective ddc-GAL4xUAS-RNAi crosses established to silence specific redox-related genes in dopaminergic and serotonergic neurons.

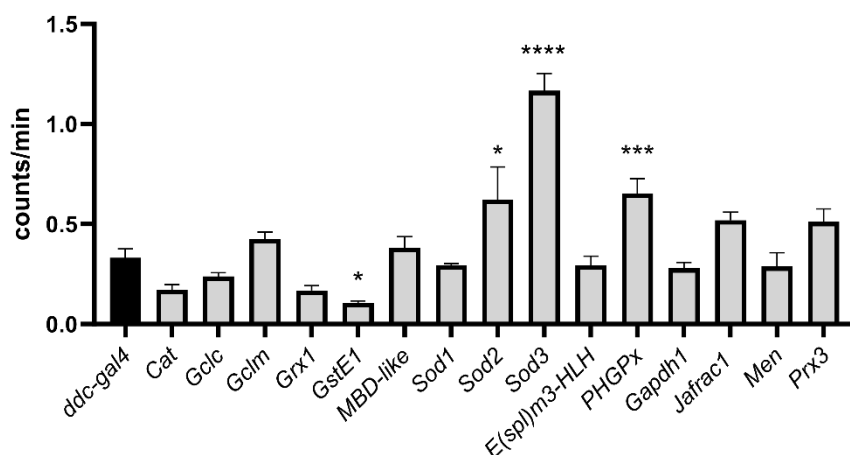


Figure 46. Silencing *GstE1*, *Sod2*, *Sod3* and *PHGPx* in dopaminergic and serotonergic neurons affects average locomotor activity. The average locomotor activity per minute was measured over a 5-day period in 3-5 days old first-generation male transgenic flies. $n=16$ flies per group.

Our analysis revealed that flies with silenced *GstE1* gene displayed significantly reduced locomotor activity compared to controls (Figure 46). In contrast, flies with silenced *Sod2*, *Sod3* and *PHGPx* exhibited increased locomotor activity relative to controls, while silencing of *Cat*, *Gclc*, *Gclm*, *Grx1*, *MBD-like*, *Sod1*, *E(spl)m3-HLH*, *Gapdh1*, *Jafrac1*, *Men* and *Prx3* did not significantly impact locomotor activity.

These findings suggest that, in most instances, silencing redox-related genes in dopaminergic and serotonergic neurons does not impact average activity of flies. However, the observed changes in locomotor activity upon silencing of *GstE1*, *Sod2*, *Sod3* and *PHGPx* underscores a distinct role for these genes in regulating locomotion in *Drosophila*.

The average duration of sleep in minutes was determined by housing individual flies in glass tubes containing food and monitoring their activity using DAMS monitors equipped with

infrared sensors. Sleep was defined as periods of continuous inactivity lasting at least 5 minutes.

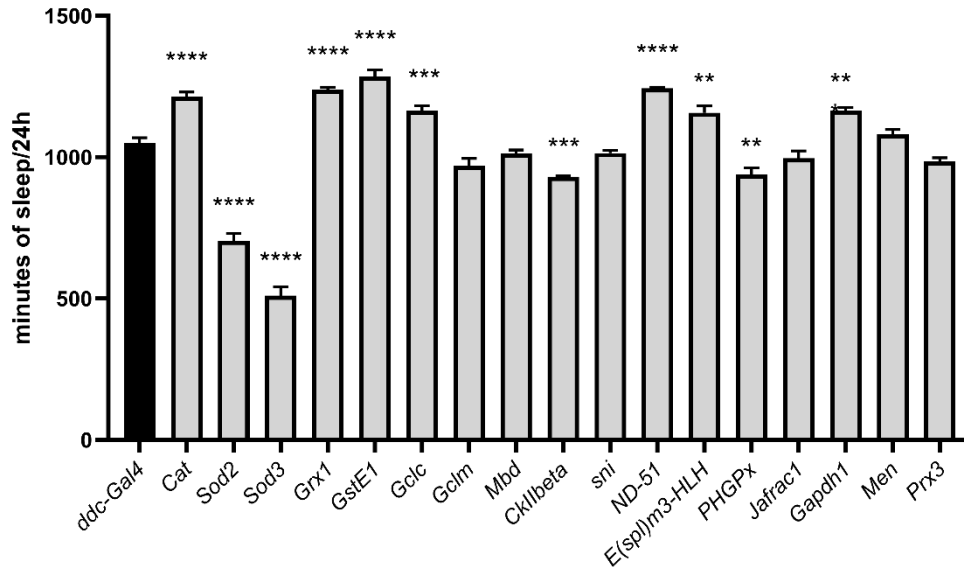


Figure 47. Silencing of redox-related genes affects the amount of sleep. *The average amount of sleep in minutes is measured for 5 days and is depicted as average for 24-hour period in 3-5 days old first-generation male transgenic flies. n=16 flies per group.*

Silencing redox-related genes in dopaminergic and serotonergic neurons significantly impacted the amount of sleep (Figure 47). Flies with silenced *Cat*, *Gclc*, *Grx1*, *GstE1*, *ND-51*, *E(spl)m3-HLH* and *Gapdh1* genes exhibited longer sleep durations compared to controls, whereas flies with silenced *Sod2*, *Sod3*, *ckllbeta* and *PHGPx* genes showed reduced sleep duration per 24 hours. Silencing *Gclm*, *MBD-like*, *sni*, *Men* and *Prx3* did not affect sleep.

These results emphasize the significant impact of altering redox-related genes specifically in dopaminergic and serotonergic neurons on sleep behavior in *Drosophila*. The manipulation

of individual genes within these neuronal populations influences the observed amount of sleep.-

4.4.3 Silencing of redox related genes in dopaminergic neurons (*ple-gal4* driver)

Focusing solely on dopaminergic neurons allows for a more targeted investigation into the specific role of redox-related genes in modulating pathways crucial for addiction-related behaviors. Dopaminergic signaling is heavily implicated in the neurobiology of addiction, playing a central role in reward reinforcement and motivational processes. By concentrating on dopaminergic neurons, we can directly assess the impact of redox gene silencing on dopamine-mediated pathways underlying addiction-like phenotypes.

Table 8. Summary of tested phenotypes for silencing of redox-related genes in the dopaminergic neurons (*ple-gal4*).

(+) - altered phenotype, (-) - normal phenotype, (blank) - no data, + - flies show sensitivity to vMETH but do not sensitize

	vMETH	Self-administration	Negative geotaxis	vCOC
<i>ple-gal4</i>	Ctrl	Ctrl	Ctrl	Ctrl
<i>Cat</i>	+		-	+
<i>Gclc</i>	+		-	
<i>Gclm</i>	+		-	
<i>Sod1</i>	+		-	
<i>Sod2</i>	+		-	
<i>E(spl)m3-hlh</i>	+		-	
<i>Gapdh2</i>	+		-	
<i>Trx-2</i>	+		-	+
<i>PHGPx</i>	+		-	

<i>Gapdh1</i>	+	-	-	+
<i>Jafrac1</i>	+		-	
<i>Men</i>	+	-	-	+
<i>Prx3</i>	+	+	-	+
<i>Prx5</i>	+		-	

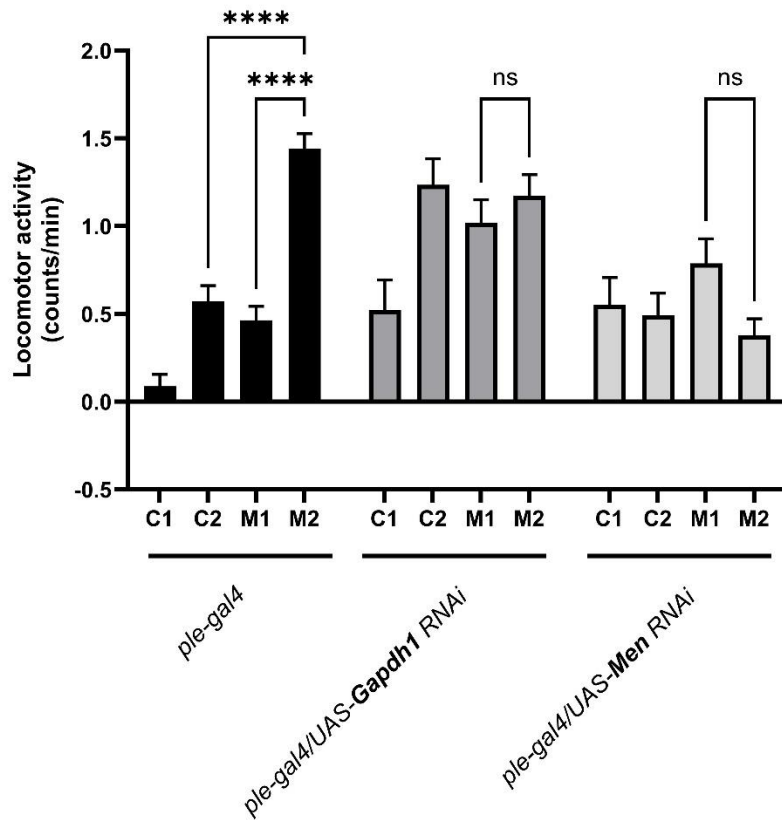


Figure 48. Silencing of *Gapdh1* or *Men* genes in dopaminergic neurons prevents the development of LS to vMETH. Change in average locomotor activity is shown after the 1st and 2nd dose of 75 μ g vMETH (experimental group – vMETH) or hot air (control group - CTRL) administered 10 hours apart. The change is calculated by subtracting the baseline activity (10 minutes before exposure) from the response to the dose (10 minutes after exposure).

We examined how silencing redox-related genes specifically in dopaminergic neurons influences sensitivity to vMETH and the development of LS in response to METH exposure. The figure shows the change in average locomotor activity following the administration of the first and second doses of 75 µg vMETH or heated air (control group - CTRL), administered 10 hours apart. This change in activity is calculated by subtracting the baseline activity recorded 10 minutes before exposure from the locomotor response measured 10 minutes after exposure.

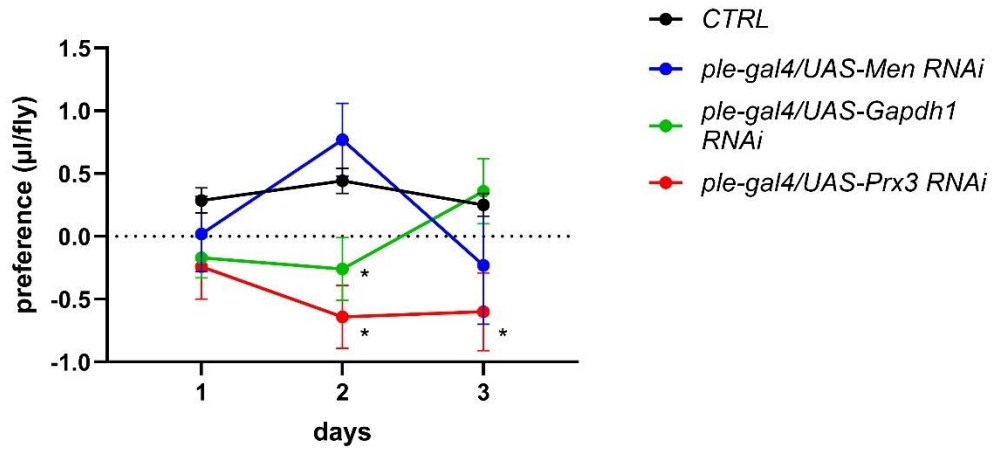
Silencing the *Gapdh1* and *Men* genes in dopaminergic neurons has no impact on sensitivity but does affect LS (Figure 48). These genes are essential in dopamine neurons for the development of LS to METH and are specific to LS.

Our experiments also yielded the following interesting cases. Genes whose silencing affects sensitivity to the first dose (flies show no response to the first dose of METH; the response is negative as activity is lower than baseline) are *Sod2*, *E(spl)m3-hlh*, *Gapdh2*, *PHGPx* (supplemental figure). These genes are essential in dopaminergic neurons for the development of sensitivity to METH.

Silencing certain genes may also affect sensitivity and/or LS to heated air, and in such cases, we can state that sensitivity and LS to METH are non-specific: *Cat*, *Gclc*, *Gclm*, *Sod1*, *Trx-2*, *Jafrac 1*, *Prx3*, *Prx5*. These genes influence the sensitivity and sensitization phenotype to air; therefore, due to limitations of the FlyBong method, we cannot confidently determine their necessity for LS to METH.

These findings imply that *Gapdh1* and *Men* in dopaminergic neurons may play critical roles in the development of LS.

A



B

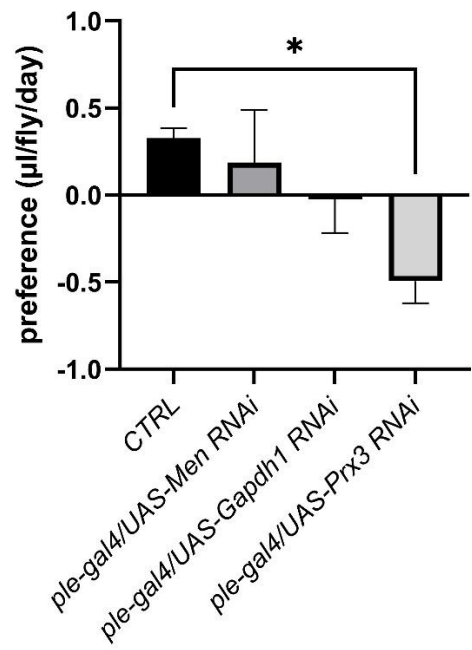


Figure 49. Silencing *Prx3* gene in dopaminergic neurons results in the loss of preference for METH. *The experimental group of flies was given a choice between food with added 0.15 mg/ml METH and regular food (yeast + sugar) over a 3-day period. The amount of consumed food was measured at 24-hour intervals. Graph A depicts preference over days, while graph B illustrates the average preference for 3 days for each line. Statistical significance: A. Two-way ANOVA, $p < 0.05$, $n=10-22$ males in each group; B. One-way ANOVA, $p < 0.05$, $n=10-22$ males in each group.*

We proceeded to assess the impact of silencing *Men*, *Gapdh1* and *Prx3* genes in dopaminergic neurons on METH preference. Flies were given a choice between food containing 0.15 mg/ml METH and regular food (yeast + sugar) over three days, with food consumption measured at 24-hour intervals.

In Figure 49, graph A depicts the preference dynamics for each group, where *Men*, *Gapdh1* and *Prx3* genes were silenced. On the first day there was no difference between experimental groups and control. On the second day *Prx3* and *Gapdh1* showed diminished preference for METH compared to controls, while on the third day the preference was significantly lower only in *Prx3* line. Graph B further supports these findings, indicating a significantly lower average preference for METH over the 3-day period in flies with silenced *Prx3*.

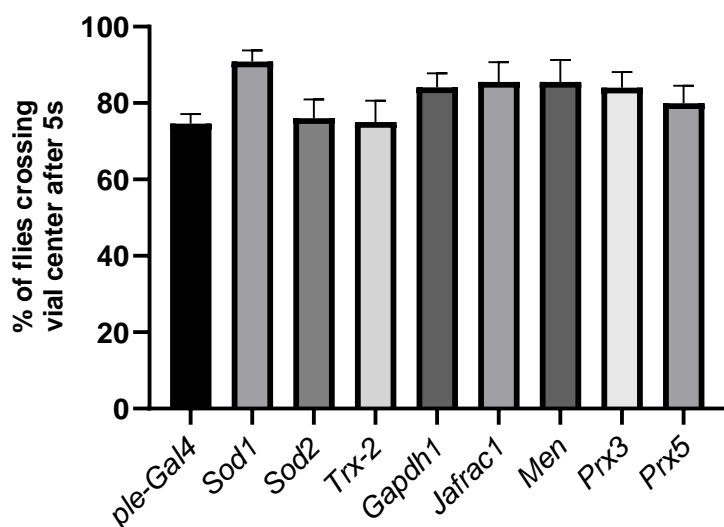


Figure 50. Silencing redox related genes in dopaminergic neurons does not affect vertical climbing ability. *Negative geotaxis was measured in 3-5 days old male flies of the first generation of transgenic flies. N=5 repetitions per experiment. The graph depicts the average percentage of flies that crossed 3 cm after 5 seconds.*

Using the average percentage of flies crossing a three-centimeter distance within five seconds as the criterion, our analysis revealed no significant difference among the experimental groups (Figure 50). Flies with silenced redox-related genes in dopaminergic neurons exhibited climbing behavior similar to that of the control group.

These findings suggest that targeting redox-related genes specifically in dopaminergic neurons has no impact on negative geotaxis behavior in *Drosophila*.

Testing the response to volatilized cocaine (vCOC) in lines not exhibiting LS to vMETH helps explore cross-sensitization between different drugs and provides insights into cocaine sensitivity and addiction-related pathways, even in lines unresponsive to vMETH, allowing for a comprehensive investigation of drug sensitivity in *Drosophila*.

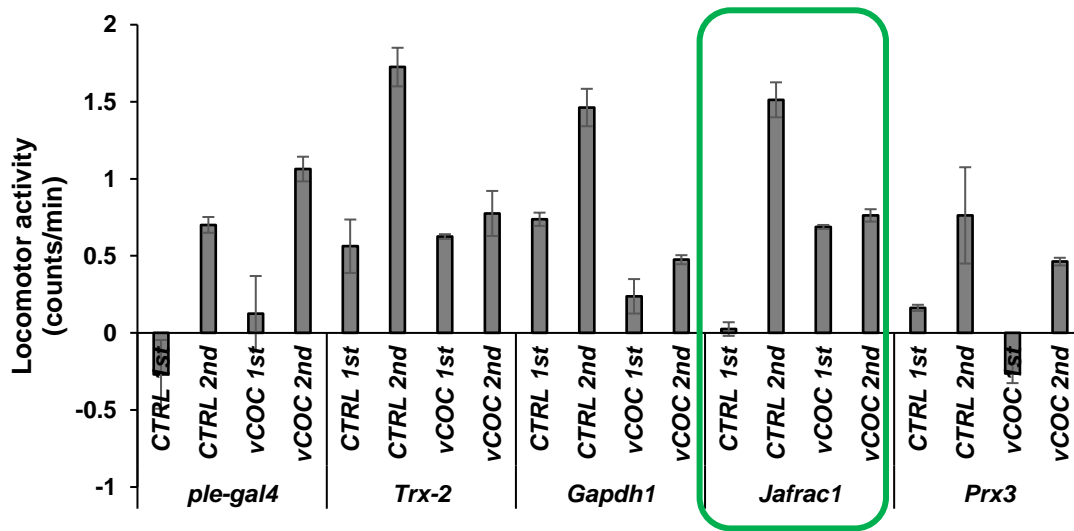


Figure 51. *Jafrac1* in dopaminergic neurons is necessary for the development of LS to vCOC. Change in average locomotor activity is shown after the 1st and 2nd doses of 75 µg vCOC (experimental group - vCOC, n=16) or hot air (control group - CTRL, n=16), administered with a 6-hour interval. The change is calculated by subtracting the baseline activity (5 minutes before exposure) from the response to the dose (5 minutes after exposure).

Flies with silenced *Jafrac1* showed increased sensitivity to the first dose of vCOC, but did not develop LS (Figure 51). Flies with silenced *Prx3* did not show sensitivity, while the response in case of silencing *Trx-2* and *Gapdh1* was not drug-specific.

These results indicate that *Jafrac1* in dopaminergic neurons is necessary for the development of LS to vCOC.

4.5 Identification of proteins involved in LS to vMETH using proteomic analysis

To correlate the findings from the genetic screen about the importance of specific genes for development of LS to vMETH with actual presence of products of those genes in the brain we performed the proteomic analysis. The goal was to validate the findings from the genetic screen and to identify new targets, proteins, that can subsequently be verified using genetic manipulations.

Male *wt* flies were exposed to two doses of vMETH 10 hours apart in a FlyBong. The flies were divided into groups based on their behavioral response, identifying those with LS to the second vMETH dose and those which did not develop LS (NLS). The control group (CTRL) experienced only heated air exposure. We identified 1894 protein groups, out of which 885 showed significant differential expression because of vMETH exposure.

4.5.1 Upregulation and downregulation of proteins in the LS group

Venn diagram analysis facilitated the visualization of protein expression alterations between the LS group and the other two groups. Figure 52 presents the distribution of upregulated proteins, pinpointing a distinct subset of 179 proteins concurrently upregulated in LS flies in comparison to both CTRL and NLS flies. This finding emphasizes the specificity of the proteomic response to the vMETH treatment in LS flies. Additionally, totally 317 proteins (138 uniquely) were upregulated in the LS group compared to CTRL, and 282 proteins in total (103 specifically) were more abundant in LS flies relative to NLS ones.

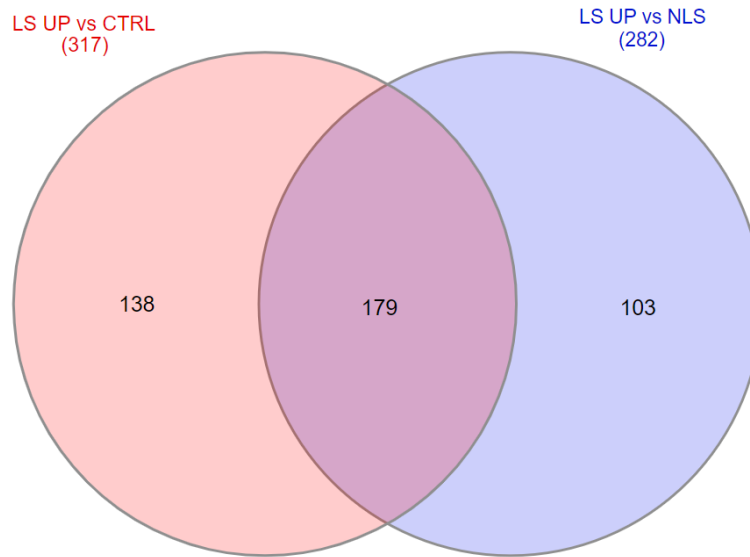


Figure 52. Venn diagram exhibiting the overlap of proteins upregulated in LS against CTRL and NLS. 317 proteins upregulated in LS compared to CTRL, 282 uniquely in LS compared to NLS, and 179 commonly upregulated in LS against both CTRL and NLS.

Figure 53. underscores the proteins with decreased expression levels within the LS group. The diagram reveals 77 proteins that were consistently downregulated in LS flies against both CTRL and NLS groups. Furthermore, there were 181 proteins (104 uniquely) less expressed in the LS group compared to CTRL and 119 (42 uniquely) downregulated compared to NLS.

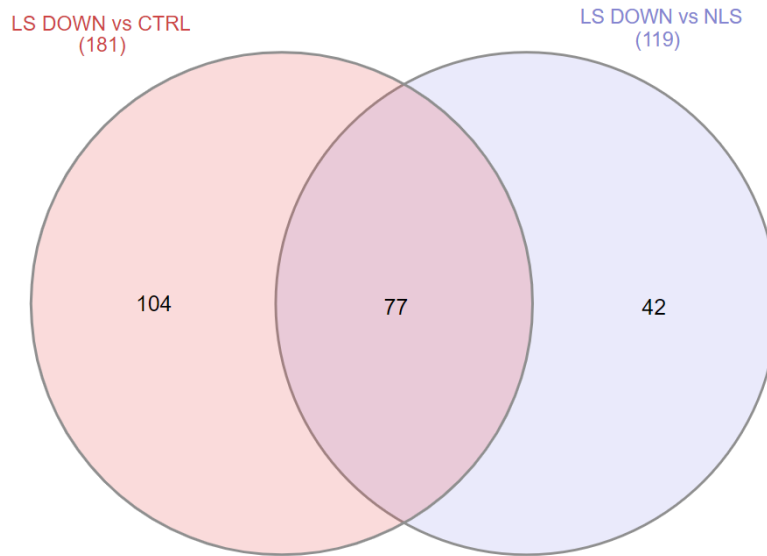


Figure 53. Venn diagram demonstrating the overlap of proteins downregulated in LS compared to CTRL and NLS. 181 proteins uniquely downregulated in LS compared to CTRL, 119 uniquely downregulated in LS compared to NLS, and 77 proteins commonly downregulated in LS against both CTRL and NLS.

4.5.2 STRING analysis of overlapping proteins

4.5.3 Proteins upregulated in LS

The 179 commonly upregulated proteins in the LS flies were further analyzed using STRING to investigate their interactions and functional enrichments. The network generated (Figure 1) revealed a significant enhancement in several key pathways, with a prominent enrichment in metabolic pathways (41 protein involved), proteasome (15 proteins), and vesicle-mediated transport (14 proteins), phototransduction (9 proteins), fatty acid metabolism (9 proteins), trehalose metabolism (5 proteins) and RNA splicing (5 proteins). We chose to focus on pathways which included five or more proteins (Figure 54.).

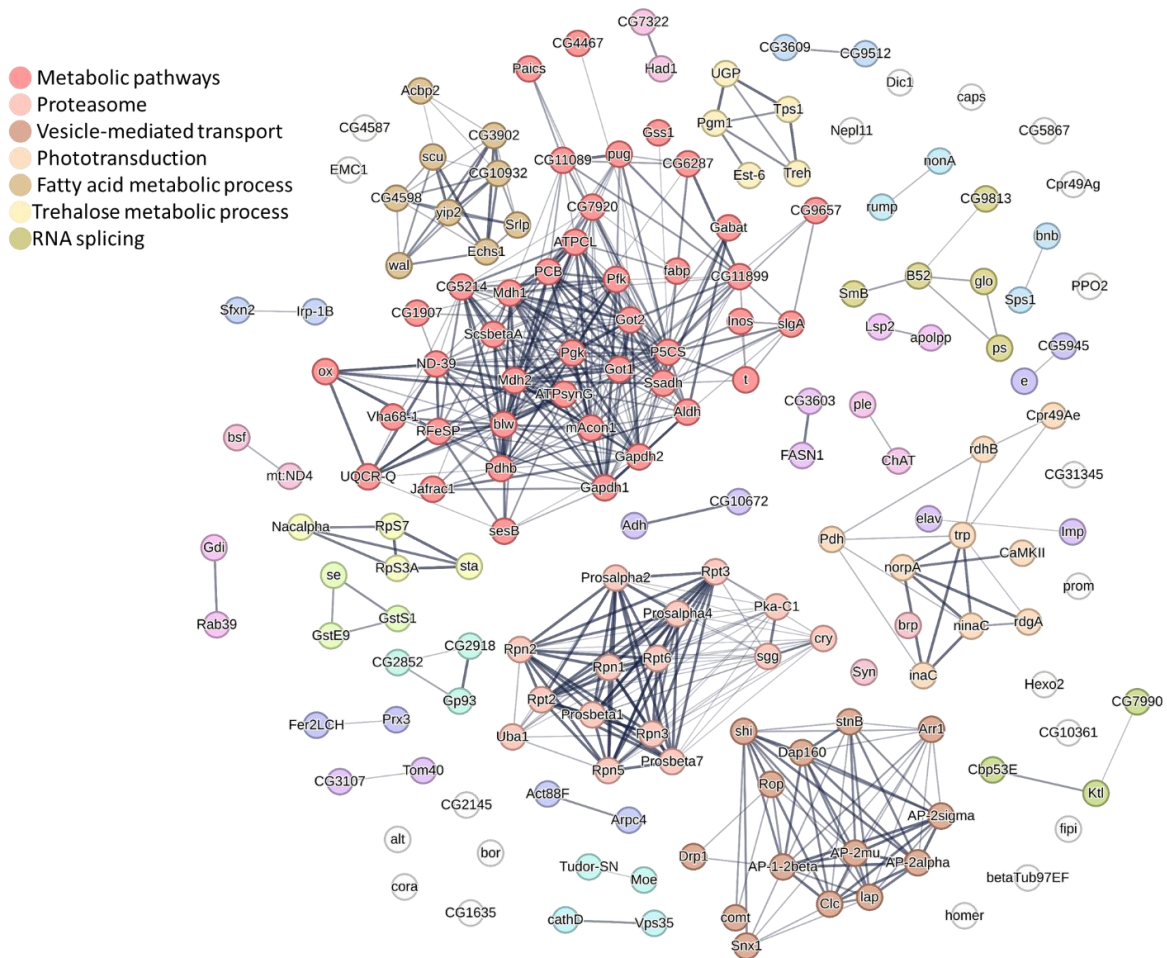


Figure 54. STRING analysis displaying the network of upregulated proteins in *Drosophila* brains of the METH-sensitized (LS) group. Each node represents a protein, with connections indicating protein-protein interactions. Pathways are color-coded as per the legend.

The network prominently features a cluster representing metabolic pathways, with enzymes like Phosphoglycerate kinase (Pgc), Phosphofructokinase-1 (Pfk) and Glyceraldehyde-3-phosphate dehydrogenase (Gapdh1 and Gapdh2) being notably upregulated, indicative of intensified glycolytic activity. Concurrently, proteins such as Aconitase (mAcon1), Malate dehydrogenases (Mdh1 and Mdh2), Succinate--CoA ligase (ScsbetaA) suggest an elevated TCA cycle flux, highlighting an enhanced need for ATP production in the LS state. Within the

proteasome cluster, components like the Regulatory particle non-ATPase (Rpn) subunits, Rpn2 and Rpn3, are upregulated, signaling an increased proteasome activity, potentially facilitating the degradation of damaged or unfolded proteins exacerbated by drug exposure. The vesicle-mediated transport cluster showcases proteins such as Synapsin (Syn), Vesicle-fusing ATPase 1 (comt), Dynamin (shi), Adaptor Protein complex 1/2, beta subunit (AP-1-2beta) and Protein stoned-B (stnB), which are critical for neurotransmitter release and synaptic vesicle recycling. Their upregulation suggests a potential amplification in synaptic communication processes. Phototransduction involves proteins like Arrestin (Arr1) and Rhodopsin (ninaC), which are upregulated, reflecting possible changes in sensory processing or circadian rhythm alterations following vMETH exposure.

Enzymes linked to the fatty acid metabolic process, such as Fatty acid synthase (FASN1) and proteins involved in fatty acid beta oxidation, such as 3-hydroxyacyl-CoA dehydrogenase type-2 (scu), Yippee interacting protein 2 (yip2) or Enoyl-CoA hydratase (Echs1), indicate a shift in lipid metabolism, while the upregulation of proteins involved in the trehalose metabolic process, like Trehalase (Treh) and Trehalose-6-phosphate synthase 1 (Tps1), underlines the role of sugar metabolism in the LS response. The RNA splicing cluster encompasses proteins such as the Pasilla (ps), Glorund (glo) and Serine-arginine protein 55 (B52). The upregulation of these components implies an enhanced post-transcriptional regulation of gene expression, which could contribute to the observed behavioral phenotypes.

Proteins associated with neuroplasticity demonstrate significant upregulation, reflecting the potential reconfiguration of synaptic connections. These proteins include Bruchpilot (brp), which is essential for the active zone structure at synaptic sites; Calcium/Calmodulin-dependent protein kinase II (CaMKII), which is integral to synaptic plasticity and long-term potentiation. Furthermore, proteins like Synapsin (Syn), which modulates synaptic vesicle trafficking and neurotransmitter release, and Homer, implicated in the regulation of post-

synaptic receptor dynamics, are also elevated, suggesting an active restructuring of synaptic networks.

4.5.3.1 *Upregulation of redox-related proteins in LS: antioxidative and metabolic proteins*

To determine which upregulated proteins in LS are related to redox processes, we identified those known to be directly involved in oxidative-reduction reactions, antioxidant defense, and cellular redox homeostasis (Table 9.). We also included proteins that indirectly affect or are affected by redox. This category includes various dehydrogenases, glutathione S-transferases, peroxiredoxins, and enzymes involved in metabolic pathways that influence redox balance. Enzymes with oxidoreductase activity or proteins modulated by redox, such as those with NADP-binding domains, were also considered.

Table 9. Redox-related proteins upregulated in LS group compared to both NLS and CTRL group

#	Short Name	Description
1	Adh	Alcohol dehydrogenase (Adh) encodes an alcohol and acetaldehyde dehydrogenase involved in alcohol and acetaldehyde metabolism. (256 aa)
2	Aldh	Aldehyde dehydrogenase (Aldh) encodes an NAD[+] dependent mitochondrial aldehyde dehydrogenase. Its functions include detoxifying endogenous aldehydes generated by lipid peroxidation, and detoxifying acetaldehyde derived from dietary ethanol. (520 aa)

- 3 **CG10672** SD02021p; Carbonyl reductase (NADPH) activity; 3-keto sterol reductase activity; oxidoreductase activity, acting on NAD(P)H, quinone or similar compound as acceptor. (317 aa)
- 4 **CG11899** Probable phosphoserine aminotransferase; Catalyzes the reversible conversion of 3-phosphohydroxypyruvate to phosphoserine and of 3-hydroxy-2-oxo-4-phosphonooxybutanoate to phosphohydroxythreonine. Belongs to the class-V pyridoxal-phosphate-dependent aminotransferase family. SerC subfamily. (364 aa)
- 5 **CG1635** LD44914p; acyl-CoA hydrolase activity. It is involved in the biological process described with: acyl-CoA metabolic process. (448 aa)
- 6 **CG3107** Presequence protease, mitochondrial; ATP-independent protease that degrades mitochondrial transit peptides after their cleavage. Also degrades other unstructured peptides (By similarity); Belongs to the peptidase M16 family. PreP subfamily. (1034 aa)
- 7 **CG3603** RH09070p; Estradiol 17-beta-dehydrogenase activity; oxidoreductase activity, acting on the CH-OH group of donors, NAD or NADP as acceptor; 3-hydroxyacyl-CoA dehydrogenase activity; quinone binding. It is involved in the biological process described with: oxidation-reduction process; fatty acid biosynthetic process. (249 aa)
- 8 **CG3609** LD06553p; Oxidoreductase activity. It is involved in the biological process described with: oxidation-reduction process. (335 aa)
- 9 **CG3902** FI09602p; Flavin adenine dinucleotide binding; acyl-CoA dehydrogenase activity. It is involved in the biological process described with: oxidation-reduction process. (414 aa)
- 10 **CG6287** GH03305p; NAD binding; phosphoglycerate dehydrogenase activity. It is involved in the biological process described with: cellular amino acid metabolic process; oxidation-reduction process; Belongs to the D-isomer specific 2-hydroxyacid dehydrogenase family. (332 aa)
- 11 **CG7322** RH57257p; Oxidoreductase activity, acting on NAD(P)H, quinone or similar compound as acceptor; carbonyl reductase (NADPH) activity; L-xylulose reductase (NADP+) activity. It is involved in the biological process described with: xylulose metabolic process; glucose metabolic process. (242 aa)

12	CG9512	GH11762p; Oxidoreductase activity, acting on CH-OH group of donors; oxidoreductase activity; flavin adenine dinucleotide binding. It is involved in the biological process described with: oxidation-reduction process; ecdysteroid metabolic process. (623 aa)
13	FASN1	Fatty acid synthase 1 (FASN1) encodes a fatty acid synthase involved in glycogen metabolism and triglyceride biosynthesis. (2540 aa)
14	Gapdh1	Glyceraldehyde 3 phosphate dehydrogenase 1 (Gapdh1) encodes a glyceraldehyde-3-phosphate dehydrogenase involved in glycolysis, myoblast fusion and the development of somatic muscle. (332 aa)
15	Gapdh2	Glyceraldehyde 3 phosphate dehydrogenase 2 (Gapdh2) encodes a glyceraldehyde-3-phosphate dehydrogenase involved in glucose homeostasis; Belongs to the glyceraldehyde-3-phosphate dehydrogenase family. (332 aa)
16	GstE9	Putative glutathione S-transferase; Glutathione S transferase E9 (GstE9) encodes an enzyme involved in glutathione metabolic processes; Belongs to the GST superfamily. (221 aa)
17	GstS1	Glutathione S-transferase S1; Conjugation of reduced glutathione to a wide number of exogenous and endogenous hydrophobic electrophiles. May be involved in the detoxification of metabolites produced during cellular division and morphogenesis. (250 aa)
18	Had1	Beta hydroxy acid dehydrogenase 1, isoform A; NAD ⁺ binding; L-gulonate 3-dehydrogenase activity; 3-hydroxyacyl-CoA dehydrogenase activity. It is involved in the biological process described with: oxidation-reduction process; fatty acid metabolic process. (315 aa)
19	Hexo2	Beta-hexosaminidase; Hexosaminidase 2 (Hexo2) encodes a beta-N-acetylglucosaminidase involved in carbohydrate metabolism. (622 aa)
20	Jafrac1	Peroxiredoxin 1; Thiol-specific peroxidase that catalyzes the reduction of hydrogen peroxide and organic hydroperoxides to water and alcohols, respectively. Plays a role in cell protection against oxidative stress by detoxifying peroxides and as sensor of hydrogen peroxide-mediated signaling events. (194 aa)
21	mAcon1	Aconitate hydratase, mitochondrial; Mitochondrial aconitase 1 (mAcon1) encodes an enzyme that harbors an iron-sulfur cluster and catalyses the first step of the Krebs Cycle

		in mitochondria, converting citrate into isocitrate; Belongs to the aconitase/IPM isomerase family. (787 aa)
22	Mdh1	Malate dehydrogenase 1 (Mdh1) encodes a L-malate dehydrogenase involved in the interconversion of malate and oxaloacetate. (337 aa)
23	Mdh2	Malate dehydrogenase 2 (Mdh2) encodes one of the enzymes in the tricarboxylic acid cycle in mitochondria; Belongs to the LDH/MDH superfamily. (336 aa)
24	Mt:ND4	NADH-ubiquinone oxidoreductase chain 4; Core subunit of the mitochondrial membrane respiratory chain NADH dehydrogenase (Complex I) that is believed to belong to the minimal assembly required for catalysis. Complex I functions in the transfer of electrons from NADH to the respiratory chain. The immediate electron acceptor for the enzyme is believed to be ubiquinone (By similarity). (446 aa)
25	P5CS	Delta-1-pyrroline-5-carboxylate synthase; Glutamate-5-semialdehyde dehydrogenase activity; glutamate 5-kinase activity; delta1-pyrroline-5-carboxylate synthetase activity. It is involved in the biological process described with: oxidation-reduction process; proline biosynthetic process; In the C-terminal section; belongs to the gamma-glutamyl phosphate reductase family. (776 aa)
26	Pdh	Photoreceptor dehydrogenase (Pdh) encodes a retinal pigment cell dehydrogenase involved in retinol metabolism; Belongs to the short-chain dehydrogenases/reductases (SDR) family. (278 aa)
27	Pdhb	Pyruvate dehydrogenase E1 component subunit beta; The pyruvate dehydrogenase complex catalyzes the overall conversion of pyruvate to acetyl-CoA and CO2. (365 aa)
28	ple	Pale (ple) encodes a tyrosine hydroxylase, the first and rate-limiting step in the synthesis of dopamine (and eventually, melanin). Dopamine has critical roles in system development. (579 aa)
29	PPO2	Prophenoloxidase 2 (PPO2) encodes a protein stored in large crystals in the crystal cells (a type of hemocyte cell) that is involved in the melanization reaction. It contributes to melanization around wounds and wasp encapsulation and is thought to be activated by proteolytic cleavage by the product of Hayan. (684 aa)

30	Prx3	Thioredoxin peroxidase 3; Peroxiredoxin 3 (Prx3) encodes an antioxidant protein involved in hydrogen peroxide catabolism and regulation of apoptosis. (234 aa)
31	pug	C-1-tetrahydrofolate synthase, cytoplasmic; Pugilist (pug) encodes the trifunctional enzyme methylenetetrahydrofolate dehydrogenase involved in the pigmentation of pteridines and ommochromes; In the C-terminal section; belongs to the formate--tetrahydrofolate ligase family. (968 aa)
32	rdhB	Retinol dehydrogenase B (rdhB) encodes a retinol dehydrogenase involved in rhodopsin biosynthesis. (248 aa)
33	RFeSP	Cytochrome b-c1 complex subunit Rieske, mitochondrial; Component of the ubiquinol-cytochrome c reductase complex (complex III or cytochrome b-c1 complex), which is a respiratory chain that generates an electrochemical potential coupled to ATP synthesis. (230 aa)
34	scu	3-hydroxyacyl-CoA dehydrogenase type-2; May function in mitochondrial tRNA maturation. Catalyzes the beta-oxidation at position 17 of androgens and estrogens, and has 3- alpha-hydroxysteroid dehydrogenase activity with androsterone. Catalyzes the third step in the beta-oxidation of fatty acids. Carries out oxidative conversions of 7-beta-hydroxylated bile acids. Also exhibits 20-beta-OH and 21-OH dehydrogenase activities with C21 steroids. Required for cell survival during embryonic development. May play a role in germline formation; Belongs to the short-chain dehydrogenases/reductases [...] (255 aa)
35	se	Pyrimidodiazepine synthase; Mediates the conversion of 2-amino-4-oxo-6-pyruvoyl-5,6,7,8-tetrahydropteridine (6-PTP; also named 6-pyruvoyltetrahydropterin) to 2-amino-6-acetyl-3,7,8,9-tetrahydro-3H-pyrimido(4,5-b)[1,4]diazepin-4-one (pyrimidodiazepine or PDA), a key intermediate in red eye pigment drosopterin biosynthesis. (243 aa)
36	slgA	Proline dehydrogenase 1, mitochondrial; Converts proline to delta-1-pyrroline-5-carboxylate. (681 aa)
37	Ssadh	Succinate-semialdehyde dehydrogenase (NAD+) activity; succinate-semialdehyde dehydrogenase [NAD(P)+] activity. It is involved in the biological process described with: oxidation-reduction process; gamma-aminobutyric acid catabolic process. (509 aa)

38	Tps1	Trehalose-6-phosphate synthase 1 (Tps1) encodes the trehalose synthesis enzyme with an N-terminal trehalose-6-phosphate (T6P) synthase domain that catalyzes the production of T6P using glucose-6-phosphate and UDP-glucose. Its C-terminal T6P phosphatase domain dephosphorylates T6P to generate trehalose. (809 aa)
39	wal	Walrus, isoform A; Walrus (wal) encodes a protein involved in the development of Malpighian tubules, gut and trachea. (330 aa)

In response to LS following vMETH exposure, *Drosophila* exhibits a substantial upregulation in proteins implicated in redox balance and neuronal plasticity. Among these upregulated proteins, several are positioned at the intersection of redox processes and neuronal plasticity, suggesting a dual role in managing oxidative stress and contributing to synaptic remodeling.

Proteins involved in antioxidant defense mechanisms include Glutathione S-transferases (GstS1 and GstE9), which detoxify harmful compounds and manage oxidative stress, and Peroxiredoxin 3 (Prx3), which reduces hydrogen peroxide and protects cells from oxidative damage. Thioredoxin peroxidase 1 (Jafrac1) also plays a significant role by reducing hydrogen peroxide and protecting against oxidative stress, supporting cellular redox homeostasis.

Proteins involved in glycolysis and other metabolic pathways that influence redox balance include Gapdh1 and Gapdh2, which are involved in cell signaling and can influence neuroplasticity beyond their metabolic roles in glycolysis. Hexosaminidase 2 (Hexo2) is also related to glycolysis and tightly linked to cellular redox state.

Key proteins from the TCA cycle that are upregulated include Mdh1 and Mdh2, which convert malate to oxaloacetate, crucial steps in the citric acid cycle, and play roles in redox balance and influencing synaptic plasticity. mAcon1, involved in the TCA cycle, acts as a

sensor for cellular redox status and modulates metabolic processes influencing synaptic function.

Proteins involved in the mitochondrial electron transport chain and energy production include Mitochondrially encoded NADH dehydrogenase 4 (Mt:ND4), which is integral to the mitochondrial ETC, and Pyruvate dehydrogenase (Pdhb), which convert pyruvate to acetyl-CoA, crucial for cellular respiration and energy production. These enzymes support energy metabolism critical for synaptic activity and are involved in metabolic regulation in addition.

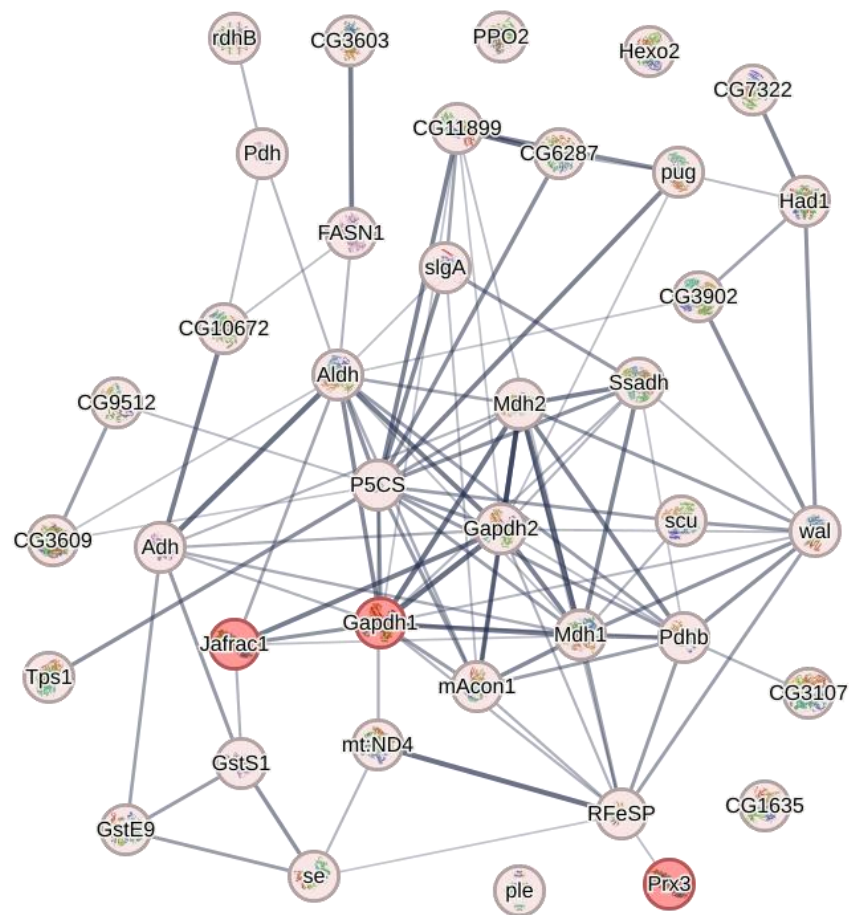


Figure 55. 39 redox-related proteins are upregulated in LS group compared to both NLS and CTRL group. *Gapdh1*, *Prx3* and *Jafrac1* are overlapping with our screen results.

This proteomic response indicates an LS fly brain actively engaged in protecting against oxidative stress while concurrently undergoing synaptic modifications. The upregulation of proteins such as GstS1 and GstE9, Prx3, Jafrac1, and others involved in cellular metabolism and redox balance highlights a coordinated effort to mitigate the effects of oxidative stress and support neuronal adaptability. This adaptation is presumably in response to the heightened activity demands imposed by vMETH exposure. Three upregulated redox-related proteins are particularly interesting, as we have shown their necessity for LS or SA through our genetic screen approach: Gapdh1, Prx3 and Jafrac1 (Figure 55.).

4.5.4 Proteins downregulated in LS

In the context of vMETH-induced LS in *Drosophila*, our proteomic analysis has highlighted significant downregulation across several critical biological pathways. Figure 56 illustrates the protein-protein interaction network depicting this downregulation, with specific clusters relating to intracellular anatomical structure (20 proteins), oxidative phosphorylation (10 proteins), ECM-receptor interaction (4 proteins), proton transmembrane transport (4 proteins), and proteolysis (3 proteins).

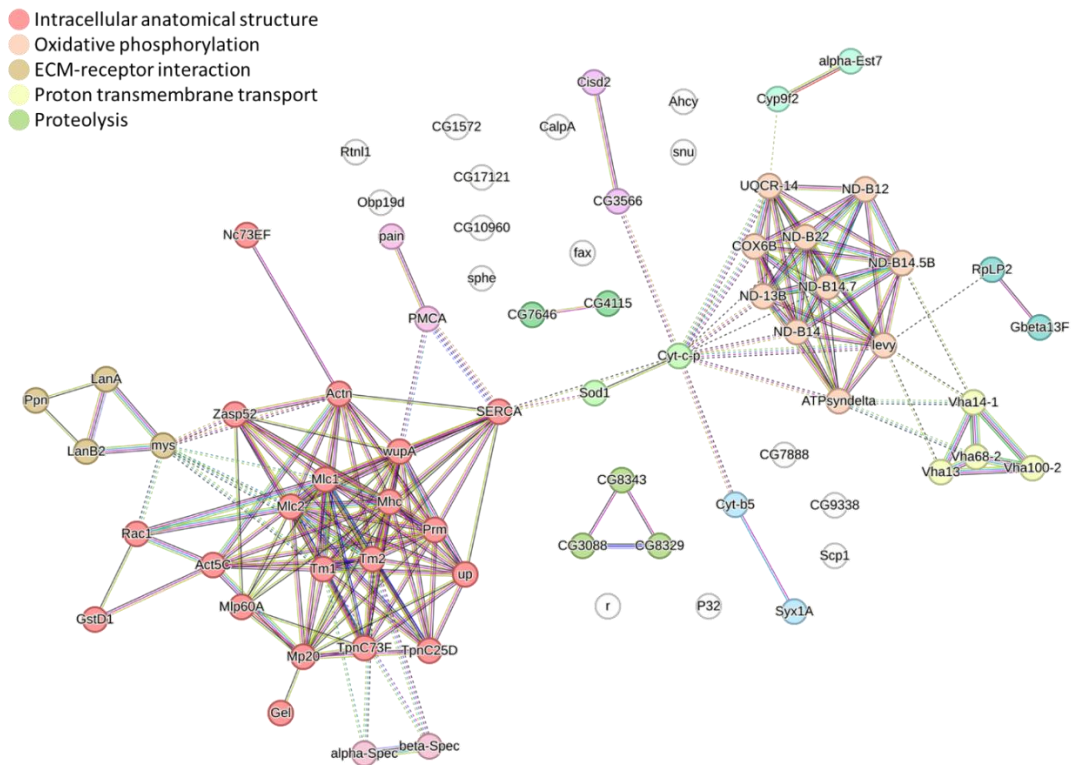


Figure 56. STRING visualization of proteins downregulated after LS in *Drosophila* brains. Color-coded clusters represent distinct functional pathways impacted, including intracellular anatomical structure, oxidative phosphorylation, ECM-receptor interaction, proton transmembrane transport, and proteolysis.

Proteins involved in maintaining the intracellular anatomical structure, such as Tropomyosin 1 and 2 (Tm1, Tm2) and Myosin light chain (Mlc1, Mlc2), are observed to be less abundant, suggesting a possible reorganization or de-emphasis of cytoskeletal integrity in LS flies. This might reflect alterations in cellular architecture associated with the behavioral changes observed. Enzymes like NADH dehydrogenases (ND-B12, ND-B14, etc.) and ATP synthase delta subunit (ATPsyndelta), key components of the oxidative phosphorylation pathway, are

notably downregulated. This decrease implies a reduction in mitochondrial energy metabolism efficiency, which may impact ATP availability and overall cellular energetics. Extracellular matrix (ECM) receptor interaction-related proteins such as Laminin (LanA, LanB2), its receptor Integrin beta-PS (mys) and Papilin (Ppn) show decreased levels, which could affect cell adhesion and signaling, processes that are essential for maintaining tissue structure and response to external stimuli. Proteins that facilitate proton transmembrane transport, including various V-type proton ATPase subunits like Vha68-2 and Vha13, also display reduced expression, indicating a potential dysregulation in maintaining proton gradients across membranes, which are vital for cellular homeostasis and signaling. Furthermore, the network points to downregulated proteolysis-related proteins such as peptidase CG8329, suggesting a possible decline in protein turnover and degradation, which are critical for protein quality control and regulation of various cellular processes.

In terms of neuroplasticity the network illustrates a downregulation in structural proteins Tm1, Tm2, Mlc1, Mlc2 which could reflect changes in the cytoarchitecture of neurons or a broader alteration in muscle plasticity, given their roles in maintaining cytoskeletal and muscular structure. Synaptic proteins such as Syntaxin-1A (Syx1A) are also less represented, potentially affecting synaptic vesicle docking and neurotransmitter release. Furthermore, the observed downregulation of peptidases might indicate a slower turnover of proteins within neurons, affecting synaptic remodeling and plasticity. The maintenance of synaptic connections and the fine-tuning of neural circuits through protein degradation and synthesis are essential for learning and memory, and alterations in these processes may contribute to the behavioral changes seen in LS.

4.5.4.1 Downregulation of redox-related proteins in LS: ETC and Sod1

Our analysis also revealed downregulation of certain proteins involved in redox balance (Table10). Among the downregulated proteins, enzymes central to redox homeostasis, such as Superoxide dismutase 1 (Sod1), which catalyzes the conversion of superoxide radicals into less reactive molecular oxygen and H₂O₂, show reduced expression. Additionally, proteins like NADH dehydrogenases, ATPases and ATP synthase important for mitochondrial oxidative phosphorylation and energy metabolism, are also less abundant. The downregulation of these proteins may imply an altered energetic state within neuronal cells, possibly affecting the capacity to cope with the increased metabolic demand following drug exposure. Sod1 is especially interesting for us because, although we showed its necessity for development of LS in genetic screen, it was downregulated in LS flies (Figure 57.).

Table 10. Redox-related proteins downregulated in LS group compared to both NLS and CTRL group

#	Short Name	Description
1	Ahcy	Adenosylhomocysteinase (Ahcy) encodes S-adenosyl-L-homocysteine hydrolase, the rate-limiting enzyme in methionine metabolism. This tetrameric enzyme catalyzes the reversible hydrolysis of S-Adenosylhomocysteine (SAH) to adenosine and L-homocysteine. The function of Ahcy product is required to maintain proper concentrations of SAH, which serves as an inhibitor of S-adenosylmethionine-dependent methylation reactions. (432 aa)
2	ATPsyndelta	ATP synthase, delta subunit, isoform A; Proton-transporting ATP synthase activity, rotational mechanism. It is involved in the biological

process described with: ATP synthesis coupled proton transport;
proton transmembrane transport. (157 aa)

3	CG17121	RH48101p; Oxidoreductase activity, acting on the CH-OH group of donors, NAD or NADP as acceptor; Belongs to the short-chain dehydrogenases/reductases (SDR) family. (361 aa)
4	COX6B	Cytochrome c oxidase subunit; This protein is one of the nuclear-coded polypeptide chains of cytochrome c oxidase, the terminal oxidase in mitochondrial electron transport. (96 aa)
5	Cyp9f2	Probable cytochrome P450 9f2; May be involved in the metabolism of insect hormones and in the breakdown of synthetic insecticides; Belongs to the cytochrome P450 family. (516 aa)
6	Cyt-b5	Cytochrome b5; Cytochrome b5 is a membrane-bound hemoprotein which functions as an electron carrier for several membrane-bound oxygenases. (134 aa)
7	Cyt-c-p	Cytochrome c-2; Electron carrier protein. The oxidized form of the cytochrome c heme group can accept an electron from the heme group of the cytochrome c1 subunit of cytochrome reductase. Cytochrome c then transfers this electron to the cytochrome oxidase complex, the final protein carrier in the mitochondrial electron-transport chain. (108 aa)
8	GstD1	Glutathione S-transferase D1; Conjugation of reduced glutathione to a wide number of exogenous and endogenous hydrophobic electrophiles. Has DDT dehydrochlorinase activity. May be involved in detoxification. (209 aa)

9	Nc73EF	Neural conserved at 73EF, isoform I; Oxoglutarate dehydrogenase (succinyl-transferring) activity; thiamine pyrophosphate binding. It is involved in the biological process described with: tricarboxylic acid cycle. (1105 aa)
10	ND-13B	NADH dehydrogenase (ubiquinone) activity; NADH dehydrogenase activity. It is involved in the biological process described with: mitochondrial electron transport, NADH to ubiquinone; respiratory electron transport chain. (124 aa)
11	ND-ACP	Acyl carrier protein, mitochondrial; Carrier of the growing fatty acid chain in fatty acid biosynthesis. Accessory and non-catalytic subunit of the mitochondrial membrane respiratory chain NADH dehydrogenase (Complex I), which functions in the transfer of electrons from NADH to the respiratory chain (By similarity); Belongs to the acyl carrier protein (ACP) family. (181 aa)
12	ND-B12	NADH dehydrogenase (Ubiquinone) B12 subunit, isoform A; NADH dehydrogenase activity. It is involved in the biological process described with: mitochondrial respiratory chain complex I assembly; mitochondrial electron transport, NADH to ubiquinone. (110 aa)
13	ND-B14	NADH dehydrogenase (Ubiquinone) B14 subunit, isoform A; NADH dehydrogenase activity. It is involved in the biological process described with: mitochondrial electron transport, NADH to ubiquinone; response to oxidative stress; Belongs to the complex I LYR family. (124 aa)
14	ND-B14.7	NADH dehydrogenase (Ubiquinone) B14.7 subunit; It is involved in the biological process described with: mitochondrial respiratory chain complex I assembly. (170 aa)

15	ND-B22	NADH dehydrogenase (Ubiquinone) B22 subunit, isoform A; NADH dehydrogenase activity. It is involved in the biological process described with: mitochondrial electron transport, NADH to ubiquinone. (144 aa)
16	Ppn	Papilin; Essential extracellular matrix (ECM) protein that influences cell rearrangements. May act by modulating metalloproteinases action during organogenesis. Able to non-competitively inhibit procollagen N- proteinase, an ADAMTS metalloproteinase; Belongs to the papilin family. (2898 aa)
17	SERCA	Calcium-transporting ATPase sarcoplasmic/endoplasmic reticulum type; Sarco/endoplasmic reticulum Ca(2+)-ATPase (SERCA) encodes an endoplasmic reticulum (ER) calcium pump with roles in ER calcium homeostasis and lipid storage. (1020 aa)
18	Sod1	Superoxide dismutase [Cu-Zn]; Destroys radicals which are normally produced within the cells and which are toxic to biological systems; Belongs to the Cu-Zn superoxide dismutase family. (153 aa)
19	UQCR-14	Cytochrome b-c1 complex subunit 7; Component of the ubiquinol-cytochrome c reductase complex (complex III or cytochrome b-c1 complex), which is part of the mitochondrial respiratory chain; Belongs to the UQCRB/QCR7 family. (111 aa)
20	Vha14-1	V-type proton ATPase subunit F 1; Subunit of the peripheral V1 complex of vacuolar ATPase essential for assembly or catalytic function. V-ATPase is responsible for acidifying a variety of intracellular compartments in eukaryotic cells. (124 aa)
21	Vha68-2	Vacuolar H[+] ATPase 68 kDa subunit 2 (Vha68-2) encodes a component of the V1 subunit of the vacuolar ATPase, which acidifies

endosomal compartments including the lysosome and influences the activity of several signaling pathways. (614 aa)

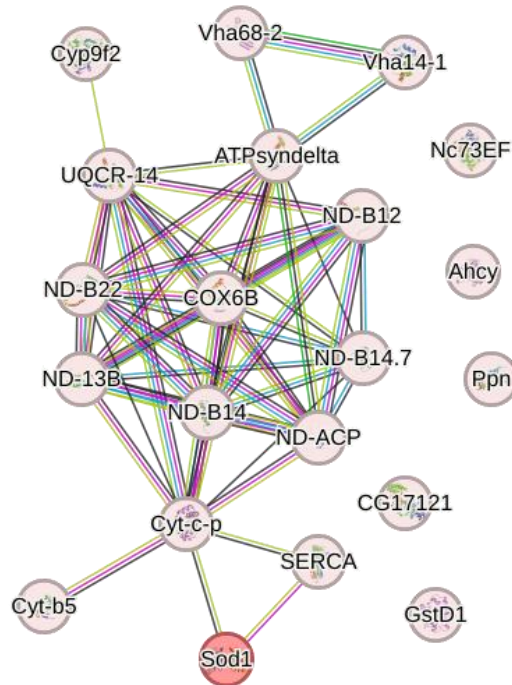


Figure 57. 21 redox-related proteins are downregulated in LS group compared to both NLS and CTRL group. *Sod1* is overlapping with our screen results.

4.6 Overlapping multiple approaches

The integration of genetic screen, selective breeding and proteomic profiling has yielded a detailed map of the genetic and molecular determinants of addiction-related behaviors. This multidimensional dataset points to a complex interplay between redox homeostasis,

metabolic pathways, and antioxidative mechanisms, which collectively modulate the propensity for, and resilience to, addiction-induced neurobehavioral changes.

The genetic contributors to LS and preferential SA, identified through pan-neuronal and neuron-specific expression analyses using genetic screen, highlight the significance of several redox related genes.

Table 11. Genes necessary for LS to vMETH:

All Neurons	Dopaminergic and Serotonergic Neurons	Dopaminergic Neurons
<i>Superoxide Dismutase 2 (Sod2)</i>	<i>Catalase (Cat)</i>	<i>Glyceraldehyde 3-phosphate dehydrogenase 1 (Gapdh1)</i>
<i>Enhancer of split m3-HLH (E(spl)m3-HLH)</i>	<i>Superoxide Dismutase 1 (Sod1)</i>	<i>Malic enzyme (Men)</i>
	<i>Superoxide Dismutase 2 (Sod2)</i>	
	<i>Glyceraldehyde 3-phosphate dehydrogenase 1 (Gapdh1)</i>	
	<i>Malic enzyme (Men)</i>	

Table 12. Genes necessary for preferential self-administration of METH:

Dopaminergic and Serotonergic Neurons	Dopaminergic Neurons
<i>Superoxide Dismutase 1 (Sod1)</i>	<i>Peroxiredoxin 3 (Prx3)</i>
<i>Glyceraldehyde 3-phosphate dehydrogenase 1 (Gapdh1)</i>	

Malic enzyme (Men)

Table 13. Genes necessary for LS to vCOC:

Dopaminergic Neurons

Peroxiredoxin 2 (Jafrac1)

Next, we checked the pathways and localization of genes identified in our genetic screen, which were shown to be necessary for the development of addiction-related behaviors, LS and SA. Then we checked the overlaps with our proteomic analyses and investigated the expression of proteins that have similar functions or belong to the same pathway. We specifically highlighted the genes/proteins that were yielded by at least two approaches (Figure 58).

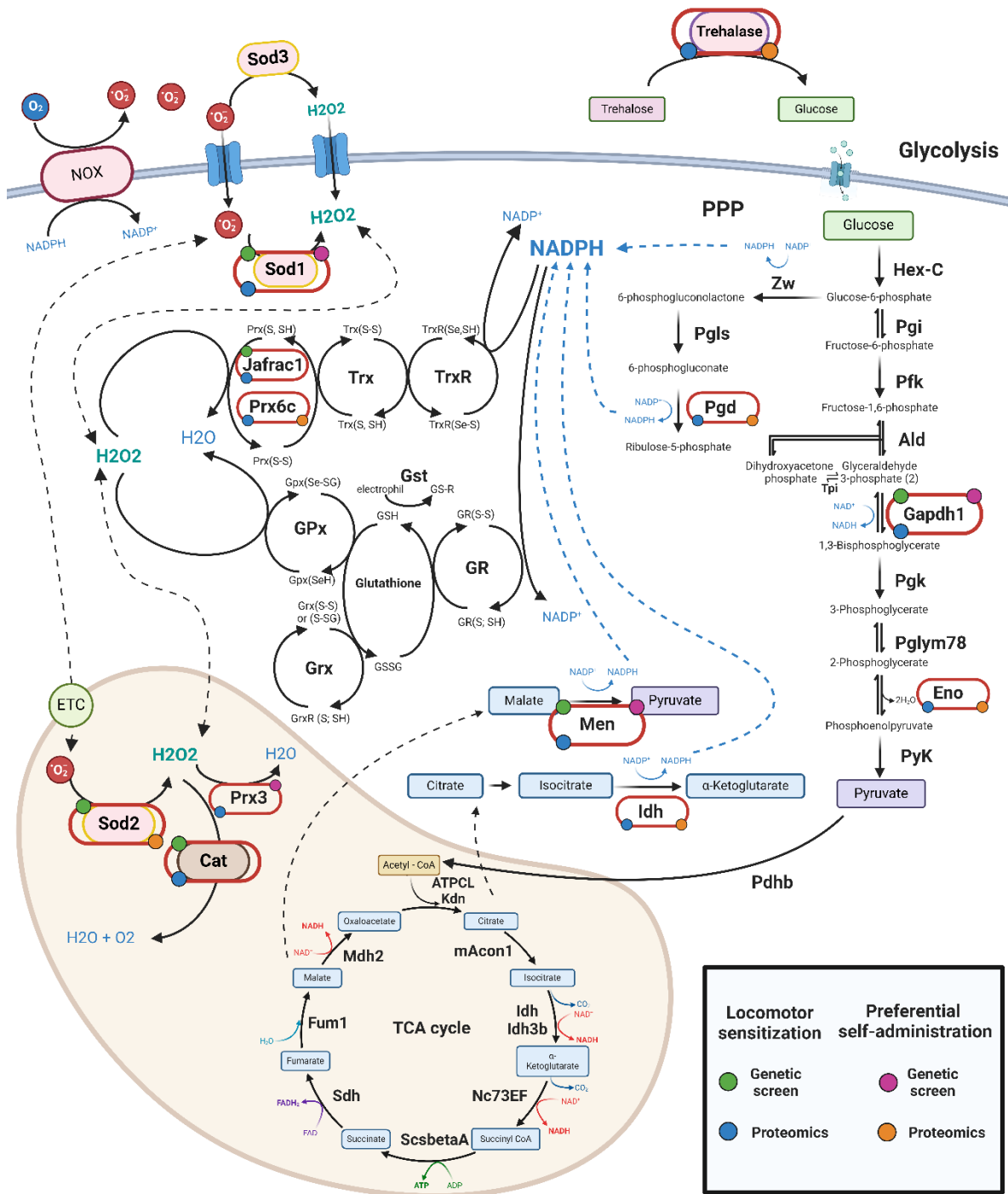


Figure 58. Schematic representation of metabolic pathways and the positions of the proteins/genes which affect LS and/or preference for METH in *Drosophila* identified by genetic screen and proteomics. Detailed schematic of metabolic pathways, highlighting the locations and roles of specific proteins and genes implicated in LS and METH preference. The

pathways include antioxidant defense system, glycolysis, the pentose phosphate pathway (PPP), and the tricarboxylic acid (TCA) cycle, along with cellular NADPH production mechanisms. In the antioxidant defense pathway, key enzymes such as Superoxide Dismutase (*Sod1*, *Sod2*, *Sod3*) catalyze the conversion of superoxide radicals into hydrogen peroxide (H_2O_2), with *Sod1* located in the cytoplasm, *Sod2* in the mitochondria, and *Sod3* in the extracellular space. Catalase (*Cat*) then converts H_2O_2 into water and oxygen, primarily within peroxisomes. Peroxiredoxins (*Prx3*, *Prx6c*) and *Jafrac1* reduce H_2O_2 to water using reducing equivalents from thioredoxin. In glucose metabolism, Glyceraldehyde 3-phosphate dehydrogenase (*Gapdh1*) catalyzes a step in glycolysis, converting glyceraldehyde 3-phosphate to 1,3-bisphosphoglycerate, while Enolase (*Eno*) converts 2-phosphoglycerate to phosphoenolpyruvate. The PPP features 6-Phosphogluconate dehydrogenase (*Pgd*), which catalyzes the oxidative decarboxylation of 6-phosphogluconate to ribulose 5-phosphate, generating NADPH. Additionally, key players in cellular NADPH production include Malic enzyme (*Men*) and Isocitrate dehydrogenase (*Idh*). This diagram features the significance of these genes and enzymes in mediating the biochemical effects of METH exposure and addiction, with their roles elucidated through genetic screen and proteomics analyses.





Figure 58 summarizes findings in a schematic of metabolic pathways, showing the locations of proteins/genes implicated in either LS and/or METH preference as uncovered across multiple methodologies. The diagram foregrounds:

- Antioxidant defense-related genes such as *Superoxide Dismutase 1 (Sod1)*, *Superoxide Dismutase 2 (Sod2)*, *Catalase (Cat)*, *Peroxiredoxin 3 (Prx3)*, and *Peroxiredoxin 6c (Prx6c)*.
- Genes included in glucose metabolism comprising *Glyceraldehyde 3-phosphate dehydrogenase 1 (Gapdh1)* and *Enolase (Eno)*.
- Key players in cellular NADPH production: *Malic enzyme (Men)*, *Isocitrate dehydrogenase (Idh)*, and *6-phosphogluconate dehydrogenase (Pgd)*.

We also looked into expression patterns of proteins that were not consistently up or downregulated in LS compared to both CTRL and NLS, but could be potentially interesting

as they are either identified in genetic screen as important for LS or they are part of the same pathway of identified genes, or have similar functions. For example, Sod2 was identified using screen, and although it didn't show statistically significant down regulation compared to NLS, it was significantly lower in LS compared to CTRL.

Table 14. Summary of redox-related genes implicated in LS and SA

<i>Gene/protein</i>	LS Genetic Screen 	LS Proteomics 	SA Genetic Screen 	SA Proteomics 
<i>Sod1</i>	Necessary for LS in dopaminergic and serotonergic neurons	Downregulated in LS group compared to CTRL and NLS	Necessary for preferential SA in dopaminergic and serotonergic neurons	
<i>Sod2</i>	Necessary for LS in all neurons and in dopaminergic and serotonergic neurons	Downregulated in LS group compared to CTRL		Detected only in P0
<i>Cat</i>	Necessary for LS in dopaminergic and serotonergic neurons	Upregulated in LS group compared to CTRL		
<i>Gapdh1</i>	Necessary for LS in dopaminergic and serotonergic neurons and in dopaminergic neurons	Upregulated in LS group compared to CTRL and NLS	Necessary for preferential SA in dopaminergic and serotonergic neurons	
<i>Men</i>	Necessary for LS in dopaminergic and serotonergic neurons and in dopaminergic neurons	Upregulated in LS group compared to CTRL *Mitochondrial isoform of malic enzyme (Men-b) was upregulated in LS compared to NLS	Necessary for preferential SA in dopaminergic and serotonergic neurons	

<i>E(spl)m3-HLH</i>	Necessary for LS in all neurons		
<i>Prx3</i>	Phenotype in flybong was not drug-specific	Upregulated in LS group compared to CTRL and NLS	Necessary for preferential SA in dopaminergic neurons
<i>GstE1</i>	Showing LS phenotype, BUT sensitivity was not drug-specific (same response to heated air)	Downregulated in LS group compared to CTRL	Detected only in P0
<i>Prx6c</i> (<i>Prx2540-2</i>)		Downregulated in LS group compared to NLS Upregulated in LS group compared to CTRL	Detected only in HP
<i>Idh</i>		Downregulated in LS group compared to NLS	Upregulated in LP group compared to HP
<i>Pgd</i>		Upregulated in LS group compared to NLS	Upregulated in LP group compared to HP
<i>Eno</i>		Upregulated in LS group compared to NLS	Downregulated in HP compared to P0
<i>Treh</i>		Upregulated in LS group compared to CTRL and NLS	Detected only in P0
<i>Bacc</i>			Detected only in LP

Integration of behavioral genetics and proteomics uncovered a common set of genes and proteins implicated in LS and SA, including antioxidant defense enzymes, metabolic regulators, and neurotransmitter modulators. We found a convergence of genes associated with antioxidant defense - *Sod1*, *Sod2*, *Cat*, *Prx3*, and *Prx6c*, glucose metabolism - *Gapdh1* and *Eno*, and genes crucial for NADPH production in the cell - *Men*, *Idh*, and *Pgd*.

5. DISCUSSION

5.1 Introduction to the Main Findings

The aim of this study was to elucidate the genetic and proteomic mechanisms underlying behavioral responses to METH in *Drosophila melanogaster*, with a particular focus on genes involved in redox regulation. Our research was driven by the hypothesis that redox processes play a crucial role in modulating neuronal plasticity and addiction behaviors. We employed a series of integrated experimental approaches to test this hypothesis, including the development of novel assay, selective breeding, and comprehensive proteomic and genetic analyses.

One of the major achievements of this study was the development of a modified Capillary Feeder (CAFÉ) assay, referred to as FlyCafe. This assay enabled precise, high-throughput measurement of METH self-administration (SA) in individual flies. The FlyCafe assay allowed us to quantify individual preferences for METH, assess locomotor activity, and monitor environmental positioning during SA. This methodological innovation represents a significant advancement in the study of drug-induced behaviors in *Drosophila* and provides a robust platform for future addiction research.

Utilizing the FlyCafe method, we identified two distinct strains of flies with high (HP) and low (LP) preferences for METH SA. This selection process facilitated the identification of genetic and proteomic factors associated with voluntary drug consumption. The HP and LP strains exhibited distinct behavioral phenotypes such as sleep, activity and negative geotaxis that were additionally quantified. The ability to select and breed flies based on their METH preference allowed us to create a model system for studying the genetic basis of addiction.

Proteomic analyses of brain tissues from these selected strains revealed significant changes in specific proteins associated with differential METH preferences. Notably, proteins involved in metabolic processes, structural integrity and protein turnover were differentially

expressed, including *Bacchus*, regulator of TA/OA conversion which was present uniquely in LP line.

Our genetic screen targeting redox-related genes identified several critical genes that regulate LS to vMETH. Genes such as *Cat*, *Sod1*, *Sod2*, *Gapdh1* and *Men* were found to be essential for LS in dopaminergic and serotonergic neurons. Furthermore, *Prx3*, an antioxidant enzyme, was required for METH SA behavior in dopaminergic neurons.

Proteomic analysis of brain tissues from flies that did or did not develop LS after two administrations of vMETH identified proteins up or downregulated in flies that developed LS. This approach enabled us to pinpoint proteins associated with the LS phenotype. The analysis revealed a complex interplay between metabolic processes, redox status, and neuronal plasticity, contributing to our understanding of the origins of addictive behaviors.

In summary, our integrative and multifaceted experimental approach has provided a comprehensive understanding of the interplay between metabolic processes, redox status, and neuronal plasticity in the development of two addictive behaviors in flies, LS and SA, with an emphasis on genes that regulate both behaviors, since we proved that those two behaviours have overlapping regulation and affect each other.

5.1.1 Summary of the experimental design and approach

The novelty of this study was to dissect the complexities of drug addiction by focusing on the role of redox processes in the modulation of neuronal plasticity and addiction behaviors, specifically in the context of METH usage. By employing *Drosophila melanogaster* as a model organism, the research utilized newly adapted Capillary Feeder assay (FlyCafe) and the FlyBong method, previously developed in our lab, to quantify two drug-induced behavioral phenotypes, LS and SA, thus revealing the interaction between genotype and addiction phenotypes.

The methodology included bidirectional selective breeding to distinguish phenotypes with varying METH preferences, genetic screen targeting genes regulating redox homeostasis, and proteomic analysis to identify critical proteins and brain regions implicated in redox-mediated addiction mechanisms. Notably, the refinement of the CAFE method to simultaneously measure food consumption and locomotion emerges as a significant advancement, offering deeper insights into the genetic and molecular basis of addiction. Through these diverse yet complementary approaches, the study aimed to clarify the complex interplay between metabolic processes, redox status, and neuronal plasticity in the origin of addictive behaviors.

5.1.2 The significance of the FlyCafe assay

The FlyCafe assay is a new research method designed to study the psychostimulant SA and preference in *Drosophila melanogaster*. This assay represents an improvement over traditional feeding behavior studies based on the CAFÉ principles due to its precision in measuring the liquid food consumption, a high-throughput concept and simultaneous locomotor activity tracking. Unlike the traditional CAFE assays, which assess liquid food consumption among a group of flies (290,292), the FlyCafe assay measures intake at the individual level, while also mitigating inaccuracies caused by evaporation and spillage. This approach allows for the detection of individual variations in feeding behavior advancing our understanding of the genetic and environmental factors that influence voluntary SA of addictive substances.

Central to the assay's innovation is its high-throughput capability, enabling simultaneous observation and measurement of up to 32 individual flies. This feature significantly increases data collection efficiency and improves the statistical reliability of findings, particularly in addiction studies where large sample sizes are important. The scalability of the FlyCafe assay is an advantage for behavioral and genetic research, facilitating the collection of large data sets in a single experimental run and thereby expediting the pace of research.

The strengths of FlyCafe assay, such as precision in measurement, high-throughput analysis, integration with genetic tools, and environmental control, make it uniquely suitable for selective breeding experiments in *Drosophila*. It enables the detailed and efficient analysis of feeding behaviors and psychostimulant preferences, crucial for identifying and selecting desirable genetic traits. Moreover, integrating tools like the UAS-Gal4 system for specific gene manipulation with FlyCafe, further enhances its utility in genetic research. This integration facilitates the identification of anatomically specific genetic expression that regulates voluntary food choice and the effects of addictive substance on motivational circuits that lead to preferential consumption.

5.1.3 Methamphetamine preference and consumption

We showed that *Drosophila* voluntarily self-administers METH food over Sugar food using the FlyCafe method. These results confirm already published evidence for preferential consumption of cocaine and METH in the CAFÉ assay (275), and suggests that despite the neuroanatomical differences between fly and mammalian brains, behavioral effects of psychostimulants are regulated at least in part by similar neuronal mechanisms.

As compared to other methods and procedures for quantification of drug consumption in flies our new FlyCafe method enables quantification of additional behavioral parameters, such as amount of locomotion in individual flies and dwell time spent by the capillary with Sugar or METH food. Interestingly, although flies consume more METH food than Sugar food during day one and two, which correlates with dwell time at METH food capillary, they do not increase the amount of locomotor activity. This is in contrast with other studies in *D. melanogaster* which show a strong motor activating effect of psychostimulants. However, in those studies drug concentrations were higher, administration was not voluntary because flies could not choose a food source, and those experiments did not allow for precise measurement of the amount of ingested food (264,293). When flies voluntarily choose between food sources the total daily food consumption (sum of METH and Sugar food) does

not differ between control and experimental group, although the experimental group consumes more METH at the expense of Sugar food. Interestingly, the amount of consumed METH food is insufficient to induce anorexic effects, which have been shown for higher concentrations of forced METH administration. Thus, in a choice paradigm such as FlyCafe flies preferentially administer METH food over highly palatable Sugar food, but the motivation to ingest METH does not lead to hyperactivity or anorexia, which are possibly perceived as aversive.

The observed voluntary SA of METH by *Drosophila* in our study provides a clear indication of substance preference, underscoring the assay's effectiveness in modeling aspects of addiction. This preference is particularly noteworthy as it demonstrates a selective behavior towards METH over Sugar food, indicating a neurobehavioral effect of the drug that motivates flies towards its consumption. Such findings are consistent with mammalian models, where voluntary SA is used as a key indicator of addictive potential (294,295). Our results align with these models, highlighting the evolutionary continuity in the basic mechanisms underlying drug preference and addiction.

5.1.4 *Per* gene is a common genetic factor underlying LS and SA

We used *D. melanogaster* as a genetically tractable model organism to investigate the hypothesis that LS to vMETH, an endophenotype with low face validity in addiction studies, influences SA of METH containing food, an endophenotype with high face validity. We show that the development of LS decreases preferential SA of METH food. Our finding agrees with a similar study using rat models, where decreased SA of METH after behavioral sensitization was explained by the increased efficacy of the drug after intermittent administration during the behavioral sensitization protocol (296).

The interaction between these two behavioral endophenotypes is further emphasized by the observation that preferential SA of METH food prevents the expression of LS to vMETH.

As the increase in the locomotor activity to the first dose of vMETH remains the same between control and experimental group, this argues for specificity of action of METH SA on neural mechanisms that regulate sensitization. SA of relatively low doses of METH food over several days likely triggers different neuromodulatory mechanisms in the brain, than acute, high concentration administration of vMETH. However, based on the mutual interaction between locomotor sensitization and preferential consumption, we propose that there is a likely overlap in the brain areas that regulate these two endophenotypes. Considering this shared mechanism, it suggests that LS and SA are two endophenotypes representing a complex addiction syndrome, similar to how addiction in humans can be analyzed through simple and measurable phenotypes. Each phenotype has its unique elements but also significant overlaps with others, ultimately resulting in addiction.

In the previous studies in our lab, we have observed apparent tolerance to motor-activating effects of vMETH at time intervals preceding those that lead to the expression of locomotor sensitization. Similar observation is reported in Filosevic et al, for vCOC (264). The simplest explanation is that both drugs lead to dysfunction of the monoaminergic system, which results in decreased locomotor activity. This dysfunction could be dependent on the metabolism of cocaine and METH which affects monoaminergic synthesis and release and could lead to monoaminergic depletion shortly after the first drug administration. This explanation does not exclude other mechanisms of adaptation, including changes in the number or sensitivity of monoaminergic receptors (297). Previous work has shown that the neurotransmitter dopamine governs cellular responses underlying LS in flies and mammals (298–300). Regulation of the dopaminergic system in areas of the rodent brain responsible for locomotor sensitization and reward are dependent on the circadian gene *mClock* (301), and sensitivity of D2-type dopaminergic receptors is changed in *per⁰¹* flies that do not develop behavioral sensitization to volatilized cocaine (293). Furthermore, chronic cocaine exposure induces expression of *mPer2* gene in striatal regions of the rodent brain (302), further alluding to the important role that circadian genes *Clock* and *per* play in the regulation of cocaine-induced phenotypes and their interaction with the dopaminergic

system. Thus, we used *per*⁰¹ mutant flies to see if this gene might be a candidate for a genetic link between locomotor sensitization and SA of METH.

wt flies develop robust LS to vMETH, and we have shown that *per*⁰¹ flies do not develop LS to METH nor do they show preferential consumption of METH food. This suggests that the function of the *period* gene is required for expression of two distinct behavioral phenotypes induced by METH. Although we do not have direct evidence for functional interactions between the *per* gene and the dopaminergic system in modulating the effect of LS on SA, based on existing evidence we propose that long term modulation at the level of dopamine synthesis, release or receptor sensitivity might be a likely mechanism that is disrupted in *per*⁰¹ mutants.

In conclusion, our results show that LS and preferential SA of METH are two types of METH-induced behaviors with partially overlapping brain mechanisms, which will have to be further investigated and characterized. LS leads to long term changes in the neuromodulatory mechanisms that last longer than the time for the expression of LS, which is ten hours. This suggests that LS is indeed a valid laboratory endophenotype that will significantly contribute to our understanding of the mechanisms of change that lead to addiction.

5.1.5 Overview of selective breeding and genetic screen

The selective breeding process, carried out over 30 generations, employed the FlyCafe assay to distinguish flies with distinct METH consumption preferences. By selectively mating individuals exhibiting extreme behaviors, we established two divergent lines: one displaying a high preference for METH (HP) and another showing low METH preference (LP). Concurrently, a genetic screen targeting redox-related genes provided critical insights into the genetic architecture of LS to vMETH. This dual approach allowed us to identify the

contributions of specific genes to two different addiction-related behaviors, with the idea of identifying other potential shared genetic mechanisms.

The genetic screen aimed to identify redox-related genes influencing the development of LS to vMETH in *Drosophila* was designed using FlyBase database for the identification of candidate genes. The focus was on genes implicated in redox processes, particularly those encoding antioxidant enzymes, oxidoreductases, and proteins involved in redox signaling pathways. Using RNA interference (RNAi) lines and anatomically specific GAL4 drivers, the study evaluated the impact of silencing selected genes on LS and other addiction-related behaviors. By employing a experimental setup that included the FlyBong assay for testing LS and additional assessments for negative geotaxis and locomotor activity, the research illuminated the roles that redox related genes play in the dopaminergic and serotonergic circuits, major circuits involved in the neuroplastic changes that lead to addiction-related phenotypes. Through selective breeding and genetic screen we sought to identify potential genetic candidates influencing neuronal plasticity induced by METH administration.

5.2 Bacchus presence, alongside efficient metabolic regulation, protein turnover and structural integrity, underlies reduced METH preference

5.2.1 Stable divergence of high and low preference for METH SA after 30 generations of selection

The implementation of a selective breeding strategy to distinguish between high and low METH preference phenotypes represents a pioneering approach in the study of genetic predispositions to substance abuse in *D. melanogaster*. After 30 generations of selective breeding for differential ingestion of METH-laced versus Sugar food we successfully selected two distinct lines of *Drosophila*: one exhibiting a high preference for METH (HP) and the

other a low preference (LP). This divergent selection underscores the genetic basis of addiction behavior, aligning with the hypothesis that genetic factors significantly influence the motivation for substance consumption.

The significant divergence in METH preference between HP and LP lines, echoes the findings from mammalian models, underlining the heritability and genetic complexity of addiction-related traits (288,303). Interestingly, the stability of these traits post-selection highlights the potential for enduring genetic changes, suggesting that the selection process may have induced enrichment of allelic variants favoring these preferences. This is in line with previous studies showing stable phenotypic changes across generations in flies selected for ethanol sensitivity (304).

Further characterization of HP and LP lines revealed differences beyond METH preference, including variations in locomotor activity, sleep patterns, vertical climbing ability, and body weight. Particularly, the LP line exhibited increased locomotor activity and body weight, and decreased vertical climbing ability, suggesting these traits were co-selected and regulated by genes that have pleiotropic function. For instance, genes involved in addiction pathways, in our case METH preference, may also affect physical traits and behaviors, meaning certain genetic profiles can predispose individuals to multiple related characteristics. These phenotypes could serve as biomarkers for addiction vulnerability, similar to how certain sleep disorders are predictive of neurodegenerative diseases like Parkinson's disease (305).

The increased body weight and decreased climbing ability observed in the LP line may be a result of genetic factors that simultaneously influence metabolism, muscle function, and behavioral tendencies. The increased locomotor activity and decreased negative geotaxis in the LP line present an intriguing paradox. While the LP line is more active overall, its reduced vertical climbing ability suggests impairments in specific motor coordination or muscle function. One possible explanation is that hyperactivity in LP flies could be disrupting their coordination or attention, leading to decreased performance in specific motor tasks. The known inverse relationship between dopamine levels and motor functions, where both

excess and deficit in DA can impair coordination, supports this hypothesis (257). Interestingly, our data show that dopamine levels, although reduced in both HP and LP compared to the parental line, are higher in LP than in HP. This suggests that while dopamine changes correlate with increased activity, other factors might explain reduced climbing ability. It is known that optimal levels of DA are required for proper motor function, with deviations in either direction leading to impairments (306). Thus, elevated dopamine or overly sensitive DA receptors in LP flies might be disrupting motor coordination despite the overall increase in activity. Regardless of significant increases in activity, LP flies did not show notable changes in sleep patterns. This suggests that the neuronal circuits regulating sleep and locomotor activity may be overlapping but are not identical. The increased activity without corresponding sleep disruption indicates changes specific to neural networks governing locomotion rather than those regulating sleep. Conversely, HP flies showed significant alterations in sleep patterns without corresponding changes in locomotor activity, implying that selection may have influenced genes regulating sleep independently of those affecting general activity.

Neurochemical analyses provided insights into the molecular differences between HP and LP lines. Besides dopamine, the neurochemicals OA, TA, GLU, ACh, and GABA were quantified. Most neurotransmitters did not show significant differences between HP and LP lines. However, in all cases, there was a significant difference between selected lines and the parental line. For example, octopamine, acetylcholine, and GABA concentrations were significantly lower in both HP and LP lines relative to the parental line but did not differ between HP and LP. This indicates that the breeding process which included exposure to METH in each generation, influenced these neurotransmitters, yet their levels were not directly correlated with the preference for METH.

The only instances where neurotransmitter concentrations differed between brains of HP versus the LP lines were for DA, Glu and TA. Dopamine and glutamate levels were significantly higher in the LP line compared to HP, while both HP and LP had significantly

lower levels of these neurotransmitters relative to the parental line. This suggests a complex interplay where reduced levels of dopamine and glutamate in both selected lines compared to the parental line could be associated with altered addiction-related behaviors. The most intriguing finding pertained to TA concentration. The LP line showed significantly elevated levels of this neurotransmitter relative to both the parental and HP lines, while there were no differences between the HP and parental lines. This suggests a unique role for TA in modulating low preference for METH, potentially mediated through its influence on neural circuits involved in addiction. This hypothesis was further supported by unique presence of *Bacchus*, a protein which negatively regulates conversion of TA to OA, in LP line, as determined in our proteomic study.

Elevated TA levels in LP flies suggest a novel neurobiological pathway influencing METH preference. TA emerges as a potential key player in modulating substance preference behaviors. TA is known to modulate various behaviors including arousal, aggression, and possibly aversion (307). Elevated TA in LP flies could be enhancing aversive responses to METH, leading to lower preference. TA could be acting as a neuromodulator that affects how METH is perceived or how its effects are processed by the nervous system. Elevated levels could modify neural circuits in a way that diminishes METH's attractiveness or rewarding effects. The high levels of TA might be providing a feedback mechanism that limits the conversion of TA to OA, maintaining octopamine at similar levels across both lines despite different behavioral responses. One explanation for the connection between elevated TA and reduced METH preference involves TA role in modulating neural circuits responsible for arousal and locomotor activity. The observed hyperactivity in LP flies, particularly in the absence of METH, might be attributed to elevated TA altering neural excitability or responsiveness in pathways shared with those affected by METH. This hyperactivity might reflect an intrinsic compensatory mechanism or altered sensitivity to external stimuli, including drugs of abuse. Furthermore, the proteomic analysis revealing the presence of *Bacchus*, a negative regulator of tyramine beta-hydroxylase, exclusively in LP flies provides at a genetic or molecular basis for the elevated TA levels. By inhibiting the

conversion of TA to OA, *Bacchus* could directly contribute to the accumulation of TA, subsequently affecting behavioral responses to METH.

In summary, the co-selected phenotypes in the LP line—hyperactivity, increased body weight, and decreased geotaxis—highlight the genetic complexity of addiction-related behaviors and emphasize the importance of phenotypic characterization in understanding addiction. The elevated TA and its regulatory mechanisms suggest novel pathways influencing METH preference.

5.2.2 A novel gene *Bacchus* defines low preference for METH

The *Bacchus* (*Bacc*) gene has been documented in the context of alcohol addiction, particularly through its role in modulating ethanol sensitivity in *Drosophila*. *Bacchus* encodes a nuclear protein that regulates the transcription of the *Tbh* gene, which in turn converts tyramine to octopamine. Disruption of *Bacc* increases *Tbh* activity and increases conversion of TA to OA. Elevated OA levels reduce ethanol sensitivity (291).

In our analysis, *Bacc* protein is detected uniquely in LP flies, which have been bred for low METH preference, but not in the parental line or HP flies. This selective expression of *Bacc* suggests that it might play a role in modulating METH preference in a manner analogous to its role in ethanol sensitivity. Elevated tyramine, resulting from *Bacchus*'s inhibition of *Tbh*, may enhance aversive responses to METH or alter reward processing, thus reducing METH preference. This modulation likely involves changes in neural excitability and the functioning of circuits associated with arousal and locomotion. Tyramine could potentially act on octopaminergic receptors, and its elevated levels could desensitize these pathways or engage alternative signaling mechanisms, contributing to the observed behavioral phenotypes (308). In the context of our findings, *Bacc* appears to mediate a neurobiological pathway that counters the rewarding effects of METH, promoting a state where METH is less attractive or rewarding to the organism. Additionally, when we silenced *Tbh* in all neurons

of *wt* flies, we observed a phenotype similar to that of LP flies, characterized by reduced preference for METH (Figure 59). This result further supports the idea that the tyramine / octopamine pathway, regulated by *Tbh* activity, is crucial not only for ethanol sensitivity but also for psychostimulant preference. The decreased METH preference upon *Tbh* silencing implies that lower octopamine levels or higher tyramine levels might contribute to a reduced inclination towards METH, aligning with the LP phenotype.

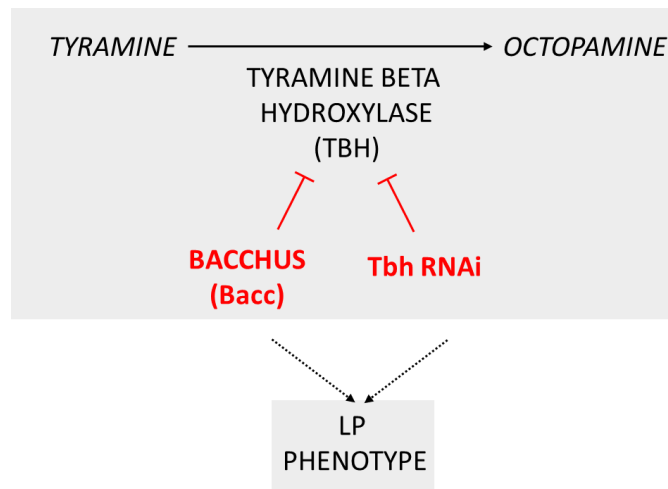


Figure 59. Blocking conversion of tyramine into octopamine results in LP phenotype.

Bacchus and Tbh RNAi.

These findings suggest a potential common pathway involving *Bacc* and *Tbh* that modulates both ethanol and METH addiction. The selective presence of *Bacc* in LP flies and the phenotypic resemblance induced by *Tbh* silencing indicate that the tyramine / octopamine neurotransmitter system could be a critical mediator of addiction-related behaviors across different substances. The differential expression of *Bacc* and the resulting neurotransmitter changes may represent a broader mechanism by which genetic and molecular factors influence substance preference and addiction susceptibility.

5.2.3 Efficient metabolic regulation, protein turnover, and structural integrity underlie reduced METH preference

The analysis of proteins unique to a *Drosophila* line selectively bred for low METH preference reveals several biological processes and pathways potentially influencing drug addiction and METH preference behaviors. These proteins were not detected in the PO nor the HP group, indicating their potential role as protective markers against METH's rewarding effects.

Here, we discuss the potential roles of Electron Transfer Flavoprotein-Ubiquinone Oxidoreductase (Etf-QO), Cytochrome P450 9f2 (Cyp9f2), Sterol Carrier Protein X (ScpX), Probable Pseudouridine-5'-Phosphatase (Gs1l), and Dihydropteridine Reductase (Dhpr) in contributing to this low preference phenotype. Etf-QO, a mitochondrial membrane-bound protein channels electrons from fatty acid oxidation into the respiratory chain, playing a crucial role in maintaining efficient energy production through oxidative phosphorylation. METH exposure induces oxidative stress and disrupts mitochondrial function, leading to neuronal damage and behavioral changes in rodents (309). The unique presence of Etf-QO in the LP group suggests that enhanced mitochondrial efficiency and robust energy production might confer resistance to METH-induced alterations in redox regulation, thereby reducing its rewarding effects. Cyp9f2, involved in the metabolism of insect hormones and the breakdown of synthetic insecticides, plays a role in the detoxification of various xenobiotics, including drugs. Previous studies have shown that METH metabolism involves the cytochrome P450 enzyme system, influencing the drug's pharmacokinetics and toxicity (310). The presence of Cyp9f2 in the LP group suggests enhanced detoxification capabilities, reducing the overall impact of METH and its reinforcing effects. ScpX, with phospholipid transporter activity, is involved in phospholipid transport and fatty acid metabolism. Proper lipid metabolism is essential for maintaining cellular membrane integrity and function, and METH disrupts lipid metabolism and membrane dynamics, contributing to neuronal damage (311). The presence of ScpX in the LP group suggests a

protective role in maintaining lipid homeostasis and membrane integrity, mitigating the deleterious effects of METH on neuronal cells. Gs1l, involved in the dephosphorylation of pseudouridine 5'-phosphate, plays a role in RNA metabolism, crucial for protein synthesis and cellular function. METH exposure alters RNA metabolism and protein synthesis pathways, leading to changes in synaptic plasticity and behavior (312). The presence of Gs1l in the LP group suggests enhanced RNA processing capabilities, maintaining normal protein synthesis and cellular function in the face of METH exposure. Dhpr, involved in the reduction of dihydropteridine to tetrahydropteridine, is essential for the synthesis of neurotransmitters such as dopamine, serotonin, and norepinephrine. METH increases the release and blocks the reuptake of these neurotransmitters, leading to their elevated levels in the brain (173). The presence of Dhpr in the LP group suggests a role in maintaining neurotransmitter balance and preventing the excessive accumulation of dopamine and other neurotransmitters induced by METH. In conclusion, the unique presence of these metabolic proteins in the LP group highlights their potential role as protective markers against METH's rewarding effects. Etf-QO, Cyp9f2, ScpX, Gs1l, and Dhpr contribute to various aspects of cellular metabolism, detoxification, and neurotransmitter regulation, collectively helping to maintain cellular homeostasis and protect against the neurotoxic effects of METH.

The presence of certain proteins involved in protein synthesis uniquely in LP line, suggests a protective role against rewarding effects of METH. These proteins include Large Subunit Ribosomal Protein Lp1 (RpLP1), Eukaryotic Translation Initiation Factor 3 Subunit H (eIF-3p40), UK114, Proteasome Subunit Beta Type-1 (Prosbeta6), and Carboxypeptidase D (svr). Their presence indicates enhanced protein synthesis and degradation capabilities, which are crucial for maintaining cellular and synaptic integrity under METH-induced stress. The presence of molecular chaperone UK114, which aids in protein folding and cellular protection under stress, suggests enhanced chaperone activity that manages protein integrity and prevents aggregation, reducing neurotoxic effects of METH and supporting cellular resilience against oxidative stress and protein misfolding. Efficient protein synthesis, facilitated by RpLP1 and eIF-3p40, ensures the production of proteins necessary for

neuronal health, countering METH's disruptive effects on these pathways. Prosbeta6 and svr contribute to the degradation of damaged proteins, preventing the accumulation of toxic aggregates and mitigating neurotoxicity. Together, these proteins support cellular homeostasis and protect against neurotoxic effects, potentially reducing drug preference. The ability to sustain normal protein production and degradation despite METH exposure could help in preserving cellular and synaptic integrity, reducing the drug's reinforcing effects.

The unique presence of structural proteins such as Lamin C (LamC), Coiled-coil-helix-coiled-coil-helix domain-containing protein 3 (Chchd3), Moesin/Ezrin/Radixin Homolog 1 (Moe), and Papilin (Ppn) in LP line suggests their collective role in reducing METH preference by maintaining cellular integrity and function. These proteins ensure the stability of nuclear, mitochondrial, cytoskeletal, and extracellular matrix structures, which are essential for normal neuronal function and resilience against METH-induced perturbations. The combined action of these proteins supports various aspects of cellular and structural integrity crucial for countering the effects of METH. Maintaining nuclear stability through proteins like LamC protects against gene expression disruptions often induced by METH, which can lead to neuronal dysfunction and contribute to addictive behaviors. Enhanced mitochondrial resilience, supported by proteins like Chchd3, is critical for preventing oxidative stress and maintaining energy production, both of which are negatively impacted by METH use. Cytoskeletal stability, ensured by proteins like Moe, preserves neuronal connectivity and signaling pathways, which are essential for proper synaptic function and plasticity. Lastly, the stability of the extracellular matrix, facilitated by Ppn, helps maintain synaptic integrity and prevent the remodeling and plasticity changes associated with addiction. Research in addiction has shown that METH disrupts cellular structures and induces neurotoxic effects through various mechanisms, including oxidative stress, mitochondrial dysfunction, and alterations in synaptic plasticity (73,313). The presence of these structural proteins in the LP group suggests that they collectively contribute to a cellular environment that is more resistant to these disruptive effects. This resistance likely

plays a significant role in reducing the rewarding and reinforcing effects of METH, thereby contributing to the observed low preference for meth in LP line. Furthermore, these proteins' roles in maintaining cellular homeostasis align with existing ideas for therapeutic approaches that target structural and functional plasticity to combat substance use disorders (314). By preserving the integrity of critical cellular structures, these proteins help mitigate the damage caused by METH, supporting neuronal health and function, and ultimately reducing drug-seeking behaviors.

The unique presence of certain signaling and regulation proteins in LP suggests their potential role in reducing METH preference by maintaining cellular signaling and homeostasis. These proteins, including Bacchus (Bacc), V-type Proton ATPase Catalytic Subunit A (Vha68-2) and Optic Atrophy 1 (Opa1), collectively contribute to cellular stability and resilience against METH-induced changes in redox homeostasis. Vha68-2, part of the ATPase complex, helps maintain cellular pH balance and supports various signaling pathways, mitigating METH-induced cellular stress and dysfunction. Opa1 is crucial for mitochondrial integrity and energy production, protecting against oxidative stress and neuronal damage induced by METH. Together, these proteins ensure robust cellular signaling, homeostasis, and detoxification, essential for reducing METH preference and supporting resilience against addiction.

In conclusion, the analysis of proteins unique to the *Drosophila* line with low METH preference reveals a complex interplay of metabolic processes, protein turnover, structural integrity, signaling pathways, extracellular matrix components, and stress responses. These findings are consistent with previous proteomic studies in rodents, suggesting that these multiple biological processes contribute to the modulation of drug preference. The unique presence of these proteins in the LP group, and their absence in the PO and HP groups, indicates that they may serve as important markers for resistance to METH's rewarding effects.

5.2.4 Selective breeding summary and potential role of redox in preference for METH

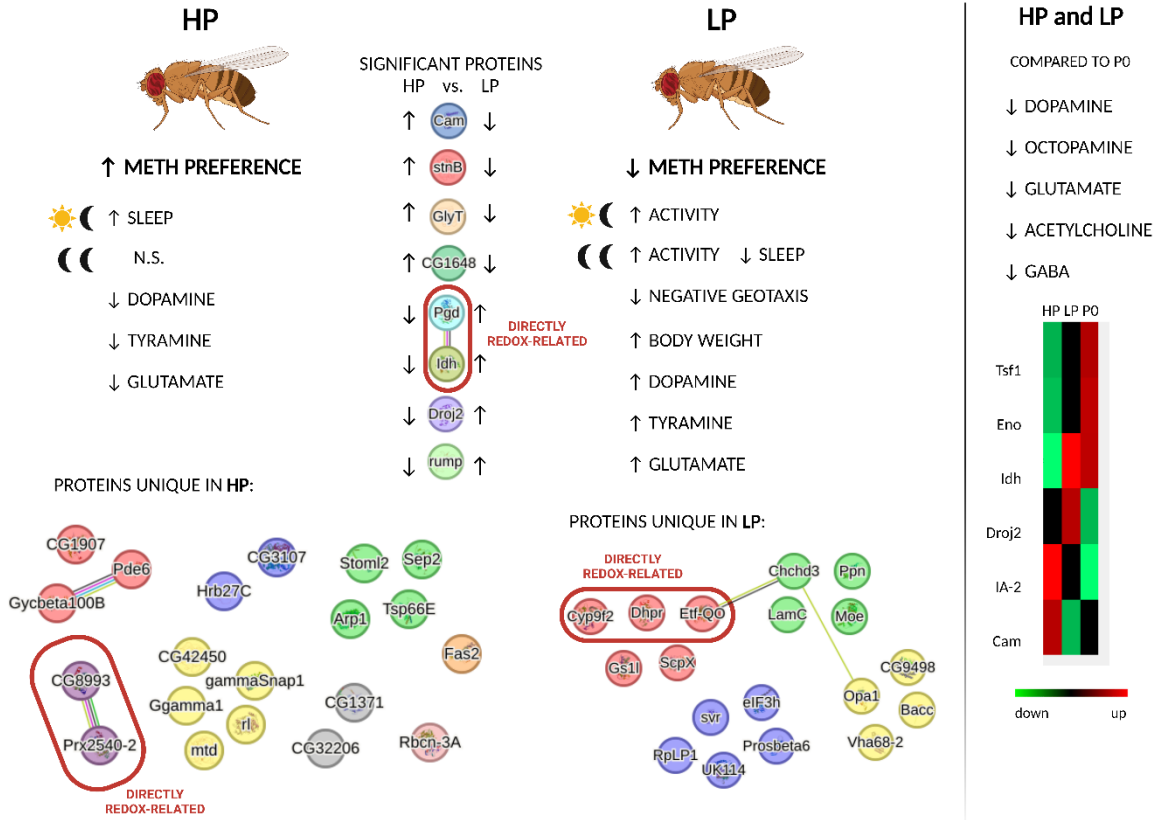
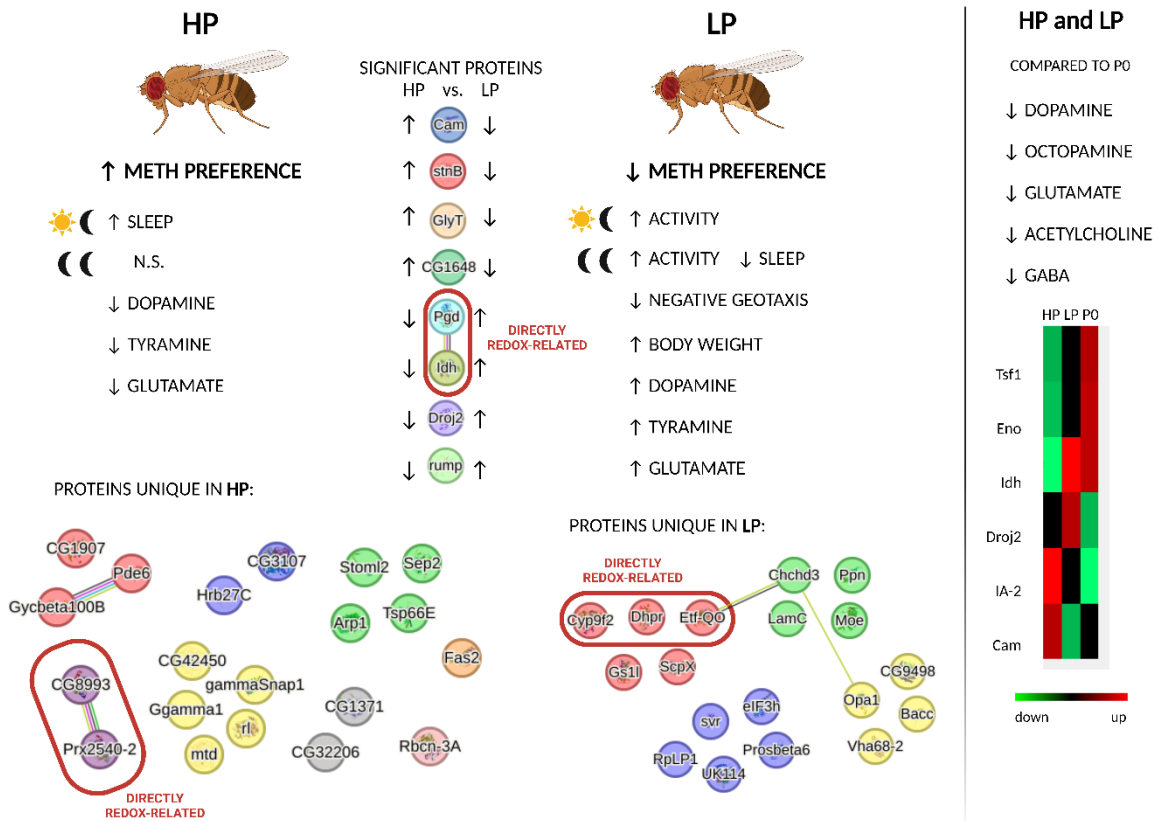


Figure 60. Summary of behavioral, neurochemical and proteomic differences between HP and LP lines.



illustrates the distinctions between HP and LP selected lines of *Drosophila*. HP flies exhibit a higher preference for METH, increased sleep in LD conditions, and decreased levels of dopamine, tyramine, and glutamate. Unique proteins in HP flies include two directly redox-related proteins: CG1893 and Prx2540-2 (also known as Prx6c). In contrast, LP flies show a reduced preference for METH, increased activity in both LD and DD conditions, higher body weight, and higher levels of dopamine, tyramine, and glutamate. Unique proteins in LP flies include Cyp9f2, Dhpr, Etf-QO which are all directly redox-related. Notably, LP flies sleep less only in DD and display decreased negative geotaxis. The significant proteins that differentiate HP from LP include lower levels of Cam, StnB, GlyT and CG1648, and higher expression of Pgd, Idh, Droj2, and rump in LP. Pgd and Idh are both directly related to redox regulation as NADPH producers. Both lines show reduced levels of dopamine, octopamine, glutamate, acetylcholine, and GABA compared to the parental line (P0). The heatmap

comparison of protein expression among HP, LP, and P0 lines highlights differential expression of proteins such as Tsf1, Eno, Idh, Droj2, IA-2, and Cam, indicating complex neurochemical and protein expression changes associated with METH preference.

In our study, we identified Bacc as a protein of interest due to its unique expression in LP flies. Although direct evidence linking Bacc to redox processes was not initially apparent, its potential role in metabolic regulation prompted us to further investigate. To explore Bacc possible connections to redox regulation, we examined its protein interactions using data from FlyBase. This analysis revealed a network of physical interactions between Bacc and several redox-related proteins, including Prx6c, suggesting that Bacc might influence METH preference through interplay with redox balance and metabolic pathways. However, the specific nature of these interactions is not yet known, and further research is needed to elucidate the exact mechanisms by which Bacc interacts with redox-related proteins.

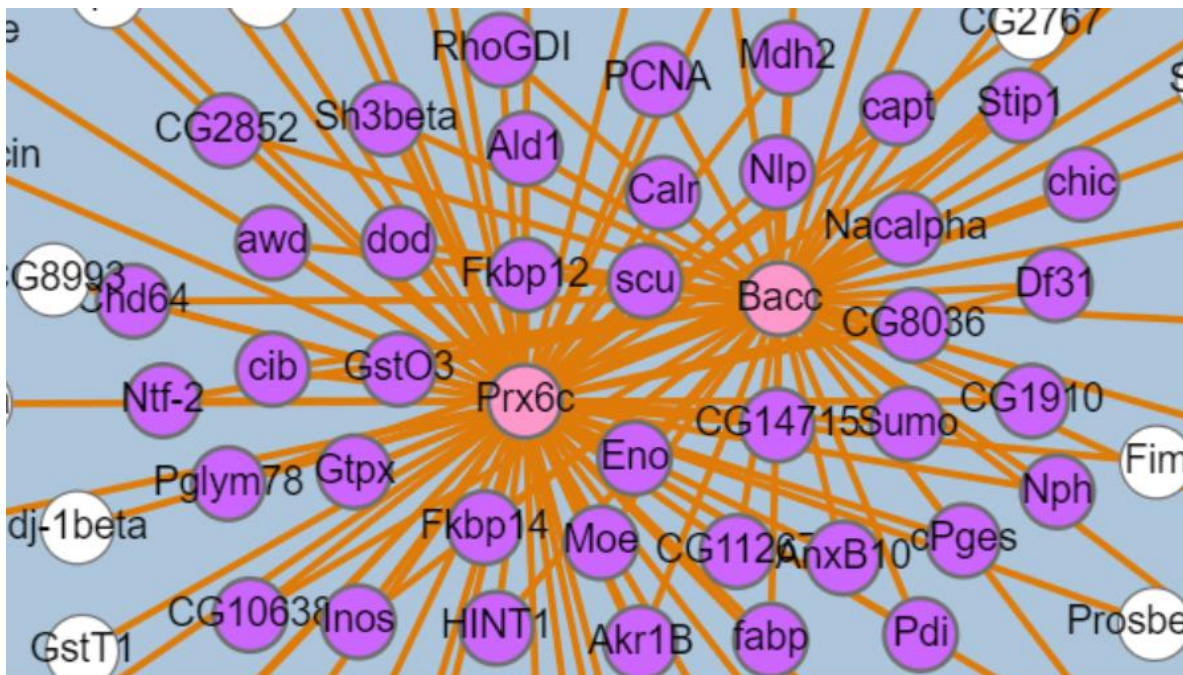


Figure 61. Bacchus could be regulated by redox through its physical interactions with Prx6c or other redox related and metabolic proteins. *Physical association of Bacc with Prx6c and their common interactors depicted in purple. Source: FlyBase*

The network depicted in Figure 61. includes common interactors of Bacc and Prx6c, represented in purple circles, which are involved in various metabolic and redox processes. These interactions suggest a complex regulatory network where Bacc could modulate cellular responses to oxidative stress and metabolic changes. This network includes proteins such as Eno, Moe, GstO3, Ald1, and others, which play roles in redox homeostasis, detoxification, and metabolic regulation. These associations support the hypothesis that Bacc influence on METH preference in the LP flies might be mediated through its sensitivity to or impact on redox balance and metabolic pathways. As Prx6c was present only in HP line, and Bacc only in LP, there is a possibility that either Prx6c negatively regulates Bacc, or vice versa, but this hypothesis should further be tested.

5.3 Redox regulation of H₂O₂ levels, glucose metabolism and NADPH production underlies LS phenotype to vMETH

5.3.1 Expression of *Cat*, *Sod1*, *Sod2*, *Men* and *Gapdh1* in the dopaminergic and serotonergic neurons is necessary for LS phenotype

The UAS-Gal4 genetic screen is a powerful tool employed in *Drosophila* research to investigate the functional significance of genes, in this case, redox-related genes, in the modulation of complex behaviors. Utilizing this binary system allows for the precise manipulation of gene expression: the UAS is a segment of DNA where transcription is initiated, while Gal4 is a yeast-derived transcription factor that binds to UAS to activate gene transcription. By genetically engineering flies to express Gal4 under specific neuronal promoters and crossing these with UAS lines carrying RNAi constructs, we can achieve targeted gene silencing in subsets of neurons.

In our study, this screening technique was used in exploring the link between redox-related gene silencing and addiction-related behaviors, with a focus on LS, preferential SA with additional characterization of other related phenotypes like negative geotaxis, sleep,

locomotor activity, and response to vCOC. Gene silencing was conducted at three levels: pan-neuronally, in dopaminergic and serotonergic neurons and in dopaminergic neurons exclusively.

Our initial efforts involved pan-neuronal gene silencing to understand the broad implications of redox regulation on neural function. However, the critical role of these genes in maintaining neuronal integrity became apparent as this wide-reaching approach led to reduced viability and fitness among the experimental flies, manifesting in low survival rates. This observation supported the significance of redox processes not just in the pathological mechanisms of addiction but in the foundational health of neural systems. To overcome these challenges and gain more specific insights, we refined our strategy to target gene silencing within particular subsets of neurons known for their roles in addiction: dopaminergic and serotonergic neurons. This more focused approach allowed us to explore the effects of redox gene manipulation in neurotransmitter systems central to reward processing on addiction behaviors. Our study has highlighted several key genes that play important roles in modulating neuronal responses and synaptic plasticity required for LS across these brain regions, which include *Sod1*, *Sod2*, *Cat*, *Gapdh1*, and *Men*, with addition of *E(spl)m3-HLH* and *Sod2* being significant in all neurons.

A gene involved in LS across all neurons is *E(spl)m3-HLH*, implicated in the Notch signaling pathway, which may regulate synaptic plasticity and the remodeling of neural circuitries underlying LS. The Notch pathway is known for its role in cell differentiation and development, which is connected to neural development and plasticity (315). The dysregulation of *E(spl)m3-HLH* and by extension, Notch signaling could result in maladaptive synaptic changes that are inconsistent with the establishment of LS, potentially due to impaired communication between neurons or a failure to maintain synaptic strength after repeated drug administration. The limitation of this approach is that we cannot determine whether *E(spl)m3-HLH* is important in all neurons or only in specific ones. Silencing *E(spl)m3-HLH* results in relatively mild changes in neuronal function that do not cause

lethality and are specific to LS. This finding does not rule out the possibility that a specific group of neurons could have a more significant impact on the impaired LS phenotype. In a previous study with the METH-induced LS model in mice researchers found that Notch1 signaling was downregulated in the medial prefrontal cortex (mPFC) of sensitized mice, but inhibition of Notch1 signaling in the mPFC attenuated METH-induced LS, while overexpression of Notch1 signaling enhanced LS (316). Genetic and pharmacological manipulations of Notch1 signaling were found to bidirectionally alter METH-induced LS and other METH-related behaviors by modulating neuronal activity (316). This complements our finding in *Drosophila* where *E(spl)m3-hlh* component of the Notch pathway is necessary for LS. Additionally, alcohol studies in flies show that Notch signaling in the mushroom body memory circuitry influences dopamine receptor expression and gene transcription, highlighting the conserved role of Notch signaling in addiction-related behaviors (274).

Our findings demonstrate the necessity of well-known antioxidative enzymes, *Cat* and *superoxide dismutases (Sod1 and Sod2)* for LS, particularly within dopaminergic and serotonergic neurons, emphasizing the role of managing oxidative stress and supporting redox-sensitive signaling pathways through fine-tuning of H₂O₂ levels (317). *Cat* and *Sod* are key enzymes in detoxifying ROS, markedly in regulating H₂O₂ levels to function as a signaling molecule and at the same time prevent it reaching toxic concentrations. *Sod* catalyzes the dismutation of superoxide radicals into H₂O₂ and oxygen, while *Cat* decomposes H₂O₂ into water and oxygen. Proper regulation of H₂O₂ levels in these neurons ensures their resilience and functionality, crucial for adaptive processes in the brain's reward circuits. This regulation of H₂O₂ is vital for maintaining the pathways that are known to be redox-sensitive, one example being the MAPK/ERK pathway, which is involved in synaptic plasticity and memory formation, and it is crucial for the acquisition of LS to cocaine or amphetamine, as shown in mice (318,319). *Sod1*, located in the cytoplasm and extracellular spaces, and *Sod2*, located in mitochondria, both ensure proper oxidative environment management and neuronal health to enable the long-term adaptations in neuronal connectivity and signaling that are essential for LS.

Flies with *Sod1* silenced in all neurons exhibited a response same as the response to the control protocol (heated air) in the FlyBong assay and did not show sensitivity to even to the first dose of vMETH. This suggests that the lack of *Sod1* impaired functions beyond the neuroplastic changes associated with LS, which is confirmed by the fact that their general locomotor activity was heightened. This hyperactivity could account for their strong response to heated air. Therefore, we cannot conclusively state that *Sod1* silencing did not affect LS; rather, it had a more systemic effect, affecting other phenotypes besides LS. As a result, we could not isolate the METH-specific effects due to the broader impact of *Sod1* silencing across all neurons. Line with pan-neuronal silencing of *Sod2* had normal sensitivity and locomotor activity but did not show LS and had reduced sleep, giving clearer picture of *Sod2* necessity for LS. The differential effects of pan neuronal *Sod1* and *Sod2* silencing on LS and general activity can be explained by their distinct cellular localizations and roles in oxidative stress management. We speculate that *Sod1*'s cytoplasmic localization makes it more likely to maintain redox balance during synaptic plasticity and neurotransmitter signaling, and its silencing leads to widespread oxidative perturbations affecting overall neuronal function. In contrast, *Sod2*'s mitochondrial localization is essential for maintaining energy production and mitochondrial health, specifically affecting the energy-dependent processes of LS and sleep without broadly disrupting general activity. This explains why *Sod2* silencing leads to the absence of LS but does not cause heightened general locomotor activity or sensitivity to non-specific stimuli, and it also supports previous findings that sleep and activity are regulated by distinct mechanisms in *Drosophila* (320,321)

To avoid systemic issues, we silenced either *Sod1* or *Sod2* specifically in dopaminergic and serotonergic neurons. This resulted in the normal sensitivity to METH but prevented the development of LS indicating that both *Sod1* and *Sod2* are crucial in dopaminergic and serotonergic neurons for the neuroplastic changes required for LS. However, the specific roles of these enzymes in general activity and sleep patterns are distinct. Flies with *Sod1* silenced in dopaminergic and serotonergic neurons exhibited normal activity and sleep patterns, suggesting that while *Sod1* is essential for the specific neuroplastic changes

associated with LS, it is not involved in the overall regulation of activity and sleep in these neurons. In contrast, flies with *Sod2* silenced in the same neurons showed increased general activity and reduced sleep. Dopaminergic and serotonergic neurons have high metabolic demands due to their role in neurotransmitter synthesis, release, and reuptake, making efficient mitochondrial function and bioenergetics particularly important. The disruption of *Sod2* in these neurons likely leads to elevated ROS levels, resulting in hyperactivity and sleep disturbances. Major sleep-regulating centers within the *Drosophila* brain are regulated by many different neurons, including dopaminergic PPL1 neurons, while activation of other populations of dopamine neurons suppresses sleep (322). Mitochondrial metabolism plays a key role in sleep regulation by influencing the excitability of sleep-control neurons through mitochondrial ROS (323). Therefore, it is not surprising that mitochondrial *Sod2* is vital for broader aspects of neuronal health, including activity regulation and sleep maintenance, due to its essential role in sustaining mitochondrial function and bioenergetics in energetically demanding dopaminergic and serotonergic neurons. To summarize, on a global, pan-neuronal level where all different types of neurons are included, cytosolic *Sod1* is more critical, so its silencing has broader, systemic effects, whereas *Sod2* is particularly important in the energetically demanding dopaminergic and serotonergic neurons. Both enzymes, however, are essential for the neuroplastic processes underlying LS.

We also showed that catalase is necessary for LS in dopaminergic and serotonergic neurons in *Drosophila*. Flies also exhibited increased sleep when *Cat* was silenced in these neurons, and when silenced in all neurons, flies showed lower overall activity and increased sleep. This suggests that catalase plays a role in regulating neuronal activity and sleep-wake cycles, likely through its function in managing the redox balance. When catalase activity is silenced, H_2O_2 accumulates, leading to an increase in ROS. This change in the oxidative environment could impair neuronal function and plasticity, which are essential for the development of LS. Previous studies on ethanol-induced LS suggested that a deficiency in brain catalase activity prevents the development of sensitization. This is also supported by findings where outbred mice with normal catalase activity did not exhibit sensitization or neuroadaptations when

catalase was pharmacologically blocked during the sensitization process (324,325). In the context of METH exposure, the lack of LS observed when Cat is silenced in dopaminergic and serotonergic neurons could similarly be due to the inability of these neurons to manage the oxidative environment effectively. Dopaminergic neurons are particularly sensitive to changes in ROS because the metabolism of dopamine itself produces ROS. Without sufficient catalase activity to precisely regulate H₂O₂, these neurons may suffer from altered function and plasticity. This could explain why LS to METH does not develop when catalase is silenced. Moreover, the increased sleep observed in flies with silenced catalase activity in dopaminergic and serotonergic neurons might indicate an attempt by the organism to mitigate the altered oxidative environment by reducing neuronal activity. Sleep is known to play a role in managing oxidative conditions and supporting neural repair. Therefore, increased sleep could be a compensatory mechanism in response to heightened ROS levels due to the absence of catalase activity.

Gapdh1 and *Men* are integral to energy metabolism in cells, with *Gapdh1* participating in glycolysis and *Men* in the NADPH production. Their requirement for LS, especially in the energy-demanding dopaminergic neurons, may relate to their roles in providing ATP and substrates for neurotransmitter production, both of which are vital for sustained neural activity and plasticity in response to stimulants. The altered expression of *Gapdh1* or *Men* could affect the availability of energy, thereby lowering the efficacy of synaptic transmission and the strength of drug-induced neuronal adaptations necessary for LS.

Gapdh1, a key glycolytic enzyme, also performs non-glycolytic functions through posttranslational modifications. Over the past two decades, studies have revealed that *Gapdh1*, beyond its glycolytic role, is involved in various cellular processes such as nucleic acid binding, telomere protection, tRNA and mRNA transport, gene regulation, and DNA repair. *Gapdh1* also mediates responses to oxidative stress, where low stress preserves its glycolytic function, and high stress induces S-nitrosylation, leading to nuclear translocation, protein degradation, and apoptosis (326). Under oxidative stress, it can undergo reversible

S-thiolation that protects *Gapdh1* from damage and redirects metabolism to the pentose phosphate pathway to maintain NADPH/NADP⁺ balance. *Gapdh1* also contributes to local NADH⁺ levels and may regulate IP3R-mediated Ca²⁺ signaling (327). The most recent studies on extracellular vesicles (EVs) have expanded our understanding of neural cell communication (328). EVs, including microvesicles and exosomes, are secreted by all neural cell types and can influence recipient cells by activating surface receptors or delivering cargo such as proteins and nucleic acids. These vesicles are regulated by neurotransmitter signaling, linking their release to neural activity, and may support neural plasticity and tissue homeostasis. A study from Dar et al. study demonstrates that *Gapdh* associates with EVs through a phosphatidylserine-binding motif, with exogenous *Gapdh* inducing EV clustering (329). Using an in vivo *Drosophila* model, the research shows that endogenous *Gapdh* is crucial for exosome clustering, the formation of central dense granules in multivesicular endosomes, and influences exosome formation and secretion. Those are examples of possible mechanisms through which *Gapdh1* could regulate neuroplastic changes upon METH-induced LS. Silencing *Gapdh1* also induces increased sleep, while other behaviors remained unchanged. This change in sleep is not surprising, since evidence indicate that sleep is closely linked to energy metabolism, energy conservation, and replenishment, and experimentally induced local energy depletion triggers increased sleep (330).

Furthermore, our study highlights the role of the Men in LS neuroplasticity. Silencing Men in dopaminergic and serotonergic neurons, or in dopaminergic neurons alone, prevents the development of LS while other phenotypes, such as general locomotor activity and sleep, were unaffected. Men functions as a crucial metabolic switch, connecting glycolysis to the TCA cycle and producing NADPH, which is vital to fuel antioxidative system. Men has been linked to alcohol resistance in flies and is implicated in fatty liver disease in heavy drinkers (331). Specific SNPs in the human Malic enzyme (ME1) gene was associated with drinking behavior in humans (332). The failure to develop LS when Men is silenced suggests that the metabolic processes regulated by Men are essential for the neuroplastic changes underlying

sensitization. Men's role in maintaining metabolic flexibility and providing necessary biochemical substrates likely supports the neuronal adaptations required for LS.

5.3.2 *Sod1, Gapdh1 and Men are common link in the overlapping regulation of LS and SA*

The requirement of *Sod1*, *Gapdh1*, and *Men* in dopaminergic and serotonergic neurons for the development of LS and the preferential SA underscores the importance of maintaining a balanced redox state and adequate energy metabolism in reward pathways. Moreover, it confirms our previous finding that LS and SA partially share molecular background. The expression of *Prx3*, which is predominantly present in the mitochondria, specifically in dopaminergic neurons is required for SA of METH. This suggests a unique sensitivity of these neurons to peroxide levels, which could influence dopaminergic signaling pathways crucial for drug reinforcement, and consequently, the importance of mitochondrial redox regulation in these neurons.

5.3.3 Pleiotropic effect of redox-related genes

Silencing specific redox-related genes in all neurons resulted in a noticeable increase in sleep duration in many fly lines, and similar outcome was observed when genes were silenced in dopaminergic and serotonergic neurons, albeit with a higher variability, depending on the gene that was being silenced. These findings support a regulatory role of redox processes for the sleep homeostasis in accordance with previous studies that have implicated oxidative homeostasis and redox signaling in circadian rhythms and sleep regulation (333,334). Our findings further support the identification of specific subsets of dopaminergic neurons as key regulators of sleep and wakefulness transition (335).

Locomotor activity was impacted by silencing redox genes in all neurons. For instance, silencing the *Sod1* gene led to increased locomotor activity, while silencing other genes such

as *Cat*, *Gclc*, *Gclm*, *Grx1*, *GstE1*, and *MBD-like* resulted in decreased activity. This specificity implies a relationship between redox balance and locomotion. However, the regulation of locomotion appears to involve other types of neurons, not dopaminergic and serotonergic, since these changes were less evident when genes were silenced only in these neurons. In terms of negative geotaxis, the performance of flies did not significantly differ from controls, indicating that the climbing ability was not compromised by the silencing of these redox-related genes. Possible explanation is that climbing ability which was measured during five second intervals was not sufficiently energetically demanding to observe the phenotype from gene silencing. Locomotor activity, in contrast, was measured during several days when disruption of redox regulation was more likely to become evident. These observations suggests that phenotypic consequences depend on multiple variables that need to be considered such as anatomical localization of the gene manipulation, and type and the duration of measured phenotype.

The absence of LS to vCOC, but not to vMETH highlights the unique role of *Jafrac1* specifically in the dopaminergic neurons. *Jafrac1*, known for its involvement in cellular redox regulation, may differentially impact the dopaminergic circuits based on the distinct mechanisms of action between vCOC and vMETH. The specific redox environment influenced by *Jafrac1* could be more critical to the neural pathways engaged by cocaine's mechanism. The absence of LS to vCOC in flies with silenced *Jafrac1* suggests an impaired adaptive response in dopaminergic pathways, crucial for neuroplastic changes associated with drug exposure. This impairment highlights the role of *Jafrac1* in modulating neural plasticity, particularly how dopamine neurons adapt to oxidative changes induced by cocaine, providing insights into the selective modulation of neuronal responses to different psychostimulants.

5.3.4 Large cluster of redox-related proteins is upregulated in flies that develop LS

The upregulation of redox-related proteins in LS, as seen in our data, points out the importance of oxidative homeostasis changes in neuroplasticity. Out of 179 proteins uniquely upregulated in LS compared to CTRL and NLS groups, 39 proteins are related to redox homeostasis, either by their antioxidative and/or metabolic functions or their sensitivity to redox changes. In LS, the overexpression of antioxidative proteins like GstS1, GstE9, Jafrac1 and Prx3 indicates an enhanced cellular response to redox perturbations caused by METH. These proteins help detoxify harmful compounds and mitigate oxidative damage, which is necessary for maintaining cellular homeostasis during the heightened neuronal activity associated with LS.

Moreover, proteins involved in glycolysis, such as Gapdh1 and Gapdh2, are upregulated, which is in line with the previous research showing increase in glucose metabolism after METH exposure (336). However, it was previously unexplored whether there is a difference in their expression between flies that developed LS and those that did not. Our proteomics results showed that multiple glycolytic enzymes are upregulated in LS group, either compared to CTRL or NLS, or both. Gapdh1 and Gapdh2 are particularly interesting because these enzymes are known to participate in cellular signaling and influence neuroplasticity, highlighting their dual functions in metabolic and redox pathways. This observation aligns with previous studies showing that glycolytic enzymes have non-metabolic roles in neuroplasticity and redox regulation. Pdhb, an enzyme that links glycolysis and the TCA cycle by converting pyruvate into acetyl-CoA, which is used in the TCA cycle, is upregulated. Additionally, key enzymes from the TCA cycle, like Mdh1, Mdh2, and mAcon1, are upregulated in LS. The intermediates from glycolysis and the TCA cycle serve as precursors for various biosynthetic pathways, supporting the synthesis of nucleotides, amino acids, and lipids which could be important for supporting the cellular growth and synaptic remodeling necessary for neuroplasticity. However, there is a concurrent downregulation of certain ETC

components in LS group, suggesting a shift towards glycolytic pathways to meet the energy and redox demands during LS.

When flies exhibit upregulation of glycolysis and TCA cycle enzymes alongside downregulation of the respiratory chain in the context of LS it suggests significant metabolic adaptations which can possibly be linked to neuroplasticity. The increased activity in glycolysis and the TCA cycle indicates a compensatory response to meet the heightened energy demands associated with enhanced neuronal activity and plasticity during LS. Despite this, the downregulation of the respiratory chain suggests a shift away from oxidative phosphorylation, implying that cells might rely more on anaerobic metabolism or alternative pathways for energy production. This shift reflects a strategic metabolic adaptation where cells prioritize rapid ATP generation through glycolysis and the Krebs cycle over the more efficient but slower oxidative phosphorylation. Such a reprogramming supports the immediate and fluctuating energy requirements during LS, facilitating sustained neuronal activity and plasticity, which are evident as enhanced LS behavior.

5.3.5 Genes and pathways associated with LS identified by screen and proteomics

5.3.5.1 Combining behavioral genetics and proteomics in addiction studies

In our study, genetic screen investigated behavioral changes resulting from gene silencing, with the aim of identifying which redox-related genes are necessary for the development of specific phenotypes such as LS or SA. This helps in identifying specific genes that play a functional role in the behavioral manifestations of addiction. Concurrently, our proteomic analysis examines how METH exposure, and more specifically sensitization to METH, alters protein expression, identifying proteins that are differentially expressed in flies that have develop the LS phenotype.

The utility of combining these two approaches lies in their ability to provide a dual perspective on the biological impacts of substance exposure and genetic manipulation. By

observing the behavioral consequences of gene silencing, we gain insights into the genetic foundations of addiction-related behaviors. Simultaneously, proteomic analysis reveals the changes at the protein level that occur in response to METH exposure, providing a list of proteins that might have either a functional role or are the consequence of the development of LS.

Combining these methodologies allows us to cross-validate findings and establish a more comprehensive understanding of addiction. For instance, if gene silencing of a specific gene leads to reduced LS and this gene's associated proteins also show altered expression in the proteomic analysis of METH-exposed flies, this correlation strengthens the evidence that this gene and its proteins are integral to addiction mechanisms. Furthermore, understanding the direct impact of METH at the protein level helps in identifying potential biomarkers for addiction and therapeutic targets. Moreover, this combined approach can highlight discrepancies between genetic predisposition and post-exposure protein changes, offering insights into how external factors like drug exposure interact with genetic backgrounds to influence behavior. Such findings are crucial for developing personalized medicine strategies and can lead to more targeted interventions in addiction treatment.

As discussed before, through our genetic screen we identified several genes which are necessary for the development of LS either in all neurons, dopaminergic and serotonergic neurons, or just dopaminergic neurons. To complement these results, we investigated the function of these identified genes and checked the results of our proteomic analysis to assess whether proteins related to these genes, or those within analogous functional pathways, showed changes in expression in the brains of flies which developed LS, thereby clarifying their roles in the development of addiction.

5.3.5.2 Antioxidative and metabolic adaptations are important for LS

The integration of genetic and proteomic data reveals a coordinated regulation of antioxidant defenses and metabolic pathways in LS. Genes involved in antioxidant defense, such as *Sod1* and *Sod2*, are crucial for LS in dopaminergic and serotonergic neurons. Despite their necessity for LS, both genes were downregulated in the LS group compared to controls and the NLS group. This downregulation suggests a reduced capacity to convert superoxide into H_2O_2 , which can be part of the mechanism for fine-tuning H_2O_2 to the right concentration that triggers neuroplastic changes, while still avoiding oxidative damage. The necessity of *Cat* for LS in dopaminergic and serotonergic neurons, along with its upregulation, indicates a compensatory mechanism to counterbalance the potentially elevated levels of ROS. This highlights the regulatory network that maintains oxidative homeostasis during LS, ensuring ROS levels are favorable for promoting plasticity without causing neuronal damage. The differential regulation of *Sod* and *Cat* implies a precise amount of H_2O_2 needed for specific signaling and neuroplasticity to occur. *Sod* downregulation results in less production of H_2O_2 , while *Cat* upregulation increases its conversion to water. Consequently, we can expect that there should be lower H_2O_2 levels in LS brains compared to NLS. However, the presence of both enzymes being necessary for LS indicates that there is still sufficient to facilitate neuroplastic changes.

The findings related to *Gapdh1* and *Men* highlight the importance of metabolic processes in LS. *Gapdh1* is necessary for LS in dopaminergic and serotonergic neurons and was upregulated in the LS group compared to controls and the NLS group. This upregulation reflects increased glycolytic activity to meet the heightened energy demands during LS, providing the necessary ATP for sustained neuronal activity and plasticity. Additionally, *Gapdh1* can indirectly regulate H_2O_2 levels by acting as a switch that shifts glycolysis to the pentose phosphate pathway, enhancing NADPH production, which fuels the redox systems of *Trx*, *Prx*, and glutathione. *Men* is also necessary for LS and was upregulated in the LS group compared to control, while its mitochondrial isoform (*Men-b*) was upregulated in LS

compared to NLS. The upregulation of Men suggests an increased need for NADPH during LS, supporting both antioxidant defenses and anabolic processes essential for neuroplastic changes.

These findings provide insights into the molecular mechanisms driving LS, highlighting the precise balance of ROS, particularly H₂O₂, required for neuroplasticity. This balance is tightly regulated by the activities of Sod and Cat, ensuring sufficient H₂O₂ levels to facilitate LS without causing oxidative damage. Additionally, Gapdh1 and Men could indirectly regulate H₂O₂ levels by fueling the redox system through their roles in NADPH production. It is also important to emphasize that with the screen, we selectively analyzed the necessity for certain genes in specific neurons, while the proteomics was performed on the entire brain. Therefore, some genes identified in the screen may not necessarily appear in the proteomics if their role is important and changes occur in a small number of neurons.

5.4 Integration of findings and broader implications

5.4.1 Connecting the dots: genetic, behavioral, and molecular insights into LS and SA

Integration of behavioral genetics and proteomics uncovered a common set of genes and proteins implicated in LS and SA, including antioxidant defense enzymes, metabolic regulators, and neurotransmitter modulators. By combining all the data, we found a convergence of genes associated with antioxidant defense - *Sod1*, *Sod2*, *Cat*, *Prx3*, and *Prx6c*, glucose metabolism - *Gapdh1* and *Eno*, and genes crucial for NADPH production in the cell - *Men*, *Idh*, and *Pgd*. *Bacchus* was identified as a regulator of preferential SA of METH and could possibly be related to these pathways based on his known physical interactions with antioxidative and metabolic proteins we identified, such as Prx6c, Eno.

Our findings demonstrate that antioxidant defense and metabolic pathways play a central role in managing oxidative perturbations and facilitating the neuroplastic changes required for both LS and SA. The convergence of genetic and proteomic data reveals a complex network where enzymes involved in redox balance, energy production, and NADPH generation work together to regulate neuronal function under repeated METH exposure. Enzymes such as Sod1, Sod2, Cat, Prx3, and Prx6c are crucial for maintaining redox homeostasis by converting ROS like superoxide and peroxide into less harmful molecules, allowing for controlled redox signaling essential for neuroadaptation. The upregulation of metabolic enzymes like Gapdh1 and Eno reflects the increased energetic demands and redox balance required during synaptic remodeling, ensuring that neurons have the energy needed to adapt to the persistent stimulus provided by METH. NADPH-producing enzymes like Men, Idh, and Pgd generate the reducing power necessary to sustain antioxidant defenses and support biosynthetic processes, highlighting their dual role in counteracting oxidative perturbations and supporting the anabolic processes involved in neuroplasticity. This interconnectedness underlines the importance of balancing oxidative perturbations and redox signaling in the development of LS, suggesting that interventions targeting these pathways could modulate the addictive behaviors associated with METH exposure. Enhancing antioxidant enzyme activity, modulating metabolic pathways, and boosting NADPH production could mitigate excessive oxidative perturbations, ensure adequate energy supply, and protect neurons, potentially leading to more effective treatments for substance use disorders.

5.4.2 Methodological considerations and experimental limitations

In our UAS-GAL4 genetic screen, we focused on crossing 22 redox-related UAS RNAi lines with neuronal drivers and testing their progeny for the ability to develop LS, including testing the driver lines alone but not the UAS lines alone as controls. Several factors influenced this decision: resource and time constraints, the significant overlap between our genetic screen

and proteomic analysis results, and our primary objective of investigating the role of redox-related genes within specific neuronal contexts. Proteomic validation provides additional confirmation for our findings, reinforcing their validity despite the absence of UAS-only controls. We recognize the importance of including these controls and plan to perform them before submitting our work for publication in a peer-reviewed journal, ensuring a comprehensive dataset that addresses potential concerns and strengthens the overall validity of our findings. Given that this study represents an initial investigation into the roles of redox-related genes in LS, our approach was designed to quickly identify promising candidate genes and pathways. Future studies, including the planned control experiments, will build on these findings and provide a more detailed understanding of the underlying mechanisms.

Screening experiments were also initially challenged by the diminished viability and condition of flies with pan-neuronal silencing of redox-related genes, a testament to the key role of these genes in neuronal health. This necessitated a shift to a more targeted approach, focusing on dopaminergic and serotonergic neuron-specific silencing. This strategic adjustment not only improved the viability of our experimental flies but also allowed for a more precise insight into localization of neurobiological mechanisms.

Interestingly, a subset of flies exhibited behavioral responses to heated air similar to the vMETH exposure or displayed reduced responses, indicating the need to differentiate drug-specific from general stress responses. Future studies could employ a titrated range of vMETH doses to refine the sensitivity of the LS assay, ensuring that observed behaviors are attributable to the drug rather than nonspecific stress. Additionally, this approach could help identify subtler phenotypic manifestations of genetic alterations that might be masked at higher drug concentrations.

5.4.3 Future directions

The results of our study provide a foundational understanding of the genetic and proteomic mechanisms underlying behavioral responses to METH in *Drosophila*. Moving forward, several key directions and experiments can be undertaken to build on these findings, with significant implications for translational research, redox interventions, and metabolic regulation.

One promising direction is the manipulation of the *Bacchus* gene and the tyramine/octopamine systems to elucidate their roles in METH preference and SA. Experiments could involve genetic and pharmacological manipulations, for example using RNAi to knock down or overexpress *Bacchus* and measure changes in tyramine and octopamine levels, followed by behavioral assays to evaluate changes in METH preference and SA. Further exploration of the role of *Bacchus* and its interaction with redox-related proteins like Prx6c in modulating METH preference should also be explored. Additionally, it could be interesting to check if *Bacchus* has a role in LS considering that tyramine, but not octopamine is involved in the development of LS to vCOC.

Further detailed characterization of generated HP and LP lines, including their response in FlyBong, pharmacological interventions to modulate monoamines, measuring the activity of antioxidative enzymes such as Sod and Cat can give deeper insights into regulation of the SA phenotype. Additional research on the HP and LP lines could explore the impact of dietary interventions, such as antioxidant-rich or restricted diets, on METH preference.

Another important direction is to conduct detailed mechanistic studies to investigate the specific roles and interactions of identified enzymes and pathways, particularly focusing on how they influence redox balance and neuroplasticity. For example, measuring H₂O₂ concentrations in the brains of flies with silenced redox-related genes (e.g., *Sod1*, *Sod2*, *Cat*) and assessing changes in neuroplasticity markers such as synaptic proteins could provide valuable insights.

Exploring the impact of manipulating NADPH production pathways on LS and SA behaviors is another area of future research. Measuring NADPH levels in flies with silenced *Men* and *Gapdh1*, silencing other enzymes related to glycolysis and NADPH production that we detected by proteomics, and assessing how these manipulations affect both LS and SA behaviors could provide insights into the metabolic requirements of addiction-related neuroplasticity. Such experiments could identify metabolic interventions to mitigate addiction by ensuring adequate energy supply and redox balance during neural adaptations.

The findings of our study have significant implications for translational research, particularly in understanding the role of redox regulation in addiction. The identification of key genes and proteins involved in redox balance and metabolism highlights potential therapeutic targets for modulating addiction-related behaviors. Focusing on redox interventions and metabolic regulation could lead to strategies that mitigate the effects of METH and other substances, ultimately resulting in more effective treatments for substance use disorders.

Furthermore, this research can provide basis for further exploration of dietary and lifestyle interventions aimed at maintaining redox balance and metabolic health. For instance, specific dietary supplements that enhance antioxidant defenses or support metabolic pathways, such as antioxidants, metabolic modulators, or NADPH boosters could be explored as adjunctive therapies for addiction.

6. Conclusion

In our study, we have specifically identified redox genes, whose expression changes in response to METH or/and which are necessary in regulating neural plasticity evident as LS and SA phenotypes. The mechanisms linking redox genes with those regulating neural plasticity warrant further discussion and analysis. Potential mediators such as peroxide (whose levels are regulated by *Cat*, *Sod* and *Prx*) may act as messengers, modulating the

metabolic pathways which are crucial for fueling energetically demanding neuroplastic processes.

Our results indicate that METH-induced LS and neuroplasticity are mediated by an interplay between peroxide signaling, enhanced glucose metabolism, and increased NADPH production, which together modulate redox-sensitive pathways and protect against oxidative stress. The upregulation of redox-related proteins suggests a coordinated response to METH-induced oxidative changes in the brain. Peroxide signaling might trigger neuroplastic changes, while enhanced glucose metabolism and NADPH production provide the necessary energy and redox balance to support these changes. Together, these processes contribute to the development and maintenance of addiction-related neuroplasticity evident as LS and SA. Additionally, our findings highlight the importance of neurotransmitter tyramine in SA behavior, indicating that elevated tyramine levels, influenced by the Bacchus protein, may modulate the neural circuits involved substance preference and consumption.

- We successfully developed a modified version of the CAFÉ assay, referred to as the FlyCafe assay, which enables precise and high-throughput measurement of METH SA in individual flies. This innovative method allows for the quantification of individual preferences for METH, locomotor activity, and environmental positioning during SA, providing a robust platform for future addiction research.
- Utilizing the FlyCafe assay, we identified and selectively bred two distinct strains of *Drosophila* with high (HP) and low (LP) preferences for METH SA. This selection process facilitated the identification of genetic and proteomic factors associated with voluntary drug consumption
- Through proteomic analysis of brain tissues from the HP and LP strains, we defined the proteomic changes accompanying differences in METH SA preference. This analysis revealed significant changes in proteins involved in metabolic processes,

structural integrity, and protein turnover, highlighting potential overlaps with the LS phenotype.

- We identified Bacchus, a negative regulator of conversion of tyramine into octopamine, as an important regulator of preferential SA for METH
- We conducted a genetic screen to identify redox-related genes that regulate LS to vMETH. This approach uncovered several critical genes, such as *Cat*, *Sod1*, *Sod2*, *Gapdh1*, and *Men*, that play functional roles in the regulation of LS, emphasizing the importance of redox processes in addiction-related neuroplasticity.
- The necessity of *Sod1*, *Gapdh1* and *Men* in dopaminergic and serotonergic neurons overlaps for both LS and SA
- Proteomic analysis of brain tissues from flies that did or did not develop LS after two administrations of vMETH identified a set of proteins unique to the LS phenotype, with an emphasis on significant changes in redox-related proteins, including upregulation of several antioxidative, glycolytic and TCA enzymes (*Cat*, *Prx3*, *Prx6c*, *Jafrac1*, *Gapdh1*, *Gapdh2*, *mAcon1*, *Mdh1*, *Mdh2*) and downregulation of enzymes related to oxidative phosphorylation (*NADH dehydrogenases*).
- By combining the results of our approaches, our study reveals that both LS and SA of METH are modulated by interconnected pathways involving peroxide regulation, glucose metabolism, NADPH production, and neurotransmitter systems:
 - Redox Regulation: Enzymes like *Sod1*, *Sod2*, *Cat*, and *Prx* manage peroxide signaling, maintaining oxidative balance crucial for neuroplasticity.
 - Glucose Metabolism: Upregulation of glycolytic and TCA cycle enzymes (e.g., *Gapdh1*, *Mdh1*, *Mdh2*) provides ATP and metabolic intermediates needed for energy-demanding neuroplastic processes.
 - NADPH Production: Enzymes like *Men*, *Pgd*, and *Idh* support NADPH production, essential for both antioxidative defense and biosynthetic activities.

- Neurotransmitter Regulation: The neurotransmitter tyramine, influenced by the Bacchus protein, modulates SA behavior, indicating its role in reward processing and METH preference.

7. REFERENCES

1. Zou Z, Wang H, d'Oleire Uquillas F, Wang X, Ding J, Chen H. Definition of Substance and Non-substance Addiction. *Adv Exp Med Biol* [Internet]. 2017 [cited 2024 Apr 18];1010:21–41. Available from: <https://pubmed.ncbi.nlm.nih.gov/29098666/>
2. McLellan AT. Substance Misuse and Substance use Disorders: Why do they Matter in Healthcare? *Trans Am Clin Climatol Assoc* [Internet]. 2017 [cited 2024 Apr 18];128:112. Available from: </pmc/articles/PMC5525418/>
3. Nathan PE, Conrad M, Skinstad AH. History of the Concept of Addiction. *Annu Rev Clin Psychol* [Internet]. 2016 Mar 28 [cited 2024 Apr 18];12:29–51. Available from: <https://pubmed.ncbi.nlm.nih.gov/26565120/>
4. Ewald DR, Strack RW, Orsini MM. Rethinking Addiction. *Glob Pediatr Health* [Internet]. 2019 [cited 2024 Apr 18];6. Available from: <https://pubmed.ncbi.nlm.nih.gov/30719491/>
5. Baler RD, Volkow ND. Drug addiction: the neurobiology of disrupted self-control. *Trends Mol Med*. 2006 Dec;12(12):559–66.
6. Hurd YL. Perspectives on current directions in the neurobiology of addiction disorders relevant to genetic risk factors. *CNS Spectr*. 2006;11(11):855–62.
7. Adinoff B. Neurobiologic Processes in Drug Reward and Addiction. *Harv Rev Psychiatry* [Internet]. 2004 Nov [cited 2022 Apr 11];12(6):305. Available from: </pmc/articles/PMC1920543/>
8. Holtz NA, Carroll ME. Animal Models of Addiction: Genetic Influences. *Animal Models of Behavior Genetics* [Internet]. 2016 [cited 2023 Sep 11];303–31. Available from: https://link.springer.com/chapter/10.1007/978-1-4939-3777-6_10
9. Maze I, Nestler EJ. The epigenetic landscape of addiction. *Ann N Y Acad Sci*. 2011;1216(1):99–113.
10. Anderson EM, Penrod RD, Barry SM, Hughes BW, Taniguchi M, Cowan CW. It is a complex issue: emerging connections between epigenetic regulators in drug addiction. *European Journal of Neuroscience*. 2019 Aug 1;50(3):2477–91.
11. Nestler EJ, Lüscher C. The Molecular Basis of Drug Addiction: Linking Epigenetic to Synaptic and Circuit Mechanisms. *Neuron* [Internet]. 2019 Apr 3 [cited 2024 Apr 18];102(1):48–59. Available from: <https://pubmed.ncbi.nlm.nih.gov/30946825/>

12. Sampedro-Piquero P, Santín LJ, Castilla-Ortega E. Aberrant Brain Neuroplasticity and Function in Drug Addiction: A Focus on Learning-Related Brain Regions. *Behavioral Neuroscience* [Internet]. 2019 Mar 15 [cited 2022 May 31]; Available from: [undefined/state.item.id](#)
13. Smelik PG. Chapter 1 Adaptation and brain function. *Prog Brain Res*. 1987 Jan 1;72(C):3–9.
14. Nestler EJ. Cellular basis of memory for addiction. *Dialogues Clin Neurosci* [Internet]. 2013 Dec [cited 2024 Apr 18];15(4):431. Available from: [/pmc/articles/PMC3898681/](#)
15. Nestler EJ. Molecular basis of long-term plasticity underlying addiction. *Nat Rev Neurosci*. 2001;2(2):119–28.
16. Uhl GR, Koob GF, Cable J. The neurobiology of addiction. *Ann N Y Acad Sci* [Internet]. 2019 Jan 1 [cited 2022 Apr 5];1451(1):5. Available from: [/pmc/articles/PMC6767400/](#)
17. Volkow ND, Morales M. The Brain on Drugs: From Reward to Addiction. *Cell* [Internet]. 2015 Aug 17 [cited 2024 Apr 18];162(4):712–25. Available from: <https://pubmed.ncbi.nlm.nih.gov/26276628/>
18. Parsegian A, See RE. Dysregulation of Dopamine and Glutamate Release in the Prefrontal Cortex and Nucleus Accumbens Following Methamphetamine Self-Administration and During Reinstatement in Rats. *Neuropsychopharmacology* [Internet]. 2014 Mar [cited 2024 Apr 18];39(4):811. Available from: [/pmc/articles/PMC3924513/](#)
19. Tanabe J, Regner M, Sakai J, Martinez D, Gowin J. Neuroimaging reward, craving, learning, and cognitive control in substance use disorders: review and implications for treatment. *Br J Radiol* [Internet]. 2019 [cited 2024 Apr 18];92(1101). Available from: [/pmc/articles/PMC6732921/](#)
20. Bressan RA, Crippa JA. The role of dopamine in reward and pleasure behaviour--review of data from preclinical research. *Acta Psychiatr Scand Suppl* [Internet]. 2005 [cited 2024 Apr 22];111(427):14–21. Available from: <https://pubmed.ncbi.nlm.nih.gov/15877719/>
21. Wise RA, Robble MA. Dopamine and addiction. *Annu Rev Psychol* [Internet]. 2020 Jan 4 [cited 2024 Apr 10];71(Volume 71, 2020):79–106. Available from: <https://www.annualreviews.org/content/journals/10.1146/annurev-psych-010418-103337>

22. Miniaci MC, Speranza L, Dresp-Langley B. From Reward to Anhedonia-Dopamine Function in the Global Mental Health Context. *Biomedicines* 2023, Vol 11, Page 2469 [Internet]. 2023 Sep 6 [cited 2024 Apr 22];11(9):2469. Available from: <https://www.mdpi.com/2227-9059/11/9/2469/htm>
23. Turton S, Lingford-Hughes A. Neurobiology and principles of addiction and tolerance. *Medicine*. 2016 Dec 1;44(12):693–6.
24. Tomkins DM, Sellers EM. Addiction and the brain: the role of neurotransmitters in the cause and treatment of drug dependence. *CMAJ: Canadian Medical Association Journal* [Internet]. 2001 Mar 3 [cited 2024 Apr 10];164(6):817. Available from: </pmc/articles/PMC80880/>
25. Di Matteo V, Di Giovanni G, Pierucci M, Esposito E. Serotonin control of central dopaminergic function: focus on in vivo microdialysis studies. *Prog Brain Res* [Internet]. 2008 [cited 2024 May 10];172:7–44. Available from: <https://pubmed.ncbi.nlm.nih.gov/18772026/>
26. Di Giovanni G, Di Matteo V, Esposito E. Serotonin-Dopamine Interaction : Experimental Evidence and Therapeutic Relevance. :665.
27. Fischer AG, Ullsperger M. An update on the role of serotonin and its interplay with dopamine for reward. *Front Hum Neurosci*. 2017 Oct 11;11:285268.
28. Sofuoglu M, Sewell RA. Norepinephrine and Stimulant Addiction. *Addiction biology* [Internet]. 2009 Apr [cited 2024 May 10];14(2):119. Available from: </pmc/articles/PMC2657197/>
29. Carboni E, Spielow C, Vacca C, Nosten-Bertrand M, Giros B, Di Chiara G. Cocaine and Amphetamine Increase Extracellular Dopamine in the Nucleus Accumbens of Mice Lacking the Dopamine Transporter Gene. *The Journal of Neuroscience* [Internet]. 2001 May 5 [cited 2024 May 10];21(9):RC141. Available from: <https://www.ncbi.nlm.nih.gov/pmc/articles/PMC6762548/>
30. Paladini CA, Williams JT. Noradrenergic Inhibition of Midbrain Dopamine Neurons. *The Journal of Neuroscience* [Internet]. 2004 May 5 [cited 2024 May 10];24(19):4568. Available from: </pmc/articles/PMC6729397/>
31. Blanc G, Trovero F, Vezina P, Hervé D, Godeheu A -M, Glowinski J, et al. Blockade of prefronto-cortical alpha 1-adrenergic receptors prevents locomotor hyperactivity induced by subcortical D-amphetamine injection. *Eur J Neurosci* [Internet]. 1994 [cited 2024 May 10];6(3):293–8. Available from: <https://pubmed.ncbi.nlm.nih.gov/7912614/>

32. Christensen B, Namen AR Van, Calipari E. Sex Differences in GABA Regulation of Dopamine Release in the Nucleus Accumbens and its Role in Cocaine Use Disorder. *Journal of Pharmacology and Experimental Therapeutics* [Internet]. 2023 Jun 1 [cited 2024 May 10];385(S3):543. Available from: <https://jpet.aspetjournals.org/content/385/S3/543>
33. Marshburn PB, Michael Iuvone P. The role of GABA in the regulation of the dopamine/tyrosine hydroxylase-containing neurons of the rat retina. *Brain Res.* 1981 Jun 15;214(2):335–47.
34. Hleihil M, Benke D. Restoring GABAB receptor expression in the ventral tegmental area of methamphetamine addicted mice inhibits locomotor sensitization and drug seeking behavior. *Front Mol Neurosci.* 2024 Feb 7;17:1347228.
35. Kalivas PW, LaLumiere RT, Knackstedt L, Shen H. Glutamate Transmission in Addiction. *Neuropharmacology* [Internet]. 2009 [cited 2024 May 10];56(Suppl 1):169. Available from: </pmc/articles/PMC3280337/>
36. Bimpisidis Z, Wallén-Mackenzie Å. Neurocircuitry of Reward and Addiction: Potential Impact of Dopamine–Glutamate Co-release as Future Target in Substance Use Disorder. *J Clin Med* [Internet]. 2019 Nov 1 [cited 2024 May 10];8(11). Available from: </pmc/articles/PMC6912639/>
37. Moeller SJ, London ED, Northoff G. Neuroimaging markers of glutamatergic and GABAergic systems in drug addiction: Relationships to resting-state functional connectivity. *Neurosci Biobehav Rev.* 2016 Feb 1;61:35–52.
38. Hogarth L. Addiction is driven by excessive goal-directed drug choice under negative affect: translational critique of habit and compulsion theory. *Neuropsychopharmacology* 2020 45:5 [Internet]. 2020 Jan 6 [cited 2024 May 14];45(5):720–35. Available from: <https://www.nature.com/articles/s41386-020-0600-8>
39. Miller NS, Dackis CA, Gold MS. The relationship of addiction, tolerance, and dependence to alcohol and drugs: a neurochemical approach. *J Subst Abuse Treat* [Internet]. 1987 [cited 2024 May 14];4(3–4):197–207. Available from: <https://pubmed.ncbi.nlm.nih.gov/3325655/>
40. Piper ME. Editor’s choice: Withdrawal: Expanding a Key Addiction Construct. *Nicotine & Tobacco Research* [Internet]. 2015 Dec 1 [cited 2024 May 14];17(12):1405. Available from: </pmc/articles/PMC4654762/>

41. Baker TB, Japuntich SJ, Hogle JM, McCarthy DE, Curtin JJ. Pharmacologic and behavioral withdrawal from addictive drugs. *Curr Dir Psychol Sci*. 2006 Oct;15(5):232–6.
42. Anton RF. What Is Craving?: Models and Implications for Treatment. *Alcohol Research & Health* [Internet]. 1999 [cited 2024 May 14];23(3):165. Available from: [/pmc/articles/PMC6760371/](#)
43. Cless MM, Courchesne-Krak NS, Bhatt K V., Mittal ML, Marienfeld CB. Craving among patients seeking treatment for substance use disorder. *Discover Mental Health* [Internet]. 2023 Dec 1 [cited 2024 May 14];3(1):23. Available from: [/pmc/articles/PMC10630178/](#)
44. Verdejo-Garcia A, T-J Chong T, Stout JC, Yücel M, London ED. Stages of dysfunctional decision-making in addiction. 2018 [cited 2024 May 14]; Available from: <http://dx.doi.org/10.1016/j.pbb.2017.02.003>
45. Krmpotich T, Mikulich-Gilbertson S, Sakai J, Thompson L, Banich MT, Tanabe J. Impaired decision-making, higher impulsivity, and drug severity in substance dependence and pathological gambling. *J Addict Med* [Internet]. 2015 May 1 [cited 2024 May 14];9(4):273. Available from: [/pmc/articles/PMC4523448/](#)
46. Milkman H, Weiner SE, Sunderwirth S. Addiction relapse. *Adv Alcohol Subst Abuse* [Internet]. 1983 Jan 31 [cited 2024 May 14];3(1–2):119–34. Available from: <https://pubmed.ncbi.nlm.nih.gov/6391101/>
47. Moon SJE, Lee H. Relapse to substance use: A concept analysis. *Nurs Forum (Auckl)* [Internet]. 2020 Jul 1 [cited 2024 May 14];55(3):523–30. Available from: <https://pubmed.ncbi.nlm.nih.gov/32350881/>
48. Sinha R. The role of stress in addiction relapse. *Curr Psychiatry Rep* [Internet]. 2007 Oct [cited 2024 May 14];9(5):388–95. Available from: <https://pubmed.ncbi.nlm.nih.gov/17915078/>
49. Spanagel R. Animal models of addiction. *Dialogues Clin Neurosci* [Internet]. 2017 Sep 1 [cited 2023 May 9];19(3):247. Available from: [/pmc/articles/PMC5741108/](#)
50. Emmett-Oglesby MW, Mathis DA, Moon RTY, Lal H. Animal models of drug withdrawal symptoms. *Psychopharmacology (Berl)* [Internet]. 1990 Jul [cited 2024 May 14];101(3):292–309. Available from: <https://pubmed.ncbi.nlm.nih.gov/1972994/>

51. Blanco-Gandía MC, Mateos-García A, García-Pardo MP, Montagud-Romero S, Rodríguez-Arias M, Miñarro J, et al. Effect of drugs of abuse on social behaviour: a review of animal models. *Behavioural Pharmacology*. 2015 Sep 1;26(6):541–70.
52. Robinson TE, Gorny G, Mitton E, Kolb B. Cocaine Self-Administration Alters the Morphology of Dendrites and Dendritic Spines in the Nucleus Accumbens and Neocortex. *Synapse*. 2001;39:257–66.
53. Acewicz A, Mierzejewski P, Dyr W, Jastrzebska A, Korkosz I, Wyszogrodzka E, et al. Cocaine self-administration in Warsaw alcohol high-preferring (WHP) and Warsaw alcohol low-preferring (WLP) rats. *Eur J Pharmacol*. 2012 Jan 14;674(2–3):275–9.
54. Gobin C, Shallcross J, Schwendt M. Neurobiological substrates of persistent working memory deficits and cocaine-seeking in the prelimbic cortex of rats with a history of extended access to cocaine self-administration. *Neurobiol Learn Mem* [Internet]. 2019 May 1 [cited 2023 May 8];161:92–105. Available from: https://drive.google.com/file/d/1DeqSEqLXiPfyIHjLNoeG0jERkxe5n3N_/view?usp=embed_facebook
55. McKendrick G, Graziane NM. Drug-Induced Conditioned Place Preference and Its Practical Use in Substance Use Disorder Research. *Front Behav Neurosci*. 2020 Sep 29;14:582147.
56. Blanco-Gandía MC, Aguilar MA, Miñarro J, Rodríguez-Arias M. Reinstatement of Drug-seeking in Mice Using the Conditioned Place Preference Paradigm. *J Vis Exp* [Internet]. 2018 Jun 7 [cited 2024 May 14];2018(136):56983. Available from: </pmc/articles/PMC6101638/>
57. Steketee JD, Kalivas PW. Drug Wanting: Behavioral Sensitization and Relapse to Drug-Seeking Behavior. *Pharmacol Rev* [Internet]. 2011 Jun [cited 2024 May 14];63(2):348. Available from: </pmc/articles/PMC3082449/>
58. Robinson TE, Berridge KC. The incentive sensitization theory of addiction: some current issues. *Philosophical Transactions of the Royal Society B: Biological Sciences* [Internet]. 2008 Oct 10 [cited 2022 May 25];363(1507):3137. Available from: </pmc/articles/PMC2607325/>
59. Bienkowski P, Kostowski W, Koros E. The role of drug-paired stimuli in extinction and reinstatement of ethanol-seeking behaviour in the rat. *Eur J Pharmacol*. 1999 Jun 25;374(3):315–9.
60. Courtney KE, Ray LA. Methamphetamine: An Update on Epidemiology, Pharmacology, Clinical Phenomenology, and Treatment Literature. *Drug Alcohol*

Depend [Internet]. 2014 Oct 10 [cited 2023 Sep 11];0(1):11. Available from: [/pmc/articles/PMC4164186/](#)

61. Shin EJ, Jeong JH, Hwang Y, Sharma N, Dang DK, Nguyen BT, et al. Methamphetamine-induced dopaminergic neurotoxicity as a model of Parkinson's disease. *Archives of Pharmacal Research* 2021 44:7 [Internet]. 2021 Jul 20 [cited 2024 May 6];44(7):668–88. Available from: <https://link.springer.com/article/10.1007/s12272-021-01341-7>
62. Bisagno V, Lud Cadet J. Methamphetamine and MDMA Neurotoxicity: Biochemical and Molecular Mechanisms. *Handbook of Neurotoxicity, Second Edition* [Internet]. 2022 Jan 1 [cited 2024 Apr 29];1:563–85. Available from: https://link.springer.com/referenceworkentry/10.1007/978-3-031-15080-7_80
63. Hogarth S, Manning E, van den Buuse M. Chronic Methamphetamine and Psychosis Pathways. *Handbook of Substance Misuse and Addictions* [Internet]. 2022 [cited 2024 May 6];1–26. Available from: https://link.springer.com/referenceworkentry/10.1007/978-3-030-67928-6_110-1
64. Nickell JR, Siripurapu KB, Vartak A, Crooks PA, Dwoskin LP. The Vesicular Monoamine Transporter-2: An Important Pharmacological Target for the Discovery of Novel Therapeutics to Treat Methamphetamine Abuse. *Adv Pharmacol* [Internet]. 2014 [cited 2024 Apr 29];69:71. Available from: [/pmc/articles/PMC4084610/](#)
65. Edwards S, Whisler KN, Fuller DC, Orsulak PJ, Self DW. Addiction-Related Alterations in D1 and D2 Dopamine Receptor Behavioral Responses Following Chronic Cocaine Self-Administration. *Neuropsychopharmacology* 2007 32:2 [Internet]. 2006 Mar 15 [cited 2024 May 6];32(2):354–66. Available from: <https://www.nature.com/articles/1301062>
66. Müller CP, Carey RJ, Huston JP, De Souza Silva MA. Serotonin and psychostimulant addiction: focus on 5-HT1A-receptors. *Prog Neurobiol* [Internet]. 2007 Feb [cited 2024 May 6];81(3):133–78. Available from: <https://pubmed.ncbi.nlm.nih.gov/17316955/>
67. Hyman SE. Addiction: A Disease of Learning and Memory. <https://doi.org/10.1176/appi.ajp.162.8.1414> [Internet]. 2005 Aug 1 [cited 2023 Mar 6];162(8):1414–22. Available from: <https://ajp.psychiatryonline.org/doi/10.1176/appi.ajp.162.8.1414>
68. Cao G, Zhu J, Zhong Q, Shi C, Dang Y, Han W, et al. Distinct roles of methamphetamine in modulating spatial memory consolidation, retrieval, reconsolidation and the accompanying changes of ERK and CREB activation in

- hippocampus and prefrontal cortex. *Neuropharmacology* [Internet]. 2013 Apr [cited 2023 May 5];67:144. Available from: [/pmc/articles/PMC3582331/](#)
69. Mao LM, Reusch JM, Fibuch EE, Liu Z, Wang JQ. Amphetamine increases phosphorylation of MAPK/ERK at synaptic sites in the rat striatum and medial prefrontal cortex. *Brain Res* [Internet]. 2013 Feb 2 [cited 2023 May 3];1494:101. Available from: [/pmc/articles/PMC3546198/](#)
 70. Thrash-Williams B, Karuppagounder SS, Bhattacharya D, Ahuja M, Suppiramaniam V, Dhanasekaran M. Methamphetamine-induced dopaminergic toxicity prevented owing to the neuroprotective effects of salicylic acid. *Life Sci*. 2016 Jun 1;154:24–9.
 71. Chen C, Hsu FC, Li CW, Huang MC. Structural, functional, and neurochemical neuroimaging of methamphetamine-associated psychosis: A systematic review. *Psychiatry Res Neuroimaging*. 2019 Oct 30;292:23–31.
 72. McKetin R, Leung J, Stockings E, Huo Y, Foulds J, Lappin JM, et al. Mental health outcomes associated with the use of amphetamines: A systematic review and meta-analysis. *EClinicalMedicine*. 2019 Nov 1;16:81–97.
 73. Cadet JL, Krasnova IN. MOLECULAR BASES OF METHAMPHETAMINE-INDUCED NEURODEGENERATION. *Int Rev Neurobiol* [Internet]. 2009 [cited 2024 May 20];88(C):101. Available from: [/pmc/articles/PMC8247532/](#)
 74. Choi HJ, Yoo TM, Chung SY, Yang JS, Kim J II, Ha ES, et al. Methamphetamine-induced Apoptosis in a CNS-derived Catecholaminergic Cell Line. *Mol Cells*. 2002 Apr 1;13(2):221–7.
 75. De Vito MJ, Wagner GC. Methamphetamine-induced neuronal damage: a possible role for free radicals. *Neuropharmacology* [Internet]. 1989 [cited 2024 May 20];28(10):1145–50. Available from: <https://pubmed.ncbi.nlm.nih.gov/2554183/>
 76. Heilig M, MacKillop J, Martinez D, Rehm J, Leggio L, Vanderschuren LJMJ. Addiction as a brain disease revised: why it still matters, and the need for consilience. *Neuropsychopharmacology* 2021 46:10 [Internet]. 2021 Feb 22 [cited 2024 Apr 22];46(10):1715–23. Available from: <https://www.nature.com/articles/s41386-020-00950-y>
 77. Dreher JC, Kohn P, Kolachana B, Weinberger DR, Berman KF. Variation in dopamine genes influences responsivity of the human reward system. *Proc Natl Acad Sci U S A* [Internet]. 2009 Jan 13 [cited 2024 Apr 22];106(2):617–22. Available from: <https://pubmed.ncbi.nlm.nih.gov/19104049/>

78. Nestler EJ. Transcriptional Mechanisms of Drug Addiction. *Clinical Psychopharmacology and Neuroscience*. 2012;10(3):136.
79. Citri A, Malenka RC. Synaptic Plasticity: Multiple Forms, Functions, and Mechanisms. *Neuropsychopharmacology* 2008 33:1 [Internet]. 2007 Aug 29 [cited 2023 Mar 16];33(1):18–41. Available from: <https://www.nature.com/articles/1301559>
80. Kauer JA, Malenka RC. Synaptic plasticity and addiction. *Nat Rev Neurosci* [Internet]. 2007 Nov [cited 2023 Mar 16];8(11):844–58. Available from: <https://pubmed.ncbi.nlm.nih.gov/17948030/>
81. Dietz DM, Dietz KC, Nestler EJ, Russo SJ. Molecular mechanisms of psychostimulant-induced structural plasticity. *Pharmacopsychiatry* [Internet]. 2009 [cited 2023 Apr 20];42 Suppl 1(Suppl 1). Available from: <https://pubmed.ncbi.nlm.nih.gov/19434558/>
82. Hidalgo C, Arias-Cavieres A. Calcium, reactive oxygen species, and synaptic plasticity. *Physiology*. 2016 May 1;31(3):201–15.
83. Nyberg F. Structural plasticity of the brain to psychostimulant use. *Neuropharmacology*. 2014 Dec 1;87:115–24.
84. Kalivas PW, O'Brien C. Drug Addiction as a Pathology of Staged Neuroplasticity. *Neuropsychopharmacology* 2008 33:1 [Internet]. 2007 Sep 5 [cited 2024 Apr 22];33(1):166–80. Available from: <https://www.nature.com/articles/1301564>
85. Robinson TE, Kolb B. Structural plasticity associated with exposure to drugs of abuse. *Neuropharmacology* [Internet]. 2004 [cited 2024 May 20];47(SUPPL. 1):33–46. Available from: <https://pubmed.ncbi.nlm.nih.gov/15464124/>
86. Zucker RS, Regehr WG. Short-term synaptic plasticity. *Annu Rev Physiol* [Internet]. 2002 [cited 2024 May 13];64:355–405. Available from: <https://pubmed.ncbi.nlm.nih.gov/11826273/>
87. Citri A, Malenka RC. Synaptic Plasticity: Multiple Forms, Functions, and Mechanisms. *Neuropsychopharmacology* 2008 33:1 [Internet]. 2007 Aug 29 [cited 2024 May 14];33(1):18–41. Available from: <https://www.nature.com/articles/1301559>
88. Muller D, Nikonenko I, Jourdain P, Alberi S. LTP, Memory and Structural Plasticity. *Curr Mol Med*. 2005 Mar 25;2(7):605–11.
89. Ungless MA, Whistler JL, Malenka RC, Bonci A. Single cocaine exposure in vivo induces long-term potentiation in dopamine neurons. *Nature* [Internet]. 2001 May

31 [cited 2024 May 20];411(6837):583–7. Available from:
<https://pubmed.ncbi.nlm.nih.gov/11385572/>

90. Sarti F, Borgland SL, Kharazia VN, Bonci A. Acute cocaine exposure alters spine density and long-term potentiation in the ventral tegmental area. *European Journal of Neuroscience*. 2007 Aug;26(3):749–56.
91. Heshmati M. Cocaine-induced LTP in the ventral tegmental area: new insights into mechanism and time course illuminate the cellular substrates of addiction. *J Neurophysiol* [Internet]. 2009 Jun [cited 2024 May 20];101(6):2735–7. Available from: <https://pubmed.ncbi.nlm.nih.gov/19297516/>
92. Ungless MA, Whistler JL, Malenka RC, Bonci A. Single cocaine exposure in vivo induces long-term potentiation in dopamine neurons. *Nature*. 2001 May 31;411(6837):583–7.
93. Fernandez-Espejo E, Rodriguez-Espinosa N. Psychostimulant Drugs and Neuroplasticity. *Pharmaceuticals* 2011, Vol 4, Pages 976-991 [Internet]. 2011 Jun 30 [cited 2024 May 21];4(7):976–91. Available from: <https://www.mdpi.com/1424-8247/4/7/976/htm>
94. Volianskis A, France G, Jensen MS, Bortolotto ZA, Jane DE, Collingridge GL. Long-term potentiation and the role of N-methyl-d-aspartate receptors. *Brain Res* [Internet]. 2015 Sep 9 [cited 2024 May 14];1621:5. Available from: </pmc/articles/PMC4563944/>
95. Heysieattalab S, Naghdi N, Hosseinmardi N, Zarrindast MR, Haghparast A, Khoshbouei H. Methamphetamine-induced enhancement of hippocampal long-term potentiation is modulated by NMDA and GABA receptors in the shell-accumbens. *Synapse* [Internet]. 2016 Aug 1 [cited 2024 May 20];70(8):325–35. Available from: <https://pubmed.ncbi.nlm.nih.gov/27029021/>
96. Avchalumov Y, Trenet W, Piña-Crespo J, Mandyam C. SCH23390 Reduces Methamphetamine Self-Administration and Prevents Methamphetamine-Induced Striatal LTD. *Int J Mol Sci* [Internet]. 2020 Sep 2 [cited 2024 May 20];21(18):1–16. Available from: </pmc/articles/PMC7554976/>
97. Brebner K, Wong TP, Liu L, Liu Y, Campsall P, Gray S, et al. Nucleus accumbens long-term depression and the expression of behavioral sensitization. *Science* [Internet]. 2005 Nov 25 [cited 2024 May 20];310(5752):1340–3. Available from: <https://pubmed.ncbi.nlm.nih.gov/16311338/>

98. La Rosa C, Parolisi R, Bonfanti L. Brain Structural Plasticity: From Adult Neurogenesis to Immature Neurons. *Front Neurosci* [Internet]. 2020 Feb 4 [cited 2024 May 14];14:512123. Available from: www.frontiersin.org
99. Gage FH. Structural plasticity of the adult brain. *Dialogues Clin Neurosci* [Internet]. 2004 [cited 2024 May 14];6(2):135. Available from: [/pmc/articles/PMC3181802/](https://pubmed.ncbi.nlm.nih.gov/15229250/)
100. Thompson PM, Hayashi KM, Simon SL, Geaga JA, Hong MS, Sui Y, et al. Structural abnormalities in the brains of human subjects who use methamphetamine. *J Neurosci* [Internet]. 2004 Jun 30 [cited 2024 May 20];24(26):6028–36. Available from: <https://pubmed.ncbi.nlm.nih.gov/15229250/>
101. Kasahara Y, Sakakibara Y, Hiratsuka T, Moriya Y, Lesch KP, Hall FS, et al. Repeated methamphetamine treatment increases spine density in the nucleus accumbens of serotonin transporter knockout mice. *Neuropsychopharmacol Rep* [Internet]. 2019 Jun 1 [cited 2024 May 20];39(2):130–3. Available from: <https://onlinelibrary.wiley.com/doi/full/10.1002/npr2.12049>
102. Li J, Liu N, Lu K, Zhang L, Gu J, Guo F, et al. Cocaine-induced dendritic remodeling occurs in both D1 and D2 dopamine receptor-expressing neurons in the nucleus accumbens. *Neurosci Lett*. 2012 May 31;517(2):118–22.
103. Iwazaki T, McGregor IS, Matsumoto I. Protein expression profile in the striatum of rats with methamphetamine-induced behavioral sensitization. *Proteomics*. 2007 Apr;7(7):1131–9.
104. Iwazaki T, McGregor IS, Matsumoto I. Protein expression profile in the striatum of acute methamphetamine-treated rats. *Brain Res* [Internet]. 2006 Jun 30 [cited 2024 May 20];1097(1):19–25. Available from: <https://pubmed.ncbi.nlm.nih.gov/16729985/>
105. Yang MH, Kim S, Jung MS, Shim JH, Ryu NK, Yook YJ, et al. Proteomic analysis of methamphetamine-induced reinforcement processes within the mesolimbic dopamine system. *Addiction biology* [Internet]. 2008 Sep [cited 2024 May 20];13(3–4):287–94. Available from: <https://pubmed.ncbi.nlm.nih.gov/18279499/>
106. Iwazaki T, McGregor IS, Matsumoto I. Protein expression profile in the amygdala of rats with methamphetamine-induced behavioral sensitization. *Neurosci Lett* [Internet]. 2008 Apr 18 [cited 2024 May 20];435(2):113–9. Available from: <https://pubmed.ncbi.nlm.nih.gov/18346852/>
107. Kamsler A, Segal M. Control of neuronal plasticity by reactive oxygen species. *Antioxid Redox Signal*. 2007 Feb;9(2):165–7.

108. Womersley JS, Townsend DM, Kalivas PW, Uys JD. Targeting Redox Regulation to Treat Substance Use Disorder using N-acetylcysteine. *Eur J Neurosci*. 2019 Aug 1;50(3):2538.
109. D'Autréaux B, Toledano MB. ROS as signalling molecules: mechanisms that generate specificity in ROS homeostasis. *Nature Reviews Molecular Cell Biology* 2007 8:10. 2007 Oct;8(10):813–24.
110. Sies H, Jones DP. Reactive oxygen species (ROS) as pleiotropic physiological signalling agents. *Nature Reviews Molecular Cell Biology* 2020 21:7. 2020 Mar 30;21(7):363–83.
111. Massaad CA, Klann E. Reactive Oxygen Species in the Regulation of Synaptic Plasticity and Memory. *Antioxid Redox Signal*. 2011 May 15;14(10):2013.
112. Hidalgo C, Carrasco MA, Muñoz P, Núñez MT. A role for reactive oxygen/nitrogen species and iron on neuronal synaptic plasticity. *Antioxid Redox Signal*. 2007 Feb;9(2):245–55.
113. Jones DP, Sies H. The Redox Code. *Antioxid Redox Signal* [Internet]. 2015 Sep 20 [cited 2023 Mar 8];23(9):734–46. Available from: <https://pubmed.ncbi.nlm.nih.gov/25891126/>
114. Zhang J, Wang X, Vikash V, Ye Q, Wu D, Liu Y, et al. ROS and ROS-Mediated Cellular Signaling. *Oxid Med Cell Longev*. 2016;2016.
115. Yang X, Wang Y, Li Q, Zhong Y, Chen L, Du Y, et al. The Main Molecular Mechanisms Underlying Methamphetamine- Induced Neurotoxicity and Implications for Pharmacological Treatment. *Front Mol Neurosci* [Internet]. 2018 Jun 4 [cited 2023 Feb 27];11:186. Available from: </pmc/articles/PMC5994595/>
116. Hong Y, Boiti A, Vallone D, Foulkes NS. Reactive Oxygen Species Signaling and Oxidative Stress: Transcriptional Regulation and Evolution. *Antioxidants* 2024, Vol 13, Page 312 [Internet]. 2024 Mar 1 [cited 2024 May 26];13(3):312. Available from: <https://www.mdpi.com/2076-3921/13/3/312/htm>
117. Song BJ, Moon KH, Upreti V V., Eddington ND, Lee IJ. Mechanisms of MDMA (Ecstasy)-Induced Oxidative Stress, Mitochondrial Dysfunction, and Organ Damage. *Curr Pharm Biotechnol* [Internet]. 2010 Aug 8 [cited 2023 May 5];11(5):434. Available from: </pmc/articles/PMC2911494/>
118. Yamamoto BK, Raudensky J. The role of oxidative stress, metabolic compromise, and inflammation in neuronal injury produced by amphetamine-related drugs of abuse. *Journal of Neuroimmune Pharmacology*. 2008 Dec;3(4):203–17.

119. Jayanthi S, Ladenheim B, Cadet JL. Methamphetamine-induced changes in antioxidant enzymes and lipid peroxidation in copper/zinc-superoxide dismutase transgenic mice. *Ann N Y Acad Sci* [Internet]. 1998 [cited 2024 May 22];844(1):92–102. Available from: <https://pubmed.ncbi.nlm.nih.gov/29090838/>
120. Bedard K, Krause KH. The NOX family of ROS-generating NADPH oxidases: Physiology and pathophysiology. *Physiol Rev*. 2007 Jan;87(1):245–313.
121. Murphy MP. How mitochondria produce reactive oxygen species. *Biochemical Journal*. 2009 Jan 1;417(1):1–13.
122. Held JM. Redox Systems Biology: Harnessing the Sentinels of the Cysteine Redoxome. *Antioxid Redox Signal* [Internet]. 2020 Apr 1 [cited 2023 Apr 28];32(10):659–76. Available from: <https://www.liebertpub.com/doi/10.1089/ars.2019.7725>
123. Berndt C, Lillig CH, Flohé L. Redox regulation by glutathione needs enzymes. *Front Pharmacol* [Internet]. 2014 [cited 2024 May 14];5. Available from: </pmc/articles/PMC4101335/>
124. Paul BD, Sbodio JI, Snyder SH. Cysteine Metabolism in Neuronal Redox Homeostasis. *Trends Pharmacol Sci* [Internet]. 2018 May 1 [cited 2023 Apr 19];39(5):513–24. Available from: <https://pubmed.ncbi.nlm.nih.gov/29530337/>
125. Sbodio JI, Snyder SH, Paul BD. Redox Mechanisms in Neurodegeneration: From Disease Outcomes to Therapeutic Opportunities. *Antioxid Redox Signal* [Internet]. 2019 [cited 2023 Apr 19];30(11):1450–99. Available from: <https://pubmed.ncbi.nlm.nih.gov/29634350/>
126. Moldogazieva NT, Mokhosev IM, Feldman NB, Lutsenko S V. ROS and RNS signalling: adaptive redox switches through oxidative/nitrosative protein modifications. *Free Radic Res* [Internet]. 2018 May 4 [cited 2023 Apr 19];52(5):507–43. Available from: <https://pubmed.ncbi.nlm.nih.gov/29589770/>
127. Trist BG, Hare DJ, Double KL. Oxidative stress in the aging substantia nigra and the etiology of Parkinson's disease. *Aging Cell* [Internet]. 2019 Dec 1 [cited 2024 May 13];18(6). Available from: <https://pubmed.ncbi.nlm.nih.gov/31432604/>
128. Milkovic L, Gasparovic AC, Cindric M, Mouthuy PA, Zarkovic N. Short Overview of ROS as Cell Function Regulators and Their Implications in Therapy Concepts. *Cells* [Internet]. 2019 Aug 1 [cited 2023 Apr 19];8(8). Available from: <https://pubmed.ncbi.nlm.nih.gov/31366062/>

129. Paulsen CE, Carroll KS. Cysteine-Mediated Redox Signaling: Chemistry, Biology, and Tools for Discovery. *Chem Rev* [Internet]. 2013 Jul 7 [cited 2023 Apr 19];113(7):4633. Available from: [/pmc/articles/PMC4303468/](https://pubmed.ncbi.nlm.nih.gov/2401137/)
130. Butterfield DA, Dalle-Donne I. FORUM EDITORIAL Redox Proteomics.
131. Boguszewska-Mańkowska D, Zagdańska MN and B, Boguszewska-Mańkowska D, Zagdańska MN and B. Protein Oxidation and Redox Regulation of Proteolysis. *Basic Principles and Clinical Significance of Oxidative Stress* [Internet]. 2015 Nov 11 [cited 2023 Apr 19]; Available from: <https://www.intechopen.com/chapters/49160>
132. Zhang J, Wang X, Vikash V, Ye Q, Wu D, Liu Y, et al. ROS and ROS-Mediated Cellular Signaling. *Oxid Med Cell Longev* [Internet]. 2016 [cited 2023 Mar 10];2016. Available from: [/pmc/articles/PMC4779832/](https://pubmed.ncbi.nlm.nih.gov/270479832/)
133. Adler V, Yin Z, Fuchs SY, Benezra M, Rosario L, Tew KD, et al. Regulation of JNK signaling by GSTp. *EMBO J* [Internet]. 1999 Mar 1 [cited 2023 Apr 19];18(5):1321–34. Available from: <https://onlinelibrary.wiley.com/doi/full/10.1093/emboj/18.5.1321>
134. Saitoh M, Nishitoh H, Fujii M, Takeda K, Tobiume K, Sawada Y, et al. Mammalian thioredoxin is a direct inhibitor of apoptosis signal-regulating kinase (ASK) 1. *EMBO J*. 1998;17(9):2596–606.
135. Tonks NK. Redox redux: Revisiting PTPs and the control of cell signaling. *Cell* [Internet]. 2005 Jun 3 [cited 2023 Apr 19];121(5):667–70. Available from: <http://www.cell.com/article/S0092867405004952/fulltext>
136. Stuart JA, Maddalena LA, Merilovich M, Robb EL. A midlife crisis for the mitochondrial free radical theory of aging. *Longevity & Healthspan* 2014 3:1 [Internet]. 2014 Apr 1 [cited 2023 Apr 19];3(1):1–15. Available from: <https://longevityandhealthspan.biomedcentral.com/articles/10.1186/2046-2395-3-4>
137. Finkel T. Signal transduction by reactive oxygen species. *Journal of Cell Biology* [Internet]. 2011 Jul 11 [cited 2023 Apr 19];194(1):7–15. Available from: www.jcb.org/cgi/doi/10.1083/jcb.201102095
138. Cadet JL, Brannock C. Free radicals and the pathobiology of brain dopamine systems. *Neurochem Int*. 1997 Aug 1;32(2):117–31.
139. Cadet JL, Krasnova IN, Jayanthi S, Lyles J. Neurotoxicity of substituted amphetamines: molecular and cellular mechanisms. *Neurotox Res* [Internet]. 2007

- [cited 2022 May 24];11(3–4):183–202. Available from:
<https://pubmed.ncbi.nlm.nih.gov/17449459/>
140. Lennicke C, Rahn J, Lichtenfels R, Wessjohann LA, Seliger B. Hydrogen peroxide – production, fate and role in redox signaling of tumor cells. *Cell Communication and Signaling* 2015 13:1 [Internet]. 2015 Sep 14 [cited 2024 May 22];13(1):1–19. Available from: <https://biosignaling.biomedcentral.com/articles/10.1186/s12964-015-0118-6>
 141. Redox and Neuroplasticity. [Internet]. [cited 2023 Apr 4]. Available from: <https://chat.openai.com/chat/3274b8cc-dee5-4dce-b920-6d76f14b5a15>
 142. Knapp LT, Klann E. Role of reactive oxygen species in hippocampal long-term potentiation: contributory or inhibitory? *J Neurosci Res* [Internet]. 2002 Oct 1 [cited 2023 Mar 29];70(1):1–7. Available from: <https://pubmed.ncbi.nlm.nih.gov/12237859/>
 143. Reczek CR, Chandel NS. ROS-dependent signal transduction. *Curr Opin Cell Biol*. 2015 Apr 1;33:8–13.
 144. D’Autréaux B, Toledano MB. ROS as signalling molecules: mechanisms that generate specificity in ROS homeostasis. *Nature Reviews Molecular Cell Biology* 2007 8:10 [Internet]. 2007 Oct [cited 2022 May 25];8(10):813–24. Available from: <https://www.nature.com/articles/nrm2256>
 145. Milton VJ, Jarrett HE, Gowers K, Chalak S, Briggs L, Robinson IM, et al. Oxidative stress induces overgrowth of the Drosophila neuromuscular junction. *Proc Natl Acad Sci U S A* [Internet]. 2011 Oct 18 [cited 2024 May 22];108(42):17521–6. Available from: </pmc/articles/PMC3198377/>
 146. Sanyal S, Sandstrom DJ, Hoeffler CA, Ramaswami M. AP-1 functions upstream of CREB to control synaptic plasticity in Drosophila. *Nature* [Internet]. 2002 Apr 25 [cited 2024 May 22];416(6883):870–4. Available from: <https://pubmed.ncbi.nlm.nih.gov/11976688/>
 147. Milton VJ, Sweeney ST. Oxidative stress in synapse development and function. *Dev Neurobiol* [Internet]. 2012 Jan [cited 2024 May 22];72(1):100–10. Available from: <https://pubmed.ncbi.nlm.nih.gov/21793225/>
 148. Gao X, Kim HK, Chung JM, Chung K. Reactive oxygen species (ROS) are involved in enhancement of NMDA-receptor phosphorylation in animal models of pain. *Pain* [Internet]. 2007 Oct [cited 2023 Apr 21];131(3):262. Available from: </pmc/articles/PMC2048490/>

149. Dukoff DJ, Hogg DW, Hawrysh PJ, Buck LT. Scavenging ROS dramatically increase NMDA receptor whole-cell currents in painted turtle cortical neurons. *J Exp Biol* [Internet]. 2014 Sep 1 [cited 2023 Apr 21];217(Pt 18):3346–55. Available from: <https://pubmed.ncbi.nlm.nih.gov/25063855/>
150. Girouard H, Wang G, Gallo EF, Anrather J, Zhou P, Pickel VM, et al. NMDA Receptor Activation Increases Free Radical Production through Nitric Oxide and NOX2. *Journal of Neuroscience* [Internet]. 2009 Feb 25 [cited 2023 Apr 21];29(8):2545–52. Available from: <https://www.jneurosci.org/content/29/8/2545>
151. Iqbal MA, Eftekharpour E. Regulatory Role of Redox Balance in Determination of Neural Precursor Cell Fate. *Stem Cells Int* [Internet]. 2017 [cited 2023 Apr 21];2017. Available from: </pmc/articles/PMC5540383/>
152. Sinenko SA, Starkova TY, Kuzmin AA, Tomilin AN. Physiological Signaling Functions of Reactive Oxygen Species in Stem Cells: From Flies to Man. *Front Cell Dev Biol*. 2021 Aug 6;9:1994.
153. Kärkkäinen V, Pomeshchik Y, Savchenko E, Dhungana H, Kurronen A, Lehtonen S, et al. Nrf2 regulates neurogenesis and protects neural progenitor cells against A β toxicity. *Stem Cells* [Internet]. 2014 [cited 2023 Apr 21];32(7):1904–16. Available from: <https://pubmed.ncbi.nlm.nih.gov/24753106/>
154. Dhawan S, Myers P, Bailey DMD, Ostrovsky AD, Evers JF, Landgraf M. Reactive Oxygen Species Mediate Activity-Regulated Dendritic Plasticity Through NADPH Oxidase and Aquaporin Regulation. *Front Cell Neurosci*. 2021 Jul 5;15:237.
155. Oswald MCW, Brooks PS, Zwart MF, Mukherjee A, West RJH, Giachello CNG, et al. Reactive oxygen species regulate activity-dependent neuronal plasticity in *Drosophila*. *Elife* [Internet]. 2018 Dec 1 [cited 2024 May 22];7. Available from: <https://pubmed.ncbi.nlm.nih.gov/30540251/>
156. Zwart MF, Randlett O, Evers JF, Landgraf M. Dendritic growth gated by a steroid hormone receptor underlies increases in activity in the developing *Drosophila* locomotor system. *Proc Natl Acad Sci U S A* [Internet]. 2013 Oct 1 [cited 2024 May 22];110(40). Available from: <https://pubmed.ncbi.nlm.nih.gov/24043825/>
157. Cuesto G, Enriquez-Barreto L, Caramés C, Cantarero M, Gasull X, Sandi C, et al. Phosphoinositide-3-kinase activation controls synaptogenesis and spinogenesis in hippocampal neurons. *J Neurosci* [Internet]. 2011 Feb 23 [cited 2024 May 22];31(8):2721–33. Available from: <https://pubmed.ncbi.nlm.nih.gov/21414895/>

158. Wilson MA. The role of cysteine oxidation in DJ-1 function and dysfunction. *Antioxid Redox Signal* [Internet]. 2011 Jul 1 [cited 2024 May 22];15(1):111–22. Available from: <https://pubmed.ncbi.nlm.nih.gov/20812780/>
159. Nave KA, Werner HB. Myelination of the nervous system: mechanisms and functions. *Annu Rev Cell Dev Biol* [Internet]. 2014 [cited 2023 Apr 21];30:503–33. Available from: <https://pubmed.ncbi.nlm.nih.gov/25288117/>
160. Smith KJ, Kapoor R, Felts PA. Demyelination: the role of reactive oxygen and nitrogen species. *Brain Pathol* [Internet]. 1999 [cited 2023 Apr 21];9(1):69–92. Available from: <https://pubmed.ncbi.nlm.nih.gov/9989453/>
161. Accetta R, Damiano S, Morano A, Mondola P, Paternò R, Avvedimento E V., et al. Oxygen species derived from NOX3 and NOX5 drive differentiation of human oligodendrocytes. *Front Cell Neurosci*. 2016 Jun 2;10(JUN):146.
162. Bongarzone ER, Pasquini JM, Soto EF. Oxidative damage to proteins and lipids of CNS myelin produced by in vitro generated reactive oxygen species. *J Neurosci Res* [Internet]. 1995 Jun 1 [cited 2023 Apr 28];41(2):213–21. Available from: <https://onlinelibrary.wiley.com/doi/full/10.1002/jnr.490410209>
163. Sies H. Hydrogen peroxide as a central redox signaling molecule in physiological oxidative stress: Oxidative eustress. *Redox Biol*. 2017 Apr 1;11:613–9.
164. Sies H. Role of Metabolic H₂O₂ Generation: REDOX SIGNALING AND OXIDATIVE STRESS*. *J Biol Chem* [Internet]. 2014 Mar 3 [cited 2023 Apr 20];289(13):8735. Available from: </pmc/articles/PMC3979367/>
165. Dringen R, Pawlowski PG, Hirrlinger J. Peroxide detoxification by brain cells. *J Neurosci Res* [Internet]. 2005 Jan 15 [cited 2023 Apr 20];79(1–2):157–65. Available from: <https://pubmed.ncbi.nlm.nih.gov/15573410/>
166. Randall LM, Ferrer-Sueta G, Denicola A. Peroxiredoxins as preferential targets in H₂O₂-induced signaling. *Methods Enzymol* [Internet]. 2013 [cited 2023 Apr 20];527:41–63. Available from: <https://pubmed.ncbi.nlm.nih.gov/23830625/>
167. Rhee SG, Woo HA, Kang D. The Role of Peroxiredoxins in the Transduction of H₂O₂ Signals. *Antioxid Redox Signal* [Internet]. 2018 Mar 1 [cited 2023 Apr 20];28(7):537–57. Available from: <https://pubmed.ncbi.nlm.nih.gov/28587524/>
168. Veal EA, Day AM, Morgan BA. Hydrogen Peroxide Sensing and Signaling. *Mol Cell*. 2007 Apr 13;26(1):1–14.

169. Kamsler A, Segal M. Hydrogen Peroxide Modulation of Synaptic Plasticity. *The Journal of Neuroscience* [Internet]. 2003 Jan 1 [cited 2023 Mar 29];23(1):269. Available from: [/pmc/articles/PMC6742148/](#)
170. Sies H. Hydrogen peroxide as a central redox signaling molecule in physiological oxidative stress: Oxidative eustress. *Redox Biol* [Internet]. 2017 Apr 1 [cited 2023 Apr 20];11:613. Available from: [/pmc/articles/PMC5256672/](#)
171. Davis S, Zhu J. Substance abuse and neurotransmission. *Adv Pharmacol* [Internet]. 2022 Jan 1 [cited 2023 May 8];93:403. Available from: [/pmc/articles/PMC9759822/](#)
172. Sulzer D, Sonders MS, Poulsen NW, Galli A. Mechanisms of neurotransmitter release by amphetamines: a review. *Prog Neurobiol* [Internet]. 2005 Apr [cited 2024 May 12];75(6):406–33. Available from: <https://pubmed.ncbi.nlm.nih.gov/15955613/>
173. Branch SY, Beckstead MJ. Methamphetamine produces bidirectional, concentration-dependent effects on dopamine neuron excitability and dopamine-mediated synaptic currents. *J Neurophysiol*. 2012 Aug 1;108(3):802–9.
174. Meiser J, Weindl D, Hiller K. Complexity of dopamine metabolism. *Cell Commun Signal* [Internet]. 2013 [cited 2024 May 12];11(1):34. Available from: [/pmc/articles/PMC3693914/](#)
175. Nestler EJ, Lüscher C. The Molecular Basis of Drug Addiction: Linking Epigenetic to Synaptic and Circuit Mechanisms. *Neuron* [Internet]. 2019 Apr 3 [cited 2024 May 21];102(1):48–59. Available from: <https://pubmed.ncbi.nlm.nih.gov/30946825/>
176. Herlinger E, Jameson RF, Linert W. Spontaneous autoxidation of dopamine. *Journal of the Chemical Society, Perkin Transactions 2* [Internet]. 1995 Jan 1 [cited 2024 May 13];(2):259–63. Available from: <https://pubs.rsc.org/en/content/articlehtml/1995/p2/p29950000259>
177. Hermida-Ameijeiras Á, Méndez-Álvarez E, Sánchez-Iglesias S, Sanmartín-Suárez C, Soto-Otero R. Autoxidation and MAO-mediated metabolism of dopamine as a potential cause of oxidative stress: role of ferrous and ferric ions. *Neurochem Int*. 2004 Jul 1;45(1):103–16.
178. Umek N, Geršak B, Vintar N, Šoštarič M, Mavri J. Dopamine Autoxidation Is Controlled by Acidic pH. *Front Mol Neurosci* [Internet]. 2018 Dec 18 [cited 2024 May 13];11:467. Available from: [/pmc/articles/PMC6305604/](#)
179. Girotto S, Sturlese M, Bellanda M, Tessari I, Cappellini R, Bisaglia M, et al. Dopamine-derived Quinones Affect the Structure of the Redox Sensor DJ-1 through

- Modifications at Cys-106 and Cys-53. *J Biol Chem* [Internet]. 2012 May 5 [cited 2024 May 13];287(22):18738. Available from: [/pmc/articles/PMC3365698/](#)
180. Solano F, Hearing VJ, García-Borrón JC. Neurotoxicity due to o-quinones: neuromelanin formation and possible mechanisms for o-quinone detoxification. *Neurotox Res* [Internet]. 2000 Sep [cited 2024 May 13];1(3):153–69. Available from: <https://pubmed.ncbi.nlm.nih.gov/12835099/>
181. LaVoie MJ, Hastings TG. Dopamine Quinone Formation and Protein Modification Associated with the Striatal Neurotoxicity of Methamphetamine: Evidence against a Role for Extracellular Dopamine. *Journal of Neuroscience* [Internet]. 1999 Feb 15 [cited 2024 May 13];19(4):1484–91. Available from: <https://www.jneurosci.org/content/19/4/1484>
182. Kussmaul L, Hirst J. The mechanism of superoxide production by NADH:ubiquinone oxidoreductase (complex I) from bovine heart mitochondria. *Proc Natl Acad Sci U S A* [Internet]. 2006 May 5 [cited 2024 May 13];103(20):7607. Available from: [/pmc/articles/PMC1472492/](#)
183. Bleier L, Dröse S. Superoxide generation by complex III: From mechanistic rationales to functional consequences. *Biochim Biophys Acta Bioenerg*. 2013;1827(11–12):1320–31.
184. Murphy MP, Holmgren A, Larsson NG, Halliwell B, Chang CJ, Kalyanaraman B, et al. Unraveling the biological roles of reactive oxygen species. *Cell Metab*. 2011 Apr 6;13(4):361–6.
185. Weidinger A, Kozlov A V. Biological Activities of Reactive Oxygen and Nitrogen Species: Oxidative Stress versus Signal Transduction. *Biomolecules* [Internet]. 2015 Apr 15 [cited 2024 May 13];5(2):472. Available from: [/pmc/articles/PMC4496681/](#)
186. Ruskiewicz J, Albrecht J. Changes in the mitochondrial antioxidant systems in neurodegenerative diseases and acute brain disorders. *Neurochem Int* [Internet]. 2015 Sep 1 [cited 2024 May 13];88:66–72. Available from: <https://pubmed.ncbi.nlm.nih.gov/25576182/>
187. Karnati S, Lüers G, Pfreimer S, Baumgart-Vogt E. Mammalian SOD2 is exclusively located in mitochondria and not present in peroxisomes. *Histochem Cell Biol* [Internet]. 2013 Aug [cited 2024 May 13];140(2):105–17. Available from: <https://pubmed.ncbi.nlm.nih.gov/23744526/>

188. Thornton C, Grad E, Yaka R. The role of mitochondria in cocaine addiction. *Biochem J* [Internet]. 2021 Feb 1 [cited 2023 Mar 6];478(4):749–64. Available from: <https://pubmed.ncbi.nlm.nih.gov/33626141/>
189. Ben-Shachar D, Zuk R, Glinka Y. Dopamine neurotoxicity: inhibition of mitochondrial respiration. *J Neurochem*. 1995;64(2):718–23.
190. Paladini CA, Robinson S, Morikawa H, Williams JT, Palmiter RD. Dopamine controls the firing pattern of dopamine neurons via a network feedback mechanism. *Proc Natl Acad Sci U S A*. 2003 Mar 4;100(5):2866–71.
191. Gluck M, Ehrhart J, Jayatilleke E, Zeevalk GD. Inhibition of brain mitochondrial respiration by dopamine: Involvement of H₂O₂ and hydroxyl radicals but not glutathione-protein-mixed disulfides. *J Neurochem*. 2002;82(1):66–74.
192. Asaoka N, Ibi M, Hatakama H, Nagaoka K, Iwata K, Matsumoto M, et al. NOX1/NADPH Oxidase Promotes Synaptic Facilitation Induced by Repeated D2 Receptor Stimulation: Involvement in Behavioral Repetition. *Journal of Neuroscience*. 2021 Mar 24;41(12):2780–94.
193. Sumimoto H, Miyano K, Takeya R. Molecular composition and regulation of the Nox family NAD(P)H oxidases. *Biochem Biophys Res Commun*. 2005 Dec 9;338(1):677–86.
194. Bedard K, Krause KH. The NOX family of ROS-generating NADPH oxidases: Physiology and pathophysiology. *Physiol Rev*. 2007 Jan;87(1):245–313.
195. Contreras ML, de la Fuente-Ortega E, Vargas-Roberts S, Muñoz DC, Goic CA, Haeger PA. NADPH oxidase isoform 2 (NOX2) is involved in drug addiction vulnerability in progeny developmentally exposed to ethanol. *Front Neurosci*. 2017 Jun 14;11(JUN):338.
196. Schiavone S, Riezzo I, Turillazzi E, Trabace L. Involvement of the NADPH Oxidase NOX2-Derived Brain Oxidative Stress in an Unusual Fatal Case of Cocaine-Related Neurotoxicity Associated With Excited Delirium Syndrome. *J Clin Psychopharmacol* [Internet]. 2016 Oct 1 [cited 2023 Apr 28];36(5):513–7. Available from: <https://pubmed.ncbi.nlm.nih.gov/27533346/>
197. Yang Z, Asico LD, Yu P, Wang Z, Jones JE, Escano CS, et al. D5 dopamine receptor regulation of reactive oxygen species production, NADPH oxidase, and blood pressure. *Am J Physiol Regul Integr Comp Physiol* [Internet]. 2006 Jan [cited 2024 May 13];290(1):96–104. Available from: <https://journals.physiology.org/doi/10.1152/ajpregu.00434.2005>

198. Park M, Hennig B, Toborek M. Methamphetamine alters occludin expression via NADPH oxidase-induced oxidative insult and intact caveolae. *J Cell Mol Med* [Internet]. 2012 Feb [cited 2023 Apr 28];16(2):362. Available from: [/pmc/articles/PMC3133868/](#)
199. Miller DK, Oelrichs CE, Sun GY, Simonyi A. Subchronic apocynin treatment attenuates methamphetamine-induced dopamine release and hyperactivity in rats. *Life Sci*. 2014 Mar 7;98(1):6–11.
200. Schröder K. NADPH oxidase-derived reactive oxygen species: Dosis facit venenum. *Exp Physiol* [Internet]. 2019 Apr 1 [cited 2023 Mar 15];104(4):447–52. Available from: <https://pubmed.ncbi.nlm.nih.gov/30737851/>
201. Dukoff DJ, Hogg DW, Hawrysh PJ, Buck LT. Scavenging ROS dramatically increase NMDA receptor whole-cell currents in painted turtle cortical neurons. *J Exp Biol* [Internet]. 2014 Sep 1 [cited 2024 May 21];217(Pt 18):3346–55. Available from: <https://pubmed.ncbi.nlm.nih.gov/25063855/>
202. Reactive oxygen species (ROS) modulate AMPA receptor phosphorylation and cell-surface localization in concert with pain-related behavior - PMC [Internet]. [cited 2024 May 21]. Available from: <https://www.ncbi.nlm.nih.gov/pmc/articles/PMC3413777/>
203. Lee DZ, Chung JM, Chung K, Kang MG. Reactive oxygen species (ROS) modulate AMPA receptor phosphorylation and cell-surface localization in concert with pain-related behavior. *Pain* [Internet]. 2012 Sep [cited 2024 May 21];153(9):1905. Available from: [/pmc/articles/PMC3413777/](#)
204. Li MH, Underhill SM, Reed C, Phillips TJ, Amara SG, Ingram SL. Amphetamine and Methamphetamine Increase NMDAR-GluN2B Synaptic Currents in Midbrain Dopamine Neurons. *Neuropsychopharmacology* 2017 42:7 [Internet]. 2016 Dec 15 [cited 2024 May 22];42(7):1539–47. Available from: <https://www.nature.com/articles/npp2016278>
205. Berríos-Cárcamo P, Quezada M, Quintanilla ME, Morales P, Ezquer M, Herrera-Marschitz M, et al. Oxidative Stress and Neuroinflammation as a Pivot in Drug Abuse. A Focus on the Therapeutic Potential of Antioxidant and Anti-Inflammatory Agents and Biomolecules. *Antioxidants* [Internet]. 2020 Sep 1 [cited 2023 May 8];9(9):1–26. Available from: [/pmc/articles/PMC7555323/](#)
206. Tan H, Trevor Young L, Shao L, Che Y, Honer WG, Wang JF. Mood stabilizer lithium inhibits amphetamine-increased 4-hydroxynonenal-protein adducts in rat frontal cortex. *International Journal of Neuropsychopharmacology* [Internet]. 2012 Oct 1

- [cited 2023 May 5];15(9):1275–85. Available from:
<https://academic.oup.com/ijnp/article/15/9/1275/671096>
207. Fisher AA, Labenski MT, Malladi S, Gokhale V, Bowen ME, Milleron RS, et al. Quinone electrophiles selectively adduct “electrophile binding motifs” within cytochrome c. *Biochemistry* [Internet]. 2007 Oct 2 [cited 2023 May 5];46(39):11090–100. Available from: <https://pubmed.ncbi.nlm.nih.gov/17824617/>
 208. Kumagai Y, Abiko Y. Environmental electrophiles: Protein adducts, modulation of redox signaling, and interaction with persulfides/polysulfides. *Chem Res Toxicol* [Internet]. 2017 Jan 17 [cited 2023 May 5];30(1):203–19. Available from: <https://pubs.acs.org/doi/full/10.1021/acs.chemrestox.6b00326>
 209. Sun WL, Quizon PM, Zhu J. Molecular mechanism: ERK signaling, drug addiction and behavioral effects. *Prog Mol Biol Transl Sci* [Internet]. 2016 [cited 2023 May 3];137:1. Available from: </pmc/articles/PMC5330621/>
 210. Liu HQ, An YW, Hu AZ, Li MH, Wu JL, Liu L, et al. Critical roles of the PI3K-Akt-mTOR signaling pathway in apoptosis and autophagy of astrocytes induced by methamphetamine. *Open Chem* [Internet]. 2019 Jan 1 [cited 2023 May 3];17(1):96–104. Available from: <https://www.degruyter.com/document/doi/10.1515/chem-2019-0015/html?lang=en>
 211. Wang SF, Yen JC, Yin PH, Chi CW, Lee HC. Involvement of oxidative stress-activated JNK signaling in the methamphetamine-induced cell death of human SH-SY5Y cells. *Toxicology*. 2008 Apr 18;246(2–3):234–41.
 212. Wang X, Northcutt AL, Cochran TA, Zhang X, Fabisiak TJ, Haas ME, et al. Methamphetamine activates Toll-like receptor 4 to induce central immune signaling within the ventral tegmental area and contributes to extracellular dopamine increase in the nucleus accumbens shell. *ACS Chem Neurosci* [Internet]. 2019 Aug 8 [cited 2023 May 3];10(8):3622. Available from: </pmc/articles/PMC8316980/>
 213. Lepsch LB, Munhoz CD, Kawamoto EM, Yshii LM, Lima LS, Curi-Boaventura MF, et al. Cocaine induces cell death and activates the transcription nuclear factor kappa-b in pc12 cells. *Mol Brain* [Internet]. 2009 Feb 1 [cited 2023 May 3];2(1):1–15. Available from: <https://molecularbrain.biomedcentral.com/articles/10.1186/1756-6606-2-3>
 214. Miller JS, Barr JL, Harper LJ, Poole RL, Gould TJ, Unterwald EM. The GSK3 Signaling Pathway Is Activated by Cocaine and Is Critical for Cocaine Conditioned Reward in Mice. *PLoS One* [Internet]. 2014 Feb 4 [cited 2023 May 3];9(2). Available from: </pmc/articles/PMC3913742/>

215. Kim M, Jang WJ, Shakya R, Choi B, Jeong CH, Lee S. Current Understanding of Methamphetamine-Associated Metabolic Changes Revealed by the Metabolomics Approach. *Metabolites* [Internet]. 2019 [cited 2023 Mar 6];9(10). Available from: [/pmc/articles/PMC6835349/](https://pubmed.ncbi.nlm.nih.gov/36039764/)
216. Zheng T, Liu L, Shi J, Yu X, Xiao W, Sun R, et al. The metabolic impact of methamphetamine on the systemic metabolism of rats and potential markers of methamphetamine abuse. *Mol Biosyst* [Internet]. 2014 Jun 3 [cited 2023 Mar 6];10(7):1968–77. Available from: <https://pubs.rsc.org/en/content/articlehtml/2014/mb/c4mb00158c>
217. Volkow ND, Chang L, Wang GJ, Fowler JS, Ding YS, Sedler M, et al. Low level of brain dopamine D2 receptors in methamphetamine abusers: association with metabolism in the orbitofrontal cortex. *Am J Psychiatry* [Internet]. 2001 [cited 2024 May 24];158(12):2015–21. Available from: <https://pubmed.ncbi.nlm.nih.gov/11729018/>
218. Kovacic P. Role of oxidative metabolites of cocaine in toxicity and addiction: Oxidative stress and electron transfer. *Med Hypotheses*. 2005;64(2):350–6.
219. Brown JM, Quinton MS, Yamamoto BK. Methamphetamine-induced inhibition of mitochondrial complex II: Roles of glutamate and peroxynitrite. *J Neurochem*. 2005 Oct;95(2):429–36.
220. Dietrich JB, Mangeol A, Revel MO, Burgun C, Aunis D, Zwiller J. Acute or repeated cocaine administration generates reactive oxygen species and induces antioxidant enzyme activity in dopaminergic rat brain structures. *Neuropharmacology*. 2005;48(7):965–74.
221. Fattore L, Diana M. Drug addiction: An affective-cognitive disorder in need of a cure. *Neurosci Biobehav Rev*. 2016 Jun 1;65:341–61.
222. Shukla M, Vincent B. Methamphetamine abuse disturbs the dopaminergic system to impair hippocampal-based learning and memory: An overview of animal and human investigations. *Neurosci Biobehav Rev*. 2021 Dec 1;131:541–59.
223. Nestler EJ, Barrot M, Self DW. Δ FosB: A sustained molecular switch for addiction. *Proc Natl Acad Sci U S A* [Internet]. 2001 Sep 25 [cited 2023 May 8];98(20):11042–6. Available from: <https://www.pnas.org/doi/abs/10.1073/pnas.191352698>
224. Kumar A, Aglyamova G, Yim YY, Bailey AO, Lynch HM, Powell RT, et al. Chemically targeting the redox switch in AP1 transcription factor Δ FOSB. *Nucleic Acids Res* [Internet]. 2022 Sep 9 [cited 2024 May 26];50(16):9548–67. Available from: <https://pubmed.ncbi.nlm.nih.gov/36039764/>

225. McKetin R, Mattick RP. Attention and memory in illicit amphetamine users: comparison with non-drug-using controls. *Drug Alcohol Depend.* 1998 Apr 1;50(2):181–4.
226. Lipaus IFS, Gomes EF, Martins CW, e Silva CM, Pires RGW, Malgarin F, et al. Impairment of spatial working memory and oxidative stress induced by repeated crack cocaine inhalation in rats. *Behavioural Brain Research.* 2019 Feb 1;359:910–7.
227. Lipaus IFS, Gomes EF, Martins CW, e Silva CM, Pires RGW, Malgarin F, et al. Impairment of spatial working memory and oxidative stress induced by repeated crack cocaine inhalation in rats. *Behavioural brain research [Internet].* 2019 Feb 1 [cited 2024 May 26];359:910–7. Available from: <https://pubmed.ncbi.nlm.nih.gov/29935277/>
228. Felipe RM, Oliveira GM, Barbosa RS, Esteves BD, Gonzaga BMS, Horita SIM, et al. Experimental Social Stress: Dopaminergic Receptors, Oxidative Stress, and c-Fos Protein Are Involved in Highly Aggressive Behavior. *Front Cell Neurosci [Internet].* 2021 Aug 17 [cited 2023 May 10];15. Available from: <https://pubmed.ncbi.nlm.nih.gov/34489642/>
229. Vujnović AF, Rubinić M, Starčević I, Waldowski RA. Influence of Redox and Dopamine Regulation in Cocaine-Induced Phenotypes Using *Drosophila*. *Antioxidants* 2023, Vol 12, Page 933 [Internet]. 2023 Apr 14 [cited 2023 May 8];12(4):933. Available from: <https://www.mdpi.com/2076-3921/12/4/933/htm>
230. Jang EY, Ryu YH, Lee BH, Chang SC, Yeo MJ, Kim SH, et al. Involvement of reactive oxygen species in cocaine-taking behaviors in rats. *Addiction biology [Internet].* 2015 Jul 1 [cited 2022 May 25];20(4):663. Available from: </pmc/articles/PMC4843775/>
231. Jang EY, Yang CH, Hedges DM, Kim SP, Lee JY, Ekins TG, et al. The role of reactive oxygen species in methamphetamine self-administration and dopamine release in the nucleus accumbens. *Addiction Biology.* 2017 Sep 1;22(5):1304–15.
232. Numa R, Kohen R, Poltyrev T, Yaka R. Tempol diminishes cocaine-induced oxidative damage and attenuates the development and expression of behavioral sensitization. *Neuroscience.* 2008 Aug 26;155(3):649–58.
233. Beiser T, Numa R, Kohen R, Yaka R. Chronic treatment with Tempol during acquisition or withdrawal from CPP abolishes the expression of cocaine reward and diminishes oxidative damage. *Sci Rep.* 2017 Dec 1;7(1).

234. Jang EY, Ryu YH, Lee BH, Chang SC, Yeo MJ, Kim SH, et al. Involvement of reactive oxygen species in cocaine-taking behaviors in rats. *Addiction biology*. 2015 Jul 1;20(4):663.
235. Jang EY, Yang CH, Hedges DM, Kim SP, Lee JY, Ekins TG, et al. The role of reactive oxygen species in methamphetamine self-administration and dopamine release in the nucleus accumbens. *Addiction Biology*. 2017 Sep 1;22(5):1304–15.
236. Zegers-Delgado J, Blanlot C, Calderon F, Yarur HE, Novoa J, Vega-Quiroga I, et al. Reactive oxygen species modulate locomotor activity and dopamine extracellular levels induced by amphetamine in rats. *Behavioural Brain Research*. 2022 Jun 3;427:113857.
237. Miller DK, Oelrichs CE, Sage AS, Sun GY, Simonyi A. Repeated resveratrol treatment attenuates methamphetamine-induced hyperactivity and [3H]dopamine overflow in rodents. *Neurosci Lett [Internet]*. 2013 Oct 25 [cited 2023 Apr 21];554:53–8. Available from: <https://pubmed.ncbi.nlm.nih.gov/24012682/>
238. Ezeriņa D, Takano Y, Hanaoka K, Urano Y, Dick TP. N-acetyl cysteine functions as a fast-acting antioxidant by triggering intracellular H₂S and sulfane sulfur production. *Cell Chem Biol*. 2018 Apr 4;25(4):447.
239. Herrmann AP, Andrejew R, Benvenuti R, Gama CS, Elisabetsky E. Effects of N-acetylcysteine on amphetamine-induced sensitization in mice. *Brazilian Journal of Psychiatry*. 2018 Apr 1;40(2):169.
240. Herrmann AP, Benvenuti R, Pilz LK, Elisabetsky E. N-acetylcysteine prevents increased amphetamine sensitivity in social isolation-reared mice. *Schizophr Res*. 2014 May 1;155(1–3):109–11.
241. Schmaal L, Veltman DJ, Nederveen A, Van Den Brink W, Goudriaan AE. N-acetylcysteine normalizes glutamate levels in cocaine-dependent patients: A randomized crossover magnetic resonance spectroscopy study. *Neuropsychopharmacology*. 2012 Aug;37(9):2143–52.
242. Corbit LH. Use of N-Acetylcysteine in Relapse and Cocaine Addiction. *The Neuroscience of Cocaine: Mechanisms and Treatment*. 2017 Jan 1;645–53.
243. Baker DA, McFarland K, Lake RW, Shen H, Toda S, Kalivas PW. N-Acetyl Cysteine-Induced Blockade of Cocaine-Induced Reinstatement. *Ann N Y Acad Sci*. 2003;1003:349–51.

244. Mousavi SG, Sharbafchi M, Salehi M, Peykanpour M, Sichani NK, Maracy M. The efficacy of N-acetylcysteine in the treatment of methamphetamine dependence: a double-blind controlled, crossover study. *Arch Iran Med*. 2015;
245. Manchester LC, Coto-Montes A, Boga JA, Andersen LPH, Zhou Z, Galano A, et al. Melatonin: An ancient molecule that makes oxygen metabolically tolerable. *J Pineal Res*. 2015 Nov 1;59(4):403–19.
246. Takahashi TT, Vengeliene V, Spanagel R. Melatonin reduces motivation for cocaine self-administration and prevents relapse-like behavior in rats. *Psychopharmacology* 2017 234:11 [Internet]. 2017 Feb 28 [cited 2023 Mar 21];234(11):1741–8. Available from: <https://link.springer.com/article/10.1007/s00213-017-4576-y>
247. Barbosa-Méndez S, Pérez-Sánchez G, Becerril-Villanueva E, Salazar-Juárez A. Melatonin decreases cocaine-induced locomotor sensitization and cocaine-conditioned place preference in rats. *J Psychiatr Res*. 2021 Jan 1;132:97–110.
248. Anderson G. Melatonin and cocaine: Role of mitochondria, immunity, and gut microbiome. *Brazilian Journal of Psychiatry*. 2020 Jul 1;42(4):452–3.
249. Chen F, Sun J, Zhang Y, Dai Y, Zhang Z, Chen C, et al. Quercetin ameliorates mitochondrial dysfunction and mitigates methamphetamine-induced anxiety-like behavior. *bioRxiv* [Internet]. 2021 Jun 30 [cited 2023 Mar 21];2021.06.29.450268. Available from: <https://www.biorxiv.org/content/10.1101/2021.06.29.450268v1>
250. Kaun KR, Devineni A V., Heberlein U. *Drosophila melanogaster* as a model to study drug addiction. *Hum Genet* [Internet]. 2012 Jun 17 [cited 2022 May 25];131(6):959–75. Available from: <https://link.springer.com/article/10.1007/s00439-012-1146-6>
251. Graham ML, Prescott MJ. The multifactorial role of the 3Rs in shifting the harm-benefit analysis in animal models of disease. *Eur J Pharmacol* [Internet]. 2015 Jul 7 [cited 2024 May 25];759:19. Available from: </pmc/articles/PMC4441106/>
252. Heigwer F, Port F, Boutros M. RNA Interference (RNAi) Screening in *Drosophila*. *Genetics* [Internet]. 2018 Mar 1 [cited 2024 Mar 8];208(3):853. Available from: </pmc/articles/PMC5844339/>
253. Yamamoto S, Seto ES. Dopamine Dynamics and Signaling in *Drosophila*: An Overview of Genes, Drugs and Behavioral Paradigms. *Exp Anim* [Internet]. 2014 [cited 2024 May 25];63(2):107. Available from: </pmc/articles/PMC4160991/>
254. Belmer A, Patkar OL, Pitman KM, Bartlett SE. Serotonergic Neuroplasticity in Alcohol Addiction. *Brain Plasticity*. 2016 Jul 1;1(2):177–206.

255. Müller CP, Homberg JR. The role of serotonin in drug use and addiction. *Behavioural Brain Research*. 2015 Jan 15;277:146–92.
256. McClung C, Hirsh J. Stereotypic behavioral responses to free-base cocaine and the development of behavioral sensitization in *Drosophila*. *Curr Biol* [Internet]. 1998 Jan 15 [cited 2024 May 25];8(2):109–12. Available from: <https://pubmed.ncbi.nlm.nih.gov/9427649/>
257. Andretic R, Van Swinderen B, Greenspan RJ. Dopaminergic modulation of arousal in *Drosophila*. *Curr Biol* [Internet]. 2005 Jul 12 [cited 2024 May 18];15(13):1165–75. Available from: <https://pubmed.ncbi.nlm.nih.gov/16005288/>
258. Hyman SE. Addiction to cocaine and amphetamine. *Neuron* [Internet]. 1996 [cited 2024 May 25];16(5):901–4. Available from: <https://pubmed.ncbi.nlm.nih.gov/8630246/>
259. Kuhn BN, Kalivas PW, Bobadilla AC. Understanding Addiction Using Animal Models. *Front Behav Neurosci* [Internet]. 2019 Nov 29 [cited 2024 Jun 9];13. Available from: </pmc/articles/PMC6895146/>
260. Miserendino MJD, Nestler EJ. Behavioral sensitization to cocaine: modulation by the cyclic AMP system in the nucleus accumbens. *Brain Res* [Internet]. 1995 Mar 20 [cited 2024 Jun 9];674(2):299–306. Available from: <https://pubmed.ncbi.nlm.nih.gov/7796110/>
261. Thomas MJ, Beurrier C, Bonci A, Malenka RC. Long-term depression in the nucleus accumbens: a neural correlate of behavioral sensitization to cocaine. *Nat Neurosci* [Internet]. 2001 [cited 2024 Jun 9];4(12):1217–23. Available from: <https://pubmed.ncbi.nlm.nih.gov/11694884/>
262. Pierce RC, Kalivas PW. A circuitry model of the expression of behavioral sensitization to amphetamine-like psychostimulants. *Brain Res Rev* [Internet]. 1997 Oct [cited 2024 Jun 9];25(2):192–216. Available from: <https://pubmed.ncbi.nlm.nih.gov/9403138/>
263. Nestler EJ, Lüscher C. The Molecular Basis of Drug Addiction: Linking Epigenetic to Synaptic and Circuit Mechanisms. *Neuron* [Internet]. 2019 Apr 3 [cited 2024 Jun 9];102(1):48–59. Available from: <https://pubmed.ncbi.nlm.nih.gov/30946825/>
264. Filošević A, Al-Samarai S, Andretić Waldowski R. High throughput measurement of locomotor sensitization to volatilized cocaine in *drosophila melanogaster*. *Front Mol Neurosci* [Internet]. 2018 Feb 5 [cited 2022 May 25];11:25. Available from: </pmc/articles/PMC5807336/>

265. McClung C, Hirsh J. Stereotypic behavioral responses to free-base cocaine and the development of behavioral sensitization in *Drosophila*. *Curr Biol* [Internet]. 1998 Jan 15 [cited 2024 May 31];8(2):109–12. Available from: <https://pubmed.ncbi.nlm.nih.gov/9427649/>
266. Lee HG, Kim YC, Dunning JS, Han KA. Recurring Ethanol Exposure Induces Disinhibited Courtship in *Drosophila*. *PLoS One* [Internet]. 2008 Jan 2 [cited 2024 Jun 9];3(1):1391. Available from: </pmc/articles/PMC2148075/>
267. Filošević A, Al-Samarai S, Andretić Waldowski R. High throughput measurement of locomotor sensitization to volatilized cocaine in *drosophila melanogaster*. *Front Mol Neurosci*. 2018 Feb 5;11:25.
268. Hasan G, Dieter Riemensperger T, Szumlinski KK, Andretić Waldowski R, Filošević A, Al-samarai S. High Throughput Measurement of Locomotor Sensitization to Volatilized Cocaine in *Drosophila melanogaster*. *Front Mol Neurosci* [Internet]. 2018 [cited 2022 May 25];11:25. Available from: www.frontiersin.org
269. Rigo F, Filošević A, Petrović M, Jović K, Andretić Waldowski R. Locomotor sensitization modulates voluntary self-administration of methamphetamine in *Drosophila melanogaster*. *Addiction Biology* [Internet]. 2021 May 1 [cited 2023 Sep 11];26(3):e12963. Available from: <https://onlinelibrary.wiley.com/doi/full/10.1111/adb.12963>
270. Devineni A V., Heberlein U. Preferential Ethanol Consumption in *Drosophila* Models Features of Addiction. *Current Biology*. 2009 Dec 29;19(24):2126–32.
271. Ja WW, Carvalho GB, Mak EM, De La Rosa NN, Fang AY, Liong JC, et al. Prandiology of *Drosophila* and the CAFE assay. *Proc Natl Acad Sci U S A*. 2007 May 15;104(20):8253–6.
272. Diegelmann S, Jansen A, Jois S, Kastenholz K, Escarcena LV, Strudthoff N, et al. The CAPillary feeder assay measures food intake in *Drosophila melanogaster*. *Journal of Visualized Experiments*. 2017 Mar 17;2017(121).
273. Kaun KR, Devineni A V., Heberlein U. *Drosophila melanogaster* as a model to study drug addiction. *Hum Genet*. 2012 Jun 17;131(6):959–75.
274. Petruccelli E, Feyder M, Ledru N, Jaques Y, Anderson E, Kaun KR. Alcohol Activates Scabrous-Notch to Influence Associated Memories. *Neuron* [Internet]. 2018 Dec 5 [cited 2024 Jun 3];100(5):1209-1223.e4. Available from: <https://pubmed.ncbi.nlm.nih.gov/30482693/>

275. Highfill CA, Baker BM, Stevens SD, Anholt RRH, Mackay TFC. Genetics of cocaine and methamphetamine consumption and preference in *Drosophila melanogaster*. *PLoS Genet* [Internet]. 2019 May 1 [cited 2024 Apr 10];15(5):e1007834. Available from: <https://journals.plos.org/plosgenetics/article?id=10.1371/journal.pgen.1007834>
276. St Johnston D. The art and design of genetic screens: *Drosophila melanogaster*. *Nature Reviews Genetics* 2002 3:3 [Internet]. 2002 [cited 2024 May 25];3(3):176–88. Available from: <https://www.nature.com/articles/nrg751>
277. Tsai LTY, Bainton RJ, Blau J, Heberlein U. Lmo Mutants Reveal a Novel Role for Circadian Pacemaker Neurons in Cocaine-Induced Behaviors. *PLoS Biol* [Internet]. 2004 Dec [cited 2024 May 25];2(12). Available from: </pmc/articles/PMC529317/>
278. Ojelade SA, Jia T, Rodan AR, Chenyang T, Kadrmas JL, Cattrell A, et al. Rsu1 regulates ethanol consumption in *Drosophila* and humans. *Proc Natl Acad Sci U S A* [Internet]. 2015 Jul 28 [cited 2024 May 25];112(30):E4085–93. Available from: </pmc/articles/PMC4522778/>
279. Arking R. Successful selection for increased longevity in *Drosophila*: analysis of the survival data and presentation of a hypothesis on the genetic regulation of longevity. *Exp Gerontol* [Internet]. 1987 [cited 2024 May 24];22(3):199–220. Available from: <https://pubmed.ncbi.nlm.nih.gov/3113991/>
280. Dierick HA, Greenspan RJ. Molecular analysis of flies selected for aggressive behavior. *Nat Genet* [Internet]. 2006 Sep 4 [cited 2023 Sep 11];38(9):1023–31. Available from: <https://pubmed.ncbi.nlm.nih.gov/16906161/>
281. Wheeler JM, Reed C, Burkhart-Kasch S, Li N, Cunningham CL, Janowsky A, et al. Genetically correlated effects of selective breeding for high and low methamphetamine consumption. *Genes Brain Behav* [Internet]. 2009 Nov [cited 2023 Jun 26];8(8):758. Available from: </pmc/articles/PMC2783502/>
282. Carroll ME, Morgan AD, Anker JJ, Perry JL, Dess NK. Selective breeding for differential saccharin intake as an animal model of drug abuse. *Behavioural Pharmacology*. 2008 Sep;19(5–6):435–60.
283. Morgan AD, Dess NK, Carroll ME. Escalation of intravenous cocaine self-administration, progressive-ratio performance, and reinstatement in rats selectively bred for high (HiS) and low (LoS) saccharin intake. *Psychopharmacology (Berl)*. 2005 Feb;178(1):41–51.

284. Carroll ME, Morgan AD, Lynch WJ, Campbell UC, Dess NK. Intravenous cocaine and heroin self-administration in rats selectively bred for differential saccharin intake: Phenotype and sex differences. *Psychopharmacology (Berl)*. 2002;161(3):304–13.
285. Yakovenko V, Speidel ER, Chapman CD, Dess NK. Food dependence in rats selectively bred for low versus high saccharin intake. Implications for “food addiction.” *Appetite* [Internet]. 2011 Oct [cited 2024 May 25];57(2):397–400. Available from: <https://pubmed.ncbi.nlm.nih.gov/21683748/>
286. Hauser SR, Katner SN, Waeiss RA, Truitt WA, Bell RL, McBride WJ, et al. Selective breeding for high alcohol preference is associated with increased sensitivity to cannabinoid reward within the nucleus accumbens shell. *Pharmacol Biochem Behav*. 2020 Oct 1;197:173002.
287. Eastwood EC, Phillips TJ. Opioid sensitivity in mice selectively bred to consume or not consume methamphetamine. *Addiction biology* [Internet]. 2014 [cited 2024 Jun 9];19(3):370. Available from: </pmc/articles/PMC3796126/>
288. Eastwood EC, Barkley-Levenson AM, Phillips TJ. Methamphetamine drinking microstructure in mice bred to drink high or low amounts of methamphetamine. *Behavioural brain research* [Internet]. 2014 Oct 1 [cited 2023 Sep 11];272:111–20. Available from: <https://pubmed.ncbi.nlm.nih.gov/24978098/>
289. Shabani S, Houlton SK, Hellmuth L, Mojica E, Mootz JRK, Zhu Z, et al. A Mouse Model for Binge-Level Methamphetamine Use. *Front Neurosci* [Internet]. 2016 [cited 2024 Jun 9];10(NOV). Available from: </pmc/articles/PMC5090006/>
290. Ja WW, Carvalho GB, Mak EM, De La Rosa NN, Fang AY, Liong JC, et al. Prandiology of *Drosophila* and the CAFE assay. *Proc Natl Acad Sci U S A* [Internet]. 2007 May 15 [cited 2022 May 25];104(20):8253–6. Available from: www.pnas.org/doi/10.1073/pnas.0702726104
291. Chen J, Wang Y, Zhang Y, Shen P. Mutations in *Bacchus* reveal a tyramine-dependent nuclear regulator for acute ethanol sensitivity in *Drosophila*. *Neuropharmacology* [Internet]. 2013 Apr [cited 2024 May 27];67:25–31. Available from: <https://pubmed.ncbi.nlm.nih.gov/23142736/>
292. Diegelmann S, Jansen A, Jois S, Kastenholz K, Escarcena LV, Strudthoff N, et al. The CAPillary FEeder Assay Measures Food Intake in *Drosophila melanogaster*. *J Vis Exp* [Internet]. 2017 Mar 17 [cited 2022 May 25];2017(121):55024. Available from: </pmc/articles/PMC5408587/>

293. Andretic R, Chaney S, Hirsh J. Requirement of circadian genes for cocaine sensitization in *Drosophila*. *Science* [Internet]. 1999 Aug 13 [cited 2024 Jun 9];285(5430):1066–8. Available from: <https://pubmed.ncbi.nlm.nih.gov/10446052/>
294. Dominguez-Lopez S, Ahn B, Sataranatarajan K, Ranjit R, Premkumar P, Van Remmen H, et al. Long-term methamphetamine self-administration increases mesolimbic mitochondrial oxygen consumption and decreases striatal glutathione. *Neuropharmacology* [Internet]. 2023 Apr 1 [cited 2023 Apr 28];227. Available from: <https://pubmed.ncbi.nlm.nih.gov/36693561/>
295. Siciliano CA, Calipari ES, Ferris MJ, Jones SR. Adaptations of presynaptic dopamine terminals induced by psychostimulant self-administration. *ACS Chem Neurosci* [Internet]. 2015 Jan 21 [cited 2023 May 5];6(1):27–36. Available from: <https://pubs.acs.org/doi/full/10.1021/cn5002705>
296. Kucerova J, Pistovcakova J, Vrskova D, Dusek L, Sulcova A. The effects of methamphetamine self-administration on behavioural sensitization in the olfactory bulbectomy rat model of depression. *Int J Neuropsychopharmacol* [Internet]. 2012 Nov [cited 2024 Apr 10];15(10):1503–11. Available from: <https://pubmed.ncbi.nlm.nih.gov/22114789/>
297. Ashok AH, Mizuno Y, Volkow ND, Howes OD. Association of Stimulants With Dopaminergic Alterations in Users of Cocaine, Amphetamine, and Methamphetamine: A Systematic Review and Meta-analysis. *JAMA Psychiatry* [Internet]. 2017 May 5 [cited 2024 Jun 9];74(5):511. Available from: </pmc/articles/PMC5419581/>
298. Martin-Iverson MT, Burger LY. Behavioral sensitization and tolerance to cocaine and the occupation of dopamine receptors by dopamine. *Mol Neurobiol* [Internet]. 1995 Aug [cited 2024 Jun 9];11(1–3):31–46. Available from: <https://pubmed.ncbi.nlm.nih.gov/8561966/>
299. Li H, Chaney S, Forte M, Hirsh J. Ectopic G-protein expression in dopamine and serotonin neurons blocks cocaine sensitization in *Drosophila melanogaster*. *Curr Biol* [Internet]. 2000 Feb 1 [cited 2024 Jun 9];10(4):211–4. Available from: <https://pubmed.ncbi.nlm.nih.gov/10704417/>
300. McClung CA, Sidiropoulou K, Vitaterna M, Takahashi JS, White FJ, Cooper DC, et al. Regulation of dopaminergic transmission and cocaine reward by the Clock gene. *Proc Natl Acad Sci U S A* [Internet]. 2005 Jun 28 [cited 2024 May 18];102(26):9377–81. Available from: <https://pubmed.ncbi.nlm.nih.gov/15967985/>

301. Spencer S, Torres-Altoro MI, Falcon E, Arey R, Marvin M, Goldberg M, et al. A mutation in CLOCK leads to altered dopamine receptor function. *J Neurochem* [Internet]. 2012 Oct [cited 2024 Jun 9];123(1):124–34. Available from: <https://pubmed.ncbi.nlm.nih.gov/22757753/>
302. Falcon E, Ozburn A, Mukherjee S, Roybal K, McClung CA. Differential Regulation of the Period Genes in Striatal Regions following Cocaine Exposure. *PLoS One* [Internet]. 2013 Jun 11 [cited 2024 Jun 9];8(6):e66438. Available from: <https://journals.plos.org/plosone/article?id=10.1371/journal.pone.0066438>
303. Grahame NJ, Li TK, Lumeng L. Selective breeding for high and low alcohol preference in mice. *Behav Genet* [Internet]. 1999 [cited 2023 Sep 11];29(1):47–57. Available from: <https://pubmed.ncbi.nlm.nih.gov/10371758/>
304. Morozova T V., Anholt RRH, Mackay TFC. Phenotypic and transcriptional response to selection for alcohol sensitivity in *Drosophila melanogaster*. *Genome Biol* [Internet]. 2007 Oct 31 [cited 2023 Sep 11];8(10):1–15. Available from: <https://genomebiology.biomedcentral.com/articles/10.1186/gb-2007-8-10-r231>
305. Bollu PC, Sahota P. Sleep and Parkinson Disease. *Mo Med* [Internet]. 2017 Sep 1 [cited 2024 May 18];114(5):381. Available from: </pmc/articles/PMC6140184/>
306. Koob GF, Volkow ND. Neurocircuitry of Addiction. *Neuropsychopharmacology* [Internet]. 2010 [cited 2022 May 23];35(1):217. Available from: </pmc/articles/PMC2805560/>
307. Huang J, Liu W, Qi Y xiang, Luo J, Montell C. Neuromodulation of Courtship Drive through Tyramine-Responsive Neurons in the *Drosophila* Brain. *Current Biology*. 2016 Sep 12;26(17):2246–56.
308. Blenau W, Baumann A. Molecular and pharmacological properties of insect biogenic amine receptors: Lessons from *Drosophila melanogaster* and *Apis mellifera*. *Arch Insect Biochem Physiol* [Internet]. 2001 Sep 1 [cited 2024 May 28];48(1):13–38. Available from: <https://onlinelibrary.wiley.com/doi/full/10.1002/arch.1055>
309. Burrows KB, Gudelsky G, Yamamoto BK. Rapid and transient inhibition of mitochondrial function following methamphetamine or 3,4-methylenedioxymethamphetamine administration. *Eur J Pharmacol*. 2000 Jun 9;398(1):11–8.
310. Dostalek M, Jurica J, Pistovcakova J, Hanesova M, Tomandl J, Linhart I, et al. Effect of methamphetamine on cytochrome P450 activity. *Xenobiotica* [Internet]. 2007 Dec

- [cited 2024 Jun 2];37(12):1355–66. Available from: <https://pubmed.ncbi.nlm.nih.gov/17922362/>
311. Jiang L, Gu H, Lin Y, Xu W, Zhu R, Kong J, et al. Remodeling of brain lipidome in methamphetamine-sensitized mice. *Toxicol Lett*. 2017 Sep 5;279:67–76.
 312. Zhu L, Li J, Dong N, Guan F, Liu Y, Ma D, et al. mRNA changes in nucleus accumbens related to methamphetamine addiction in mice. *Sci Rep [Internet]*. 2016 Nov 21 [cited 2024 Jun 2];6. Available from: <https://pubmed.ncbi.nlm.nih.gov/27869204/>
 313. Davidson C, Gow AJ, Lee TH, Ellinwood EH. Methamphetamine neurotoxicity: Necrotic and apoptotic mechanisms and relevance to human abuse and treatment. *Brain Res Rev [Internet]*. 2001 [cited 2024 May 27];36(1):1–22. Available from: <https://pubmed.ncbi.nlm.nih.gov/11516769/>
 314. Pandey S, Miller CA. Targeting the cytoskeleton as a therapeutic approach to substance use disorders. *Pharmacol Res [Internet]*. 2024 Apr 1 [cited 2024 May 27];202:107143. Available from: [/pmc/articles/PMC11034636/](https://pubmed.ncbi.nlm.nih.gov/11034636/)
 315. Bray SJ. Notch signalling: a simple pathway becomes complex. *Nature Reviews Molecular Cell Biology* 2006 7:9 [Internet]. 2006 Sep 19 [cited 2024 Jun 9];7(9):678–89. Available from: <https://www.nature.com/articles/nrm2009>
 316. Ni T, Zhu L, Wang S, Zhu W, Xue Y, Zhu Y, et al. Medial prefrontal cortex Notch1 signalling mediates methamphetamine-induced psychosis via Hes1-dependent suppression of GABAB1 receptor expression. *Molecular Psychiatry* 2022 27:10 [Internet]. 2022 Jun 22 [cited 2024 Jun 3];27(10):4009–22. Available from: <https://www.nature.com/articles/s41380-022-01662-z>
 317. Wang Y, Branicky R, Noë A, Hekimi S. Superoxide dismutases: Dual roles in controlling ROS damage and regulating ROS signaling. *J Cell Biol [Internet]*. 2018 Jun 6 [cited 2024 Jun 4];217(6):1915. Available from: [/pmc/articles/PMC5987716/](https://pubmed.ncbi.nlm.nih.gov/3117716/)
 318. Valjent E, Corvol JC, Trzaskos JM, Girault JA, Hervé D. Role of the ERK pathway in psychostimulant-induced locomotor sensitization. *BMC Neurosci [Internet]*. 2006 Mar 2 [cited 2024 Jun 4];7. Available from: <https://pubmed.ncbi.nlm.nih.gov/16512905/>
 319. Abe MK, Kartha S, Karpova AY, Li J, Liu PT, Kuo WL, et al. Hydrogen peroxide activates extracellular signal-regulated kinase via protein kinase C, Raf-1, and MEK1. *Am J Respir Cell Mol Biol [Internet]*. 1998 [cited 2024 Jun 4];18(4):562–9. Available from: <https://pubmed.ncbi.nlm.nih.gov/9533945/>

320. Lee SH, Cho E, Yoon SE, Kim Y, Kim EY. Metabolic control of daily locomotor activity mediated by tachykinin in *Drosophila*. *Communications Biology* 2021 4:1 [Internet]. 2021 Jun 7 [cited 2024 Jun 9];4(1):1–14. Available from: <https://www.nature.com/articles/s42003-021-02219-6>
321. Shafer OT, Keene AC. The Regulation of *Drosophila* Sleep. *Current Biology*. 2021 Jan 11;31(1):R38–49.
322. Shafer OT, Keene AC. The Regulation of *Drosophila* Sleep. *Current Biology*. 2021 Jan 11;31(1):R38–49.
323. Hartmann C, Kempf A. Mitochondrial control of sleep. *Curr Opin Neurobiol*. 2023 Aug 1;81:102733.
324. Correa M, Sanchis-Segura C, Pastor R, Aragon CMG. Ethanol intake and motor sensitization: the role of brain catalase activity in mice with different genotypes. *Physiol Behav*. 2004 Sep 15;82(2–3):231–40.
325. Correa M, Sanchis-Segura C, Aragon CMG. Brain catalase activity is highly correlated with ethanol-induced locomotor activity in mice. *Physiol Behav* [Internet]. 2001 [cited 2024 Jun 10];73(4):641–7. Available from: <https://pubmed.ncbi.nlm.nih.gov/11495670/>
326. Tristan C, Shahani N, Sedlak TW, Sawa A. The diverse functions of GAPDH: views from different subcellular compartments. *Cell Signal* [Internet]. 2011 Feb [cited 2024 Jun 4];23(2):317. Available from: </pmc/articles/PMC3084531/>
327. Patterson RL, Van Rossum DB, Kaplin AI, Barrow RK, Snyder SH. Inositol 1,4,5-trisphosphate receptor/GAPDH complex augments Ca²⁺ release via locally derived NADH. *Proc Natl Acad Sci U S A* [Internet]. 2005 Feb 2 [cited 2024 Jun 10];102(5):1357. Available from: </pmc/articles/PMC547892/>
328. Schnatz A, Müller C, Brahmer A, Krämer-Albers EM. Extracellular Vesicles in neural cell interaction and CNS homeostasis. *FASEB Bioadv* [Internet]. 2021 Aug 1 [cited 2024 Jun 4];3(8):577. Available from: </pmc/articles/PMC8332475/>
329. Dar GH, Mendes CC, Kuan WL, Speciale AA, Conceição M, Görgens A, et al. GAPDH controls extracellular vesicle biogenesis and enhances the therapeutic potential of EV mediated siRNA delivery to the brain. *Nat Commun* [Internet]. 2021 Dec 1 [cited 2024 Jun 10];12(1). Available from: </pmc/articles/PMC8602309/>
330. Porkka-Heiskanen T, Kalinchuk A V. Adenosine, energy metabolism and sleep homeostasis. *Sleep Med Rev* [Internet]. 2011 Apr [cited 2024 Jun 4];15(2):123–35. Available from: <https://pubmed.ncbi.nlm.nih.gov/20970361/>

331. Morozova T V., Mackay TFC, Anholt RRH. Genetics and genomics of alcohol sensitivity. *Molecular Genetics and Genomics* [Internet]. 2014 [cited 2024 Jun 10];289(3):253. Available from: [/pmc/articles/PMC4037586/](#)
332. Morozova T V., Ayroles JF, Jordan KW, Duncan LH, Carbone MA, Lyman RF, et al. Alcohol sensitivity in *Drosophila*: Translational potential of systems genetics. *Genetics*. 2009;183(2):733–45.
333. Terzi A, Ngo KJ, Mourrain P. Phylogenetic conservation of the interdependent homeostatic relationship of sleep regulation and redox metabolism. *Journal of Comparative Physiology B* 2024 [Internet]. 2024 Feb 7 [cited 2024 Jun 3];1–12. Available from: <https://link.springer.com/article/10.1007/s00360-023-01530-4>
334. Hartmann C, Kempf A. Mitochondrial control of sleep. *Curr Opin Neurobiol*. 2023 Aug 1;81:102733.
335. Kempf A, Song SM, Talbot CB, Miesenböck G. A potassium channel β -subunit couples mitochondrial electron transport to sleep. *Nature* [Internet]. 2019 Apr 11 [cited 2024 Jun 9];568(7751):230–4. Available from: <https://pubmed.ncbi.nlm.nih.gov/30894743/>
336. Sun L, Li HM, Seufferheld MJ, Walters KR, Margam VM, Jannasch A, et al. Systems-Scale Analysis Reveals Pathways Involved in Cellular Response to Methamphetamine. *PLoS One* [Internet]. 2011 [cited 2024 Jun 10];6(4):e18215. Available from: <https://journals.plos.org/plosone/article?id=10.1371/journal.pone.0018215>

8. LIST OF ABBREVIATIONS

- 5-HT = 5-Hydroxytryptamine (Serotonin)
- ADH = Alcohol Dehydrogenase
- ALDH = Aldehyde Dehydrogenase
- AMPA = α -Amino-3-hydroxy-5-methyl-4-isoxazolepropionic Acid
- AP-1 = Activator Protein 1
- CAFÉ = Capillary Feeder Assay
- CaMKII = Calcium/Calmodulin-Dependent Protein Kinase II
- cAMP = Cyclic Adenosine Monophosphate
- CAT = Catalase
- cGMP = Cyclic Guanosine Monophosphate
- COC = Cocaine
- COMT = Catechol-O-Methyltransferase
- CPP = Conditioned Place Preference
- CREB = cAMP Response Element-Binding Protein
- DA = Dopamine or 4-(2-aminoethyl)benzene-1,2-diol
- DAMS = Drosophila Activity Monitoring System
- DAT = Dopamine Transporter
- DDC = DOPA Decarboxylase
- Dj-1beta = DJ-1 beta (Parkinsonism Associated Deglycase)

- DOPAC = 3,4-Dihydroxyphenylacetic Acid
- DOPAL = 3,4-Dihydroxyphenylacetaldehyde
- ERK = Extracellular Signal-Regulated Kinase
- ETC = Electron Transport Chain
- GABA = Gamma-Aminobutyric Acid
- GAL4 = (Yeast) Galactose-Responsive Transcription Factor
- GPx = Glutathione Peroxidase
- GRx = Glutaredoxin
- GSH = Glutathione
- GSSG = Glutathione Disulfide
- H₂O₂ = Hydrogen Peroxide
- HAT = Histone Acetyltransferase
- HDAC = Histone Deacetylase
- HP = line with high preference for METH generated by selective breeding
- HVA = Homovanillic Acid
- LP = line with low preference for METH generated by selective breeding
- LS = Locomotor Sensitization
- LTD = Long-Term Depression
- LTP = Long-Term Potentiation
- MAHDR = High Drinking Inbred Strain of Mice
- MALDR = Low Drinking Inbred Strain of Mice

- MAO = Monoamine Oxidase
- MAPK = Mitogen-Activated Protein Kinase
- MAPK/ERK = Mitogen-Activated Protein Kinase/Extracellular Signal-Regulated Kinase
- METH = Methamphetamine
- NAC = N-Acetylcysteine
- NAc = Nucleus Accumbens
- NAD⁺ = Nicotinamide Adenine Dinucleotide (oxidized form)
- NADH = Nicotinamide Adenine Dinucleotide (reduced form)
- NET = Norepinephrine Transporter
- NF-Kb = Nuclear Factor Kappa B
- NMDA = N-Methyl-D-Aspartate
- NO = Nitric Oxide
- NOX = NADPH Oxidase
- OA = Octopamine
- PBN = Phenyl-N-tert-butyl Nitron
- per = Period gene
- PFC = Prefrontal Cortex
- PI3K = Phosphoinositide 3-Kinase
- PKC = Protein Kinase C
- PKG = Protein Kinase G
- Prx = Peroxiredoxin

- PTEN = Phosphatase and Tensin Homolog
- RNAi = Ribonucleic Acid Interference
- ROS = Reactive Oxygen Species
- RTK = Receptor Tyrosine Kinase
- SA = Salicylic Acid
- SENS = Sensitivity
- SERT = Serotonin Transporter
- SOD = Superoxide Dismutase
- TA = Tyramine
- TEMPOL = 4-Hydroxy-2,2,6,6-Tetramethylpiperidine 1-Oxyl
- UAS = (Yeast) Upstream Activating Sequence
- vCOC = Volatilized Cocaine
- VMAT = Vesicular Monoamine Transporter
- VMAT2 = Vesicular Monoamine Transporter 2
- vMETH = Volatilized Methamphetamine
- VTA = Ventral Tegmental Area

9. LIST OF FIGURES

Figure 1. Addictive drugs “hijack” synaptic plasticity mechanisms in key brain circuits.	3
Figure 2. Mesolimbic and mesocortical dopamine pathways.	4
Figure 3. Chemical structures of dopamine and METH	9
Figure 4. Dopamine Neurotransmission under Baseline and METH-Exposed Conditions. ...	10
Figure 5. Basic neuroplasticity types.	14
Figure 6. The Impact of ROS Levels on Cellular Signaling and Outcomes.	19
Figure 7. Reactive Oxygen Species (ROS) and Antioxidant Defense Mechanisms.....	21
Figure 8. Main sources of ROS in the neurons upon psychostimulant abuse.	28
Figure 9. Neuronal DA metabolism and ROS production.	30
Figure 10. Reactive oxygen species are an inherent by-product of oxidative phosphorylation in the mitochondrial ETC.....	32
Figure 11. FlyCafe: a novel method for measuring preferential consumption of food in individual flies.....	58
Figure 12. FlyBong platform for measuring changes in locomotor activity of <i>Drosophila</i> after delivery of psychostimulants.	61
Figure 13. Transgenic flies used in the genetic screen were generated using the Gal4/UAS expression system.....	72
Figure 14. Flow chart of the genetic screen for the identification of redox-related genes involved in LS in <i>Drosophila melanogaster</i>	73
Figure 15. Flow chart of the selective breeding for the high and low METH preference. ...	75
Figure 16. Proteomic analyses of fly brains after selective breeding for high and low METH preference (Proteomics 1) or exposing <i>wt</i> flies to two doses of vMETH (Proteomics 2).....	76
Figure 17. FlyBong test procedure for exposing <i>wt</i> flies to two doses of vMETH before Proteomics 2.....	79
Figure 18. Criteria for segregation into CTRL, LS and NLS groups for proteomic analysis. ...	80
Figure 19. Evaporation of liquid food is significantly lower when the capillaries are placed in evaporation control system (ES).	83
Figure 20. Experimental group (EXP) consumes more METH food than regular food, but the total amount does not differ from the control group during 3-day experiment.....	84
Figure 21. <i>Drosophila</i> males preferentially consume METH food over regular food.	88
Figure 22. Preferential self-administration of METH food is long lasting.	91
Figure 23. Two highly divergent lines of flies with Low Preference (LP) and High Preference (HP) for METH were generated through 30 generations of selective breeding.	94
Figure 24. Phenotypes of high and low preferential consumption of METH are stable after the end of selective breeding.	96
Figure 25. Increased locomotor activity in LD and reduced sleep in DD conditions in LP. ..	98

Figure 26. LP male flies have reduced vertical climbing ability compared to P0.	100
Figure 27. LP male flies have increased body weight compared to <i>wt</i> and HP.	101
Figure 28. LP flies have increased tyramine compared to P0, while other neurotransmitter concentration are lower in HP and LP lines compared to P0.	103
Figure 29. Proteomic analysis of P0, HP and LP lines yielded a list of differentially expressed proteins among those 3 groups.....	106
Figure 30. Bacchus, a negative regulator of tyramine beta-hydroxylase, is detected among proteins present only in the brains of LP flies and is not present in HP nor CS lines.	110
Figure 31. Panneuronal silencing of <i>Tbh</i> mimics LP phenotype.....	112
Figure 32. Preferential self-administration of METH precludes LS to vMETH.	113
Figure 33. Flies exposed to heated air after the SA experiment show no LS.	114
Figure 34. LS to vMETH precludes preferential self-administration of METH food.....	116
Figure 35. Mock treatment with heated air in the FlyBong does not affect preferential consumption of METH in the FlyCafe.	117
Figure 36. <i>per</i> ⁰¹ mutant flies do not develop LS to vMETH and do not preferentially self-administer METH food.....	119
Figure 37. There is no difference in baseline locomotor activity between <i>wt</i> and <i>per</i> ⁰¹ flies.	120
Figure 38. Hypothetical results and their controls.	122
Figure 39. Panneuronal silencing of <i>Sod2</i> or <i>E(spl)m3-hlh</i> prevents the development of LS	125
Figure 40. Redox-related genes do not affect negative geotaxis.....	127
Figure 41. Flies with panneuronally silenced <i>Cat</i> , <i>Gclc</i> , <i>Gclm</i> , <i>Grx1</i> , <i>GstE1</i> , and <i>MBD-like</i> exhibit significantly reduced, while <i>Sod1</i> shows increased locomotor activity.	127
Figure 42. Silencing redox-related genes in all neurons affects the amount of sleep.....	129
Figure 43. Silencing of <i>Cat</i> , <i>Sod1</i> , <i>Sod2</i> , <i>Gapdh1</i> or <i>Men</i> in dopaminergic and serotonergic neurons prevents LS to vMETH.....	132
Figure 44. Silencing <i>Sod1</i> , <i>Gapdh1</i> , and <i>Men</i> genes in dopaminergic and serotonergic neurons results in the loss of preference for METH.....	135
Figure 45. Silencing redox related genes in dopaminergic and serotonergic neurons does not affect climbing ability.	136
Figure 46. Silencing <i>GstE1</i> , <i>Sod2</i> , <i>Sod3</i> and <i>PHGPx</i> in dopaminergic and serotonergic neurons affects average locomotor activity.	137
Figure 47. Silencing of redox-related genes affects the amount of sleep.	138
Figure 48. Silencing of <i>Gapdh1</i> or <i>Men</i> genes in dopaminergic neurons prevents the development of LS to vMETH.	141
Figure 49. Silencing <i>Prx3</i> gene in dopaminergic neurons results in the loss of preference for METH.	144

Figure 50. Silencing redox related genes in dopaminergic neurons does not affect vertical climbing ability.....	145
Figure 51. <i>Jafrac1</i> in dopaminergic neurons is necessary for the development of LS to vCOC.	146
Figure 52. Venn diagram exhibiting the overlap of proteins upregulated in LS against CTRL and NLS.	148
Figure 53. Venn diagram demonstrating the overlap of proteins downregulated in LS compared to CTRL and NLS.....	149
Figure 54. STRING analysis displaying the network of upregulated proteins in <i>Drosophila</i> brains of the METH-sensitized (LS) group.	150
Figure 55. 39 redox-related proteins are upregulated in LS group compared to both NLS and CTRL group.	158
Figure 56. STRING visualization of proteins downregulated after LS in <i>Drosophila</i> brains.	160
Figure 57. 21 redox-related proteins are downregulated in LS group compared to both NLS and CTRL group.	166
Figure 58. Schematic representation of metabolic pathways and the positions of the proteins/genes which affect LS and/or preference for METH in <i>Drosophila</i> identified by genetic screen and proteomics.....	169
Figure 59. Blocking conversion of tyramine into octopamine results in LP phenotype.	185
Figure 60. Summary of behavioral, neurochemical and proteomic differences between HP and LP lines.	190
Figure 61. Bacchus could be regulated by redox through its physical interactions with Prx6c or other redox related and metabolic proteins.	192

10. LIST OF TABLES

Table 1. List of RNAi lines obtained from Vienna Drosophila Resource Center (VDRC) and Bloomington Drosophila Stock Center (BDSC)	54
Table 2. Composition for 50 mL RIPA (RadioImmunoPrecipitation Assay).....	66
Table 3. Composition of Laemmli Buffer	67
Table 4. Example of amount of ingested food and preference calculations for FlyCafe assay.	86
Table 5. Proteins unique in LP line.....	106
Table 6. Summary of tested phenotypes for pan-neuronal silencing of redox related genes.	124
Table 7. Summary of tested phenotypes when redox-related genes were silenced in dopaminergic and serotonergic neurons.	130
Table 8. Summary of tested phenotypes for silencing of redox-related genes in the dopaminergic neurons (ple-gal4).	139
Table 9. Redox-related proteins upregulated in LS group compared to both NLS and CTRL group.....	152
Table 10. Redox-related proteins downregulated in LS group compared to both NLS and CTRL group.....	162
Table 11. Genes necessary for LS to vMETH:.....	167
Table 12. Genes necessary for preferential self-administration of METH:.....	167
Table 13. Genes necessary for LS to vCOC:.....	168
Table 14. Summary of redox-related genes implicated in LS and SA.....	171
Table 15. Summary of redox-related genes implicated in LS and SA.....	Error! Bookmark not defined.

11. SUPPLEMENT

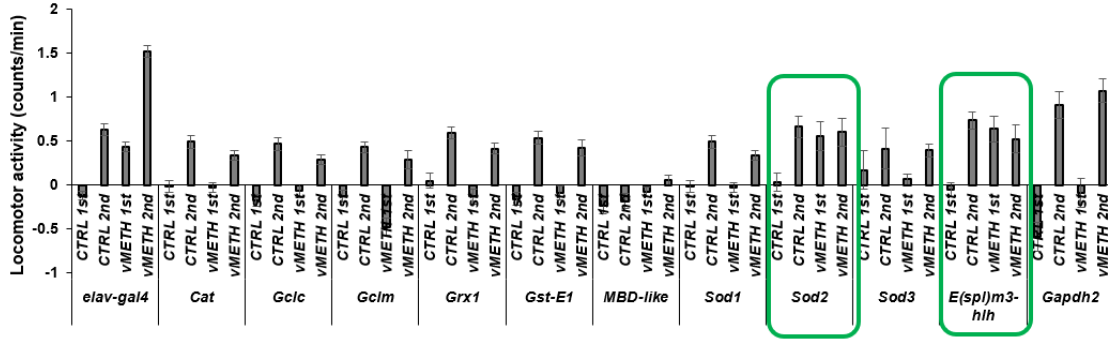


Figure1. elav-gal4

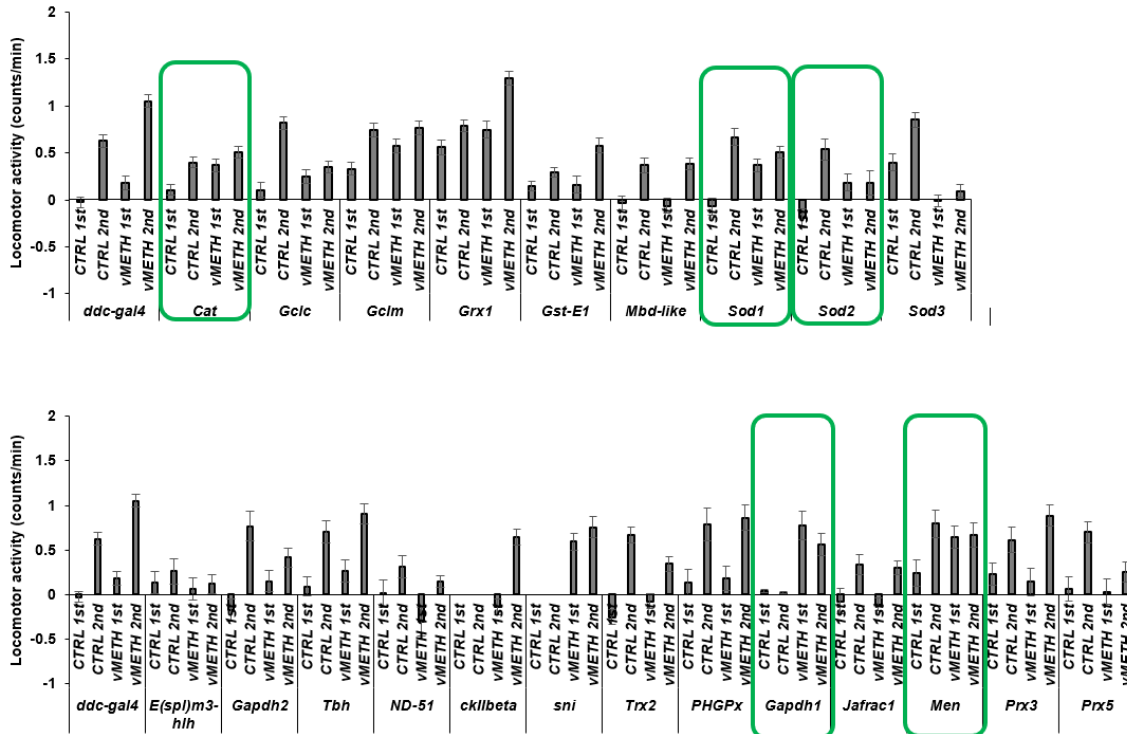


Figure 2. ddc-gal4

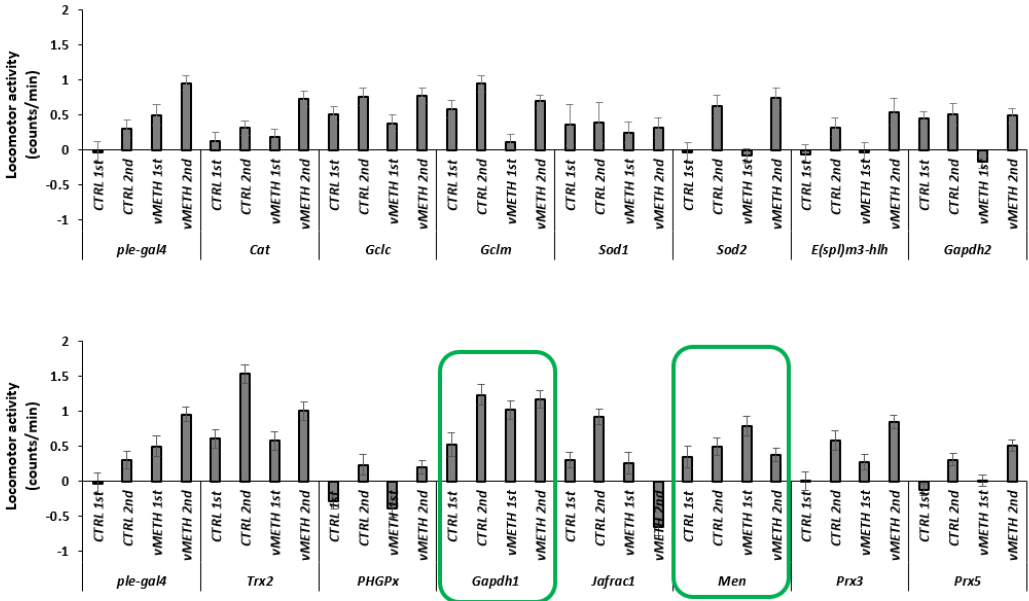


Figure 3. ple-gal4

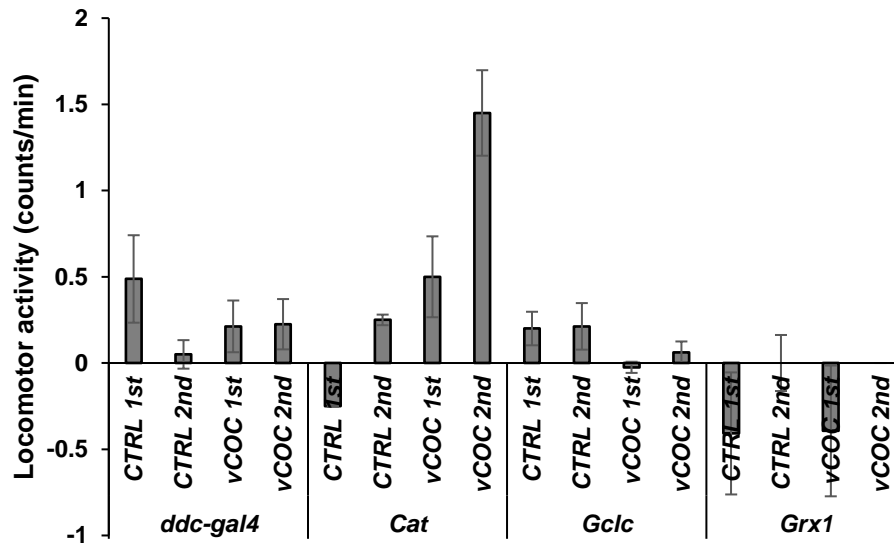


Figure 4. Representation of locomotor activity in transgenic male flies after two doses of 75 µg vCOC given at a 6-hour interval. Average locomotor activity after the 1st and 2nd doses of 75 µg vCOC (experimental group - vCOC, n=16) or hot air (control group - CTRL, n=16), administered with a 6-hour interval. The change is calculated by subtracting the baseline activity (5 minutes before exposure) from the response to the dose (5 minutes after exposure). progeny of the respective GAL4xUAS-RNAi crosses.